Electroanalysis of microbial biofilms and antibiofilm drug testing

By

Kayode Olaifa

Submitted In Partial Fulfillment of the Requirements for the Degree of Doctor of Philosophy in Science, Engineering and Technology

2022

Electroanalysis of microbial biofilms and antibiofilm drug testing

By

Kayode Olaifa

Submitted In Partial Fulfillment of the Requirements for the Degree of Doctor of Philosophy in Science, Engineering and Technology

School of Engineering and Digital Sciences
Nazarbayev University

Supervised by
Prof. Daniele Tosi
Prof. Damira Kanayeva
Prof. Carlo Santoro
Prof. Enrico Marsili

November 2022

Declaration

I, Kayode Olaifa, declare that the research contained in this thesis, unless otherwise formally indicated within the text, is original. The thesis has not been previously submitted to this or any other university for a degree and does not incorporate any material already submitted for a degree.

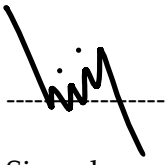

Signed
Dated 29th November 2022

Abstract

Microbial biofilms are responsible for about 80% of infectious diseases in humans, resulting in high morbidity and mortality rates. Biofilm confers protection to the microbial cells from stressors, including antimicrobial treatments. Biofilms are more difficult to remove/kill, thus, contributing to antimicrobial resistance phenomenon. Unfortunately, existing methodologies routinely employed for microbial biofilms and evaluation of anti-biofilm compounds are flawed with varying limitations. Therefore, an urgent need for the design/development and adoption of new diagnostic platforms is exigent. Additionally, the need for new therapeutic options cannot be overemphasized.

In this work, a bioelectrochemical platform that uses simple, low-cost, and commercially available screen-printed electrodes was implemented for real-time evaluation of selected antimicrobials against clinically relevant biofilm-forming species. We also adopted a drug repurposing strategy against a model resistant bacterial strain using the developed bioelectrochemical platform. Finally, attempt was made to detect a model fungal pathogen in human urine samples also via the developed platform.

In general, both biochemical and electroanalytic methods suggests that complete inhibition of biofilm formation would require concentrations higher than that needed for planktonic cells. Further optimization of the methodology on *C. albicans* biofilms indicated that the antifungal activity of the tested compounds is in the order of complex Ag3>Amphotericin B>Fluconazole, while the conventional XTT indicated the order of Amphotericin B > Fluconazole >complex Ag3. This variability further reiterates the necessity for a multi-method approach to validate the antibiofilm efficacy of any compound. However, this study demonstrated, for the first time, the real-time antibiofilm assessment of selected antimicrobials using electroanalytical approach and offers consistent findings as early as 10 h following inoculation.

Additionally, both biochemical and bioelectrochemical results validate that fungicide repurposing against bacterial biofilms could be the missing piece in the puzzle of fight against bacterial resistance, as crystal violet assay demonstrated 90.5 %, 81.2 %, and 69.1 % biofilm inhibition, while electroanalysis demonstrated 92.5 %, 84.7 %, and 57.8 %

reduction in current output of *A. baumannii* biofilm, exposed to Ciprofloxacin, Itraconazole, and Fluconazole, respectively. Though both approaches complement each other, the latter offers a simple and real-time platform for antibiofilm assessment. Finally, the developed bioelectrochemical platform detected *C. albicans* cells in human urine samples within approximately 10 h with a limit of detection (LOD) of ~39 CFU/mL. This work presented the first report on electrochemical-based detection of a fungal pathogen in human urine sample using unmodified screen-printed carbon electrodes.

Acknowledgements

***"Enter his gates with thanksgiving* and his courts with praise; give thanks to him and praise his name. For the Lord is good and his love endures forever; his faithfulness continues through all generations* - Psalm 100:4-5".**

The story of my journey to Kazakhstan began on one fateful evening in March 2019 during a long phone conversation with one of my advisors, Dr. Obinna Ajunwa, who informed me about Nazarbayev University (NU), its ongoing PhD application, and the possibility of working with one of the top researchers in the field of microbial electrochemistry, Prof. Enrico Marsili, if I eventually get admitted. Strangely, that was my first-time hearing about Kazakhstan not to talk of NU, but after that phone call, I swung into action immediately, first with getting acquainted with the university and then with the application process. Today, three years after, I am writing the acknowledgements section of my PhD thesis at NU supervised by Prof. Enrico Marsili. Therefore, I say with great joy in my heart, To God be the glory for his faithfulness**,** indeed**,** endures forever.

A perfect thesis, they say, is a completed thesis. However, in completing this thesis, I received help of all kinds from people, and it is only fair to acknowledge them specially and properly. This will however take no specific or particular order.

To the government of Kazakhstan and NU management, I say thank you for the Abay Kunanbayev scholarship award. I am also grateful to the former Director of PhD programs in SET, Prof. Luis Rojas, and the current Director, Prof. Konstantinos Kostas, for their immeasurable support, timely and constructive feedbacks during presentations and willingness to answer and provide clarifications when I am in doubt or need help from the school office. I acknowledge the supportive roles of the former and current Managers for Academics and Students Affairs in the school office, Makpal Shomenova and Zura Zhodorova, respectively. You all made my PhD study and research, a memorable one.

To my advisor, Prof. Enrico Marsili, thank you for the opportunity to work under your supervision, to learn from you and through you, and for trusting me. You are supportive beyond my expectation. Your quest to ensure I am doing fine all the time, academically, psychologically, and health-wise is highly appreciated. You are a great manager, and a compassionate advisor, and I consider you a role model. Thank you for the training, the academic cum research pressures, the criticism, the guidance and feedback, the

opportunities, and most importantly the freedom to explore my own ideas, make mistakes and learn new things. I have not only learnt about doing research and writing papers over the past three years, I have also acquired adequate knowledge about lab management, project management, budget and procurement processes, and human resource management. I am grateful for these privileges and for preparing me for the next big phase of my life. Your financial and moral support throughout my graduate program, especially while I was sick a couple of times, while I contracted COVID-19 twice, and just recently during the period of grief of my father's death, will forever live with me. No doubt I will miss you, but I take solace in the belief that we would continue to work together, either directly or indirectly. With a heart full of gratitude, I say thank you!

To my internal and external co-advisors, Prof. Damira Kanayeva and Prof. Carlo Santoro, respectively, I would like to specially express my sincere gratitude for your support throughout my PhD study. Thank you.

Once again, special thanks to Dr Obinna Ajunwa for his propitious support, meticulous guidance, motivation, and encouragement. Your ceaseless and great assistance over the years were exemplary. I bless the Supreme Being for making my path cross yours; it has been a great privilege and an experience that would live with me beyond forever. May God continue to bestow His mercy and blessings on you and yours. I am equally thankful to my academic mentors and former advisors, Prof. Abiodun A. Onilude and Dr Oluwaseun Garuba. Their support before I enrolled in PhD and during the PhD is beyond description. Their mentorship during my master's degree study at University of Ibadan provided me with moral and mental capacity that sustained me till this time. Your help with letters of recommendation and other kinds is what metamorphosed into today's success. Thank you for everything you have been doing for me.

To my friends and lab members, Neda Eghtesadi and Aisholpan Kaziullayeva, and colleagues in PhD SET – Saule Mergenbayeva, Samal Kaumbekova, Abat Zhuldassov, Soudabeh Gorginezhad, Motahereh Naseri, and Yerkanat Kanafin, thanks for the friendship and support throughout this program. I am grateful to you all. Also, special thanks to Dr Aidos Baumuratov and other staff members of Core Facilities, NU, and to Dr Dinara Begimbetova of National Laboratory Astana (NLA), for their technical support,

even when it is not convenient to do so. I want to specially acknowledge Maulen Yergaziyev of Office of International Scholars and Students for his immense and all-round support. He literally made living in Kazakhstan easy and seamless. This is same for all other administrative staff I have had the privilege of meeting, working, or interacting over the past few years. Many thanks to you all.

To my friends, I mean friends, including those who stayed true to our friendship despite my inability to keep up for reasons beyond my control, I say thank you – Femi Awodokun, Oke Adeyinka, Sunday Oguntomi, Shuiab Badmus, Abayomi Akanbi, Peter Oyedeji, Bolanle Olujimi, Ibrahim Adedayo. Thank you all! It is equally very important to thank and appreciate all other persons whose name I couldn't mention but whose support made this work a success. May God in His infinite mercy continues to guide and protect us all.

I have been lucky to meet new people in NU. My colleagues in the Nigerian community, the African community, and the international community. Amazing people all round. Thank you all for the meals shared together, the laughs, arguments, talks and conversations, the soccer games, game nights, travels, and all. Thank you for making NU fun and fulfilling. Rizwan Muneer, Mariam Shakeel, Sagidolla Batay and his wife, Hamza Tariq and his wife, Zhanat Makhataeva, Zhadyra Onshanova, Ahmad Javeed and his wife, Moshin, Muhammad Salman, Evans Asare, Enoch Adotey, Ebenezer Owusu – You guys represent an important part of my journey, and I am grateful for the support, beautiful moments and all other good things we share.

Sadly, my father died on April 2, 2022. I didn't see it coming. I became disinterested in everything. I was broken beyond words, even till now. I spoke with him on phone just few days before that tragic date, and as usual, he jokingly called me a doctor. Unfortunately, he is no more to witness me become it. Before his death, he was a great and supportive father. He is a lover of education and academic excellence. He enrolled me in the best of schools available to us right from childhood and supported me fully till the moment he departed this earthly surface. He loved me beyond words. I am grateful to him for everything, his upright teachings – moral and social, and for imbibing in me the values of hard work, honesty, commitment, love, humility, and absolute faith in God. My father is not dead, I believe. He is too good to die. His legacy lives on, and I take solace in this. I promise to

continue to always live by his legacy of 'humanity first'. May his sins be forgiven, and may he find rest in the afterlife. Amen.

To my loving, strong and amazing mother, Chief (Mrs) Florence Modupe Olaifa, thank you for all the support. May you live long in good health to enjoy the fruit of your labour, Amen. I love you, Mama. To my siblings: *Egbon* Babatunde, *ati awon aburo mi*: Damilola, Oluwatobiloba and Olumide, I sincerely acknowledge your support in all ramifications. May God continue to keep us strong in love, health, and unison. May we blossom and become great. May we not die a sudden death. Amen. Cheers to the amazing tomorrow! Love you all.

I am grateful for the constant support I receive from my grandpa, Baba Fola Omitade, from childhood till now. His constant encouragement and words of affirmation is part of what kept me strong till this moment. God bless you grandpa. To Akin Olaifa, my uncle who now doubles as my daddy, thank you Sir for been there when it matters. Your weekly Sunday calls is one I cherish and appreciate. May God's grace, blessing and mercy never depart from you.

Finally, to my amazing fiancée, hearty friend, partner and confidant, Omolabake Alake Grace, Omo Baba Adegboye, I say a big thank you for the all-round support, understanding and patience. I admire your attitude towards life, your zeal, hard work, diligence, and perseverance. You are a great partner with whom I am eager to live the rest of my life with. The moment is closer, even than we could think! I love you baby 😍😍. Thank you for being my peace and best friend. May God continue to bless us and answer our prayers, Amen. Cheers to the beautiful future we would share together!

Kayode Olaifa

November 2022

Table of Contents

List of Figures

Fig. 4.2. (A) Comparative biofilm and planktonic estimates of *C. albicans* (n =4) and the current output (n=3). **(B)** Current output of *C. albicans* biofilm at varying applied potential (V) (n = 3).

Fig.4.3. (A) Effect of tested antifungals on the current output of *C. albicans* biofilms: cells with $K_3[Fe(CN)_6]$ only (black trace); cells with DMSO (dotted black trace); cells with complex 3 (green trace), Flz (red trace), AmB (blue trace); cells only (thin blue trace); $K_3[Fe(CN)_6]$ and complex 3 only (thin dotted green trace); $K_3[Fe(CN)_6]$ only (thin red trace). **(B)** Total Q after 24 h of incubation at E = 0.4 V (n=3). The differences between controls and antifungal experiments are statistically significant ($p < 0.05$).

Fig. 4.4: (A) OD of planktonic cells in different experimental conditions after 24 h growth at E = 0.4 *vs*. Ag pseudo-reference electrode. **(B)** Biofilm cells estimates obtained via crystal violet assay for the different experimental conditions after 24 h growth at E = 0.4 *vs*. Ag pseudo-reference electrode. The difference between each pair of conditions is statistically significant ($p < 0.05$), with smaller OD and biofilm formation in the presence of Flz, AmB and complex 3. (n = 3).

Fig. 4.5. Cyclic voltammograms of *C. albicans* ATTC 10231 at 24 h at 1 mV s^{-1}.

Fig. 4.6. Modulus of impedance with time. Cells with $K_3[Fe(CN)_6]$ (black trace); cells with complex 3 (red trace), Flz (blue trace), and AmB (green trace).

Fig. 4.7. Representative Raman images of *C. albicans* ATCC 10231 on the WE area after 48 h potentiostatic experiment

Fig. 4.8. Representative of *C. albicans* ATCC 10231 on the WE area after 48 h potentiostatic experiment obtained via scanning electron microscopy. **(A)** Cells not exposed to antimicrobials demonstrating massive biofilm matrix and hyphal proliferation. **(B)** Cells exposed to Flz demonstrating limited hyphal growth. **(C)** Cells exposed to AmB demonstrating scanty yeast cells with membrane damage. **(D)** Cells exposed to complex 3 also demonstrated scanty yeast cells.

Fig. 4.9. Biofilm formation by *C. albicans* following addition of Flz, AmB and Ag3 at inoculation at two different concentrations (1×MIC and 10×MIC) evaluated by XTT reduction assay

Fig. 5.1. Effect of **(A)** Amp, **(B)** Flz, **(C)** Itz and **(D)** Cip on growth (OD_{600}) of *A. baumannii.* Except for Amp, the difference between treatments vs control is significant ($p < 0.05$).

Fig. 5.2. Effect of Cip, Flz and Itz on *A. baumannii* biofilm formation. **(A)** Addition of drugs at inoculation; **(B)** Addition to preformed biofilm. (n=4). The difference between treatments vs control is significant ($p < 0.05$).

Fig. 5.3. (A) Chronoamperometry of *A. baumannii* biofilms with and without the drugs: cells not exposed to drugs (black trace); cells exposed to Flz (red trace); cells exposed to Itz (blue trace); cells exposed to Cip (green). **(B)** Total Q obtained after 24 h of incubation at E = 400 mV (C). Crystal violet estimates of biofilms on the WE surface determined after

List of Tables

Thesis output

Publications

K. Olaifa, O. Ajunwa, E. Marsili (2022). Electroanalytic evaluation of antagonistic effect of azole fungicides on *Acinetobacter baumannii* biofilms. *Electrochimica Acta* **405**, 139837. https://doi.org/10.1016/j.electacta.2022.139837

K. Olaifa, J. Nikodinovic-Runic, B. Glišić, F. Boschetto, E. Marin, F. Segreto, E. Marsili (2021) Electroanalysis of *Candida albicans* biofilms: a suitable real-time tool for antifungal testing, *Electrochimica Acta* **389**, 138757. https://doi.org/10.1016/j.electacta.2021.138757

N. Savić, B. Petković, S. Vojnovic, M. Mojicevic, K. **Olaifa**, E. Marsili, J. Nikodinovic-Runic, M. Djuran, B. Glisic (2020) Dinuclear silver(I) complexes with pyridine-based macrocyclic type of ligand as antimicrobial agents against clinically relevant species: the influence of counter anion on the structure diversification of the complexes, *Dalton Transactions* **49**, 10880–10894. https://doi.org/10.1039/D0DT01272F

Gauhar Akhmetzhan, **Kayode Olaifa**, Michael Kitching, Paul A. Cahill, Tri T. Pham, Obinna M. Ajunwa, Enrico Marsili, Biochemical and electrochemical characterization of biofilms formed on everolimus-eluting coronary stents, Enzyme and Microbial Technology,Volume 163, 2023, 110156, ISSN 0141-0229, https://doi.org/10.1016/j.enzmictec.2022.110156.

Eghtesadi, N., **Olaifa, K.**, Perna, F. M., Capriati, V., Trotta, M., Ajunwa, O., & Marsili, E. (2022). Electroactivity of weak electricigen Bacillus subtilis biofilms in solution containing deep eutectic solvent components. Bioelectrochemistry (Amsterdam, Netherlands), 147(July), 108207. https://doi.org/10.1016/j.bioelechem.2022.108207

Yang, Q., **Olaifa, K.**, Andrew, F. P., Ajibade, P. A., Ajunwa, O. M., & Marsili, E. (2022). Assessment of physiological and electrochemical effects of a repurposed zinc dithiocarbamate complex on Acinetobacter baumannii biofilms. Scientific Reports, 1–14. https://doi.org/10.1038/s41598-022-16047-z

Conferences

Olaifa K, Ajunwa O, Marsili E. New use for old/existing drugs: repurposing antifungal drugs against bacterial biofilms. **[Oral presentation]. 2nd Eurasian International Workshop on Antimicrobial and Biosensing Nanotechnologies, 13-15th May 2022.**

Olaifa K, Qing O, Ajunwa O, Marsili E. Repurposing fungicides against bacterial biofilms – biochemical and bioelectrochemical assessment. **[Oral presentation**]. **72nd Annual Meeting of the International Society of Electrochemistry held in Jeju Island, Korea.** 29 August to 3 September 2021.

Olaifa K, Nikodinovic-Runic J, Glišić B, Boschetto F, Marin E, Segreto F, Marsili E. Electroanalysis of *Candida albicans* biofilms: a suitable real-time tool for antifungal

testing. **[Oral presentation]. 1st Eurasian International Workshop on Antimicrobial and Biosensing Nanotechnologies, May 2021**.

Marsili E, **Olaifa K**, Savić ND, Nikodinović-Runić J, Glišić BĐ. Antibiofilm activity of dinuclear silver(I) complexes with pyridine-based macrocyclic type of ligand against clinically relevant species. [**Oral presentation**]. **71st Annual Meeting of the International Society of Electrochemistry held in Belgrade, Serbia.** 31 Aug-1 Sep 2020.

Chapter One: Introduction

1.1 Background of study and problem statements

Microbiology involves the study of tiny living cells (usually less than about one millimeter in diameter, e.g., bacteria, fungi, yeasts, viruses, archaea etc.), and electrochemistry is a field of study that deals with the relation of electrical activity to chemical changes. Consequently, the term microbial electrochemistry can be described as an interdisciplinary field that combines the concepts and techniques of microbiology and electrochemistry to create a versatile toolbox for both fundamental and applied research. It is a subfield of bioelectrochemistry that, *ab initio*, was considered a basic scientific discipline borne out of curiosity, and focuses on microbe-electrode interactions and their applications (Schröder et al., 2015). Nevertheless, the developments in this area of research have since resulted in diverse electrochemical technologies in which microbial cells are employed, solely or as supporting materials, for bioproduction/biosynthesis, biodegradation/bioremediation, waste treatment, biosensing etc. (Czerwińska-Główka & Krukiewicz, 2020; Sánchez et al., 2020). The field has continued to evolve, with diverse interfaces yet unexplored, or underexplored as in the case of its emerging applications in clinical and biomedical settings, with great potential for actual biosensing devices.

Biofilms are an aggregate of microbial cells formed as micro-structured communities on solid surfaces and surrounded with self-produced polymeric matrix within which growth and other metabolic processes take place (Flemming et al., 2016). The confirmation of the existence of electric currents in microbial biofilms led to the concept of applying electrochemical methods for biofilm detection and analysis. Historically, more than a century ago, a scientist named Michael Cressé Potter was the first to report that microbial activity and metabolism, particularly physiological processes that involve the use and/or transformation of chemical compounds (e.g., breakdown of nutrients/organic compounds like glucose) is associated with the release and/or expression of electrical activity in the form of electrical current/energy. This observation was believed to have originated from his interest and knowledge of the unique physiological ability of microorganisms to generate and release electrons during utilization of any kind of organic compound in their

quest for cellular energy, and that, some sort of electrical energy is also released during these processes. To confirm his curiosity, the fermentative activity of microbial cells was investigated. Specifically, culture of yeast cells and certain bacterial cells were grown in a glucose-rich nutrient medium while the electrical activity was estimated with a galvanic cell with platinum electrodes, which produced an electrical potential of 0.3 and 0.5 V (Potter, 1911). This fascinating phenomenon of microbe-electrode interactions is the basis of electroanalytical techniques and technologies and has since witnessed a tremendous advancement, sophistication, and applications in industrial, environmental, biomedical and clinical settings (Czerwińska-Główka & Krukiewicz, 2020).

Moreover, as electric current is simply electrons in an ordered motion, and since electrons are continually generated via metabolic processes involving oxidation-reduction reactions and transported mostly through the electron transport chain (ETC) within the cytoplasmic matrix and/or to the outside cell via extracellular electron transfer mechanisms, the rate of this transfer is mostly a function of biofilm formation, growth, and metabolic activity of the microbial cells (Masi et al., 2015; Prindle et al., 2015; Schofield et al., 2020). There are also new proofs that support the correlation between pathogenicity and electroactivity of microbial biofilms (Astorga et al., 2019). Therefore, extracellular respiration rate measured as EET in microorganisms is now being considered as a suitable parameter for the determination of the metabolic state and activity of the microbial cells rather than the conventional cell growth measurement (Hassan & Bilitewski, 2013).

The current methodologies and chemical methods routinely employed in the analysis of microbial biofilms and evaluation of the effectiveness of anti-biofilm compounds are mostly insensitive, not-standardized, expensive, requires high technical knowledge and/or time-consuming (Ernst, 2007; Lass-Flörl et al., 2010; Sanguinetti & Posteraro, 2018). The need, therefore, for a more sensitive diagnostic tool and technique for rapid analysis and characterization of microbial biofilms, and evaluation of their sensitivity and/or resistance to therapeutic compounds cannot be overemphasized.

In most microorganisms, the respiratory system is embedded in the cytoplasmic matrix where largest percentage of the available oxygen is used up as terminal electron acceptor

in the ETC. Hence, monitoring and estimating the electron transport to oxygen or another electron acceptor of similar physicochemical properties is a direct reflection of the microbial respiration and their cellular activity. This is more adaptable to biofilms as their electron transport can easily be intercepted on the solid surface (electrodes, as in the case of laboratory conditions) upon which their cells are growing. In the same context, since the definitive effect of any antibiotic/antimicrobial is to either kill, remove/disperse, or significantly inhibit growth, their activity can be inferred from the respiratory process rate and change with time following antibiotic/antimicrobial application. Furthermore, while bacterial growth is a slow process (i.e., the generation time of model microorganism is in the range of hours) and is often impossible under defined laboratory conditions, respiration is a much faster process, thus respiration-based assays of antibiotic/antimicrobial activity are much faster and do not depend on the growth rate of the microorganisms. Hence, this phenomenon can be implicated as a diagnostic tool for a fast and sensitive analysis of microbial biofilms either in the presence or absence of antimicrobial treatment (Prévoteau & Rabaey, 2017). Therefore, electrochemical-based techniques appear to be useful and efficient to complement and/or replace the existing conventional methods of analysis of microbial biofilms, and assessment of antibiofilm efficacy (Czerwińska-Główka & Krukiewicz, 2020).

Additionally, more than 80 % of microbial infections is caused by biofilms, and this remain the major cause of high hospitalization and death rates owing to therapeutic failure and occurrence of antimicrobial resistance (Van Dijck et al., 2018). Interestingly, despite the diversity of microbial pathogens, most healthcare-associated infections are initiated by only a few opportunistic pathogens (e.g., *Pseudomonas aeruginosa*, *Staphylococcus aureus*, *Acinetobacter baumannii*, *Candida* spp etc.), with inherent biofilm-forming ability and extensive antibiotic/antimicrobial resistance (Simoska et al., 2019). Unfortunately, their rapid detection and real-time monitoring remain a practical challenge of worthy relevance, especially in achieving effective antimicrobial treatment options.

Although the development of effective antimicrobial drugs/treatments remains the main goal in the medical research community, the design and development, and implementation of biosensing platforms for detection and monitoring of early biofilm formation signatures,

coupled with real-time assessment of drug efficacy is equally paramount. In the past, various approaches including the conventional culturing, straining, and counting methods, molecular methods, microscopy-based and mass spectrometry techniques, have been adopted. While a few of them are sensitive, these procedures are mostly costly, difficult to perform and execute, mostly qualitative, and are generally destructive for the object of study (Huang et al., 2020; Meireles et al., 2015). The way out, therefore, is to develop a fast and sensitive platform with a real-time measurement feature for microbial biofilms analysis and assessment of their drug susceptibility profile.

Microbial electrochemical systems (MES) are simple, relatively easy to setup, use and implement, and are based on the ability of naturally- or artificially induced electrochemically active microorganisms to generate/consume and transfer to/from polarized electrodes. While cathodic MES (i.e., those in which electrons are transferred from the electrode to the biofilm) are relevant to bioelectrosynthesis and electrochemical fermentation, the anodic MES (i.e., those in which electrons are transferred from the biofilm to the electrode) are more relevant to the development of biofilm sensors and antibiotic/antimicrobial assay. Thus, in the following, the discussion will be limited to anodic MES.

The oxidation current rate and density obtained from the microbe-electrode interactions in anodic MES is directly correlated to the metabolic state of the organisms (Uria et al., 2020). The use of exogenous redox mediator in MES has been well documented as an efficient means of increasing the measurement range and current density because it mediates and facilitates extracellular electron transfer in weak electrogenic microorganisms (Martinez & Alvarez, 2018a) as would be the case of the two microbial biofilms under study in this thesis – *C. albicans* (a dimorphic fungus) and *A. baumannii* (a bacterium). Our choice of ferricyanide as exogenous redox mediator for *C. albicans* is based on its high solubility in water and low toxicity potential to microbial cells (Bharatula et al., 2019; Congdon et al., 2013; Uria et al., 2020), while - hydroxy-1,4-naphthoquinone (2-HNQ) was adopted for *A. baumannii* due its biocompatibility property (Astorga et al., 2020; Santoro et al., 2016).

Furthermore, a two- or three-electrode system is the conventional set-up that is commonly adopted for electroanalysis of microbial biofilms (Babauta et al., 2012; Besant et al., 2015; Bimakr et al., 2018; Lv et al., 2014; Sá et al., 2020). It consists of a working electrode (WE) where the biofilm attachment and growth take place, the counter/auxiliary electrode (CE) to maintain charge balance, and the reference electrode (RE) (Aiyer & Doyle, 2021). Each electrode is acquired/made/fabricated and processed/cleaned separately, thus, contributing to high cost and tediousness.

In recent years, however, there has been a growing interest in the application of Screen-Printed Electrodes (SPEs) as disposable, portable, simple-to-use, low cost, and highly sensitive biosensing device for analysis, detection, and characterization of different microbial pathogens. In addition, SPEs offer advantages such as mild cleaning/processing, versatility and amenability for specific and/or extensive modifications (Alonso-Lomillo et al., 2010). Also, the need for a more rapid diagnosis that allows real-time *in situ* drug susceptibility profiling has further made the use of SPEs a tool of first choice (Munteanu et al., 2018). Nevertheless, the electroanalysis of *C. albicans* and *A. baumannii* biofilms, in addition to evaluation of anti-biofilm activity of clinically relevant antimicrobial drugs using commercial SPE as a diagnostic tool is yet to be investigated.

1.2 Hypothesis

Electrochemical techniques could provide real-time information on the physiology and growth kinetics (Bressel et al., 2003; Marsili et al., 2010), interfacial and/or extracellular electron transfer (respiratory mechanisms) (Carmona-Martínez et al., 2013; Qiao et al., 2017) of microbial biofilm as a function of their attachment, growth on suitable surfaces, either in the presence or absence of antimicrobial treatment. The technique has been successfully applied to a variety of clinical bacterial pathogens such as *S. epidermidis, S. aureus, E. coli, Neisseria gonorrheae, P. aeruginosa, Listeria monocytogenes, Salmonella typhimurium, Aeromonas hydrophilia* (Simoska & Stevenson, 2019), and fungal/yeast pathogens (e.g., *Saccharomyces cerevisiae*) (Arthur et al., 2019; Soley et al., 2005), and also for detection of antimicrobial compounds (Munteanu et al., 2018). Thus, the method continues to attract attention for other applications due to its real-time feature, simplicity,

low cost, rapidness, portability, sensitivity, versatility in medical, food and water, and environmental applications, and its promising potential to improve clinical diagnosis. Upon these bases, we hypothesized that *C. albicans* and *A. baumannii* biofilms, in the presence of ferricyanide and hydroxyquinone, respectively, can be used to monitor their biofilm formation and estimate the effect of selected antimicrobial drugs/compounds.

1.3 Justification of study

While there is dearth of information on the electrochemistry of the two microbial biofilms of choice in this thesis - *C. albicans* (a dimorphic fungus) and *A. baumannii* (a bacterium), it is important to emphasize that existing literatures on electroanalysis of most microbial pathogens were reported using the conventional two- or three-electrode system which is complex and difficult to set-up and/or manage, and expensive relative to the simple, portable, and cheap screen-printed electrodes.

Fungal infections, largely potentiated by members of the genus *Candida*, account for about 1.7 million deaths per year and this continues to pose a huge challenge to the global health with its increasing morbidity and mortality rates as well as the devastating socio-economic impacts (Kainz et al., 2020). In a similar context, *A. baumannii* has been categorized by the World Health Organization as a priority one pathogen with an urgent need of new treatment options (WHO, 2017), and by the center for disease control and prevention (CDC) as among pathogens that pose imminent threat to human and public health (CDC, 2019), owing to its very high prevalence, morbidity and mortality rates, and high antibiotic resistance in clinical settings (Kamurai et al., 2020).

Therefore, the electroanalysis of these biofilms and electroanalytic evaluation of anti-biofilm activity of clinically relevant drugs using the cheap and commercially available SPEs as a diagnostic tool is worthy of investigation.

1.4 Aim and specific objective

The aim of this thesis is to develop an electrochemical-based platform for assessment of drug efficacy against clinically relevant microbial biofilms.

To achieve this aim, the following specific objectives were formulated:

1. To evaluate the antimicrobial/antibiofilm efficacy of newly synthesized drug candidates against selected clinically relevant microbial species via electroanalysis.
2. To develop an electroanalytic methodology for antibiofilm drug testing against *Candida* biofilms.
3. To evaluate selected azole fungicide via electroanalysis for their antibiofilm potential against antibiotic-resistant *A. baumannii* biofilm (drug repurposing strategy).
4. To develop an electroanalytic methodology for detection and characterization of *C. albicans* biofilm in urine sample.

1.5 Structure/overview of the thesis

Chapter one introduces the key elements of the thesis topic. It provides background information on electrochemistry and microbiology as independent disciplines, and how the former could be adopted as a tool to better the study and understanding of the latter. Also, the inter-relatedness and how these two disciplines evolved into what is today referred to as microbial electrochemistry or electromicrobiology is highlighted. The study hypothesis, problem statements and study justification are all described in this chapter.

In chapter two, extensive but cogent and up-to-date review of existing literatures on microbial electroanalysis is presented. This includes the historical perspective, current studies, and future outlook of the subject under discussion. The state of electrochemical techniques in reference to their applications in most spheres of science; the challenges with existing methodologies commonly adopted for microbial analysis and drug testing; the gaps in knowledge on bioelectrochemical studies of clinically relevant microbial species, and how to bridge these gaps are all presented in this chapter.

In chapter three, a first report on electrochemical-based evaluation of newly synthesized drug candidate (kindly provided by Dr Jasmina Nikodinovic-Runic of Institute of Molecular Genetics and Genetic Engineering, University of Belgrade, Belgrade, Serbia) is presented. This provided the motivation for subsequent studies and optimization of our methodology.

Chapter 4 is focused on electroanalysis of *C. albicans* biofilm. Specifically, attempts were made to compare the gold standard culture-dependent technique with our electroanalytic platform. We also investigated and compare these two approaches for antifungal testing.

Based on our knowledge on the menace and public-health challenges of antimicrobial resistance (as established in chapter two), we explored the emerging drug repurposing strategy and evaluated clinically relevant antifungal drugs against a model resistant bacterium. Both conventional and our bioelectrochemical methodologies were employed. The remarkable results obtained from this study are presented in chapter 5.

The possible application of our bioelectrochemical platform for detection of microbial pathogens in clinical samples is presented in chapter 6. *C. albicans* as in index organism of candiduria used, while human urine samples collected from healthy individual was employed.

Finally, in chapter seven, I provide some concluding remarks and suggestions for future research as I envisage a build-up on the findings reported in this thesis.

1.6 Candidate's contribution and extent of collaboration

This thesis is a product of my work – conceptualization of ideas; experimental investigation; data collection, analysis, and curation; writing: original draft and writing: review, editing and formatting. The microbial isolates and two of the drug compounds used in this thesis were provided by our collaborators, and described in detail in the corresponding sections, where applicable. The thesis was supported through the Abay Kunanbayev scholarship award and funded by Faculty Development Competitive Research Grant Program (Grant number: 110119FD4537), School of Engineering and Digital Sciences, Nazarbayev University, and by the Collaborative Research Program 021220CRP0522, Nazarbayev University, Kazakhstan. All aspects of this thesis have been reviewed by the supervisory team.

Chapter Two: Literature review

2.0 Microbial biofilms: what they are and their relevance

Different definitions of microbial biofilm are available in the literature. Nevertheless, three distinctive elements are often central to these definitions, and these include: (1) the microorganism; (2) a suitable surface, and (3) an extracellular polymeric matrix or what could be simply described as 'cement' (Winkelströter et al., 2014).

Just as microorganisms are ubiquitous, some are inherently capable of colonizing all kinds of surfaces, whether biotic or abiotic; smooth or rough; large or small etc. (Ghosh et al., 2020). This property is what confers the morphological appearance of a micro-structured arrangement of cells called biofilm. Microbial biofilms are generally highly organized, comprising sessile and irreversibly attached, heterogenous communities of prokaryotic (bacteria) and/or eukaryotic (fungi/yeast) cells enclosed in a matrix made from biomaterials secreted by members of the microbial community (Aliane & Meliani, 2021).

The formation of biofilm is a multistep process (Figure 2.1) that always begin with initial attachment of cells to a suitable surface, followed with proliferation and subsequent synthesis and accumulation of polymeric extracellular matrix consisting of molecules/compounds (e.g., proteins, lipids, polysaccharides and nucleic acids) in varying proportions (Achinas et al., 2019; Ghosh et al., 2020), and may sometimes include other molecules such as those involved in cellular communications (Chen et al., 2019; Czerwińska-Główka & Krukiewicz, 2020; VanArsdale et al., 2020; Whited & Levin, 2019). The formation cycle also involves maturation of the biofilm architecture cells and detachment or dispersal of cells leading to recurrent biofilm growth cycles (Meireles et al., 2015).

Microbial biofilms provide an array of morphological and physiological functions to the cells that constitute the biofilm community. The most significant of it all is the protection it offers against several physical and chemical environmental attacks including antimicrobial treatments, probably due to its high resistance and tolerance ability (Babapour et al., 2016; Richter et al., 2017; Shenkutie et al., 2020). Consequently, biofilm-forming microbes are considered the most difficult to control/manage of all known human

microbial infections. This is primarily because biofilm-associated infections are typified by the morphogenesis of biofilm on/in human tissues and organs or even on medical implants/devices, thus, making these infections more complex and complicated to manage (Cepas et al., 2019a; Malott et al., 2014; Mathur et al., 2018). In addition, the structural arrangement of the biofilm also enables the constituent microbial species to acquire and adapt new virulence and pathogenic properties including antimicrobial resistance genes (Kumar et al., 2021; Limoli et al., 2015; Zhu et al., 2019).

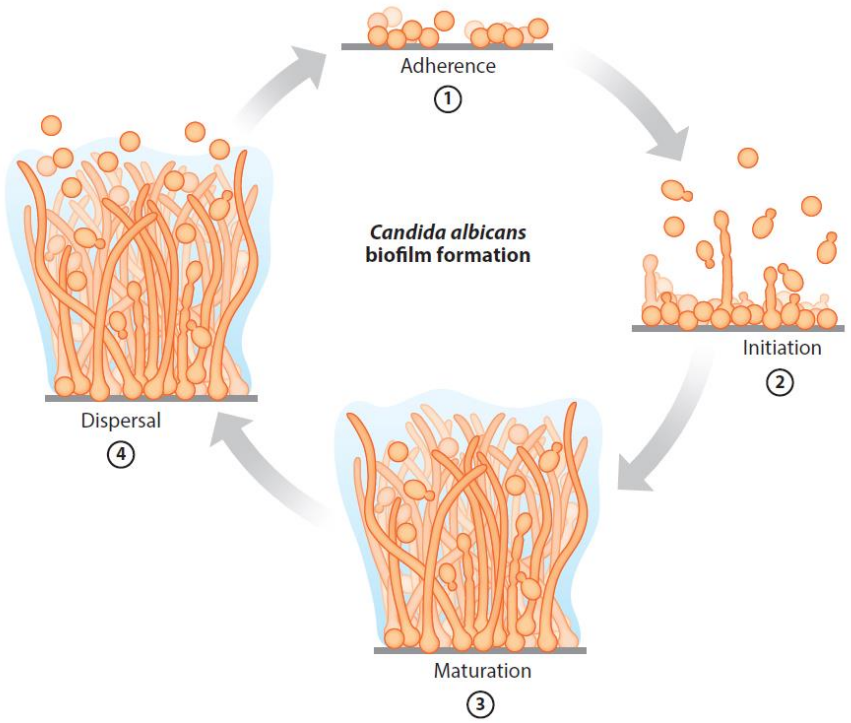

Fig. 2.1: Sequential phases of *Candida albicans* biofilm formation (Nobile & Johnson, 2015). This schematic representation is similar to biofilm formation and development stages in most microbial biofilms.

Antimicrobial resistance has become a global; rapidly emerging public health challenge, with debilitating socio-economic impacts, and a projected mortality rate of ten million deaths by the year 2050 (Aslam et al., 2018; Miró-Canturri et al., 2019). Biofilm-forming microbial species are enclosed in a structural matrix that delimits the diffusion of drugs, thus, making the cells either resistant or more tolerant to antimicrobial agents and also to the host immune soldiers (Abebe, 2020). Antimicrobial-resistant microbes are prevalent in biofilm form and are now considered a primary agent in the etiology of chronic infections

(Bowler, 2018). Presently, it is estimated that about 80% of microbial infectious diseases in humans are caused by biofilm microbes. Unfortunately, conventional antimicrobial medications are becoming less- or ineffective (Li & Lee, 2017). This problem is complicated, among other factors, by biofilm formation which provides survival and tolerance strategy to the microbial pathogens.

Among antimicrobial-resistant microbes, ESKAPE bacterial pathogens that include *Enterococcus faecium, Staphylococcus aureus, Klebsiella pneumoniae, Acinetobacter baumannii, Pseudomonas aeruginosa* and *Enterobacter* spp, and *Candida* yeasts are responsible for most clinical infections with alarming mortality and morbidity rates (Kainz et al., 2020; Wang et al., 2020). The consensus strategy to mitigating this challenge has been identified as early and rapid diagnosis in addition to effective antimicrobial therapy.

Unfortunately, existing diagnostic approaches (as would be discussed in subsequent paragraphs) are characterized with one limitation or the other, thus, negatively impacting the therapeutic outcome. Therefore, the design/development, promotion, and adoption of new rapid diagnostic platforms to reduce the duration of microbial diagnosis which would in turn minimize, drastically, the nonempirical use of antimicrobial drugs, is in high demand (Davenport et al., 2017; Dincer et al., 2019; Goeres et al., 2019; Holm et al., 2017; Islam et al., 2020; Karbelkar & Furst, 2020). In addition, the search for new antimicrobial therapeutic options to manage antimicrobial-resistant pathogens, through bioprospecting of new and novel compounds or repurposing of old, existing clinically viable drugs has also become very exigent (Cepas et al., 2019b; Frassinetti et al., 2020; Konreddy et al., 2018; Uchil et al., 2014).

Therefore, with utmost consideration of clinical relevance, public health impact, and most importantly, the dearth of information in the literature on the electrochemical-based analysis and anti-biofilm assessment of antimicrobial compounds, this thesis is focused on *A. baumannii* and *C. albicans* biofilms. The former is a bacterium and a classical ESKAPE pathogen, while the latter is a yeast and a unique fungal pathogen.

2.1 *Candida* biofilms

For several reasons including but not limited to immunosuppression in the elderly, cancer and organ transplant patients, the global incidence of fungal associated infections is on the rise (Lockhart & Guarner, 2019). Interestingly, *Candida* spp are considered the most frequently encountered among known etiological agents of fungal/microbial infections, and in general, ranked top, even higher than *Staphylococcus aureus* and *Pseudomonas aeru*ginosa (de Barros et al., 2020). In this thesis, however, the biofilm formation, pathology, clinical significance, detection and antibiofilm testing methods of *Candida* biofilms is discussed, with a focus on *C. albicans* – a yeast known for its public health and socio-economic impacts.

2.1.1 *C. albicans* biofilms

C. albicans is part of the normal, naturally existing microbiota, found asymptomatically on different niches of humans including the skin, nasal and oral cavities, other mucosal surfaces, gastrointestinal and urinogenital tracts. It is one of the few fungal species that are pathogenic in humans and could cause diseases ranging from superficial mucosal and dermal infections (e.g., thrush, vaginal yeast infections, and diaper rash), to severe candidiasis (Dadar et al., 2018; Soll & Daniels, 2016).

In healthy individuals, *C. albicans* coexists mutually with other species of the local microbiota, and thus remain safe and non-pathogenic (Nobile & Johnson, 2015). Nevertheless, perturbations of the host microbiota (e.g., due to poor hygiene practices, abuse, or misuse of antibiotics), or the host immune system (e.g., during illness due to stress or infection by another pathogen, or during chemo- and/or other immunosuppressant therapy), or alterations in the local environment (e.g., changes in temperature, pH, or humidity) can lead to excessive growth of *C. albicans,* thereby causing infection. These infections could be potentially complicated in individuals with compromised immune system (e.g., those living with cancer, HIV/AIDS, or transplanted organs) and individual with implanted medical devices. The mortality rate is almost 40% in some cases (Gulati & Nobile, 2016).

One unique virulence property of *C. albicans* is its ability to form well-structured biofilms made up of different cell types including budding yeast-form cells, hyphal and pseudo-hyphal cells, all embedded in a polymeric extracellular matrix (Polke et al., 2015). They can exhibit this property on both biotic (e.g., tissues and organs) and abiotic surfaces (e.g., implanted medical device such as catheters, dentures, pacemakers, contact lenses, mechanical heart valves, and joint prostheses) (Tuddenham & Sears, 2015). Once the biofilm is fully formed, they become highly resistant to physical and chemical agents, with a potential to birth systemic and invasive infections with a consequent menacing health and socio-economic impacts (Gulati et al., 2018).

For instance, an estimated 100,000 deaths from *Candida*-related infections, and 6.5 billion USD in excess expenditure of treatment and management costs are recorded annually in the United States only. Furthermore, due to the high resistance of fungal biofilms to current antifungal therapies, high doses of antifungal drugs and/or frequent removal/change of the colonized medical implants are commonly adopted in the treatment/management of infections (Nobile & Johnson, 2015). While high drug doses could cause physiological/hematological shock and severe and irreversible damage to vital internal organs (e.g., kidney and liver), removal of some implants (e.g., artificial heart valves) is expensive and, in some cases, difficult. Thus, early diagnosis and prompt administration of effective antifungal therapy remains highly exigent.

2.2 Biofilm formation processes in *Candida* spp

As with other microbial biofilms, the formation and development of *C. albicans* biofilms is complex and multifaceted. Regardless, four distinct phases can be recognized (Figure 2.1):

(1) Adherence: young and active yeast cells attach to a suitable surface.

(2) Initiation: the attached cells undergo multiple divisions and secretion of essential molecules to form a conspicuous entity.

(3) Maturation: where cells proliferate and differentiate into varying cell types: hyphae, pseudo-hyphae, and yeast-form cells, all enclosed in a matrix, and

(4) Dispersion: progeny cells are released from the mature biofilm for colonization of other surfaces.

The time course for *C. albicans* biofilm formation is lengthy as the process proceeds via early, intermediate, and mature developmental phases. The early phase may require about 11 h to take place, resulting in the formation of conspicuous colonies; the intermediate phase may require approximately 12–30 h, as it involves the synthesis of the extracellular matrix materials, while maturation may require 38-72 h as it involves the development of an organized network of densely packed thick layer of matrix consisting of yeast and hyphal cells (Cavalheiro & Teixeira, 2018; Mukherjee & Chandra, 2004). Maturation phase is mostly followed by dispersal and release of the young cells for further propagation of infection and colonization of other ecological/body niches.

One observation worthy of emphasis is that most studies on *C. albicans* biofilm formation were done *in vitro*. Nevertheless, a good correlation between *in vitro* and *in vivo* studies has been recorded as both study models follow a comparable time-dependent pattern in formation and exhibit a high degree of similarity in their architecture (Gulati and Nobile, 2016).

2.3 Biofilm formation and antifungal resistance in *Candida albicans*: the nexus and clinical implications

In general, drug resistance is said to have occurred when a drug known to be effective against a particular microbial pathogen gradually or suddenly becomes less effective or ineffective. This phenomenon can be described either as microbiological or clinical. Microbiological resistance occurs when a microbial pathogen is insensitive to an antimicrobial agent when contrasted with other isolates of the same species as evaluated by *in vitro* sensitivity testing. This can be further grouped as innate or acquired resistance. While innate resistance occurs naturally among a few microbial species without any known cause, acquired resistance often develop gradually in susceptible microbial strains following prior drug exposure and/or gene mutations.

On the other hand, resistance may be said to be clinical when a microbial infection persists despite treatment with what is considered to be effective antimicrobial therapy. Interestingly, microbiological resistance may promote the occurrence of clinical resistance, however, other factors such as biofilm forming capacity of the etiological pathogen, underlying diseases (e.g., cancer, HIV/AIDS), compromised host immune functions etc. may also be predisposing factors (Maurizio Sanguinetti et al., 2015).

Furthermore, in contrast to the multiplicity of classes and diverse distinctive modes of activity of antibacterial drugs, existing antifungal drugs are limited in spectrum and availability, partly due to the fact that fungi, just like their human hosts, are eukaryotic, and so toxicity is always a bottleneck during antifungal drug design and development (Prasad et al., 2016; Tsui et al., 2016). Consequently, there are four antifungal classes (namely, nucleoside analogs, echinocandins, polyenes and azoles) available and clinically recognized for the treatment and management of fungal infections (Gulati et al., 2017; Gulati & Nobile, 2016). Nucleoside analogs (e.g., flucytosine) are not antifungal drugs per say but could intrinsically disrupt nucleic acid synthesis in fungal cells while mimicking any of the nucleosides, eventually leading to cell cycle arrest and cell death. Therefore, it is safe to conclude that only three classes of antifungal drugs are known. Azoles and polyenes were presented in the 1900s while echinocandins were approved for clinical use in the early 2000s (Kim et al., 2020).

Azoles (e.g., miconazole, clotrimazole, fluconazole etc.), are the most important and the most researched antifungal drugs with the highest number of lead candidates in clinical trial, and consequently the most prescribed class of antifungal drugs in clinical practice. They exhibit their antifungal activity through inhibition of ergosterol biosynthesis. Similarly, polyenes (e.g., nystatin, amphotericin B etc.), are a broad spectrum antifungal drug with high binding affinity to ergosterol, a prevalent steroid molecule in the fungal cell wall and membrane, thereby causing depolarization and increased permeability of ions (K^+ and Na^+), resulting in leakage and ultimately cell death. Also, echinocandins (e.g., caspofungin), are a class of fungicidal drug effective against most *Candida* species through inhibition of β-1,3-glucan synthase enzyme, an essential precursor constituent in fungal cell walls synthesis (Campoy & Adrio, 2017; Shafiei et al., 2020).

Additionally, the strong resistance to antifungal drugs frequently encountered in *C. albicans* is mostly associated to their biofilm mode of growth. The azoles, for instance, are no longer effective against *C. albicans* biofilms as evident in the work of Melo et al. (2011). Similarly, in a study conducted by Hawser and Douglas, approximately five-fold increase in resistance to most antifungal drugs was observed by *C. albicans* biofilms relative to their planktonic cells after 48 h of exposure (Hawser & Douglas, 1995). These results highlight how problematic these infections portend in terms of management, and hence, the urgent need for the development effective therapies against the biofilm cells (Cavalheiro & Teixeira, 2018).

In addition to high morbidity and mortality rates associated with resistant *Candida* infections, other clinical consequence of antifungal drug resistance may include failure of therapeutic management, poor treatment outcome, development of breakthrough infection in patients receiving antifungal prophylaxis, increased treatment costs, prolonged hospitalization periods, among many others (Maurizio Sanguinetti et al., 2015). It is therefore evident from the foregoing that antifungal therapeutic options are not only limited in number but also in efficacy. Consequently, incidences of antifungal resistance among fungal pathogens are imminent and unavoidable, and this make fungal diseases a human health problem of global proportion (Campoy & Adrio, 2017). In general, nevertheless, early detection of drug-resistant microbial pathogens remains a top priority to achieving excellent treatment and patient outcomes.

2.4 Mechanism(s) of antifungal resistance in *C. albicans* biofilm

Biofilm formation plays a central in antifungal resistance of *C. albicans*. However, there is more to it than just biofilm development. Factors and conditions leading to and/or contributing to antifungal resistance in *C. albicans* biofilm are complex and multifaceted. The metabolic state of the biofilm cells, activation of efflux pumps and enzymes, the physical barriers created by the presence of extracellular matrix and, also the membrane sterol compositions all play a role, either independently or in combination (Gómez-Gaviria & Mora-Montes, 2020; Seneviratne et al., 2008; Tsui et al., 2016; Wilson, 2019).

2.4.1 Extracellular matrix

Extracellular matrix offers physical barrier to permeability of antifungal drugs in addition to contributing to the general morphological sanctity of the biofilm structure. The chemical composition of the matrix makes these roles functionally possible. For instance, the *C. albicans* biofilm matrix is largely made up of 55% proteins and glycoproteins, 25% carbohydrates, 15% lipids, and 5% nucleic acids (chiefly extracellular DNA). Also, more than 500 enzymatically active proteins have been identified to be free-flowing in the matrix (Zarnowski et al., 2014). In addition, polysaccharides consisting largely of mannan-glucan complexes, particularly β-1,6-glucan have been empirically shown to contribute to drug resistance. For example, in a study by Nett and colleagues, it was established that β-1,3-glucan in the matrix binds to amphotericin B (Amb) and fluconazole (Flz), thus limiting their penetration into the cells, while in its absence, penetration was optimal with enhanced susceptibility spectrum (Nett et al., 2007).

2.4.2 Efflux pump

Membrane-bound drug efflux pumps have been linked to antifungal resistance in *C. albicans*. However, unlike in their planktonic counterpart where these efflux pumps are activated only in response to the presence of an antifungal drug, in biofilm state, they are activated throughout the biofilm developmental phases, whether an antifungal drug is present or not. This automatic activation of efflux pumps in *C. albicans* biofilms therefore play a definitive role in antifungal resistance (Gulati & Nobile, 2016; Nobile & Johnson, 2015). Similarly, modulations in membrane sterol compositions during biofilm formation and proliferation phases has also been correlated to antifungal resistance in *Candida* spp including *C. albicans* biofilms, with exacerbated resistance during the maturation phase (Cavalheiro & Teixeira, 2018; Mukherjee & Chandra, 2004).

2.4.3 Physiological state of biofilm

The plasticity of *C. albicans* biofilms and the metabolic state of biofilm cells is another important factor responsible for sensitivity and/or resistance to antifungal drugs (Soll & Daniels, 2016). For instance, in the early biofilm growth phase of *C. albicans* on synthetic resin strips, the minimum inhibitory concentrations (MICs) of Amb and Flz were determined as 0.5 and 1 μg/mL, respectively. Surprisingly, after 72 h of biofilm growth,

MICs had significantly increased to 8 and 128 μg/mL for of Amb and Flz, respectively (Cavalheiro & Teixeira, 2018; Chandra et al., 2001).

This finding suggests two fundamental things; (1) that the older the biofilm, the more resistant it becomes; and (2) that early and rapid detection is central to solving the antifungal resistance problem in *C. albicans* biofilms. In addition, the presence of persister cells – metabolically dormant cells, within *C. albicans* biofilms is also a critical physiological factor worthy of note. Owing to their dormancy and non-dividing properties, they exhibit a very extreme level of tolerance/resistance to antimicrobial drugs (Cavalheiro & Teixeira, 2018; LaFleur et al., 2006).

2..5 *Acinetobacter baumannii* biofilms

2.5.1 *Acinetobacter baumannii* biofilms: clinical relevance and antibiotic resistance phenomenon

A. baumannii is a Gram-negative, major opportunistic pathogenic bacterium commonly found in various environmental niches including soil, water, hospital environment, human skin, bloodstream, and gastro-urogenital tract (Whiteway et al., 2022). Those of environmental origin habitually harbor antimicrobial resistance elements and may thus serve as major reservoirs for resistance factors that transmute into clinically relevant strains (Wong et al., 2017). This implicated in various infections, including respiratory pneumonia, skin and soft tissue infections, nosocomial meningitis, and even urinary tract infections (Madadi-Goli et al., 2017; Nocera et al., 2021; Vázquez-López et al., 2020).

A. baumannii was previously referred to as ‘iraqibacter’ because of its prevalence among the US veterans and soldiers that participated in the wars in Iraq and Afghanistan (Eze et al., 2018; Lee et al., 2017). Afterwards, it became a huge concern in clinical practice across the globe due to its unusual and remarkably heightened resistance to almost all known antimicrobials and host immunological responses. Consequently, existing therapeutic options against *A. baumannii* infections became ineffective, making the pathogen one of the most dreaded in medical practice (Almaghrabi et al., 2018; Gonzalez-Villoria & Valverde-Garduno, 2016; Rao et al., 2020; Vázquez-López et al., 2020).

Several phenotypic- and genomic-based virulence properties of *A. baumannii* have been described, including possession of reduced membrane porins and, capsular and lipo-polysaccharides to delimit diffusion of antibiotics into the cell, metal chelating systems, versatile enzyme (e.g., phospholipases and proteases) and protein secretion systems. Similarly, diverse resistance mechanisms such as membrane modification, enzymatic lysis of antibiotics and activation of multi-drug efflux pumps, have been identified and explicitly described in the literature (Kurihara et al., 2020; Kyriakidis et al., 2021; Lee et al., 2017; Monem et al., 2020; Moubareck & Halat, 2020; Sarshar et al., 2021; Vázquez-López et al., 2020).

The ability to form biofilm form is a strong virulence for *A. baumannii*, which contributes to its adaptation, tolerance, and survival strategies under harsh conditions such as antibiotics treatments (Bowler, 2018; Eze et al., 2018; Shenkutie et al., 2020). In fact, studies have established that a significant correlation between biofilm formation and antibiotic resistance exist in *A. baumannii* (Babapour et al., 2016; Yang et al., 2019).

Furthermore, *A. baumannii* is one of the few known microbial pathogens that have been designated as not only a multidrug-resistant (MDR) and extreme/extensive drug-resistant (XDR) but also as pan drug-resistant (PDR) because of its unconventional frequency of resistance to all known and existing antibiotics including fluoroquinolones, aminoglycosides, carbapenem and polymyxins (Moubareck & Halat, 2020; Shenkutie et al., 2020). It was on this basis that the Center for Disease Control and Prevention (CDC) and World Health Organization (WHO) declared *A. baumannii* as an ‘emergency’, top priority class 1 pathogen, posing imminent risk and danger to human and public health, and to which new therapeutic options are required (CDC, 2019; WHO, 2017).

Another related challenge, complicating the diagnosis and managements of *A. baumannii* infections is the delay clinicians often experience while waiting for the antimicrobial susceptibility assay results, as this is principal to making therapeutic decisions (Wang et al., 2020). The gold standard methods of broth microdilution and agar diffusion and their commercial prototypes (e.g., Vitek-2) for *in vitro* determination of MICs are flawed with time and resource constraints (Almaghrabi et al., 2018; Babapour et al., 2016; Madadi-Goli et al., 2017; Perez et al., 2007; Pulido et al., 2013; Qi et al., 2016). This further strengthens

the need, not just for new therapeutic options, but also for rapid and low-cost testing platforms.

2.5.2 Treatment options for *Acinetobacter baumannii* biofilms: current status and future perspective

While the development and spread of resistance mechanisms to existing clinically relevant antibiotics, including those meant to be the last resorts, remain unabated, recent studies have revealed the rising severity of *A. baumannii* infections and the consequent high morbidity and mortality rates (D'Onofrio et al., 2020; Dahdouh et al., 2017). Due to the evident limitations of single-antibiotic therapy (monotherapy), combination therapy that involves joint administration of two or more antibiotics was initially adopted as an alternative to improve treatment results (Wang et al., 2020; Wong et al., 2017). A combination of colistin and tigecycline (Peck et al., 2012), colistin and rifampicin (Aydemir et al., 2013), minocycline and tigecycline (Castanheira et al., 2014), levofloxacin, ampicillin-sulbactam and tigecycline (Madadi-Goli et al., 2017), among many others, with successful clinical outcomes have been described in the literature. Nonetheless, a significant limitation of this approach in the long term, is the inevitable development of resistance to each antibiotic that constitute the combined therapy, due to selective pressure (Davies, 1996; Vrancianu et al., 2020).

It is worthy to note that no new antibiotic has been produced in the last decade as most pharmaceutical industries have slowed down or discontinued new antimicrobial discovery programs, citing high cost of investment, slow pace of drug making (approximately 20 years for a drug to become marketable) and low profit returns (Kaul et al., 2019) as reasons for their decision, thus making WHO to declare a 'post-antibiotic era' and the urgent need for the research community to make a paradigm shift and develop non-antibiotic strategies (Kumar et al., 2021; Miró-Canturri et al., 2019; Peyclit et al., 2019; Richter et al., 2017).

Another source of worry is the recent statistics that indicate that by the year 2050, about 444 million people would be affected by antibiotic-resistant infections (Aslam et al., 2018) with a minimum of about 300 million deaths (Rangel-Vega et al., 2015) and an unprecedented global economic loss of 100 trillion USD (Kaul et al., 2019). Therefore,

research efforts have since been redirected to novel strategies such as use of bacteriophage therapy (Jubeh et al., 2020; Liu et al., 2020), phototherapy and vaccination (Wong et al., 2017), antimicrobial peptides (Mathur et al., 2018; Vrancianu et al., 2020), probiotics (Lee et al., 2017) and quorum sensing inhibitors (Eze et al., 2018; Imperi et al., 2013; Richter et al., 2017). Each of these alternatives is faced with at least, a significant challenge (Pacios et al., 2020). Peptides are not cheap; they are liable to enzymatic digestion and pose toxicity concern. Phages are prone to the host immunological attack, while resistance against inhibitors of quorum sensing systems have been observed (Eze et al., 2018; Rangel-Vega et al., 2015; Vrancianu et al., 2020).

Another promising strategy to combating microbial infections and antibiotic resistance menace is to redirect/reposition/repurpose old, existing drugs for the treatment and management of pathogens outside the spectrum of their original targets (Balasundaram et al., 2018; Konreddy et al., 2018; Moraes & Ferreira-Pereira, 2019; Parvathaneni et al., 2019; Pushpakom et al., 2018). This approach, drug repurposing, has attracted interest within and outside the medical research community, as reflected in the frequency of published articles in the last decade (Domínguez et al., 2016; Domínguez et al., 2020). Mostly because the pharmacokinetic, pharmacodynamic, toxicity, efficacy spectrum and safety profiles of these drugs are already known or readily available, leveraging these data will foster quick and appropriate re-application and dose administration for other pathogens/infections. Additionally, it saves the time and cost normally required for extensive clinical trials (Cha et al., 2018; Farha & Brown, 2019; Kim et al., 2020).

Several drug types including anthelmintic, antitumor, anti-inflammatory, antipsychotic, among other, have been repurposed for antimicrobial and antibiofilm activity (Kaul et al., 2019; Miró-Canturri et al., 2019; Oliveira et al., 2020). Specifically, Kamurai and colleagues repurposed ten non-antibiotic drugs including amodiaquine (an antimalarial drug) and ibuprofen (an anti-inflammatory drug) against *S. aureus* and *P. aeruginosa* (Kamurai et al., 2020). In another study by Zeng and others, an FDA-approved antipsychotic drug, penfluridol, was repurposed for antibacterial and antibiofilm activity against *E. faecalis* biofilm (Zeng et al., 2020). The applicability of drug repurposing strategy is therefore significant, even as it continues to gain more research attention.

Furthermore, Peyclit et al. (2019) recently reviewed the drug types and current status of different repurposed drugs against different antibiotic-resistant bacteria including *A. baumannii*, and further emphasized the significance of this approach to solving antimicrobial resistance problem. Nonetheless, this approach is yet to be fully maximized, as there are still arrays of drugs and other antimicrobial compounds yet to be evaluated outside the spectrum of their natural medical indications. Specifically, there is a dearth of information on repurposing of clinically relevant antifungal drugs against bacterial biofilms. In this same way, electrochemical-based testing of antifungals against bacterial biofilms is yet to be explored. These areas are worthy of investigation, as evident from the literature review.

2.6 Antibiofilm testing methods / Antifungal sensitivity/resistance estimation methods

In general, antimicrobial sensitivity/resistance is often estimated using the minimum inhibitory concentration (MIC) in which the growth response of a microbial pathogen in the presence of a defined range of drug concentrations is assessed over a specific period. The lowest concentration at which no growth is observed is termed the MIC (Lass-Flörl et al., 2010; Van Dijck et al., 2018).

Several existing methods for assessment of antimicrobial sensitivity/resistance in microbial biofilms, are in principle based on methods for their planktonic counterpart (Beauvais & Latgé, 2015; Di Domenico et al., 2018; Ramage & Williams, 2013; M. Sanguinetti & Posteraro, 2017) as methods for antibiofilm assessment is more or less non-existent. Fundamentally, this is problematic as prevention/inhibition/eradication of biofilms would nominally require higher drug concentrations than planktonic cells (Perlin et al., 2017). This is further complicated by lack of standardization of existing methods, as results from same or even different laboratories are always in disagreement, thus, making reproducibility difficult (Kuper et al., 2012).

Therefore, the development of complementary/alternative method(s) for precise, repeatable, non-destructive, and real-time estimation of microbial biofilms sensitivity/resistance to antimicrobial treatments is exigent. This would also enable a rapid routine testing practice in clinical settings, thus, shortening the actionable time required for

therapeutic management. In addition, this would abate the emerging socio-economic burden resulting from microbial infections and antimicrobial resistance menace.

2.6.1 Conventional methods

2.6.1.1 Broth-based methods

Over the years, two recognized international bodies; namely, the Clinical Laboratory Standards Institute (CLSI) and the Antifungal Susceptibility Subcommittee of the European Committee on Antimicrobial Susceptibility Testing (EUCAST-AFST), have both developed protocols based on broth micro-/macro-dilutions approach (Lass-Flör et al., 2008; Lass-Flörl et al., 2010, 2018). Several revisions have also been made with a collective attempt of achieving a synchronized standard methodology for antimicrobial testing. The protocols by these two bodies are dependent on the replication ability of the cells (i.e., culture-dependent) following the addition of an antimicrobial/antibiofilm compound. They are, however, different in their inoculum size and culture media requirements, and MIC interpretations. Hence, an extreme intra- and inter-laboratory result differences exist between the two procedures (Maurizio Sanguinetti et al., 2015; Maurizio Sanguinetti & Posteraro, 2018).

The inclusion of dyes (mostly fluorescent dyes) or other compounds such as crystal violet (CV), propidium iodide (PI) fluorescein diacetate (FA), resazurin, tetrazolium compounds MTT (2H- Tetrazolium, 2-(4,5-dimethyl-2-thiazolyl)-3,5-diphenyl-, bromide) or XTT (2H-Tetrazolium, 2,3-bis(2-methoxy-4- nitro-5-sulfophenyl)-5-[(phenylamino)carbonyl]-hydroxide) in the microtiter plates is commonly adopted pre- or post- spectrophotometric incubation for easy estimation of biomass or metabolic viability of the cells (Van Dijck et al., 2018).

XTT is the most common assay for biofilm analysis as it considered to be simple, reliable, and reproducible. However, the technique is only effective for testing antimicrobial efficacy within a specific single strain and not among strains (Ramage, 2016). It also requires an expensive micro-plate reader, and a minimum of 48 h to complete (Gulati et al., 2018; Kuhn et al., 2003; Pierce et al., 2008).

Furthermore, an optimized, high throughput spectrophotometric-based assay (for *C. albicans* biofilm, for instance) was recently reported (Lohsea et al., 2017). The biofilms are grown in 96- and 384-well plates in the presence of the test compound and optical density (OD) measurements at a specified wavelength (usually 600 nm) is adopted as an index of the biofilm estimate. Lohse and colleagues opined that the resultant OD represents an accurate estimate of the biofilm. While the results are reproducible, they are unreliable as most spectroscopic-based biofilm assays lack the sensitivity to distinguish between dead and viable cells, except an additional processing step involving plate culturing post-spectrophotometry, is engaged. In general, broth-based dilution methods are technically difficult and time- (and other resource) demanding, and thus, not suitable for routine testing practice (Perlin et al., 2017; M. Sanguinetti & Posteraro, 2017).

2.6.1.2 Agar-based methods

Using this approach, a Petri-plate containing a specified agar medium is seeded with the test organism and the test antimicrobial compound of interest. During the incubation period, the test compound diffuses into the agar to exert its activity, thereby resulting in formation of areas/zones of growth inhibition, the size of which is suggestive of the degree of sensitivity/resistance of the test organism to the test drug. A commonly adopted methodology is the disc diffusion test where known concentrations of the test drugs is pre-impregnated on a paper; pre-cut into disk-like form, and then gently placed on the agar medium previously seeded with the test organism (Hudzicki, 2012).

Agar-based approach generally provides a more simple, rapid, and relatively cheap platform for resistance/sensitivity profiling (Ernst, 2007; Johnson, 2008). However, this approach is more qualitative than quantitative, as only zones of growth inhibitions, subject to other analysis and interpretations, can be obtained (Moriarty et al., 2014; Van Dijck et al., 2018). It is however more efficient for testing hydrophilic compounds (e.g., fluconazole against *Candida* spp.), partly due to the high diffusion coefficient of the agar, which in turn makes measurement of zones of inhibition easy. The choice of agar medium and period of incubation often vary among laboratories depending on whether CLSI or EUCAST

protocol is followed, thus making reproducibility of results difficult (Lass-Flörl et al., 2010).

2.6.2 Commercial kits

Due to technological advancement in recent years, commercial kits developed based on the testing principles of either CLSI or EUCAST are now available in some clinics and microbiology laboratories, especially in the cities and highbrow areas. Examples include Sensititre™ YeastOne™ Y09 AST Plate (ThermoFisher, USA) whose working principle is based on broth-dilution procedure, and Etest® (BioMerieux, USA) whose working principle is based on agar dilution approach. These two kits can be manually operated (Gulati et al., 2018; Lohsea et al., 2017).

An alternative is the automated Vitek® (also developed by BioMerieux, USA) with high flexibility and excellent comparative efficiency to CLSI/EUCAST methods (Almaghrabi et al., 2018; Franco-Duarte et al., 2019; Gómez-Gaviria & Mora-Montes, 2020). They are all generally simple and easy to use, and produce reliable and reproducible results (Perlin et al., 2017). Nevertheless, high cost remains a bottleneck, making their availability in rural and middle-class diagnostic centers, a difficulty. There are also concerns about compatibility and efficiency when used for some antimicrobial compounds (Sanguinetti & Posteraro, 2018).

2.6.3 Other biofilm methods

Other methods often adopted for microbial biofilm studies, whether in the presence or absence of antimicrobial treatments, include microscopy, flow cytometry, microfluidic devices, and molecular techniques. Extensive reviews on these methods are available in the literature (Azeredo et al., 2017; Huang et al., 2020; Rajapaksha et al., 2019). A summary of most biofilm methods and their limitations is presented in Table 2.1. In general, these methods are predisposed to high cost, heavy instrumentations that may occupy large space, extended turnaround times, high-depth technical knowledge for operation and interpretation of results, and destructiveness of samples.

Table 2.1. Summary of microbial biofilms methods

Method	Limitations	Reference
(A) Microbiological: culturing and counting	Time consuming; Difficult and laborious to conduct manual enumeration; On site application is practically impossible; A subpopulation of biofilm cells can be viable but non-culturable (VBNC) and would not be detected by the CFU approach.	(Lohsea et al., 2017; Meireles et al., 2015; Maurizio Sanguinetti & Posteraro, 2018)
(B) Molecular methods (e.g., PCR technology)	Expensive technology/instrumentation and chemicals are required; Expertise for technical handling of the protocols; Overestimation of cells due to the presence of eDNA	(Azeredo et al., 2017; Harba et al., 2012; Rajapaksha et al., 2019)
(C) Gravimetric method: indirect measurement of biofilm biomass by dry or wet weight	Time consuming; Low sensitivity and accuracy	(Achinas et al., 2019)
(D) Chemical methods involving dye staining (e.g., crystal violet assay, XTT)	Lack of reproducibility; Lack of sensitivity; Overestimation or underestimation of biofilm biomass; A standardized protocol is not available; It takes approximately two days or more for analysis	(Pierce et al., 2008; Ramage, 2016; Veloz et al., 2019)
(E) Microscopy (SEM, TEM, AFM, CLSM)	High cost; High level of maintenance; Sample damage; No standardized protocol is not available	(Achinas et al., 2019; Y. Huang et al., 2020; Meireles et al., 2015)
(F) Flow cytometry	High cost; Not readily available; Numerous dilution steps needed causing low sensitivity; The need for cells to be in a suspension makes cell architecture examination difficult; Data is cumbersome, hence, can be tedious	(El-Nahas et al., 2013; Harba et al., 2012; Veloz et al., 2019)

All of these challenges have a debilitating impact on clinical diagnosis and disease management, thereby contributing to high morbidity and mortality rates, especially in rural and poor communities around the world.

2.7 Microbial electrochemistry – a promising field for biomedical applications

2.7.1 Historical perspective – how and when it began

The genesis of microbial electroactivity began more than a century ago when microorganisms, specifically yeast – *Saccharomyces cerevisiae* and certain species of bacteria, were demonstrated to produce electrical output via interactions with a platinum electrode in a galvanic cell (Potter, 1911). This microbe-electrode interactions in a nutrient-rich medium, leading to breakdown of compounds and release of electrons is termed microbial electrochemistry or electromicrobiology (Schröder et al., 2015), and has since metamorphosed into an independent field of study with a broad variety of technological applications, including but not limited to waste water treatment, desalination, biorecovery, bioremediation, synthesis of value added chemicals, and biosensing (Aulenta et al., 2018; Bosire et al., 2016a; Kannan et al., 2019; Khater et al., 2015; Liang et al., 2018; Lv et al., 2014; Simoska, Sans, Fitzpatrick, et al., 2019; Tharali et al., 2016; Verma et al., 2021).

The above-mentioned, and many other biotechnological applications that require or involve microbe-electrode interactions, are collectively referred to as microbial electrochemical technology (MET). In METs, different electrical/electronic gadgets are employed to either monitor, control or measure microbial metabolism and the resulting electrochemical reactions. In 1911, Potter used a crude set-up that consisted of a glass jar, two platinum electrodes, an analog ammeter, and a Morse condenser. This apparatus has since witnessed tremendous improvement in terms of design, size, automation, and sophistication (Sánchez et al., 2020). The discovery of solid-state electronics (e.g., semi-conductors) in the 20th century and the optimization that followed up to the development of integrated circuits created a new platform for design, configuration and application of electronic devices (Enke, 2015).

Fast forward to 1952, Hans Wenking created a three-electrode chamber with an electrode potential control system – the potentiostat (Doelling, 1998). A potentiostat provides a means to effectively control the potential difference between the reference and the working electrodes. A working electrode is the electrode of interest under study. This, therefore, provide stability to the system whether the system properties (e.g., electrode type and surface, electrolyte conductivity etc.) change or not (Doelling, 2000).

2.7.2 The potentiostat

The potentiostat (or a galvanostat, depending on its functional mode) is basically an amplifier circuit that can control the potential differences between the working electrode (WE) and the counter electrode (CE). When it is used to apply potential difference at WE–CE while measuring the resulting current, it is said to be a potentiostat, and when it is used to apply current at WE–CE while monitoring the resulting potential, it is said to be a galvanostat. A two-electrode system is made up of the WE and the CE only. In addition to WE and CE, a three-electrode system comprised a reference electrode (RE) of a known, reversible electrochemical reaction to which the potential at the WE is compared (Sánchez et al., 2020). The three-electrode system allows precise control of the potential difference at WE-RE, thus increasing the sensitivity and repeatability of the electrochemical analysis.

In a typical three-electrode system, a resistance known as the uncompensated resistance, is developed between the RE and the WE; this leads to an ohmic potential drop that may affect the system performance, especially at high currents. Unfortunately, the potentiostat cannot mitigate the resistance between RE and WE as this is not involved on its feedback loop. Nevertheless, reducing the distance between the WE and RE would resolve this lapse. In some other cases, a small glass capillary (Luggin capillary) may be used to abate the uncompensated resistance. This may, however, gets clogged, especially during long-term experiments, leading to instability due to voltage drifts, and thus cause poor electrochemical performance (Zhang et al., 2011).

Furthermore, the properties of the components that constitute the electrochemical system (e.g., electrodes, electrolytes, microorganisms) always change over time. This often results in an unstable current flow, making the assessment of the individual components difficult.

While the potentiostat is designed to control the potential at the WE by compensating the resistance between the RE and CE (Fig. 2.2) regardless of fluctuations within the electrochemical cell or changes at the electrodes, especially in a typical three-electrode system, this can only be achieved within the compliance voltage range of the device, specifically based on the limitation of the potential control amplifier (Fig. 2.2). However, a large WE can result in uneven potential distribution, resulting in heterogenous biofilm growth and/or loss of efficiency by the electrochemical system (Hernández-Fernández et al., 2015; Oliot et al., 2017), therefore, electrodes with smaller surface areas are better for sensing and analytical applications (Sánchez et al., 2020).

It is worthy to note that the traditional potentiostats (e.g., Fig. 2.2(B)) is relatively bulky, thus, expensive and unfit for off-site applications (Sánchez et al., 2020). Advancement in technology has however birthed the development of portable and even smartphone-based potentiostats that are affordable and simple to use (Huang et al., 2018). Furthermore, conventional two- and three-electrode systems used in laboratory research require purchase, preparation, and maintenance of separate electrodes (RE, CE and WE), which increase the cost and the specialized labor required for the experiments, thus are not easily adaptable for biosensing and bio-analytical applications.

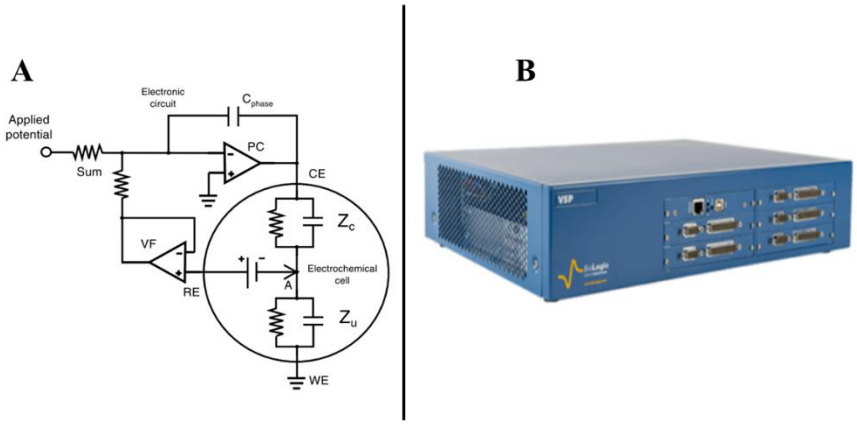

Fig. 2.2. (A) Schematic configuration of circuit, showing the working principle of a potentiostat for a three-electrode system; the potential control (PC) amplifier ensures a constant potential is maintained at point A; the RE serves as voltage source between the controlled point A and the PC, while the voltage buffer (VF) amplifier shields this voltage

to prevent loading that can interfere with the voltage source; Zc is operational amplifier (op-amp) that compensates for the impedance at CE while Zu is the uncompensated impedance between the controlled point A and the ground. **(B)** A typical, ready-to-use multi-channel VSP potentiostat (BioLogic, France).

Scree-printing technology is being adopted to bridge these limitations via fabrication of integrated, miniaturized, low-cost, versatile, easy-to-use-and-produce screen-printed electrode (SPEs) (Alonso-Lomillo et al., 2010; Metters et al., 2011; Yamanaka et al., 2016). SPEs are simple, adaptable to (1) low-volume samples – typical of biomedical settings, (2) portable devices and with various electroanalytical methods (García-Miranda Ferrari et al., 2021; Munteanu et al., 2018).

While there are concerns, especially with the possibility of replacing the standard methods, the potential of SPEs is enormous and their applications are increasingly being explored, particularly in biosensing and clinical diagnosis,

2.7.3 Screen-printed electrodes (SPEs) – the 'eureka' of biosensing and microbial diagnosis

A typical SPE corresponds to a traditional three-electrode cell, consisting of WE, RE and CE integrated into a single configuration, as schematically presented in Fig. 2.3. Traditionally, the RE is usually made of silver or silver/silver chloride layer (Ag or Ag/AgCl), while the CE is usually carbon, platinum or even gold. For WE, carbon is mostly used because of it low cost, easy availability, great functionalization potential, and excellent electrochemical features that includes low background current, wide potential range, chemical inertness, and high amenability with other materials/molecules (Munteanu et al., 2018).

Fig. 2.3 (C) shows a representative step-by-step process involved in making a typical SPE. The fabrication process often follows a similar pattern - the electrodes are designed, configured, and then manufactured via ink-printing on successive layers of ceramic or plastic materials depending on its intended use(García-Miranda Ferrari et al., 2021; Metters et al., 2011; Yamanaka et al., 2016).

SPEs in combination with electrochemical techniques have shown promising potential to serve as alternative to the conventional analytical methodology. This approach has been successfully applied for quality control assessment of food and drinks samples (Albanese et al., 2014; Andrei et al., 2016; Pierini et al., 2020; Soulis et al., 2020; Torre et al., 2020; Vasilescu et al., 2019), environmental pollution monitoring and analysis (Della Pelle et al., 2018; Dincer et al., 2019; Garciá-Miranda Ferrari et al., 2020; Kannan et al., 2019; Uria et al., 2020), forensic analysis (Elbardisy et al., 2019; C. D. Lima et al., 2020; Ott et al., 2020; Smith et al., 2013), detection of cancer biomarkers and other relevant biomolecules (Attoye et al., 2020; Ibáñez-Redín et al., 2019; Moreira et al., 2016; P. Yáñez-Sedeño et al., 2019; Paloma Yáñez-Sedeño et al., 2018), fundamental microbial studies (Guette-Marquet et al., 2021), or detection and characterization of microbial pathogens and/or their metabolites (Chalenko et al., 2012; Golichenari et al., 2019; Posseckardt et al., 2018; Simoska et al., 2019(a); Simoska et al., 2019(b); Sypabekova et al., 2019; Ward et al., 2018).

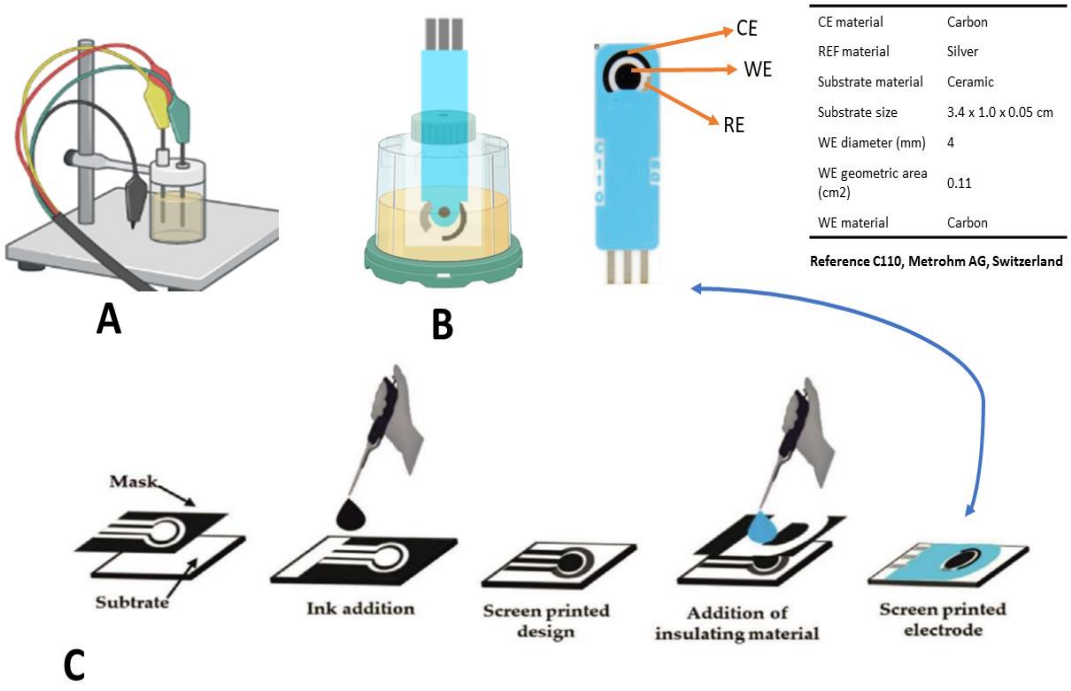

Fig. 2.3. (A) A typical conventional three-electrode electrochemical set-up. (B) A typical SPE cell; basic design and material configuration of an SPE. (C) Schematic illustration of the fabrication strategies involved in making a typical SPE.

The propensity of SPEs for rapid bioelectrochemical analysis, sensitive detection and characterization, cost-effectiveness, ease of manufacture and commercial availability, and minimal or no need for additional treatment and/or modification has been widely demonstrated (Alonso-Lomillo et al., 2010; García-Miranda Ferrari et al., 2021; Metters et al., 2011; Simoska & Stevenson, 2019; Uria et al., 2020). Thus, using SPEs in other spheres of biosensing and microbial analysis including characterization of clinically relevant microbial biofilms and antibiofilm assessment of old and/or new drugs is worthy of further research.

2.7.4 Microorganism as an electrical circuit – an electrochemist perspective

The perspective with which a microbe is viewed vary from one discipline to another. To a biotechnologist or an industrial microbiologist, a microbe is seen as a cell factory or a biological catalyst (Fig. 2.4(A)), required for bioconversion of organic raw materials into a value-added product (e.g., sugar molasses to ethanol) or for other bioprocesses (bioremediation, wastewater treatment etc.) (Su et al., 2020).

While this perspective is true and logical, it is worthy of note that the metabolic machinations and chemical transformations occurring during the bioprocess are facilitated via electrochemical reactions, leading to the generation, flow, and release of electrons, for the prime purpose of achieving a steady and active metabolic state, cellular growth, and metabolite (chemical) synthesis. Thus, a microbial electrochemist views a microbial cell as an electronic circuit (Fig. 2.4(B)) whose activity, structural and functional, can be detected and monitored electrochemically, during growth (Koch & Harnisch, 2016; Turick et al., 2019; VanArsdale et al., 2020).

Furthermore, the internal structure of a typical microbial cell is composed of water, ions, charged molecules and a variety of other solutes, compartmentalized from the outside environment by membranes (Fig. 2.4(C)), thereby creating electrical and chemical potential differences, and electrochemical gradients both within and across the membranes. Consequently, a membrane potential and ionic motive force – involved in the regulation of cellular and metabolic processes (e.g. electron transport, ATP synthesis, motility etc.), is formed (Nealson, 2017; Schofield et al., 2020). Interestingly, electron transport

phenomenon in microbial biofilms is empirically correlated with metabolism (Czerwińska-Główka & Krukiewicz, 2020; Saito et al., 2019), and thus, can serve as an indicator for determining microbial growth and cellular activity, even under drug treatments (Miran et al., 2021).

2.7.5 Electroactive versus non-electroactive microorganisms

Broadly, electroactivity as a phenomenon is often used interchangeably with the term extracellular electron transport (EET). This is because no standard definition exists in the literature yet, as different nomenclatures such as electric bacteria, cable bacteria and electricigens are commonly used for microbes that exhibits electroactivity (Koch & Harnisch, 2016; Logan et al., 2019; Nealson, 2017). Regardless, the ability to perform EET appears to be a common denominator. It is also important to emphasize that the term electricigen is more robust, and appears to be gaining acceptance over others (Verma et al., 2021). Throughout this text, the term electricigen will also be used strictly, except when stated otherwise.

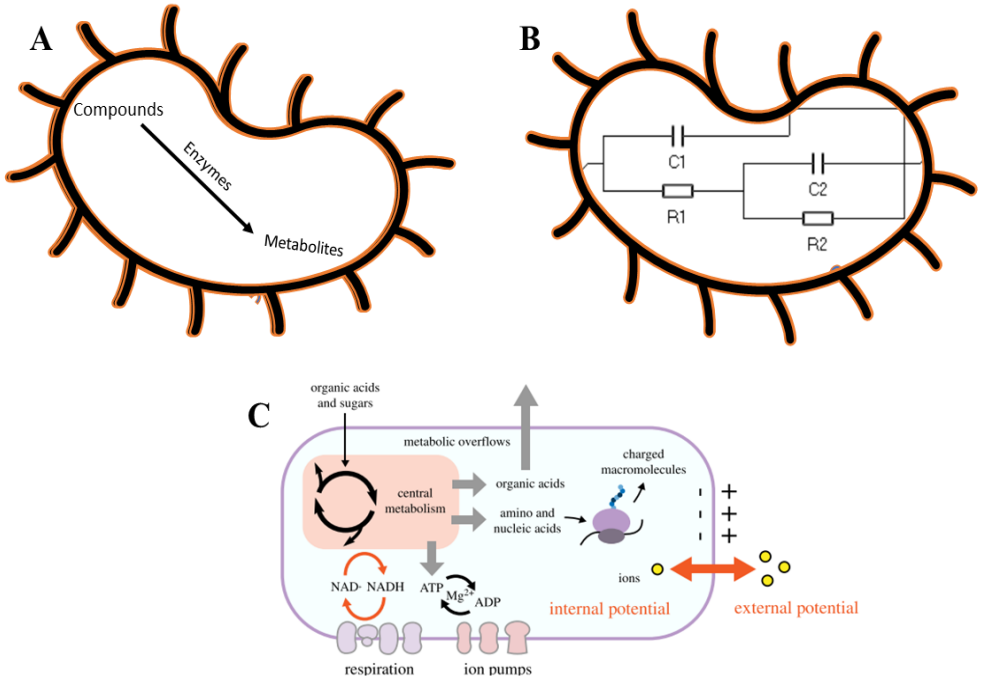

Fig. 2.4. A schematic representation of microorganism as a cell factory (A), electronic circuit (B), expanded version showing cell configuration, redox reactions, and electron flow (C).

As the term indicates, EET involves electron transport from the internal cellular space, across the membrane, to a conductive solid support, and/or vice versa. When electrons are transported from the cell to the solid support, it is said to be anodic/oxidative EET, and when reverse is the case (i.e., electron flow from the conductive solid to the cells), it is said to be cathodic/reductive EET.

The conductive solid may take the form of an electrode (e.g., SPE, as previously discussed), typical of laboratory studies, or a metal (e.g., iron), typical of what occurs in soils and other natural environmental niches (Doyle & Marsili, 2018a). EET is predominant in biofilm-forming microbial species (Masi et al., 2015; Miran et al., 2021).

Electron flow is an inherent phenomenon in all living organisms (prokaryotes and eukaryotes - plants, animals, microbes) but EET is not (Nealson, 2017). The first evidence of EET in prokaryotes (bacteria and yeasts) was reported by Potter in 1911. Afterwards, bacteria capable of direct EET, *Geobacter* and *Shewanella*, were discovered, and for long, these two bacteria served as model organisms for EET studies, owing partly to the earliest misconception that electroactivity is limited to microbes in metal-rich soils and sediments, a reflection of the environment from which *Geobacter* and *Shewanella* were first isolated from (Aiyer & Doyle, 2021).

Extensive research in the last decade has, however, proved that EET is a phylogenetically diverse feature in microorganisms (Koch et al., 2018; Koch & Harnisch, 2016), and that under favorable conditions, most microorganisms are capable of EET. It is on this basis that microbial electroactivity is now being redefined as a spectrum (Fig. 2.5), to accommodate all groups of microorganisms (Aiyer & Doyle, 2021; Doyle & Marsili, 2018a).

2.7.5.1 Mechanism of electron transport

The mechanism of EET is largely dependent on the type of organism involved. Today, three major mechanisms have been described (Fig. 2.6). First is direct electron transfer (DET) to the solid support (the solid surface, acting as the electron acceptor) using membrane-bound c-type cytochromes (Hubenova et al., 2016; Saito et al., 2019; Teravest & Angenent, 2014). This mechanism is common in strong electricigens (e.g., *Geobacter*

and *Shewanella*) (Aiyer & Doyle, 2021; Nealson, 2017). Second is the use of thin, structural appendages extending outward from the cell surface. These structures are electrically conductive, facilitating EET at a distance, and are called e-pili or nanowires (Reguera, 2018; Schofield et al., 2020). The third mechanism is mediated electron transfer (MET) where soluble electron shuttles or redox molecules, endogenously secreted by the cells (Elabed et al., 2021; Marsili, et al., 2008) or exogenously added (Astorga et al., 2019; Bosire et al., 2016b; Bosire & Rosenbaum, 2017; Kannan et al., 2019; Ramanavicius et al., 2017; J. Sun et al., 2019), facilitate electron transfer between the cell and the electron acceptor (Martinez & Alvarez, 2018b).

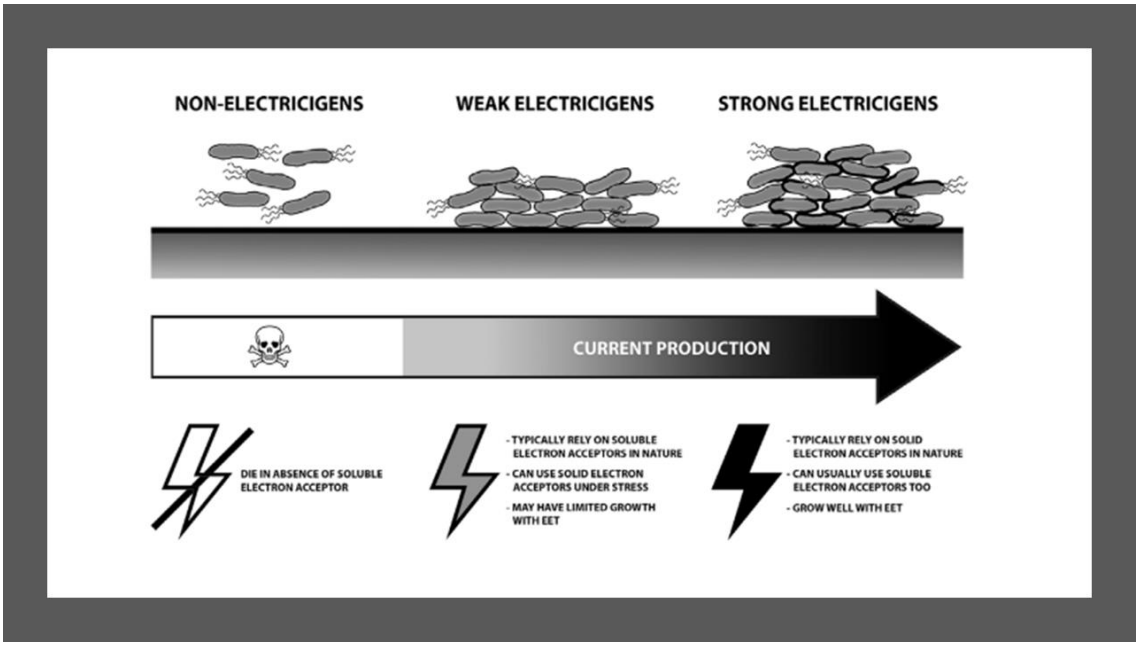

Fig. 2.5. Spectrum-based definitions of electricigen (Doyle & Marsili, 2018a).

Other EET mechanisms recently described in the literature include use chelators or siderophores to take in the solid electron acceptor, solubilize them and then ferry them into the cell (Paquete, 2020), and use of extracellular polymeric substances in the biofilm matrix (Xiao et al., 2017). Worthy of note, is that, only a thin line of difference exist among these mechanisms, as a single microbial species may adopt one or more depending on its prevailing environmental/cultural conditions (Doyle & Marsili, 2018a).

2.7.5.2 Weak electricigens – the focus of this thesis

A weak electricigen is a microbe that performs EET as a side strategy to conserve energy in lack of soluble electron acceptors. Further, the electron flow is generally low, in the range of 10-100 μA/cm^2, which is insufficient for power production and large scale energy conversion. This is due to the intrinsic genetic and physiological configurations of weak electricigen (Aiyer & Doyle, 2021; Doyle & Marsili, 2018b). However, the majority of microbial pathogens belong to this group, hence, their clinical relevance and the need for their electrochemical-based studies.

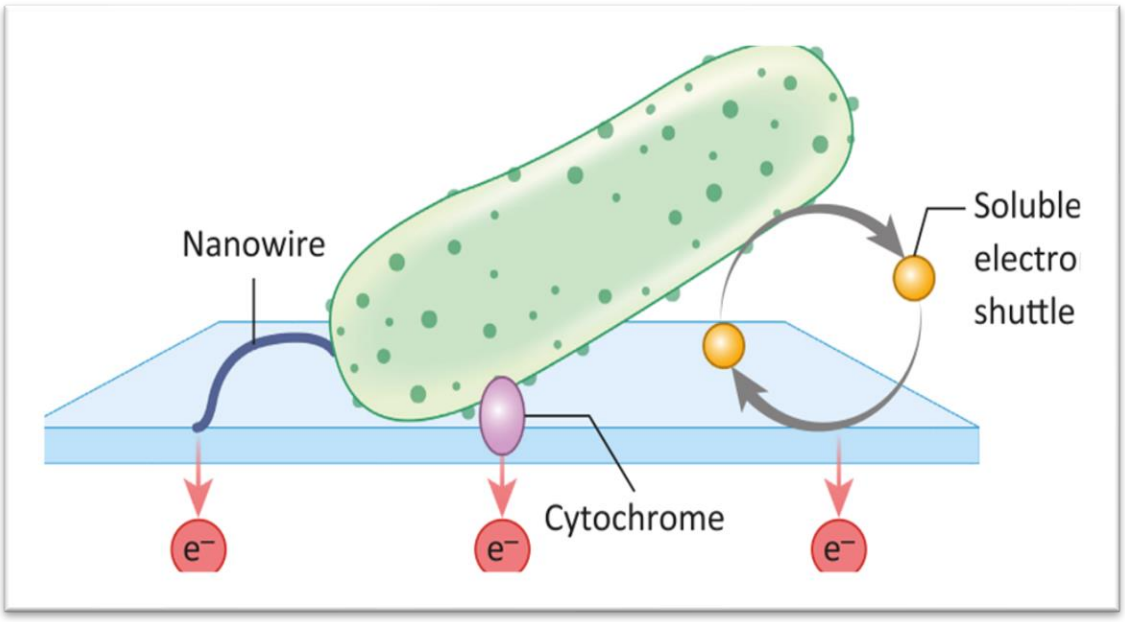

Fig. 2.6. The three major mechanism of EET (Aiyer & Doyle, 2021).

The human gastrointestinal tract (GIT), dental cavity and other micro-niches have been discovered to provide enabling conditions for microbial electroactivity (Naradasu et al., 2019; Schwab et al., 2019; Wang et al., 2019). Additionally, several clinically relevant, weak electricigenic microbial species have been identified in the last decade. These include members of the genera *Escherichia*, *Aeromonas*, *Bacillus*, and *Enterobacter* (Doyle et al., 2017; Y. Qiao et al., 2008; Seviour et al., 2015; Tian et al., 2019).

Others include *Staphylococcus aureus* (Bhuvaneswari et al., 2013), *S. mutans* (Naradasu et al., 2020a), *Enterococcus faecalis* (Keogh et al., 2018; Pankratova et al., 2018), *Pseudomonas aeruginosa* (Bharatula et al., 2019; Bosire et al., 2016a; Seviour et al., 2015), *Listeria monocytogenes* (Light et al., 2018), *Corynebacterium matruchotii*, *Porphyromonas gingivalis*, *Aggregatibacter actinomycetemcomitans* (Naradasu et al., 2020b; Naradasu et al., 2020c), *Clostridium cochlearium*, (Schwab et al., 2019) and *Capnocytophaga orchracea* (Zhang et al., 2020). Following this array of studies, the following inferences are worthy of note:

1. There is a dearth of information on the vast majority of clinically relevant, weak electricigenic microbial species, particularly the biofilm forming ones, and those of special status with respect to antimicrobial resistance.
2. Since a correlation has been established between electrical output of microbial pathogens and their metabolic activity, this could be exploited for real-time assessment of drug efficacy on microbial growth and metabolism (Miran et al., 2021). Surprisingly, this much-needed intervention to ameliorate the challenges facing clinical diagnosis and effective antimicrobial therapy remains underexplored.

2.7.5.3 The necessity of exogenous redox mediator for weak electricigen studies

Just as the name suggests, weak electricigens are described as such because of their inability to perform DET, though possess EET functionality. Thus, they rely on the presence of soluble redox molecules or electron shuttles, secreted by the cells or exogenously added (Aiyer & Doyle, 2021). They may however evolved into DET-abled cells over time and under certain growth conditions, as previously reported for *E. coli* (Qiao et al., 2008) and *S. aureus* (Bhuvaneswari et al., 2013).

Nevertheless, the necessity of exogenous addition of a redox mediation is a common practice while working with weak electricigens (Doyle & Marsili, 2018a). Table 2.2 shows a summary of synthetic redox mediator commonly adopted in electrochemical studies of weak electricigens. The choice of mediator often depends on solubility, toxicity, redox potential, photostability and sensitivity, biocompatibility with the system under study, efficiency, cost, ease of availability, among many others. As presented in Table 2.2,

quinones are the most used synthetic redox compound. This may be attributed to its high solubility and low redox potential in aqueous system, low toxicity, compatibility with biomembranes, and photostability (Doyle & Marsili, 2018a; Santoro et al., 2016).

Table 2.2. A review of redox mediators commonly used for weak electricgens.

Redox mediators	Weak electricigens	References
Flavins	*Bacillus megaterium* *Listeria monocytogenes*	(L. X. You et al., 2018) (Light et al., 2018)
Quinones e.g., 2-hydroxy-1,4-naphthoquinone (HNQ) and anthraquinone-2,6- disulfonate (AQDS),	*Enterococcus faecalis* *Escherichia coli* *Klebsiella pneumoniae* *Lactobacillus lactis* *Enterobacter* sp *Saccharomyces cerevisiae*	(Hederstedt et al., 2020) (Astorga et al., 2019; Kannan et al., 2019; Santoro et al., 2016; Sun et al., 2019) (X. Li et al., 2013) (Freguia et al., 2009) (Doyle et al., 2017) (Ramanavicius et al., 2017)
Pyocyanin	*P. aeruginosa*	(Bosire et al., 2016a)
Potassium ferricyanide	*P. aeruginosa* *Enterococcus faecalis* *S. cerevisiae* *Candida albicans* *E. coli and Clostridium sporogenes*	(Bharatula et al., 2019) (Pankratova et al., 2018) Ramanavicius et al., 2017) (Congdon et al., 2013) (Ertl et al., 2000)
Iron (III)/iron (II)	*Enterococcus faecalis*	(Keogh et al., 2018)
2,6-dichlorophenolindophenol (DCIP)	*Candida albicans*	(Hassan & Bilitewski, 2013)

2.8 Electroanalytical methods for antibiofilm testing

The convergence of microbiology and electrochemistry opened an exciting opportunity in biosensing and bio-analytics. Electrochemistry investigates electron transport phenomena arising from chemical changes (e.g., oxidation-reduction reactions), and applies this approach to the study of physiological phenomena in microorganisms. This has helped, greatly, in overcoming the limitations associated with the conventional methods (McEachern et al., 2020; Turick et al., 2019) that were previously discussed. Although their application for detection and/or monitoring of microbial pathogens is well documented in the literature (Amiri et al., 2018; Islam et al., 2020; Karbelkar & Furst, 2020; Kuss et al., 2018; Lv et al., 2014; Muir et al., 2011; Sheybani & Shukla, 2017; Simoska et al., 2019; Tokonami & Iida, 2017), little is known about their application for antibiofilm drug assessment and/or other therapeutic compounds.

This has become more necessary now, considering that most infections involving biofilm-forming microbial species are resistant to treatments, resulting in high mortality and economic burdens (Abebe, 2020; Kumar et al., 2021). Consequently, the demand for novel therapeutic strategies including assessment methods is high (Hards & Cook, 2018; Miran et al., 2021).

Also, the need for novel methodology for assessment of antimicrobial agents targeting the metabolic machineries of pathogenic microbes cannot be overemphasized, as traditional culture-dependent methods require extended incubation time, are not suitable for non-culturable organisms, and cannot distinguish between killing and inhibitory effects of drugs (Richards et al., 2020; Tao et al., 2017). Furthermore, existing advanced technologies such as adenosine triphosphate bioluminescence and single-cell Raman Spectro-microscopy, could monitor the metabolic activity of microbial biofilms via isotope or fluorescent labelling (Lee et al., 2017; Wang et al., 2020). Nevertheless, these approaches are destructive, expensive, and not suited for a real-time and label-free monitoring of biofilm cells metabolism. Although there is a wide array of electrochemical techniques for biological applications, only those suitable for biofilm-forming weak electricigens offering high signal-to-noise ratio, a reflection of the focus of this thesis, will be discussed. Table

2.3 shows an overview of microbes and the electrochemical techniques commonly employed for their detection and/or physiological studies.

2.8.1 Chronoamperometry (CA) / Chronocoulometry (CC)

CA is used to monitor current output over time, while CC – the integral of current, estimates charge (Furst & Francis, 2019), and maybe more informative for diagnostic decision due to the inherent low current density of weak electricigens (Doyle & Marsili, 2018a). CA and CC are fixed-potential techniques (Saito et al., 2019), thus, they do not elicit charging current that may interfere with the electrochemical signals, making them well suited for weak electricigens (Aiyer & Doyle, 2021). CA allows a direct, real-time measurement of electroactivity (Turick et al., 2019) and could provide reliable physiological details on the metabolic state of cells in the biofilm, thus, makes it a suitable approach for distinguishing between live and dead cells – an essential feature lacking in all conventional gold standard methods.

In CA, the WE electrode is mostly poised at a single potential, optimal for the organism under study, as too low or high potential may be insufficient to elicit a measurable EET rate or negatively impact the organism, leading to membrane damage, respectively (Bosire & Rosenbaum, 2017; Liu & Li, 2020; Teravest & Angenent, 2014; Wei et al., 2010). At high potential, the electrode itself or certain medium components may participate directly in the redox reactions, thus affecting the accuracy and reliability of the current output. Therefore, control experiments are always needed to ascertain that the current output is generated only from the biofilm cells. There is a dearth of information on the application of CA for assessment of antibiofilm agents (Miran et al., 2021). There is however a dearth of information on the application of CA for assessment of antibiofilm agents. This is intriguing and worthy of investigation, especially as a strong correlation between biofilm formation and electroactivity has been established (Czerwińska-Główka & Krukiewicz, 2020; Light et al., 2018; Masi et al., 2015; Naradasu, Guionet, Miran, et al., 2020).

Furthermore, a typical CA curve for early biofilm formation on a flat electrode (Fig. 2.7) is like the sigmoid growth curve of any microbe, as current output often rises gradually within the first few hours, corresponding to rapid attachment and growth of cells, and

becomes stable after a certain period, as the accumulation of non-conductive biofilms matrix block part of the electrode surface. Depending on the prevailing conditions, the current may remain stable for some time, and then decays over time, suggesting growth suppression, cell removal from the electrode surface or even death due to a combination of depleted nutrients and accumulation of toxic metabolites. Therefore, to determine the efficacy of a drug for biofilm inhibition or on pre-formed biofilm, the drug should be introduced at inoculation, or when the current becomes stable, respectively.

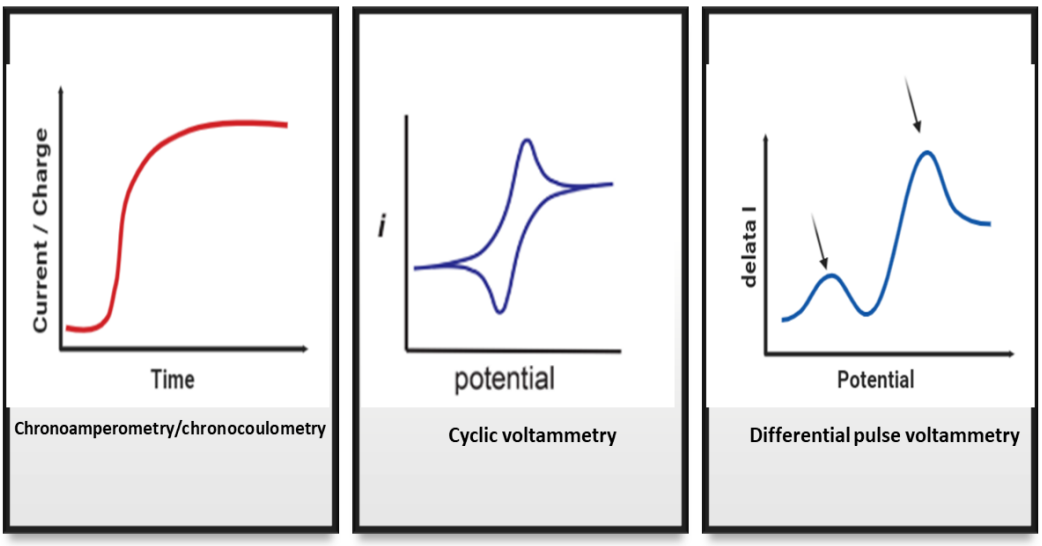

Fig. 2.7. Representative plots of selected electrochemical techniques.

2.8.2 Voltammetric-based methods (cyclic voltammetry (CV), differential pulse voltammetry (DPV))

Voltammetry is generally used for detection, characterization and quantification of redox species in relation to electron transfer processes (Saito et al., 2019; Turick et al., 2019). Contrary to amperometry (CA), voltammetry provides information only about the interfacial electron transport at the electrode surface, but not metabolic current, at least at high scan rate values (Saito et al., 2019). Multiple cycles are however a possibility, making

it a technique of choice in studying intermediate reactions, and in monitoring stability of the redox species (Furst & Francis, 2019).

In cyclic voltammetry (CV), the potential is scanned within a range, and in both forward/positive and reverse/negative directions, while the resulting current is recorded. The appearance of peak current(s) in the presence of biofilm cells, but absent in the control with no biofilm cells, is indicative of redox species produced by the biofilm cells that ferry electrons to the electrode surface (Saito et al., 2019). The intermittent varied potentials may however produce charging currents, so appropriate caution is advised when CV is applied for weak electricigens. CV at low scan rate (e.g., < 5 mV/s) are suitable to observe turnover redox reactions, while higher scan rates are adopted to characterize redox reactions under non-turnover conditions. The pulse methods (e.g., DPV and square wave voltammetry (SWV)), where the potential is either held constant or varied at a constant rate, could be used to mask the charging currents, thus increasing the analytical sensitivity (Aiyer & Doyle, 2021). In a typical pulse voltammetry method, a potential pulse (+/-) is over-imposed on a potential slope, and a short time between the pulses allows the redox pool at the interface to be recharged. The current is recorded before and after each pulse, and the difference (delta I) is plotted as a function of the pulsed potential (Fig. 2.7) (Furst & Francis, 2019).

2.8.3 Electrochemical impedance spectroscopy (EIS)

Microbial biofilms are a complex structural community of cells whose electrochemical features are also not fully defined. The interiors of the cells in the biofilm comprises different charged molecules and ions, making it somewhat conductive (~ 1 S/m), while the cell membranes are made up of phospholipid bilayers and glycoproteins, making it somewhat insulating (~ 10^{-7} S/m). The biofilm matrix consisting of proteins, lipids and extracellular DNA also contribute to the conductive and/or insulating property of the biofilm. Consequently, as cells bind to the electrode surface during biofilm development, the electrode surface area is reduced and access to redox species becomes limited, resulting in increased interface impedance (Furst & Francis, 2019). Therefore, EIS can be suitable for characterization of thin biofilm formed by weak electricigens, as it allows monitoring

and detection of early biofilm formation through estimation of changes in interfacial impedance.

In EIS, a sinusoidal voltage of a given frequency is applied to the biointerface, while the resulting sinusoidal current is recorded to estimate the impedance (Z). This can be repeated over a range of frequencies, such that different parameters relating to the biological system can be obtained. Bharatula and colleagues recently reported an EIS-based detection of weak electricigen *P. aeruginosa* within 24 h post-incubation using a flexible indium tin oxide-coated polyethylene terephthalate substrate (Bharatula et al., 2019). However, because EIS responses are different under turn-over and non-turn-over conditions, it is almost impossible to establish a quantitative correlation between biofilm formation (impedance) and metabolic activity (electroactivity) (Babauta & Beyenal, 2014), partly because it is easily perturbed by many intrinsic factors (Ward et al., 2014). Additionally, the analysis of EIS data cannot be automated (yet), thus its application for routine biofilm detection is not appropriate.

2.9 Noteworthy inferences from literature review

As presented in Table 2.3, application of electrochemical techniques for microbial studies is not a new adventure. Nonetheless, the following inferences from the literature review show the gap-in-knowledge and the need for improvement/further research.

1. Most studies were done using the two/three-electrode system. Relative to the SPEs, this approach is expensive, in that, each electrode (WE, CE, and RE) is acquired separately; complex and tedious, in that, each electrode is washed/treated/processed separately, and thus unsuitable for drug testing as it requires large volume of samples.

2. There is little or no information on the electrochemistry of *Candida albicans* and *Acinetobacter baumannii* biofilms. This is worthy of research, owing to the reports by CDC and WHO ascribing high risk status to these two microbial species, with an emphasis on the need for new therapeutic options.

3. There is dearth of information on electrochemical-based assessment of antibiofilm agents. Use of SPEs, for instance, requires small volume of sample and antimicrobials,

making it feasible for high-throughput screening. In addition, this simple and low-cost concept may possibly accelerate the discovery of antibiofilm drugs, as a significant collection of compounds could be rapidly tested. This approach could serve as an alternative or a complementary technology for assessing the effectiveness of antimicrobials.

4. There is dearth of information on repurposing of clinically relevant antifungals against *A. baumannii* biofilm. Same with electrochemical-based assessment of antimicrobials against *A. baumannii* biofilm.

Table 2.3: Overview of recent studies on electrochemical characterization of microbial biofilms

Electrochemical Technique(s)	Microbial species/strain	References
CV	*Geobacter sulfurreducens*	(Babauta & Beyenal, 2014; Marsili et al., 2008; Srikanth et al., 2008)
	Mixed culture biofilm	(Bressel et al., 2003)
	Staphylococcus epidermidis	(Becerro et al., 2016)
	Shewanella oneidensis	(Carmona-Martínez et al., 2013; Marsili, Baron, et al., 2008; Teravest & Angenent, 2014)
	Pseudomonas aeruginosa	(Qiao et al., 2017; Wang et al., 2013; Yong et al., 2014))
	Lactobacillus rhamnosus GG	(Jarosz et al., 2019)
	Acidithiobacillus thiooxidans	(Méndez-Tovar et al., 2019)
	Gut microbiota (undefined)	(Wang et al., 2019)
	Bacillus cereus and *Rhodococcus ruber*	(Tian et al., 2019)
	S. aureus, B. megaterium, E. faecalis, Lactococcus lactis, Hansenula fabianii, B. subtilis, E. coli	(Astorga et al., 2019; Bhuvaneswari et al., 2013; Chen et al., 2019; Elabed et al., 2021; Freguia et al., 2009; Hederstedt et al., 2020; L. X. You et al., 2018)
DPV	*Geobacter sulfurreducens*	(Marsili et al., 2008)
	S. epidermidis, Streptococcus mutans, P. aeruginosa, B. megaterium, Bacillus sp., *Pichia stipites, E. coli, Corynebacterium matruchotii*	(Becerro et al., 2016; Besant et al., 2015; Naradasu et al., 2020a; Naradasu et al., 2020b; Seviour et al., 2015; Xiao et al., 2017; You et al., 2018)

	Gut bacteria: *Enterococcus avium* and *Klebsiella pnuemoniae*	(Naradasu et al., 2019)
	Candida albicans	(Congdon et al., 2013)
	Mycobacterium tuberculosis	(Golichenari et al., 2019)
	Vibrio cholerae and *Salmonella typhimurium*	(Amiri et al., 2018)
CA	*Lactobacillus rhamnosus GG, Aeromonas* and *Enterobacter* sp, *S. mutans*, *C. matruchotii*, *B. cereus* and *Rhodococcus ruber*, *S. aereus*, *B. megaterium*, *E. faecalis*, *L. lactis*, gut bacteria, *B. subtilis*, *Saccharomyces cerevisae*, *E. coli*, *P. aeruginosa*	(Astorga et al., 2019; Bhuvaneswari et al., 2013; Chen et al., 2019; Doyle et al., 2017; Freguia et al., 2009; Hederstedt et al., 2020; Jarosz et al., 2019; Naradasu, Guionet, Miran, et al., 2020; Naradasu, Miran, & Okamoto, 2020; Ramanavicius et al., 2017; Santoro et al., 2016; Tian et al., 2019; V. B. Wang et al., 2013; W. Wang et al., 2019; L. X. You et al., 2018)
	Geobacter sulfurreducens	(Marsili et al., 2010)
EIS	*Pseudomonas aeruginosa*	(Bharatula et al., 2019)
	E. coli biofilms; *Salmonella* sp	(Astorga et al., 2019, 2020; Liu et al., 2018)
	Aeromonas and *Enterobacter* sp	(Doyle et al., 2017)
	Mycobacterium tuberculosis	(Golichenari et al., 2019; Sypabekova et al., 2019)
	Enterococcus faecalis	(Pankratova et al., 2018)
	Saccharomyces cerevisae	(Posseckardt et al., 2018)

Chapter Three: Evaluation of dinuclear silver(I) complexes containing pyridine-based macrocyclic form of ligand as antimicrobial agents against clinically relevant microbial species: conventional microtiter vs electrochemical-based methods.

3.1 Introduction

Infectious diseases caused by biofilm-forming microbial species has become a well acknowledged global health challenge, which requires an immediate intervention (Miró-Canturri et al., 2019). As previously emphasized in the literature review section (Chapter 2), treatment and management of infectious diseases is further complicated by antimicrobial resistance phenomenon in microbial biofilms, as existing and commonly used antimicrobial treatments are mostly ineffective (de Kraker et al., 2016; Tacconelli & Pezzani, 2019), partly because of the self-formed extracellular polymeric matrix that surrounds the biofilm cells (Dieltjens et al., 2020; Flemming et al., 2016). Consequently, the necessity for the development of new antimicrobials, either for monotherapy, combination therapy, or functionalization with existing clinically available drugs for enhanced effectiveness, cannot be overemphasized.

Recently, combination of organic ligands with metal ions of known antimicrobial potential has become an emerging strategy in the fight against antimicrobial resistance (Farrer & Sadler, 2011). Although, silver and/or its salt, silver nitrate, have shown broad and efficient activity against planktonic and biofilm-forming microbial pathogens (Klasen, 2000; Maillard & Hartemann, 2013; Medici et al., 2019), their use as an antimicrobial compound is however limited, because it precipitates easily and quickly under physiological conditions, thus, silver ions are unable to reach the target pathogens following the precipitation process (Kędziora et al., 2018; Mansour & Radacki, 2019). This could however be circumvented by coordinating ligands to the Ag(I) ion, to regulate its stability and release, thereby enhancing its antimicrobial efficacy (Sainis et al., 2016).

Polyazamacrocycles are an important family of ligands for the creation of stable complexes in terms of metal ion dissociation (Haque et al., 2017; Yudin, 2015). As a result of the macrocyclic effect, the stability of a copper (II) complex of tetraazamacrocycle is significantly higher than that of its open-chain complex counterpart ligand (Haque et al.,

2017). Furthermore, 1,4,8,11-tetraazacyclotetradecane (cyclam) and its substituted derivatives are among the most investigated azamacrocycles, and have been utilized in a variety of medical applications including as anti-cancer and anti-HIV medications (Mewis & Archibald, 2019). When 2-pyridylmethyl pendant arms are added to the cyclam framework, *N,N',N'',N'''*-tetrakis(2-pyridylmethyl)-1,4,8,11-tetraazacyclotetradecane (tpmc) is formed, which contains eight potential coordination sites and may form mono- and dinuclear metal complexes (Narayanan et al., 2002). So far, quite a few metal complexes containing the tpmc ligand have been synthesized and evaluated for antimicrobial applications (Krstić et al., 2019; Petković et al., 2013; Ruiz-Herrera et al., 2016; Tanasković et al., 2012).

In clinical diagnosis and infectious disease management, it is not enough to have a potent antimicrobial drug; the time required to obtain the antimicrobial sensitivity/resistance profile of the test pathogen is equally crucial. This is partly because in an ideal situation, clinical decision(s) cannot be taken without it. Consequently, the need for a platform that allows rapid and sensitive evaluation of antimicrobial/antibiofilm compounds is also exigent. In this study, two new silver(I) complexes with tpmc ligand, $Ag_2(NO_3)(tpmc)]NO_3.1.7H_2O$ and $[Ag_2(tpmc)](BF_4)_2$, previously synthesized and extensively characterized by our collaborators at the University of Kragujevac, Serbia, and herein referred to as complex 1 and complex 3, respectively, were evaluated for antimicrobial/antibiofilm efficacy against a list of carefully selected clinically relevant microbial pathogens using both conventional method and electroanalytical approach.

3.2 Materials and Methods

3.2.1 Materials

All chemicals including Potassium ferricyanide ($K_3[Fe(CN)_6]$) ethanol, dimethyl sulfoxide (DMSO) and phosphate buffered saline (PBS), are of analytical grade, and were prepared according to the manufacturers' directive.

All microbial strains used in this thesis were kindly provided by Dr Jasmina Nikodinovic-Runic of the Institute of Molecular Genetics and Genetic Engineering, University of Belgrade, Belgrade, Serbia.

The complete synthesis and characterization details of complexes 1 and 3, including their elemental analysis, nuclear magnetic resonance spectra, UV-Vis spectroscopic and crystallographic analyses, stability, and cytotoxicity details have been extensively documented and published (Savić et al., 2020).

For electroanalysis, graphite screen-printed electrodes (reference code C110, Metrohm DropSens, Spain). Each SPE has a silver pseudo-reference electrode, graphite counter electrode and 4 mm diameter graphite working electrode (0.126 cm2 surface area). Prior to use, the SPEs were sterilized twice in 70% (v/v) ethanol, and thereafter washed in sterile deionized water and then air-dried. The electrochemical cells were maintained at 37 °C in steel beads dry bath throughout the experiment.

3.2.2 Methods

3.2.2.1 Determination of minimum inhibitory concentration (MIC)

Prior to testing, fresh stock solutions of silver(I) complexes 1 and 3, silver(I) sulfadiazine (AgSD), and $K_3[Fe(CN)_6]$ were prepared in dimethyl sulfoxide. The MIC of complex 1 and 3 against *Acinetobacter baumannii* ATCC 19606 was determined in Luria-Bertani broth (tryptone, 10 g/L; yeast extract, 5 g/L; NaCl, 10 g/L; pH 7.2),while RPMI 1640 medium augmented with 2% of glucose was adopted for MIC determination against *Candida* species (*C. albicans* ATCC 10231, *C. parapsilosis* ATCC 22019, and *C. albicans* isolate 24) according to the protocols recommended by CLSI for broth microdilution test for bacteria and yeast, respectively. The starting inoculum was 1×10^5 CFU/mL while the highest tested concentration was 0.5 mM. MIC values were recorded as the lowest concentration of the compounds that causes no growth after 24 h of incubation at 37 °C.

3.2.2.2 Antibiofilm testing

Antibiofilm activity of complex 1 was determined via electroanalysis using chronoamperometric (CA) and cyclic voltammetric (CV) measurements with a VSP multichannel potentiostat (BioLogic, France). The CV settings were *Ei* = -0.3 V *vs.* Ag, *Ef* = 0.4 V *vs.* Ag, 1 mV/s scan rate, current averaged over the last 50 % of the step length and recorded over N = 10 voltage steps. The parameters for CA were *Ei* = 0.4 V *vs.* Ag, and they were recorded every 60 s for 24 h.

At first, the yeast and bacterial strains were cultured on Sabouraud Dextrose Agar (SDA) and Tryptic Soy Agar (TSA). Unless otherwise noted, all subsequent experiments were performed in RPMI 1640 medium augmented with 2% (w/w) glucose. All biofilm-forming species were grown in 15 mL electrochemical cells with an initial optical density ($OD_{600\ nm}$) of 0.3 in the presence of 0.1 mM $K_3[Fe(CN)_6]$ as a redox mediator, while complex 1 dissolved in DMSO was added at the MIC previously obtained for the planktonic cells. Electroanalysis was carried out using CA and CV, while the results were analyzed with the EC-Lab software (V11.33, BioLogic, France). A schematic representation of the electroanalytic approach is presented in Scheme 3.1.

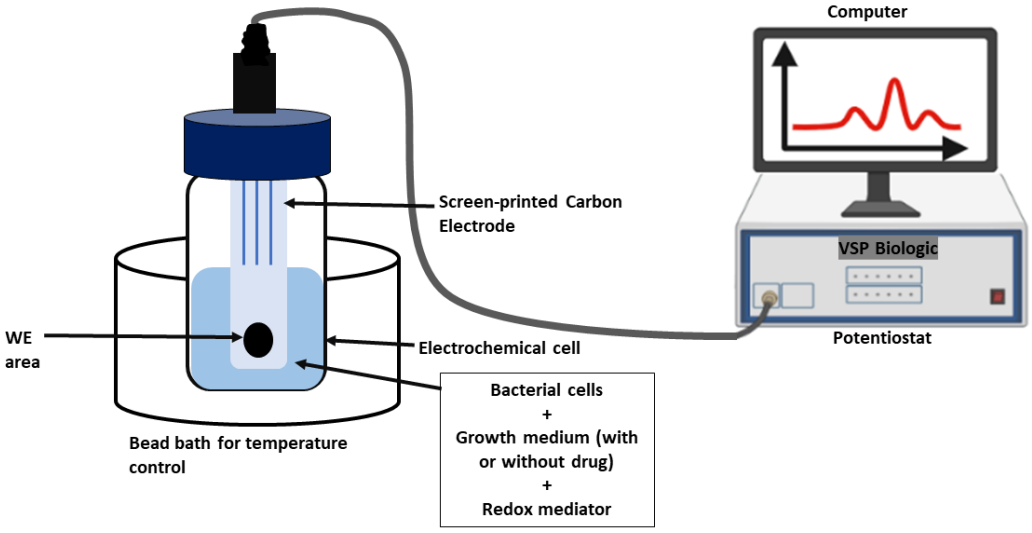

Scheme 3.1. Graphical representation of the electroanalytic method.

Additionally, the biofilm growth on the working electrode was also quantified via the conventional crystal violet assay. A minimum of three biological replicates were carried out for each experiment. Each strain was experimented in four different conditions: a) cells + redox mediator; b) cells + redox mediator + complex 1; c) cells + complex 1; d) redox mediator + DMSO, with a) and d) as controls. Additional

diagnostic information was obtained by measuring and analyzing the optical density of planktonic cells post-electroanalysis, as well as the pH of the spent medium.

Complex 1 was further tested via the conventional microtiter plate assay for its capacity to suppress the formation of *Candida* biofilms or disrupt the already formed biofilm. The formed biofilm mass was measured using crystal violet assay (absorbance at 590.0 nm) and tetrazolium salt (XTT) reduction assay (absorbance at 492.0 nm). A minimum of three biological replicates were carried out for each experiment.

3.3 Results and Discussion

3.3.1 Conventional methods

Previously described silver(I) complexes were strongly cytotoxic, limiting their therapeutic potential (Glišić et al., 2016; Savić et al., 2016), while complexes 1 and 3 evaluated in this study showed a very mild cytotoxic effect to a healthy human fibroblast cell line (MRC-5), making them ideal candidates for additional biological testing (Savić et al., 2020). Hence, our motivation to further evaluate their antimicrobial/antibiofilm potential.

In this study, complexes 1 and 3 were evaluated, *in vitro*, for their antimicrobial efficacy against one Gram-negative bacterial strain and three *Candida* spp. These microbial pathogens are well known for their debilitating disease-causing abilities in humans (Castanheira et al., 2014; Opulente et al., 2019; Sarshar et al., 2021; Tsay et al., 2018; Tsubouchi et al., 2020; Wilson, 2019). The complexes' antimicrobial effectiveness was compared to that of the clinically utilized AgSD. As presented in Table 3.1, complexes 1 and 3 showed significant antimicrobial activity against the tested strains with MIC (μM) in the range of 0.4 to 3.2. Interestingly, the complexes showed higher efficacy than the AgSD, which has MIC (μM) in the range of 2.5 to 10.

Table 3.1. Antimicrobial activity in terms MIC (μM) of complexes 1 and 3 relative to the tpmc ligand and the clinical silver-based drug AgSD.

	Complex 1	Complex 3	AgSD
Test organism			
A. baumannii ATCC 19606	1.7	3.2	NT
C. albicans ATCC 10231	2.1	2.1	10
C. albicans isolate 24	2.1	2.1	5.1
C. parapsilosis ATCC 22019	0.9	0.4	2.5

NT—Not tested; Standard error is between 1 – 3%.

Silver(I) complexes containing aromatic N-heterocycles, such as diazines, benzodiazines, and tricyclic phenazine, with significant antibacterial and antifungal efficacy have been previously reported (Glišić et al., 2016; Savić, et al., 2016). Similarly, silver(I) complexes with metronidazole (mtz), exhibited considerable antibacterial action against *E. coli and P. aeruginosa*, and minimal antifungal activity against *C. albicans* (Kalinowska-Lis et al., 2015).

Using the conventional crystal violet and tetrazolium salt (XTT) reduction assays, the ability of complexes 1 and 3 in the presence of $K_3[Fe(CN)_6]$, to inhibit biofilm formation of test *Candida* spp was determined (Table 3.2), with *C. parapsilosis* strain being the most sensitive (Tables 3.1 and 3.2), The minimal biofilm inhibition concentration (MBIC) values ranged from 13 to 29 μM, with MBIC values being 10-fold higher than the MIC values. This is consistent with the discovery that several antifungal drugs, including fluconazole, may only prevent biofilm formation at doses more than 1000-fold of the MIC.

Table 3.2. Minimal biofilm inhibition concentration (MBIC) of complexes 1 and 3 (μM) via crystal violet and tetrazolium salt (XTT) assay

	Crystal violet assay		**XTT reduction assay**	
Test organism	Complex 1	Complex 3	Complex 1	Complex 3
C. albicans ATCC 10231	21.4 ± 0.8	26.2 ± 0.4	24.2 ± 0.8	28.4 ± 0.2
C. albicans 24 (isolate)	26.7 ± 0.4	26.2 ± 0.2	25.5 ± 0.4	25.2 ± 0.4
C. parapsilosis ATCC 22019	13.4 ± 0.6	13.1 ± 0.5	15.3 ± 0.6	15.8 ± 0.3

3.3.2 Electroanalytical method

Antibiofilm activity was also investigated electro-analytically to enable for non-destructive, real-time, and continuous monitoring of the effect of complex **1** on early biofilms. At first, the effect of the redox mediator, $K_3[Fe(CN)_6]$, on growth and viability of tested microbial strains was assessed, and the findings revealed that the redox mediator is not toxic to the cells even at a concentration as high as 0.5 mM (Fig. 3.1). In the subsequent electroanalytic experiments, therefore, the mediator was used at the optimum concentration of 0.1 mM. This concentration supported adequate biofilm growth, as sufficient current output, which is dependent on biofilm growth and metabolism, were obtained when the cells were grown in the presence of the mediator only (Appendix 3.1), and thus, chosen for further experiments in this study.

The working electrode was poised at a potential 400 mV (*vs.* Ag pseudo-reference electrode) throughout the experiment. Under this circumstance, part of the electron flow caused by nutrient oxidation in the growth medium is ferried extracellularly and intercepted at the electrode. It has been established that that the current output and overall coulombic charge over a defined period is correlated to biofilm growth or its inhibition depending on the presence or absence of an antibiofilm agent, respectively (Kannan et al., 2019; Keogh et al., 2018).

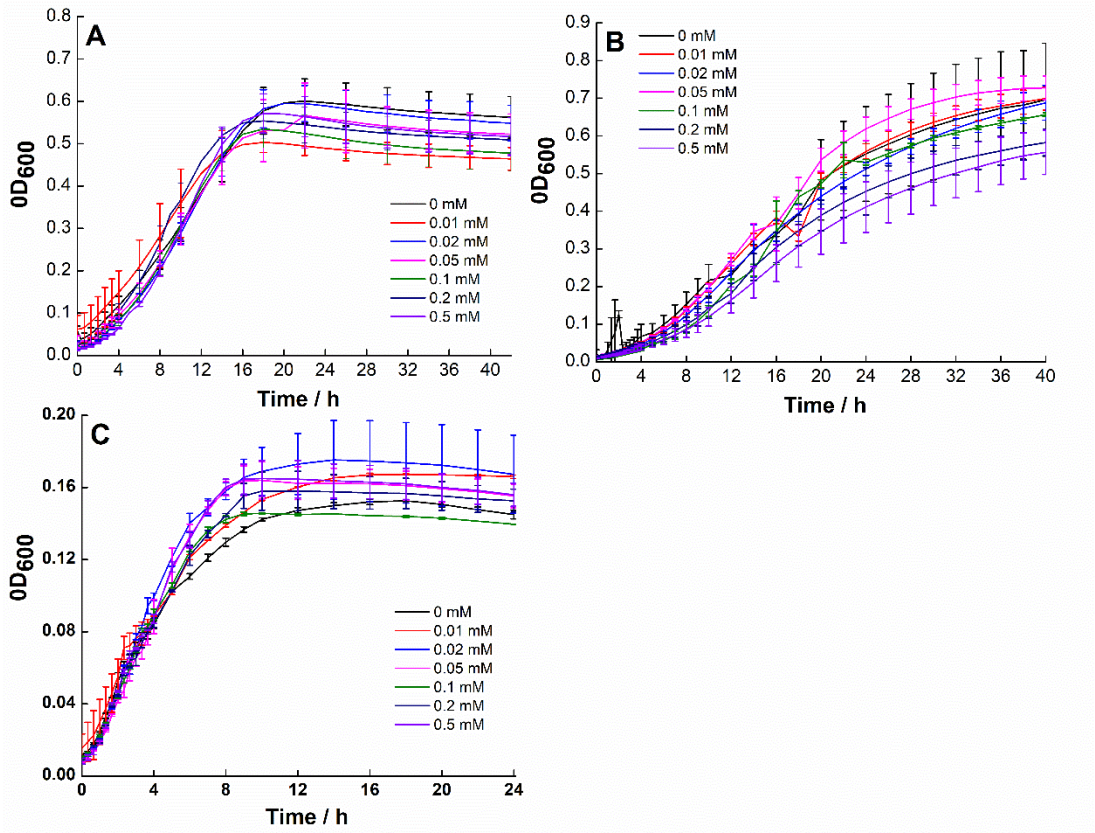

Fig. 3.1 Growth curves of tested strains at different concentrations of the redox mediator. (A) *C. parapsilosis* ATCC 22019; (B) *C. albicans* ATTC 10231; (C) *A. baumannii* ATCC 19606. Each dataset shows the average and standard deviation of three independent biological replicates (n=3).

The chronoamperometric traces revealed that complex 1 had a minimal impact on *A. baumannii* biofilm activity (Fig. 3.2 (A)). Additionally, the cyclic voltammograms (CVs) under non-turnover condition at 0 h were identical with and without the antimicrobial complex 1, but the CVs under turnover conditions at 24 h are substantially lower in the presence of complex 1, indicating that complex 1 negatively impacts bacterial metabolism and decreases the extracellular electron transfer rate (Fig. 3.2 (B)). These findings showed that the MIC for biofilm cells is greater than that required for their planktonic counterpart, which is consistent with the results of the conventional microtiter plate-based assay. Moreover, the chronoamperometric results validated the antibiofilm activity against *C. parapsilosis* (Fig. 3.3), but there was no clear trend for the other two *Candida* strains, suggesting that more work on optimizing this methodological approach for *Candida* spp. is needed.

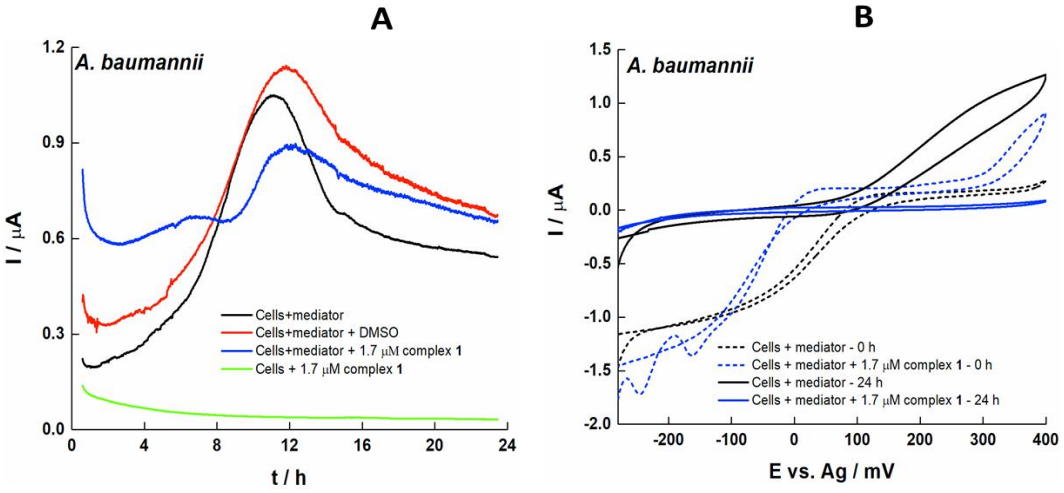

Fig. 3.2. Effect of complex 1 on early biofilm *A. baumannii* determined via electroanalysis. (A) Chronoamperometry (CA). (B) Cyclic voltammogram (CV) at 1 mV/s. CA results are the average of at least two independent biological replicates, while the CV is a representative trace.

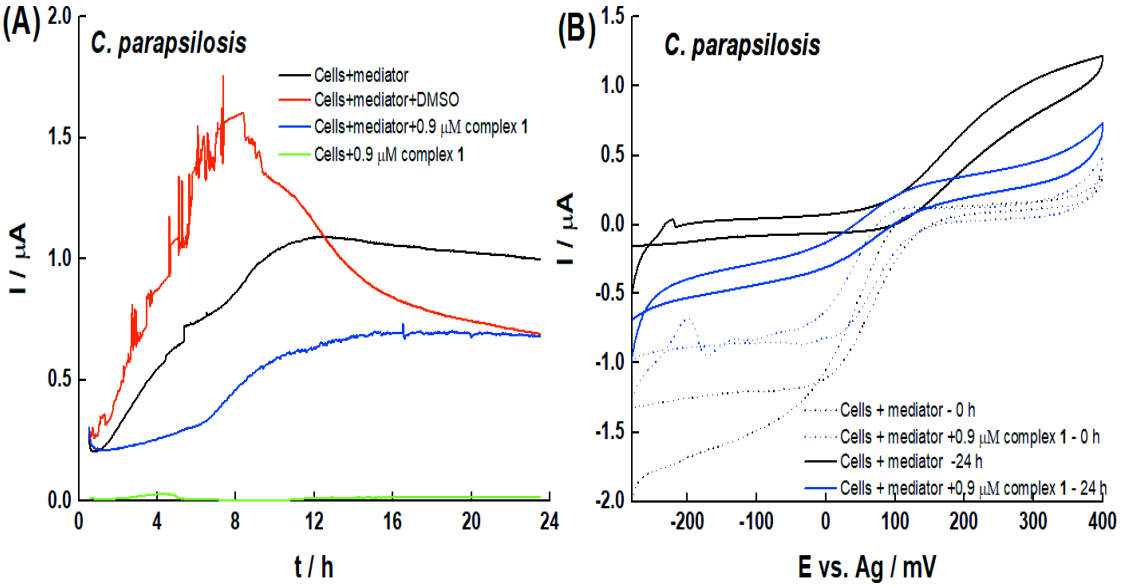

Fig. 3.3. Effect of complex 1 on early biofilm *C. parapsilosis* determined via electroanalysis. (A) Chronoamperometry (CA). (B) Cyclic voltammogram (CV) at 1 mV/s. CA results are the average of at least two independent biological replicates, while the CV is a representative trace.

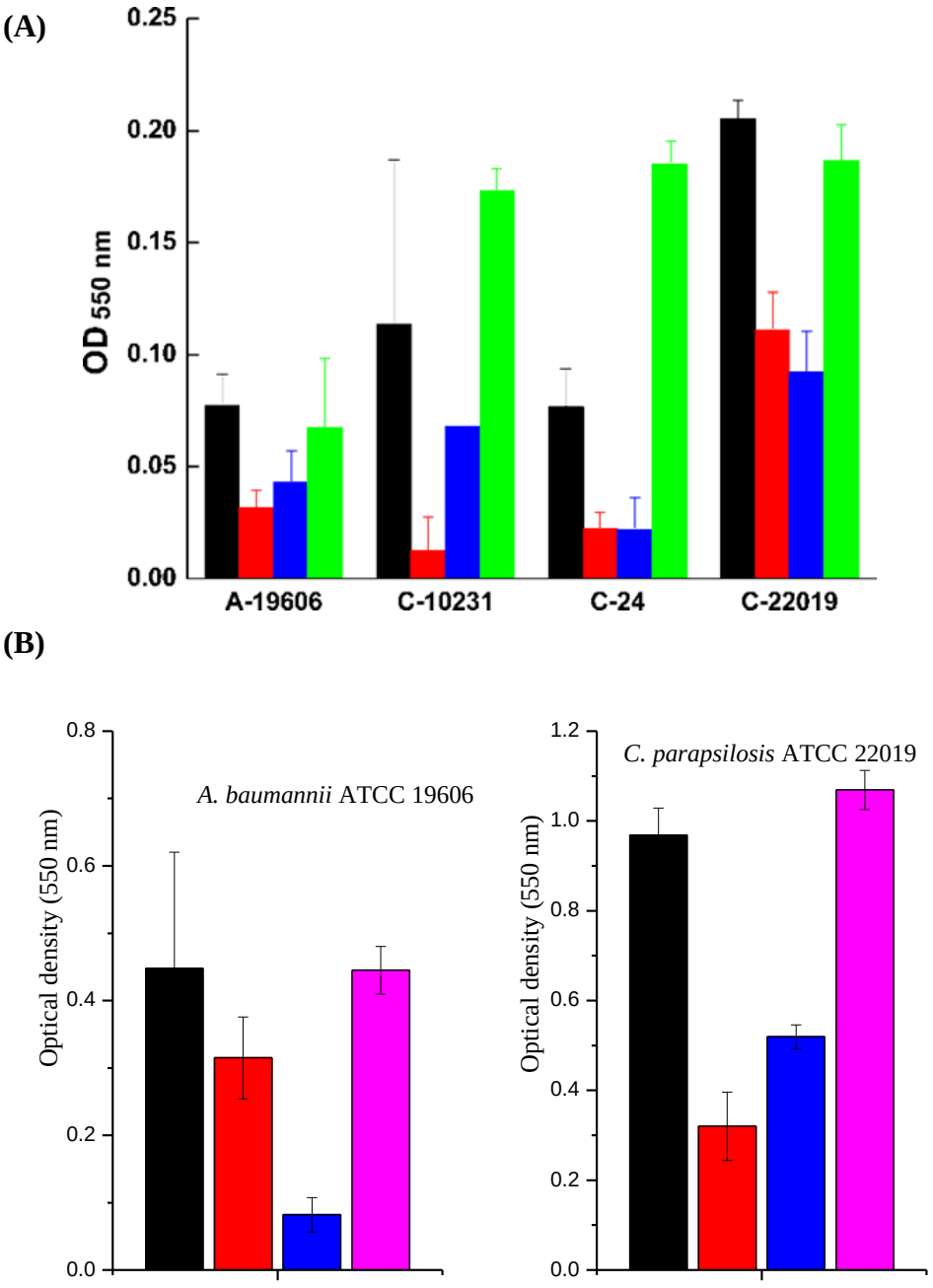

Fig. 3.4 (A) Biofilm amount quantified with crystal violet assay for the four tested, post-electroanalysis. Cells + mediator (black bars); Cells + mediator and DMSO (green bars); Cells + mediator and the MIC of complex 1 in planktonic culture (red bars). Cells + complex 1 (blue bars). The results are statistically significant for *A. baumannii* 19606 and *C. parapsilosis* 22019 ($p<0.05$), with lower biofilm production in the presence of complex 1. (B) Optical density of planktonic cells post-electroanalysis. Cells with mediator only (black); cells with mediator + DMSO (violet); cells with mediator + complex 1 (red); cells with complex 1 (blue).

Post-electroanalysis, the biofilm biomass on the graphite WE were determined for *A. baumannii*, *C. albicans* ATCC 10231, *C. albicans* isolate 24 and *C. parapsilosis* ATCC 22019 via the crystal violet staining assay (Fig. 3.4 (A)). Because of the several washing procedures, the crystal violet test likely underestimates the biofilm biomass as seen from the low absorbance (Fig. 3.4 (A)). Furthermore, after 24 h of potentiostatic experiments at E = 400 mV *vs.* Ag pseudo-reference electrode, the optical density of planktonic cells was also measured (Fig. 3.4 (B)). In general, electrochemical tests reveal that a significantly greater concentration of complex 1 is required to produce a robust antibiofilm inhibitory action, despite the fact that the impact may be seen at planktonic MIC concentrations.

3.4 Summary

Two previously synthesized silver (1) complexes were evaluated for their antimicrobial/antibiofilm efficacy against selected clinically relevant microbial pathogens. Complex 1 showed considerable potential to inhibit biofilm formation of *C. parapsilosis* even at concentrations equal to planktonic MIC values. However, in general, both conventional and electroanalytic methods indicate that complete inhibition of biofilm formation would require at least 10-fold greater concentrations than that needed for planktonic cells. Additionally, the observed discrepancies in biofilm evaluation methods reiterates the necessity for a multi-method approach to validate the antibiofilm efficacy of any antimicrobial/antibiofilm agent. This work, however, is one of the first reports on electroanalytic platforms for antibiofilm drug assessment against clinically relevant yeast strains. This study motivated us to further develop and optimize this methodology, as would be presented in the subsequent chapters.

3.5 Outcome

Savić, N., Petković, B., Vojnovic, S., …**Olaifa, K**., Marsili, E., Nikodinovic-Runic, J., Djuran, ssM., & Glisic, B. (2020). Dinuclear silver(I) complexes with pyridine-based macrocyclic type of ligand as antimicrobial agents against clinically relevant species: the influence of counter anion on the structure diversification of the

complexes. *Dalton Transactions*, *49*, 10880–10894. https://doi.org/10.1039/D0DT01272F

Chapter Four: Electroanalysis of *C. albicans* biofilms – A new approach for antifungal testing

4.1 Introduction

Approximately 1.7 million people die each year as a result of fungal diseases (Kainz et al., 2020). Candidemia, i.e., the presence of *Candida* in blood, is just one of them, accounting for about 50,000 cases each year in the United States alone (Tsay et al., 2018). *Candida* species are also common nosocomial infections in Europe, ranking among the top ten with a frequency of 1.9 to 4.8 cases per 100,000 people (Sanguinetti et al., 2015).

C. albicans is the most common fungal pathogen and can cause infections ranging from localized cutaneous thrush to deadly systemic candidiasis in immunocompromised, aged, or intensive-care unit patients (Cavalheiro & Teixeira, 2018; Mayer et al., 2013). It can also infect the cardiovascular system, bones, and brain, and have a death rate of about 40% (Gunsalus et al., 2016). Lately, it has been linked to bipolar illness and schizophrenia (Dadar et al., 2018). Unfortunately, *Candida* biofilms are more virulent than their planktonic counterparts (Cavalheiro & Teixeira, 2018), cause persistent infections (Dadar et al., 2018; Gunsalus et al., 2016) and exhibit heightened resistance to both antifungal therapies and the individual's innate immunological defense systems. As a result, early detection and treatment appears to be the only viable option.

Routine antifungal testing was not prevalent in the past given that the existing antifungal drugs at the time were effective. However, as the number of people with deteriorated immune systems rises, thanks in part to incidences of HIV/AIDS, chemotherapy, and organ transplantation, effective approaches for detecting fungal infections and means of establishing antifungal efficacies became exigent (Cantón et al., 2009). While there is no yet common standard methodology for antimicrobial testing against biofilms, the single-tube technique (Goeres et al., 2019), crystal violet assay (Melo et al., 2011), XTT reduction method (Hawser, 1996; Pierce et al., 2008) are widely used to evaluate antimicrobials in the lab, and as previously highlighted in Chapter 2 (section 2.6.1), these procedures and the existing commercial platforms are limited with diverse constraints, and thus not suited

for routine antimicrobial testing (Table 2.1). As a result, a simple and low-cost diagnostic platform for testing of antifungal drugs is in urgent demand (Van Dijck et al., 2018). For this, electroanalytical approaches might be utilized (Munteanu et al., 2018; Simoska & Stevenson, 2019).

Bioelectrochemical approach can be faster, convenient and of low cost in comparison with the traditional culture-based procedures when a rapid assessment of an antibiofilm compound is required (Hassan & Bilitewski, 2013). Extracellular electron transfer rate, mediated by exogenous redox molecules (e.g., flavins (Light et al., 2018), quinones resazurin, and humic acid (Astorga et al., 2019; Martinez & Alvarez, 2018b), has been previously adopted to determine the initial attachment, growth, and viability of early microbial biofilms (Cesewski & Johnson, 2020; Rao et al., 2020). Remarkably, bioelectrochemical testing of anti-*Candida* biofilm compounds is yet to be investigated.

In the past, Congdon et al. had described the detection of *Candida* biofilm using electrochemical techniques using porous reticulated carbon electrodes. Also, Hassan and Bilitewski (2013) previously described growth of *C. albicans* in a mediated electrochemical system. In this work, the effect of various antifungal drugs on early *C. albicans* biofilm in the presence of $K_3[Fe(CN)_6]$ as a redox mediator was investigated using bioelectrochemical methods, while conventional methods were adopted to validate our findings. To the best of our knowledge, this is the first study on evaluation of antifungal drugs against *Candida* biofilm using electrochemical methods.

4.2 Materials and methods

4.2.1 Materials

Two clinically relevant antifungals – fluconazole (Flz) and amphotericin B (AmB) and a new drug candidate, complex 3, previously described in chapter 3 (section 3.2.1), were tested. Dimethyl sulfoxide was adopted as standard solvent for preparation of stock solutions, while potassium ferricyanide ($K_3[Fe(CN)_6]$) was used as redox mediator. Except complex 3, all analytical chemicals including absolute ethanol were acquired from Acros Organics, China. SPEs (Reference code: C110, Metrohm DropSens, Spain) same as described in chapter 3 (section 3.2.1) were used for all bioelectrochemical experiments,

while *C. albicans* was initially grown on Sabouraud Dextrose Agar (SDA) (Condalab, Spain), while RPMI 1640 medium (Sigma Aldrich, Kazakhstan) was used in all subsequent experiment, except otherwise stated.

4.2.2 Methods

4.2.2.1 Optimization of redox mediator

Growth and viability of *C. albicans* cells was evaluated at various doses, 0 to 0.5 mM, of $K_3[Fe(CN)_6]$ in 96-wells microtiter plates. 18-24 h old cultures were diluted to an OD_{550} of 0.05 in fresh medium and used as inoculum. Wells with no $K_3[Fe(CN)_6]$ serve as control. Growth was measured with the Gen5TM Microplate Reader and Imager Software (BioTek Instruments). This was repeated three times using independent biological replicates, and the results recorded as mean standard ± deviation (Fig. 4.1).

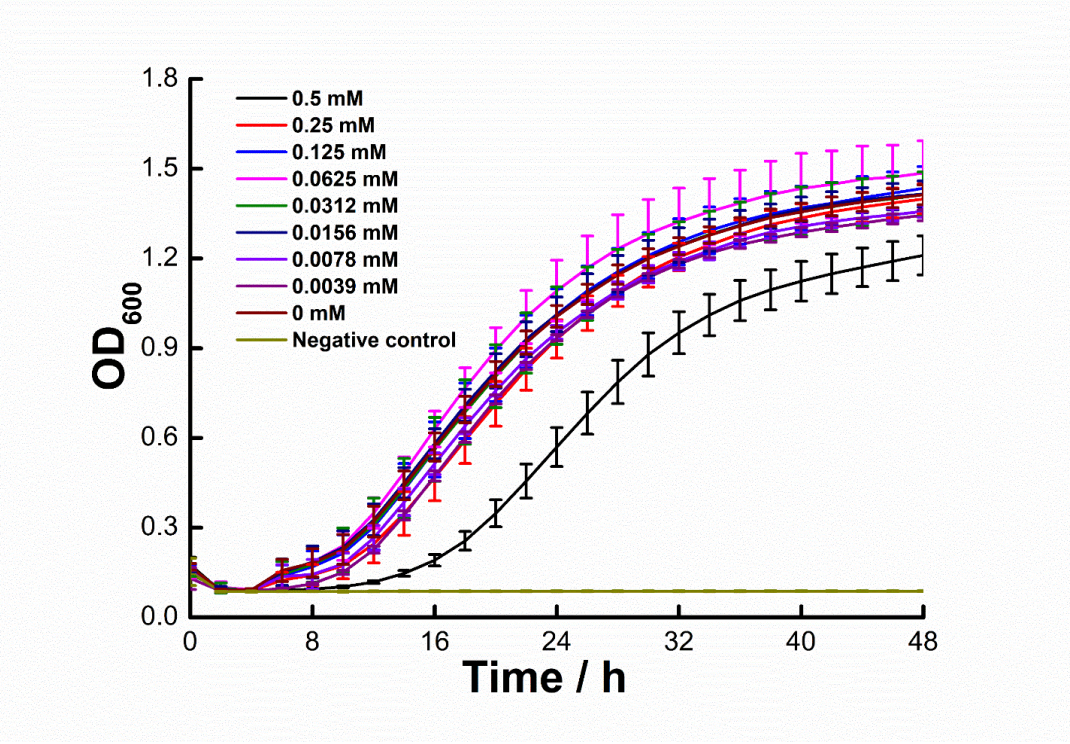

Fig. 4.1. Viability of *C. albicans* ATTC 10231 in different $K_3[Fe(CN)_6]$ concentrations. Results indicate that 0.1 mM is non-toxic (n = 3).

4.2.2.2 Electroanalysis

The antifungal efficacy of Flz, AmB, and complex 3 against the biofilm-forming strain *C. albicans* ATCC 10231 was determined via CA, CV, EIS. CA and CV were carried out in succession, while EIS was carried out in a separate series of experiments at an open circuit potential. While CA proceeded for 48 h, CVs were recorded intermittently at 0, 24 and 48 h. The parameters for CA and CV were same as those described in chapter 3 (section 3.2.2.2) The EIS analysis was performed with a 10 mV potential amplitude in a frequency range of 100 kHz to 50 mHz.

All bioelectrochemical experiments were carried out in a steel-beads dry bath constantly maintained at 37 °C (scheme 3.1). Before every experiment, the SPEs were surface sterilized twice in 70 percent v/v ethanol to remove oil, dust, and other possible contaminants, and thereafter rinsed in sterile deionized water, and finally carefully blotted to dry.

4.2.2.3 Post-electroanalysis: crystal violet assay, Raman spectroscopy and microscopic imaging of the working electrode area were performed to validate the electrochemical results.

For crystal violet, planktonic cells and leftover medium components were removed while the electrodes were gently washed in PBS to maintain the physiological state of the biofilm cells. They were thereafter incubated for 15 minutes in 0.1% crystal violet solution, then rinsed in sterile distilled water and finally air-dried. The biofilm-crystal violet matrix was then dissolved with 30% acetic acid solution, and the absorbance measured at 550 nm with a SmartSpecTM 3000 Spectrophotometer (Bio-Rad Laboratory, Moscow).

A confocal Raman microscope (Ramantouch; Nanophoton Corporation, Osaka, Japan) with a single monochromator linked to a thermoelectric-cooled CCD detector (1340 points 400 pixels) was used to acquire Raman imaging maps of the *C. albicans* biofilm formed on the WE area, while the native software of the same equipment was used for image analysis. Additionally, a crossbeam 540 scanning electron microscopy (SEM) (Carl Zeiss, Germany) was used to acquire biofilm morphologies of *C. albicans* ATCC 10231 formed

on the WE surface. To achieve this, the SPEs were carefully taken out of the electrochemical cells and rinsed in phosphate buffer solution (pH 7.3), followed by dehydration in absolute ethanol, and fixation in 4% v/v formaldehyde, and finally dried in a desiccator at room temperature. Prior to microscopic imaging, a Turbomolecular Pumped Coater Q150T (Quorum Technologies, UK) was used to coat the sample with gold (5 nm for 120 s).

4.2.2.4 Conventional XTT assay for antibiofilm assessment

2,3-bis-(2-methoxy-4-nitro-5-sulfophenyl)-2H-tetrazolium-5-carboxanilide (XTT) reduction assay was carried out using the 96-well plate method (Pierce et al., 2008). The antifungal compounds were added following inoculation at two different concentrations (1×MIC and 10×MIC) at varying times of 0, 8, and 12 h to determine their biofilm inhibition efficacy. Fresh cell culture grown in RPMI medium augmented with 2 % wt. glucose was used as inoculum, while all of the wells had 0.1 mM $K_3[Fe(CN)_6]$ in them so as to mimic the electroanalytic method. After 24 h incubation, the planktonic cells and medium component were carefully discarded while the wells were gently rinsed with PBS to eliminate non-adherent cells.

For biofilm removal assay, round-bottom 96-well microtiter plates were used to grow the biofilms, first for 48 h under static condition at 37 °C. After this, planktonic cells and old medium were removed from the wells. This was immediately followed by washing with PBS. Thereafter, fresh RPMI medium diluted with the antifungal compounds in increasing doses of 1×, 10× and 100×MIC, were dispensed into the wells having the already-formed biofilms. All wells were also supplemented with 0.1 mM $K_3[Fe(CN)_6]$ to mimic the electroanalytic experimental conditions. The plates were then incubated for another 24 h, also at 37 °C. The resultant biofilm estimates were recorded via crystal violet (XTT) assay using absorbance measurement at 490 nm in a Tecan Infinite 200 Pro multiplate reader (Tecan Group Ltd., Männedorf, Switzerland).

4.3 Results and Discussion

4.3.1 Electroanalysis

The possible impact of exogenous redox mediator, $K_3[Fe(CN)_6]$, on growth/viability of *C. albicans* growth was initially investigated in micro-titer experiments for 48 h. A range concentration of 0 to 0.5 mM was tested as presented in Fig. 4.1. It was observed that $K_3[Fe(CN)_6]$ was biocompatible under the range of concentration tested. 0.1 mM was however chosen for subsequent electrochemical experiments. At neutral pH and at 37 °C, $K_3[Fe(CN)_6]$ has a redox potential of 0.239 V, which is lower than the applied voltage (0.4 V), therefore, the extracellular current can be captured at the electrode. Control experiments at 0.6 and 0.8 V, resulted in reduced current output (Fig. 4.2 (B)). This is consistent with previous observations that applied potential greater than 0.4V could negatively impact cell membrane integrity, leading to reduced growth and suboptimal extracellular electron transfer (Teravest & Angenent, 2014).

4.3.1.1 Chronoamperometry

Because current output is an indirect indicator of cell growth and biofilm development (Sánchez et al., 2020), the chronoamperometric response of untreated *C. albicans* biofilms was initially compared to crystal violet estimate for biofilm cells ands and OD_{600} of planktonic cells, all obtained under the same experimental conditions. As presented in Fig. 4.2 (A), the current trend obtained during a 48-h period, as well as the OD/crystal violet estimates at 3, 6, 12, 24, and 48 h, follow a similar pattern. The current peaks at 10 h, which correlates to the early growth phase (8–11 h) of *C. albicans* biofilm (Rodríguez-Cerdeira et al., 2020), while OD and crystal violet estimates peak around 24 h. Because there is no statistically significant difference between the planktonic and biofilm estimates (Appendix 4.1(A), Appendix 4.2), the current output appears to be a function of cell growth and metabolism in the biofilm phase (Appendix 4.3). Additional control experiments were carried out to validate the hypothesis. *C. albicans* biofilm formed on the working electrode surface area were imaged at varying time intervals to monitor the colonization pattern of the biofilm on the electrode (Appendix 4.1(B)). A Fluorescence

Stereo Zoom Microscope (ZEISS Axio Zoom.V16) was employed for this purpose. All images were acquired with 25× magnification lens. Few cells indicating initial attachment of cells to the electrode surface were observed between 0-1 h, which increases with time up to 5 h. At 10-15 h, there is proliferation of biofilm cells coupled with expression of extracellular polymeric matrix, this may have contributed to the saturation of the current out as observed in the chronoamperometric trace, as the surface area is almost entirely clouded with biofilm. At 25 h, there seems to be more EPS covering the biofilm cell, thus, contributing to the reduced fluorescence (Appendix 4.1(B)). At this time, the nutrient depletion in the medium would lead to a lower current output, independently from the concentration of biofilm. The washing steps included in the crystal violet method and the inability to distinguish between viable and dead cells in OD measurement might have contributed to the different pattern observed with respect to electrochemical methods. However, as the time of saturation of the current output corresponds to the early-stage biofilm formation of *C. albicans*, it validates that our method is sensitive to detect and monitor early attachment and development of the biofilm cells. Finally, it is important to note that respiration and growth are different, though related. The former is more sensitive and reliable in biosensing for diagnostic applications as only living cells can respire. Consequently, of all the methods, only chronoamperometry could successfully capture the respiratory processes, thus, making it a suitable approach for distinguishing between live and dead cells – an essential feature lacking in OD and crystal violet measurements.

This finding contrasts earlier studies, which found that cells in both the biofilm and planktonic phases contributed to the electrochemical response (Astorga et al., 2019; Borole et al., 2011). However, Astorga and associates recently attributed the charge output of *E. coli* biofilm growth obtained in a 24 h potentiostatic condition to biofilm formation processes only because the concentration of cells in the planktonic phase did not change significantly (Astorga et al., 2020). Consequently, more research is needed to validate the independent contribution of planktonic and biofilm biomass to electrochemical responses. Nevertheless, it is interesting to note that the current output observed in this study increases rapidly than the OD/crystal violet assay, validating the sensitivity of our approach, with a promising potential for real-time biosensing applications.

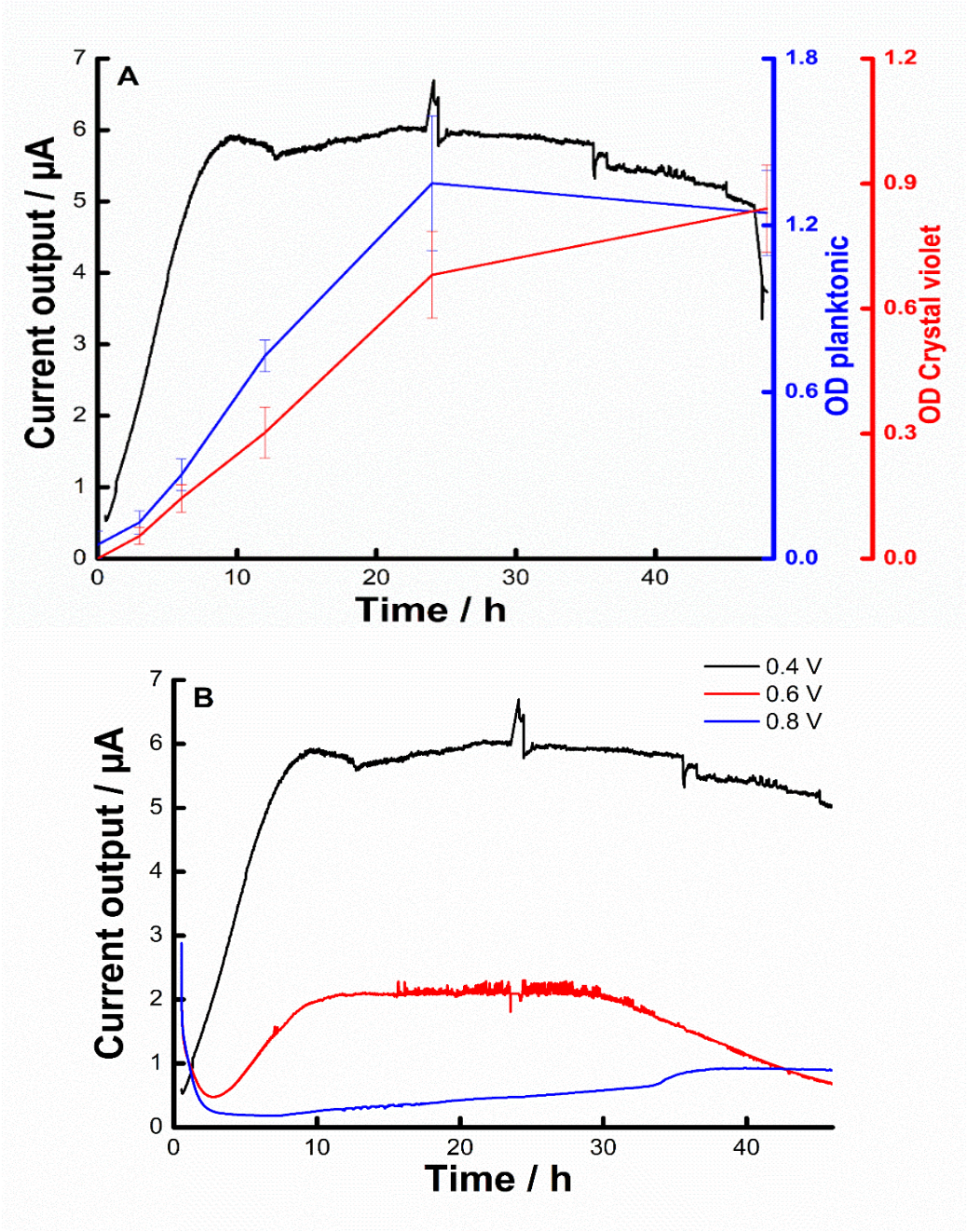

Fig. 4.2. (A) Comparative biofilm and planktonic estimates of *C. albicans* (n =4) and the current output (n=3). (B) Current output of *C. albicans* biofilm at varying applied potential (V) (n = 3).

Furthermore, the current output of *C. albicans* biofilm was drastically reduced when treated with the tested antifungal compounds (Fig. 4.3 (A)). At 10 h, the current output was ~ 6.0±1.4 µA for untreated biofilms, while ~3.1±0.2 µA, 1.6±0.1µA and ~0.7±0.1 µA for biofilms treated with Flz, AmB, and complex 3, respectively. Similarly, the estimates for both planktonic and biofilm cells obtained post-electroanalysis via crystal violet assay (Fig. 4.4B) and optical density measurement (Fig. 4.4A) for treated biofilm reduced significantly in comparison with untreated biofilm (Fig. 4.4). For context, Flz, AmB, and complex 3 exhibited 47.3 %, 54.2 %, and 74.8 % inhibition of planktonic cells, and 84.6 %, 77 %, and 98.5 % inhibition of biofilm cells, respectively, as compared to the control (Appendixes 4.2 and 4.3).

Additionally, the total charge output (Q, mC), which is the integral of current output with time, could also be used to describe the antifungal drugs' effect. As presented in Fig 4.3(B), the total charge outputs of untreated and treated biofilms differ significantly ($p < 0.05$) (Appendix 4.4). Relative to the untreated *C. albicans* biofilm, Flz, AmB, and complex 3 showed 43.1 %, 84.2 %, and 90.1 %, reduction in Q (mC), respectively, at 24 h (Appendix 4.4). Therefore, the efficacy of antifungal drugs on early fungal biofilms can be conveniently evaluated using both current and charge output measurements.

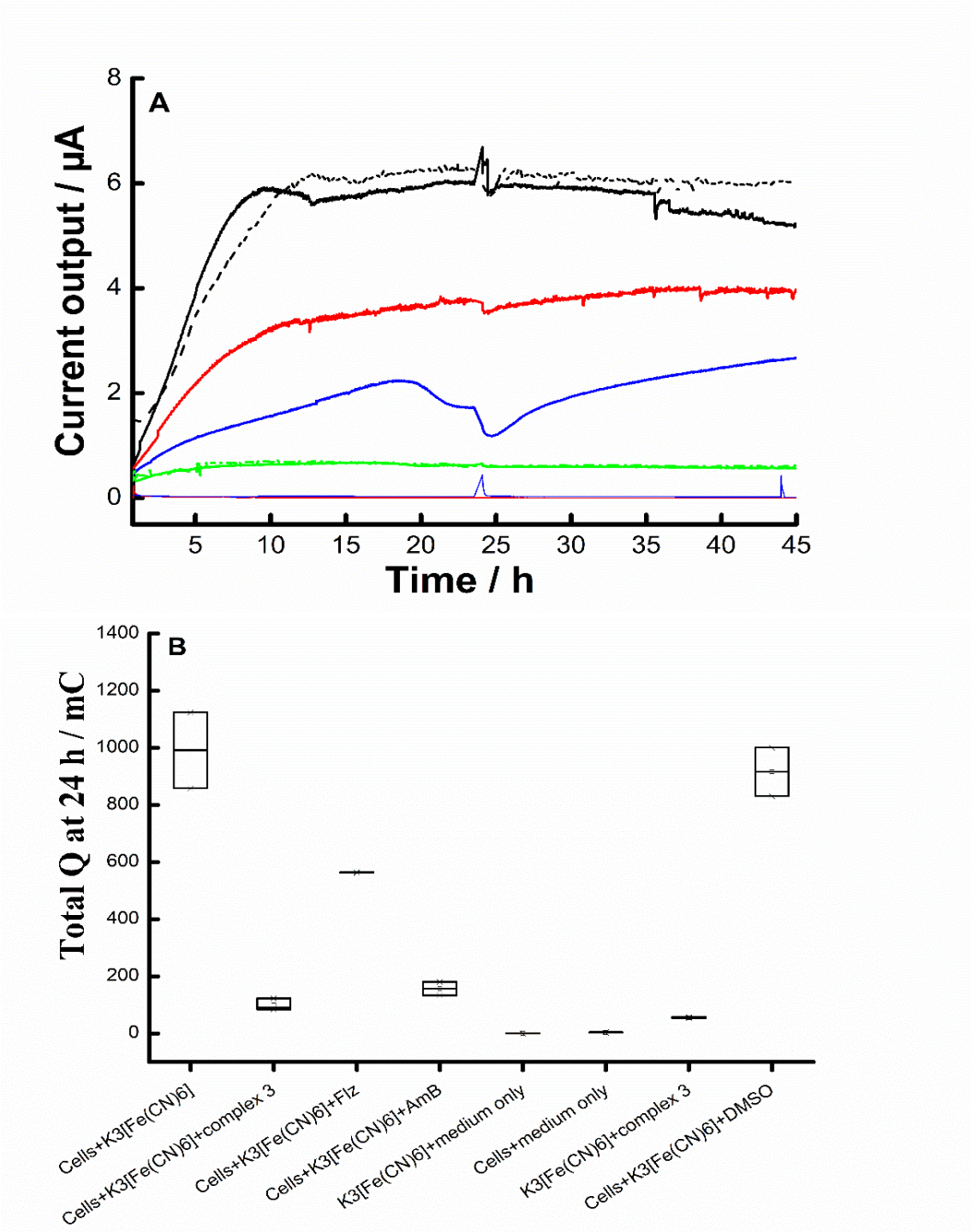

Fig.4.3. (A) Effect of tested antifungals on the current output of *C. albicans* biofilms: cells with $K_3[Fe(CN)_6]$ only (black trace); cells with DMSO (dotted black trace); cells with complex 3 (green trace), Flz (red trace), AmB (blue trace); cells only (thin blue trace); $K_3[Fe(CN)_6]$ and complex 3 only (thin dotted green trace); $K_3[Fe(CN)_6]$ only (thin red trace). (B) Total Q after 24 h of incubation at E = 0.4 V (n=3). The differences between controls and antifungal experiments are statistically significant ($p < 0.05$) (Appendix 4.4).

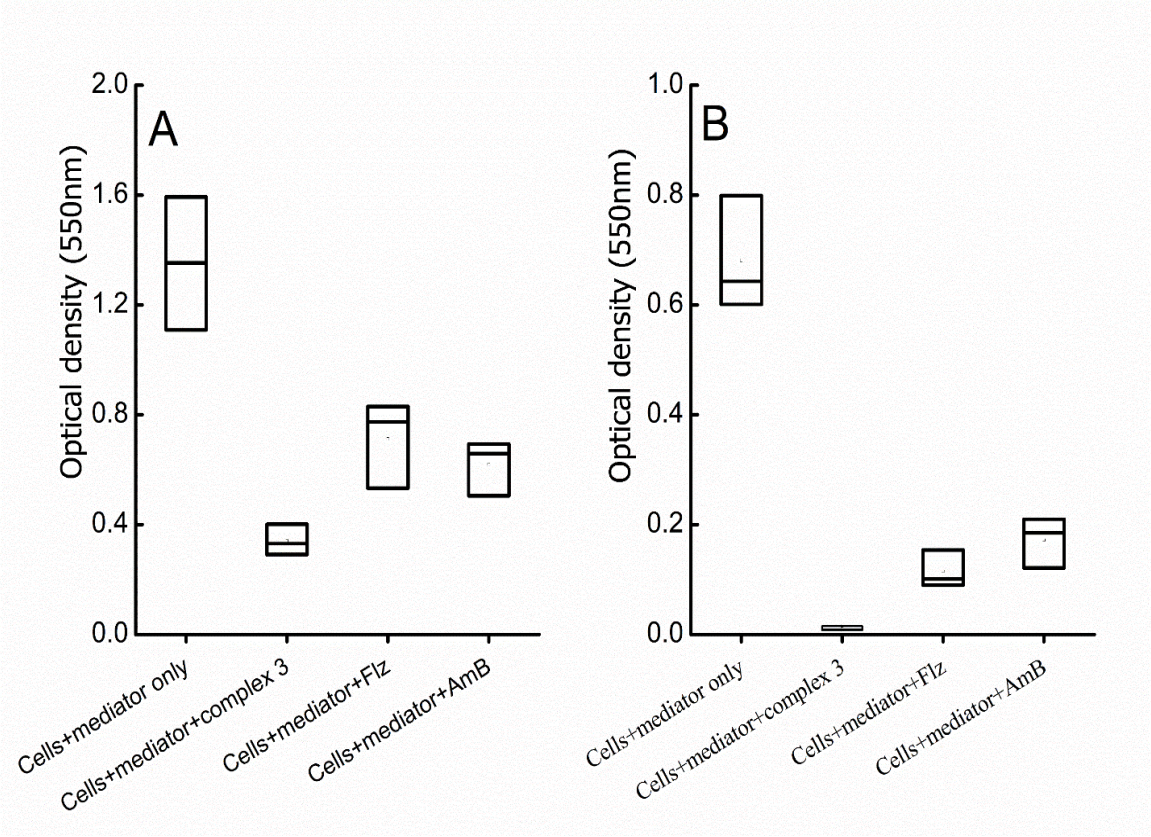

Fig. 4.4: (A) OD of planktonic cells in different experimental conditions after 24 h growth at E = 0.4 *vs*. Ag pseudo-reference electrode. (B) Biofilm cells estimates obtained via crystal violet assay for the different experimental conditions after 24 h growth at *E* = 0.4 *vs*. Ag pseudo-reference electrode. The difference between each pair of conditions is statistically significant ($p < 0.05$), with smaller OD and biofilm formation in the presence of Flz, AmB and complex 3. (n = 3).

4.3.1.2 Cyclic voltammetry (CV)

CV can be used to monitor the metabolic state of adhered biofilm cells (Babauta et al., 2012; Marsili et al., 2010) either in the absence or presence of antimicrobial treatments (Chalenko et al., 2012). Even though low scan rates (1-5 mV/s) are often adopted for microbial studies because they allow detection of slow interfacial electron transport features in biofilms. But because there was no prior understanding of the voltammetric behavior of *C. albicans* biofilm in the presence of antifungals, scan rates of 1 and 10 mV/s at three-time intervals (0, 24, and 48 h) were carried out. Interestingly,

the voltammograms produced at both scan rates were identical, suggesting that the EET rate was rapid, allowing detection of the antifungal effect.

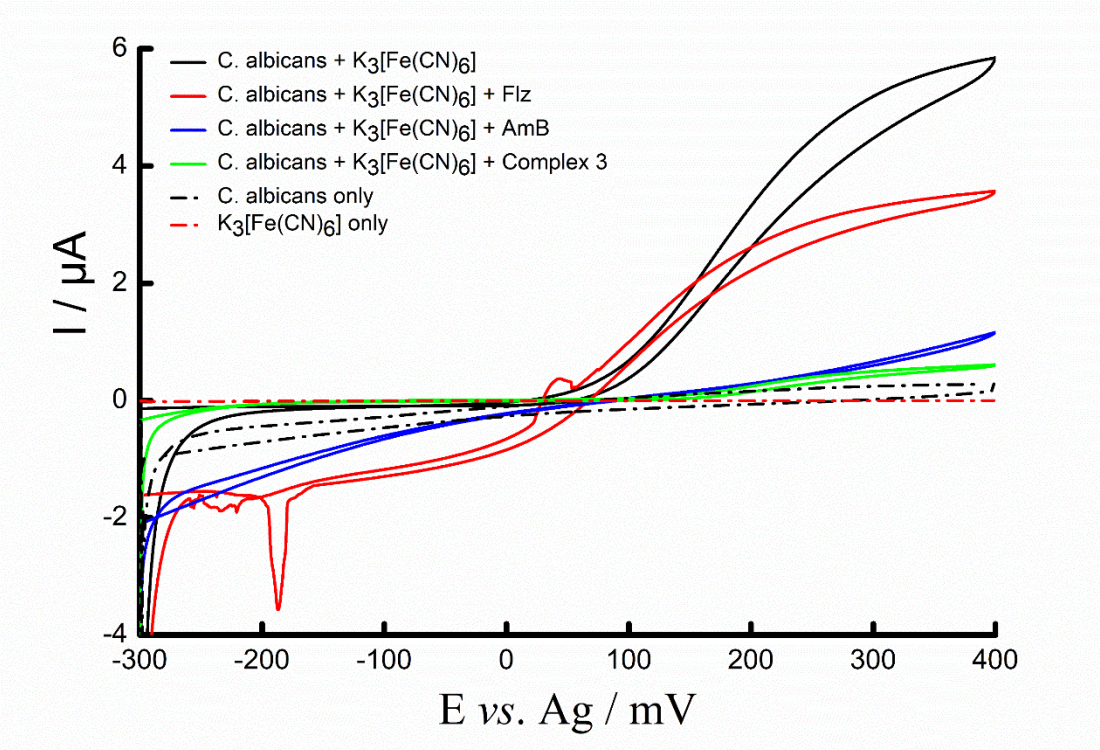

Fig. 4.5. Cyclic voltammograms of *C. albicans* ATTC 10231 at 24 h at 1 mV s^{-1}. (n = 3).

At 1 mV/s scan rate, the CVs at 0 h, (i.e., the CVs at inoculation and within 0 h of antifungal treatments) were identical for all experimental conditions (Fig. 4.5), showing turnover reduction of $K_3[Fe(CN)_6]$ and near-zero anodic current. The cathodic current had an onset potential of 140 mV, with the exception of the complex 3, which had an onset potential of 60 mV. At 24 h, however, the $K_3[Fe(CN)_6]$ turnover oxidation was observed. Anodic current was maximum in the absence of antifungal drugs and lowest in the presence of complex 3. These findings are similar to those of the CA, however the effect of AmB appears to be higher in the CV than in the CA. At a scan rate of 10 mV/s, a similar pattern was observed (Appendix 4.5). Overall, the CV results support the CA analysis.

The behavior of the redox mediators used under the experimental electrochemical conditions as reported in the thesis do not show unique peak characteristics as often observed in most cyclic voltammograms, especially when tested alone in all control experiments or under non-turnover conditions in other experimental conditions as evident in all cyclic voltammograms presented in the thesis. This may be attributed to the low concentrations (50 – 100 μM) adopted in our studies. However, under turn-over conditions in the presence of the *Candida* cells, its supports efficient cellular respiration and provides sufficient electrochemical response, quantifiable as total oxidative current.

Since voltammetry provides information only about the interfacial electron transport at the electrode surface (Saito et al., 2019), the rate and amount of electron transport at the electrode surface could be correlated to the total mass of metabolically active cells at the electrode surface (biofilm formation). Therefore, the higher the total oxidative current (i.e., electrons transfer from the biofilm to the electrode), the likelihood of the more biofilms formed on the electrode surface, and vice versa. For example, in Fig. 4.5, the red dotted trace corresponds to the redox mediator ($K_3[Fe(CN)_6]$) in absence of cells, which produced a flat voltammogram without identifiable peaks or features, while in the presence of *C. albicans* (solid black trace), it produces the maximum oxidative current attributable to the actively growing biofilm cells on the electrode. Furthermore, under antimicrobial treatments, the total oxidative current reduced significantly in relation to the control, in the order of Flz (solid red trace), AmB (solid blue trace) and complex 3 (solid green trace), suggesting that these antibiofilm molecules had inhibitory effect on biofilm formation and/or metabolic/respiratory processes of the biofilm cells at the electrode.

4.3.1.3 Impedance analysis

EIS has been used to characterize bioelectrochemical interactions in the past (McEachern et al., 2020; Sánchez et al., 2020). The biofilm thickness and composition at the electrode surface (Astorga et al., 2019) as well as other factors often contribute to impedance measurements. As a result, EIS may possibly be used to evaluate the impact of antimicrobial treatments on biofilms. Earlier investigations have used a two-time constant equivalent circuit to model the EIS results. However, due to the high variability of the

results in this study, it is difficult to discern a clear trend. It was, however, noted that the single frequency EIS at 50 mHz showed a distinctive pattern between treated and control cells.

Therefore, only this EIS data was presented. The impedance was higher for untreated biofilm (control) (Fig. 4.6), probably due to unrestricted cell growth and extracellular matrix of the biofilm, while for treated biofilms, the impedance was lower, probably due to reduced cell and biofilm growth upon exposure to the drugs. The strong effect of complex 3 observed in the CA and CV results, were however lacking in the EIS result. While the EIS results are intriguing, they exhibit more variability than the CA, indicating that EIS may be unsuitable for monitoring of *Candida* biofilms under the experimental conditions described in this study.

4.3.2 Raman spectroscopic analysis of electrode surface

The effect of the antifungals on biofilm attachment and components was assessed using Raman imaging of the electrodes after the electrochemical measurements were completed. In comparison to treated biofilms, the untreated biofilm appears to include a hyphal matrix containing biomolecules such as proteins, lipids, and carbohydrates, as revealed by the Raman spectra (Fig. 4.7).

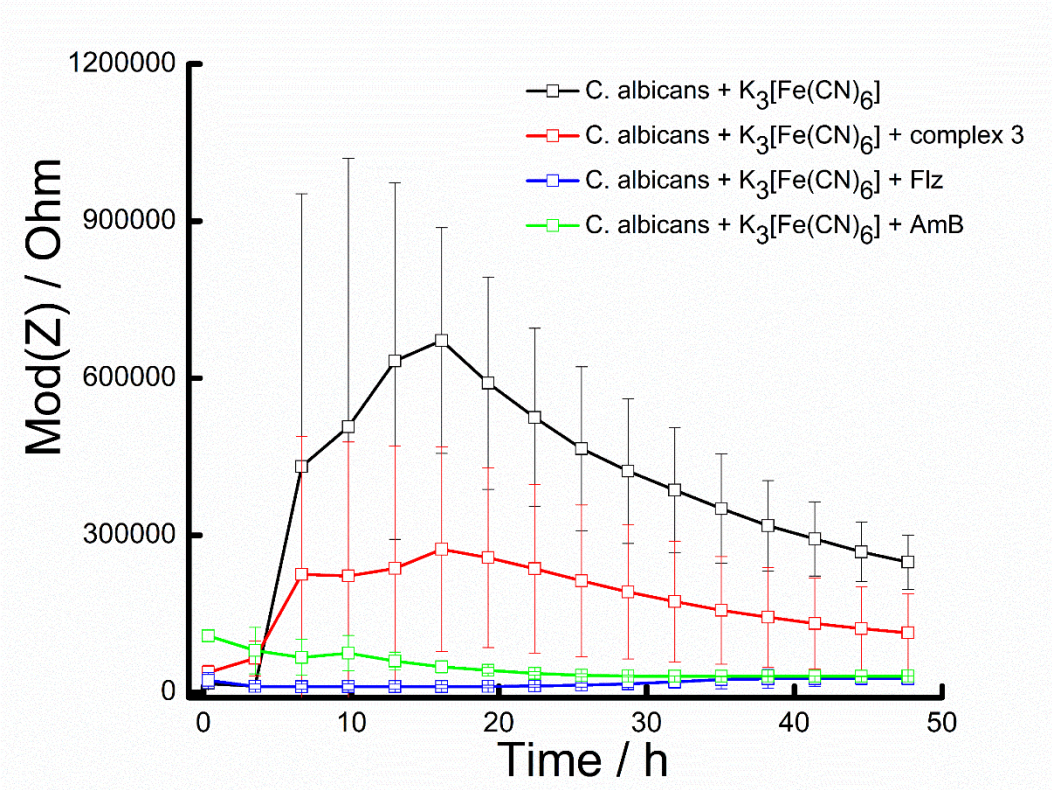

Fig. 4.6: Modulus of impedance with time. Cells with $K_3[Fe(CN)_6]$ (black trace); cells with complex 3 (red trace), Flz (blue trace), and AmB (green trace).

It has been observed that Raman imaging can be used to analyze and characterize biological samples, including microbial cells (Hrubanova et al., 2018). However, to induce excitation and get Raman scattering, a laser beam focused on a tiny sectional sample is usually applied (Huang et al., 2020). Due to the low strength of the Raman scattering signal, single bands associated with specific chemical binding could not be recognized in this study. The D (disordered) and G (graphite) bands specific to the graphitic substrate occupy the spectral range (150 and 2460 cm^{-1}) and are dominated at around 1350 and 1560 cm^{-1} which may have impacted the identification of peaks important for cellular vibrational modes. Also, the signal of numerous bands related to vibrational modes and associated with the cellular and extracellular components of *C. albicans* that are found primarily between 1100 and 1650 cm^{-1}, as reported in literature (Potocki et al., 2019), was covered by high intensity of the two substrate bands. Nonetheless, Fig. 4.7 shows images that provide an estimate of fluorescence levels and could be used to detect cells and organic materials.

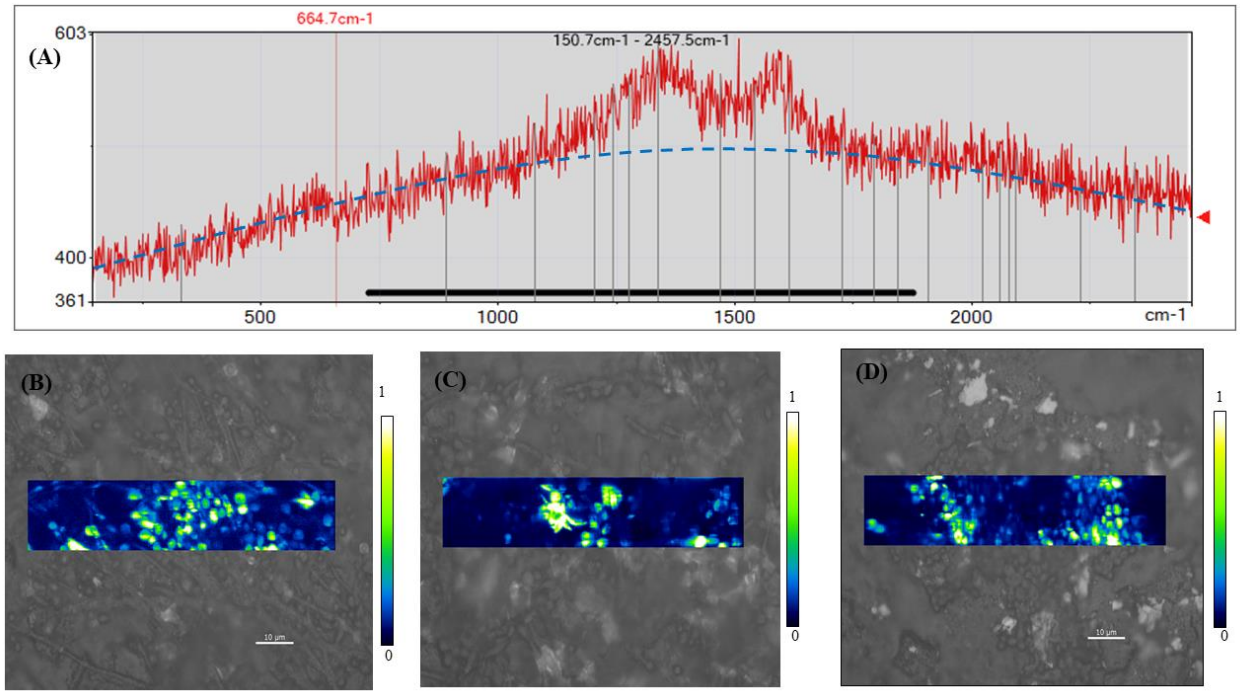

Fig. 4.7. Representative Raman images of *C. albicans* ATCC 10231 on the WE area after 48 h potentiostatic experiment.

Fig. 4.7(A) shows Raman spectra collected on C. albicans in the spectral band 400-2900 cm^{-1}, with the intensity (y-axis) commencing at about 400 counts due to fluorescence. As the spectral baseline (blue dotted line) increases, the fluorescence increases. Aromatic and heterocyclic chemicals such as proteins, lipids, and carbohydrates are frequently responsible for fluorescence in biological products. These components are abundant in the fungal biofilm's exterior matrix. By contrasting these images to the Green (biofilm) images, it is easy to differentiate between cells and biofilm.

Fig. 4.7(B) shows Raman imaging of untreated cells, which show uniform and high cell counts surrounded by hyphal materials, whereas Fig. 4.7(C) and Fig. 4.7(D) shows Raman imaging of cells treated with Flz and complex 3, respectively. The intensity scale next to each image helps to understand how cells in Fig. 4.7(C) and Fig. 4.7(D) are not homogeneously dispersed as in 5B, and how the decreased cell number indicates an

influence on growth caused by the two antifungal compounds. For each sample, three areas were scanned, and the spectra compiled.

4.3.3 Scanning electron microscopic (SEM) analysis of electrode surface

Post-electroanalysis, SEM analysis was also used to visualize biofilm formation on the WE surface. In the untreated biofilms, an extended hyphal growth surrounded by a matrix of polymeric substances (Fig. 4.8(A)), whereas biofilm cells treated with Flz (Fig. 4.8(B)), AmB (Fig. 4.8 (C)), and complex 3 (Fig. 4.8 (D)) showed sparsely dispersed cells with a strong likelihood of membrane disruption and/or other morphological injury.

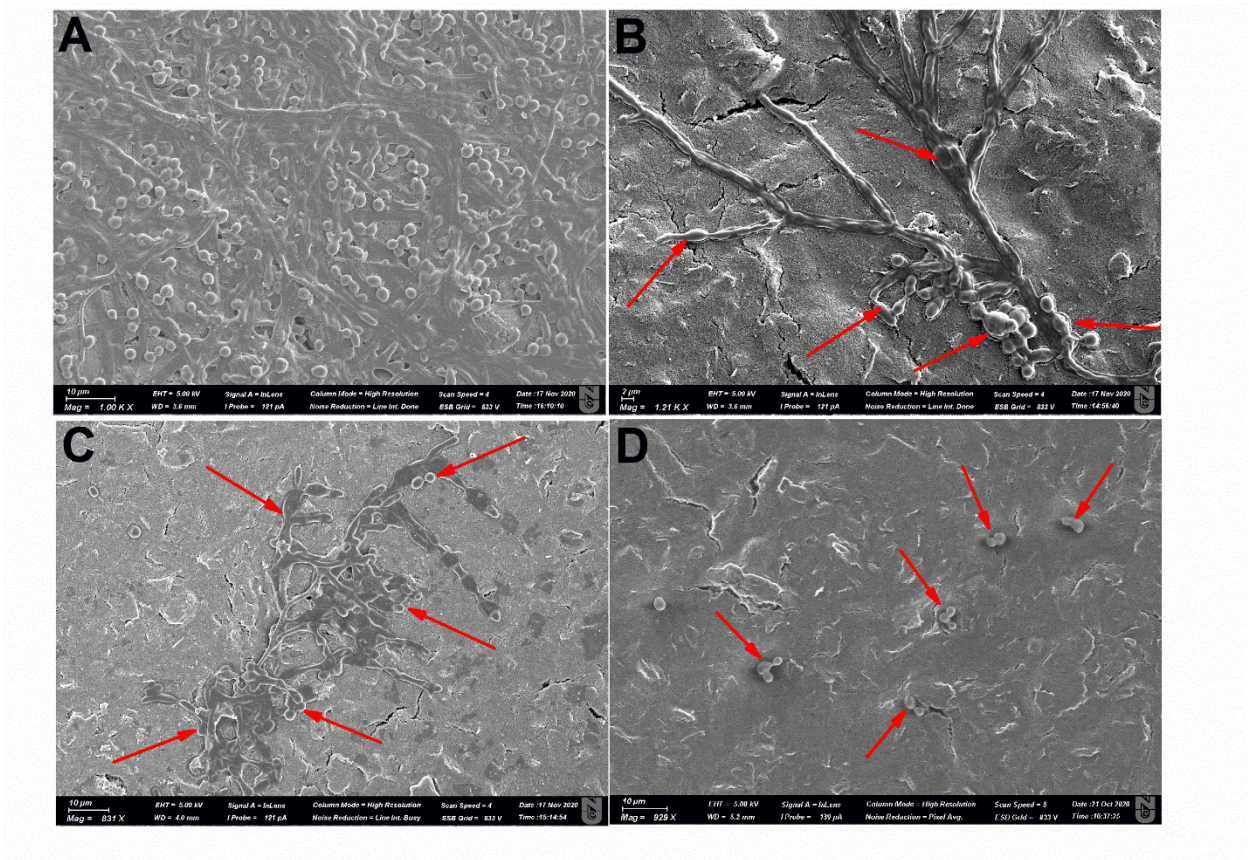

Fig. 4.8. Representative of *C. albicans* ATCC 10231 on the WE area after 48 h potentiostatic experiment obtained via scanning electron microscopy. (A) Cells not exposed to antimicrobials demonstrating massive biofilm matrix and hyphal proliferation. (B) Cells exposed to Flz demonstrating limited hyphal growth. (C) Cells exposed to AmB demonstrating scanty yeast cells with membrane damage. (D) Cells exposed to complex 3 also demonstrated scanty yeast cells.

4.3.2 Gold standard method – XTT assay

Spectrophotometric XTT assays are commonly employed for high-throughput monitoring of microbial activity and evaluation of antimicrobial agents (Kuhn et al., 2003; Meshulam et al., 1995). This approach is, however, destructive, as the biofilm cannot be further examined, at the end of the assay. Nevertheless, it is important to compare or validate our electroanalytic results with XTT results. When the antifungal compounds were added at inoculation and at 1×MIC, a considerable antibiofilm impact was observed, especially with AmB (Fig. 4.9). However, their relative effect to what is observed from electroanalysis (Figure 4.3(A)) is different. The application of a considerably larger dose (10×MIC) of the tested compounds resulted in complete biofilm inhibition (Fig. 4.9).

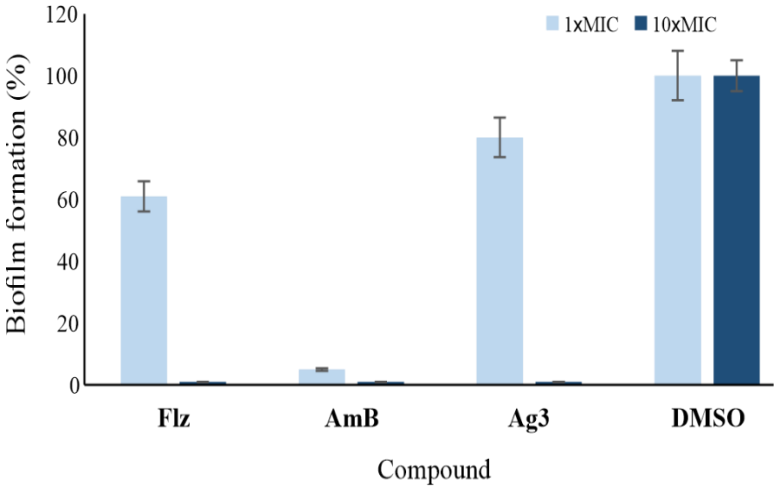

Fig. 4.9. Biofilm formation by *C. albicans* following addition of Flz, AmB and Ag3 at inoculation at two different concentrations (1×MIC and 10×MIC) evaluated by XTT reduction assay.

The same approach was adopted to evaluate the antibiofilm activity when the cells were grown, first for 8 h to allow early biofilm formation (Appendix 4.6(A)). 1×MIC, all the three compounds did not remove already-formed biofilms, while 10×MIC, complex 3 and AmB caused 90% and 40% of biofilm removal, respectively, relative to DMSO treated controls (Appendix 4.6(A)). Allowing longer durations (12 and 16 h) before adding antifungal drugs resulted in no measurable antibiofilm activity (data not shown). Only

100×MIC demonstrated some biofilm removal activity against 48 h old pre-formed biofilms, with complex 3 being the most effective (Fig. 4.6(B)).

4.4 Summary

Electroanalysis indicated that the antifungal activity of the compounds evaluated in this study are in the order of complex 3>AmB>Flz, while the conventional XTT indicated the order of AmB>Flz>complex 3. Interestingly, AmB and Complex 3 exhibited comparable activity when measured using the OD measurements for both biofilm and planktonic cells. Furthermore, EIS did not demonstrate a definite activity order due to the considerable heterogeneity of the results. In general, these findings support the necessity for multi-method antifungal activity characterization.

The inconsistency observed with respect to the different assay methods is not surprising, as this is a common problem with the exiting conventional antibiofilm testing methods (Ernst, 2007; Maurizio Sanguinetti & Posteraro, 2018). This problem is partly because several of these methods are, in principle, based on methods for their planktonic counterpart (Beauvais & Latgé, 2015; Di Domenico et al., 2018; Ramage & Williams, 2013; M. Sanguinetti & Posteraro, 2017) as methods for antibiofilm assessment is more or less non-existent. Fundamentally, this is problematic, and often results in inconsistency, even among different laboratories, thus, making reproducibility difficult (Kuper et al., 2012). In addition to the inherent irreproducibility of biofilms concentration and microstructure (Azevedo et al., 2021), the destructive nature of biofilm detection methods and the lack of standardized protocols contribute to the observed inconsistencies. This is part of our motivations for this thesis, and why electrochemical approaches are being proposed as additional/complementary method.

Electrochemical techniques are not destructive (or, at least, much less destructive) and the protocols have been standardized over many years of research in the related areas of batteries and capacitors, so adoption among different laboratories will provide consistent results. Further, CA allows a direct, real-time measurement of electroactivity (Turick et al., 2019) and could provide reliable physiological details on the metabolic state of cells in the biofilm, thus, makes it a suitable approach for distinguishing between live and dead cells

– an essential feature lacking in the conventional methods for biofilm quantification. Therefore, critical assessment of the rankings indicates that the one obtained from electroanalysis may be more reliable and should be compared in future with emerging standard methods like the single tube method (Goeres et al., 2019).

Conclusively, in this study, we have demonstrated, for the first time, the real-time antibiofilm assessment of selected antifungal compounds against *C. albicans* using an electroanalytical approach. However, in addition to being simple to understand, chronoamperometric results are more informative, and offers consistent findings as early as 10 h following inoculation. This electrochemical approach can be used to identify antifungal drug-resistant strains. If adopted in health-care settings, could aid in the efficient use of antifungal drugs, limiting the establishment and spread of antifungal resistance strains. However, a potential limitation of this approach may concern antifungal drugs that maybe electroactive or exhibit degradation upon exposure to applied potentials, as this might lead to misinterpretation of the results.

As a result of the intriguing results obtained in this study, and our desire to provide an alternative, viable, simple, and low-cost therapeutic platform for effective diagnosis and management of clinically relevant microbial pathogens, particularly antibiotic-resistant strains, we extended the use of our bioelectrochemical platform to the analysis of another dreaded pathogen, this time using a drug repurposing strategy, as would be present in the next chapter.

4.5 Outcome

Olaifa, K., Nikodinovic-Runic, J., Glišić, B., Boschetto, F., Marin, E., Segreto, F., & Marsili, E. (2021). Electroanalysis of Candida albicans biofilms: a suitable real-time tool for antifungal testing. *Electrochimica Acta*, *389*, 138757. https://doi.org/10.1016/j.electacta.2021.138757.

Chapter Five: New use for old drugs: repurposing antifungals against resistant bacterial biofilms via biochemical and bioelectrochemical assessment

5.1 Introduction

Antibiotic resistance (AR) is one of the most serious global healthcare issues of the twenty-first century (Wang et al., 2020). Antibiotic-resistant bacteria infect more than two million individuals in the United States each year, resulting in the death of more than 23,000 people annually (CDC, 2019). In the United States, resistant bacterial infections cost more than $20 billion per year (Ibberson & Whiteley, 2020), with an estimated global cost of more than $35 billion per year (Aslam et al., 2018). As previously discussed in sections 2.3 and 2.5.1, this phenomenon is prevalent in biofilm forming microbial species (Leão et al., 2020; Pacios et al., 2020).

AR is a complex phenomenon, and it causes are multifaceted, hence there is no single or simple remedy available yet (Aslam et al., 2018). Sadly, the discovery and development of new antimicrobials cannot match up with the rate of rise and spread of AR (Leão et al., 2020), therefore, innovative approaches are needed to prevent/minimize treatment failure. Combination therapy that requires joint administration of two or more antibiotics (Konreddy et al., 2018; Wang et al., 2020) and drug repurposing (Kamurai et al., 2020; Peyclit et al., 2019; Rangel-Vega et al., 2015) have gained attention in recent years.

The use of drugs to control pathogens outside their natural medical indications is referred to as drug repurposing (Richter et al., 2017). This approach was originally borne out of curiosity/luck/mistake, but it is now being clinically adopted, with multiple success stories already reported in the literature (Pushpakom et al., 2018). It is also now being projected as an approach that will speed up the discovery of novel drugs effective against resistant pathogens (Kaul et al., 2019). Because these drugs' safety reports and other pharmacological details are known, this strategy offers low risk of toxicity, reduced costs as well as time (Oliveira et al., 2020).

Mourenza et al. (2020) reported an extensive review on therapeutic management of *Mycobacterium tuberculosis* using drug repurposing strategy. Kamurai et al. (2020) had also described repurposing strategy of non-antibiotic drugs including antimalarial and anti-

inflammatory against *S. aureus* and *P. aeruginosa* biofilms. Similarly, Niclosamide and pentamidine, which are anti-helminthic and antiprotozoal, respectively, were repurposed against *P. aeruginosa* and other bacteria (Imperi et al., 2013; Stokes et al., 2017). Recently, tamoxifen, a well-known anticancer medicine, was repurposed for the treatment of *C. albicans* and other fungal infections (Farha & Brown, 2019). Also, Siala et al. (2016) found that the antifungal caspofungin significantly inhibited *S. aureus* biofilms. Benzimidazole, a fungicide, has also been used to mitigate *S. aureus* biofilm in a few trials (Kong et al., 2018). These successes, which came about mostly as a result of unintended applications and observations, boost the quest for more repurposed drugs, especially against biofilms and antibiotic-resistant bacteria. Nevertheless, a drug repurposing strategy investigating the effect of clinically relevant fungicides on the viability and biofilm development of *A. baumannii* is yet to be deservedly explored. As previously noted in chapter 2 (section 2.5.1), this bacterium has a special status designated by WHO and CDC and requires urgent therapeutic intervention.

Using biochemical and electroanalytical techniques, the effect of selected fungicides on *A. baumannii* biofilm is examined in this work.

5.2 Materials and methods

5.2.1 Materials

The bacterial strain – *A. baumannii* ATCC 19606 was used. It was initially sub-cultured nutrient agar and grown in LB broth in subsequent experiments.

Dimethyl sulfoxide (DMSO), Fluconazole (Flz) Itraconazole (Itz), Ampicillin (Amp), ciprofloxacin (Cip), absolute ethanol, nutrient agar, crystal violet, and 2- hydroxy-1,4-naphthoquinone (2-HNQ), Luria-Bertani (LB) broth, glacial acetic acid. All drugs and chemicals were of analytical grade, and were acquired from Sigma Aldrich, Kazakhstan.

Screen-Printed Carbon Electrodes, same as previously described in chapter 3 (section 3.2.1) were used for all bioelectrochemical experiments.

5.2.2 Biochemical methods

5.2.2.1 Bacterial viability and determination of MIC

Using absorbance measurement at 600 nm in 96-well plates with a Gen5TM Microplate Reader and Imager Software (BioTek Instruments), the viability of the test strain was assessed following addition of different concentrations of the test drugs (Amp, Cip, Flz, and Itz) in LB broth, and incubated at 37 °C for 24 h under static condition. Except for Cip which was dissolved in sterile double-distilled water, stock solutions of Amp, Flz and Itz were prepared in DMSO. OD_{600} of 0.1 (~1×10^6 CFU/mL) prepared from an overnight culture was used as an inoculum. Three independent biological replicates were carried out, and results analyzed and recorded as mean ± standard deviation. The highest drug concentration tested was 100 μM, while the MIC was determined and recorded according to the method previously described in section chapter 3 (3.2.2).

5.2.2.2 Biofilm formation/inhibition assay

The conventional crystal violet staining method in 96-well plate, previously described in chapter 4 (section 4.2.2.4) was adopted but with slight modification. Briefly, an 18 h old culture of *A. baumannii* culture in LB broth adjusted to an OD_{600} of 0.5 was used as inoculum. The drugs were added at 1×MIC and 10xMIC. 0.1 mM 2-HNQ was also added to all the wells to mimic the electroanalytic condition. Wells with the inoculum but without the drug are used as control. Following incubation at 37 °C for 24 h, the medium and planktonic cells were gently removed, and the wells were rinsed twice with sterile water. After that, the biofilms were fixed for 10-15 minutes in absolute methanol, rinsed twice with sterile water, and left at room temperature to dry. Thereafter, the biofilm was stained and processed as previously described in section 4.2.2.4. This was independently repeated three times, and the results reported as percentage of biofilm inhibition relative to the control.

Additionally, the effectiveness of the test drugs to remove preformed biofilm of *A. baumannii* were also assessed also in 96-well microtiter plates as previously described in section 4.2.2.4. Similarly, the procedure was repeated three times using independent

inoculum, and the results expressed as percentage of biofilm inhibition relative to the control which was calculated using the formula below;

$$\text{Percentage (\%) biofilm inhibition/removal} = \frac{\text{OD570 of Control} - \text{OD570 of Treatment}}{\text{OD570 of Control}} \times 100$$

5.2.3 Bioelectrochemical methods

The antibiofilm efficacy of Cip, Flz and Itz against *A. baumannii* biofilms were also determined by electroanalysis using chronoamperometric method (scheme 3.1). As emphasized in chapter 4 (section 4.4), chronoamperometry is simple to interpret and provides efficient diagnostic information (Olaifa et al., 2021). In addition, the approach is primarily poised at a single potential, hence, constraints such as excessive background current and signal-to-noise ratios are greatly reduced (Aiyer & Doyle, 2021). Hence, our choice of electrochemical method in this work.

0.1 mM 2-HNQ as redox mediator and a working electrode voltage of 400 mV were found to be suitable for electroanalysis based on preliminary studies (Appendix 5.1). *A. baumannii* cells were cultivated in 8 mL electrochemical cells with an initial OD_{600} of 0.5 with Cip, Flz, and Itz added at their MIC. Control tests with LB broth, 2-HNQ, and DMSO were included. A computer-controlled VSP multichannel potentiostat (BioLogic, France), as previously described in section 3.2.2.2, was used. For each set of experiments, a minimum of three biological replicates were carried out, and the results reported as mean ± SD.

Chronoamperometry was also adopted to evaluate the effect of the test drugs (Cip, Flz, and Itz) on preformed *A. baumannii* biofilms. To achieve this, a sterile analytical grade micro-syringe was used to gently add the drugs into the electrochemical cells, usually at 12-15 h post-inoculation when the current output has become stable (Kannan et al., 2019). The working electrode was maintained at 400 mV for all chronoamperometric measurements while the average current was recorded every 60 s throughout the experiment. Prior to electroanalysis, all SPEs were pre-treated as previously described in section 3.2.1.

5.2.4 Post-electroanalysis: crystal violet assessment and microscopic imaging

Crystal violet assay and microscopic imaging of selected SPEs were carried out after bioelectrochemical studies to support the biochemical and bioelectrochemical results on the efficacy of tested drugs on *A. baumannii* biofilms. The crystal violet test and scanning electron microscopy were carried out according to the instructions in section 4.2.2.3. For each experimental condition, a minimum of three biological replicates were assayed/examined. For confocal laser scanning microscopy (CLSM 780; Carl Zeiss, Germany), images were taken using a 20×objective (Plan-Apochromat; NA = 0.8) with resolutions of 424.89×424.89 μm frame size with a pixel dwell duration of 1.6 μs. The thickness of the biofilms varied, but the 1.073 μm z-step widths were consistent across all samples. Autofluorescence was obtained in the epi-illuminated geometry by the objective between 585 and 734 nm using a 561-laser line. Zen Zeiss imaging software was used to analyze the images.

5.2.5 Data analysis

One-way analysis of variance (ANOVA) was used to compare independent biological replicates, followed by Tukey's test for multiple comparisons. The statistical significance was determined using a p value of 0.05.

5.3 Results and Discussion

5.3.1 Biochemical analyses

The efficacy of two commonly used antifungals, Itz and Flz, in addition to two commonly used antibacterial, Amp and Cip, were tested *in vitro* against *A. baumannii* biofilms. Presented in Fig. 5.1 and Table 5.1 are the results of the viability tests and the comparative MICs. With the exception of Amp (Fig. 5.1A), the test organism was sensitive to Itz, Flz, and Cip within the concentration ranges investigated (Fig. 5.1). Itz, Flz, and Cip showed a statistically significant dose-dependent activity ($p<0.05$) in comparison to untreated cells (Appendixes 5.2 and 5.3). Quantitatively, starting at 1 μM, a marked reduction in growth was seen as the concentrations of Itz, Flz, and Cip increased (Fig. 5.1). Cip had the most activity with the lowest MIC of 5.5 μM. (Fig. 5.1D). However, within

the dose ranges investigated, Amp showed no apparent effect against *A. baumannii*. With MIC values (µM) of 53.8 and 62, Itz (Fig. 5.1C) and Flz (Fig. 5.1B), respectively, had significantly higher activity than Amp and were only 10 times smaller than Cip (Appendix 5.3), making them promising candidates for additional testing against *A. baumannii* biofilms.

Table 5.1. Susceptibility profile (MICs, µM) of *A. baumannii*

	Minimum inhibitory concentrations (MICs, µM)			
	Amp	Cip	Itz	Flz
Test organism *A. baumannii*	> 100	5.5± 0.4	53.8± 2.5	62± 5.3

Result is presented as mean ± SD. At $p = 0.05$, all means are significantly different.

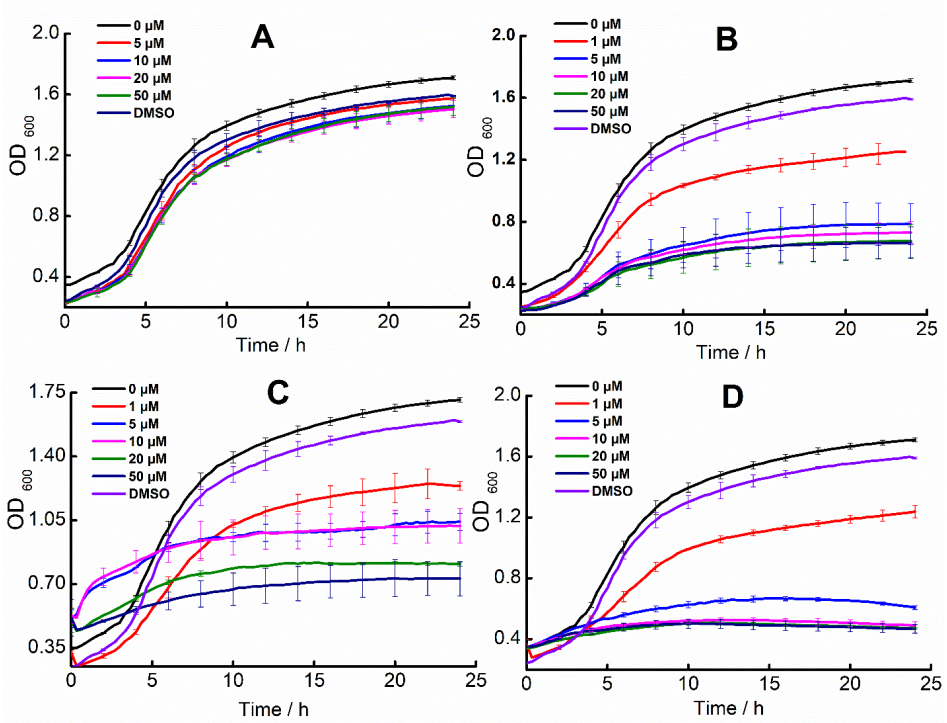

Fig. 5.1. Effect of (A) Amp, (B) Flz, (C) Itz and (D) Cip on growth (OD_{600}) of *A. baumannii*. Except for Amp, the difference between treatments vs control is significant ($p < 0.05$) (Appendixes 5.3A-5.3D).

Though bacterial strains capable of exhibiting resistance to nearly all available antibacterial drugs in the global arsenal are known to be emerging (Lenhard et al., 2017), the rising rate of antibiotic-resistant *A. baumannii* is alarming, as evidenced by data on resistance surveillance and prevalence studies conducted worldwide (Sarshar et al., 2021; Vrancianu et al., 2020). Reports of its resistance to levofloxacin, tetracycline, ceftriaxone, ceftazidime, Amp, and even Cip among many others are well documented in the literature (Babapour et al., 2016; Madadi-Goli et al., 2017; Nocera et al., 2021).

The resistance to Amp (a beta-lactam antibiotic) as presented in Fig. 5.1A is not surprising, as this bacterium was previously classified as a sequence type 52 strain with heightened resistance to beta-lactam antibiotics (Tsubouchi et al., 2020). The study of Tadesse et al. (2019) on the susceptibility patterns of pathogenic bacteria from pediatric patients indicated that 85.2% of the isolates including *A. baumannii* exhibited resistance to Amp. Its ability to form and exist as biofilms, in addition to its other resistance mechanisms, provides protection against physical and chemical attacks, including antimicrobials (Shenkutie et al., 2020).

Itz, Flz and Cip were further investigated for their biofilm inhibition/removal capacity in the standard microtiter plate-based crystal violet assay. Fig. 5.2A depicts the % biofilm inhibition when the drugs are added at inoculation, while Fig. 5.2B depicts % biofilm removal when the drugs were added 48 h post-incubation. 1×MIC of Cip, Itz, and Flz exhibited 59.2±1.0, 68±6.4, and 77±5.1 biofilm inhibition (%) (Fig. 5.2A), respectively, while 10×MIC exhibited a near 100% inhibition with Cip, Itz, and Flz yielding 97.13.4, 93.61.2, and 94.30.7 inhibition (%) (Fig. 5.2A), respectively. Statistically, there was no significant difference between Cip, Itz, and Flz in terms of biofilm inhibition (%) (Appendix 5.4), while significant difference existed between Cip and Flz in terms of biofilm removal (%) at 10×MIC alone (Appendix 5.5). While our results are consistent with previous studies on resistance profile of *A. baumannii* (Qi et al., 2016), there are no previous research on its antifungal susceptibility.

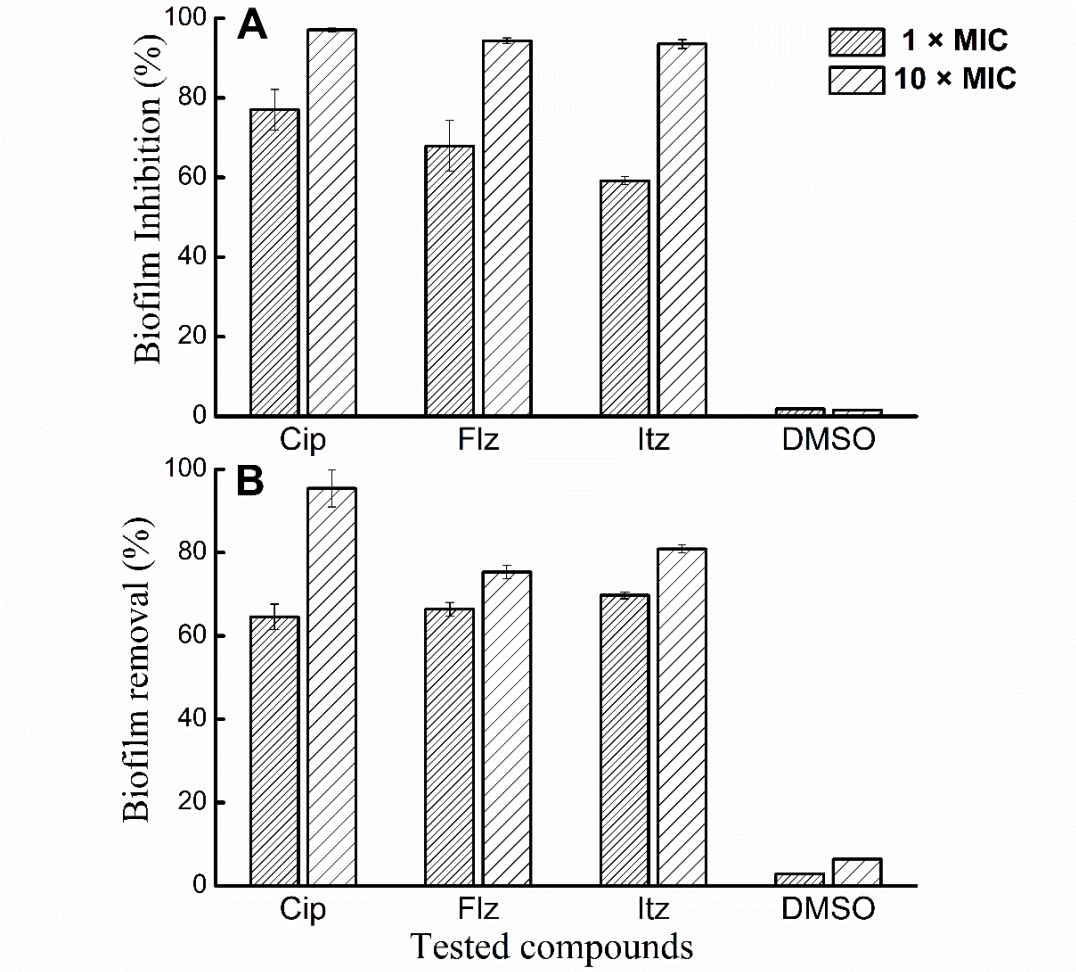

Fig. 5.2. Effect of Cip, Flz and Itz on *A. baumannii* biofilm formation. (A) Addition of drugs at inoculation; (B) Addition to preformed biofilm. (n=4). The difference between treatments vs control is significant ($p < 0.05$) (Appendixes 5.4 and 5.5).

5.3.2 Bioelectrochemical analyses

The sensitivity of *A. baumannii* biofilm to the selected antifungal drugs were also studied electro-analytically under two experimental conditions: a) addition of the drugs at inoculation for biofilm inhibition studies; and b) addition of drugs at 12-15 h after inoculation for biofilm removal studies. These conditions are complementary to the biochemical analyses and mimic an early *vs*. late treatment options using Itz, Flz, and Cip. Based on our prior research on bioelectrochemical characterization antibiofilm drugs against microbial pathogens (Olaifa et al., 2021; N. Savić et al., 2020), only CA was adopted in this work. Other approaches, such as EIS and voltammetry (e.g., differential pulse or square-wave voltammetry), may provide more information, but they have

low reproducibility than CA. Unlike other bioelectrochemical approaches, CA is non-destructive and well-suited for real-time monitoring of microbial growth (Turick et al., 2019; Uria et al., 2020).

The electroactivity of *A. baumannii* is low, as evidenced by control experiment in short-term experiments (24 h) (Appendix 5.6). To induce a stable electrochemical reaction, therefore, a redox mediator was utilized. However, as previously established for *E. coli* cells that show an electrogenic phenotype when cultured in microbial fuel cells for long period (> 20 days) (Qiao et al., 2008), it cannot be assumed that *A. baumannii* does not produce extracellular redox mediators or electrical charges at longer durations. However, sterile control experiments as presented in Appendix 5.6 confirm that the chronoamperometric output observed in this study is a function of the 2-HNQ redox coupling mediated by metabolically active biofilm cells on the electrode, resulting in extracellular electron transfer.

Furthermore, comparative control experiments of crystal violet assay and OD measurement for biofilm and planktonic cells, respectively, obtained under conventional (no applied potential) and potentiostatic conditions (Appendix 5.7B), and also with and without redox mediator (Appendix 5.7A), are not significantly different ($p<0.05$).

Similarly, preliminary experiments showed that 400 mV is optimum for the bacteria under study, as it supports efficient membrane modulation and electron transfer process. This is also supported by previous study on other clinically relevant microbial biofilms (Astorga et al., 2019; Naradasu, Guionet, Okinaga, et al., 2020; Santoro et al., 2016). Control experiments at applied potentials lower than 400 mV did not produce optimal current output, while higher potentials may have tensioned the cell membrane, resulting in unstable current response (Appendix 5.8). We, however, did not test negative potentials because of our previous knowledge on the electrochemistry of clinically relevant microbial biofilms, and also on the basis of literature reports (Bosire et al., 2016a; Wei et al., 2010; J. You et al., 2021). Nevertheless, preliminary experiments and optimization are necessary in determining the appropriate potential, as too low or high may negatively impact the electrochemical response (Bosire & Rosenbaum, 2017; Teravest & Angenent, 2014).

Consequently, electroanalysis was done at a constant applied potential of 400 mV in 8 mL cells using carbon screen-printed electrodes, while the drugs were added at their corresponding MIC values and in the presence of 0.1 mM 2-HNQ as mediator. Under this state, the oxygen in the electrochemical cell is used up quickly during the initial rapid bacterial growth, while a part of the electron flow resulting from growth and metabolism can be intercepted at the electrode. This simple approach has been repeatedly employed to characterize biofilm formation (Keogh et al., 2018) with or without antimicrobial treatments (Kannan et al., 2019; Olaifa et al., 2021; Savić et al., 2020).

Before addition of drugs, biofilm estimates via crystal violet assay and OD of planktonic cells were comparatively evaluated with the chronoamperometric response. Graphical representations of both OD and crystal violet estimates produced a similar pattern (Appendix 5.9), while the chronoamperometric data (Appendix 5.9), showed a slow current output in the early hours (0 - 7 h), before a rapid growth began. This is indicative of complex combined roles of initial cell attachment, biofilm formation and growth, and stimulation of extracellular electron transfer mediated by 2-HNQ redox coupling by actively growing metabolic cells. Chronoamperometric results validated that Itz, Flz, and Cip significantly affected *A. baumannii* biofilm formation (Figure 5.3A, Appendix 5.10).

Presented in Fig 5.3A is the chronoamperometric traces *A. baumannii* biofilms with and without drug treatments. This result can be qualitatively described and separated into three parts: a) slow growth characterized with initial cell attachment to the solid electrode (0-6 h); b) rapid biofilm formation and growth, (7-15 h); c) limited biofilm growth phase (16-24 h) due to nutrients and diffusional limitations; d) death phase (48 h and beyond) due to high death rate and increased number of inactive biofilm cells at the bottom layers.

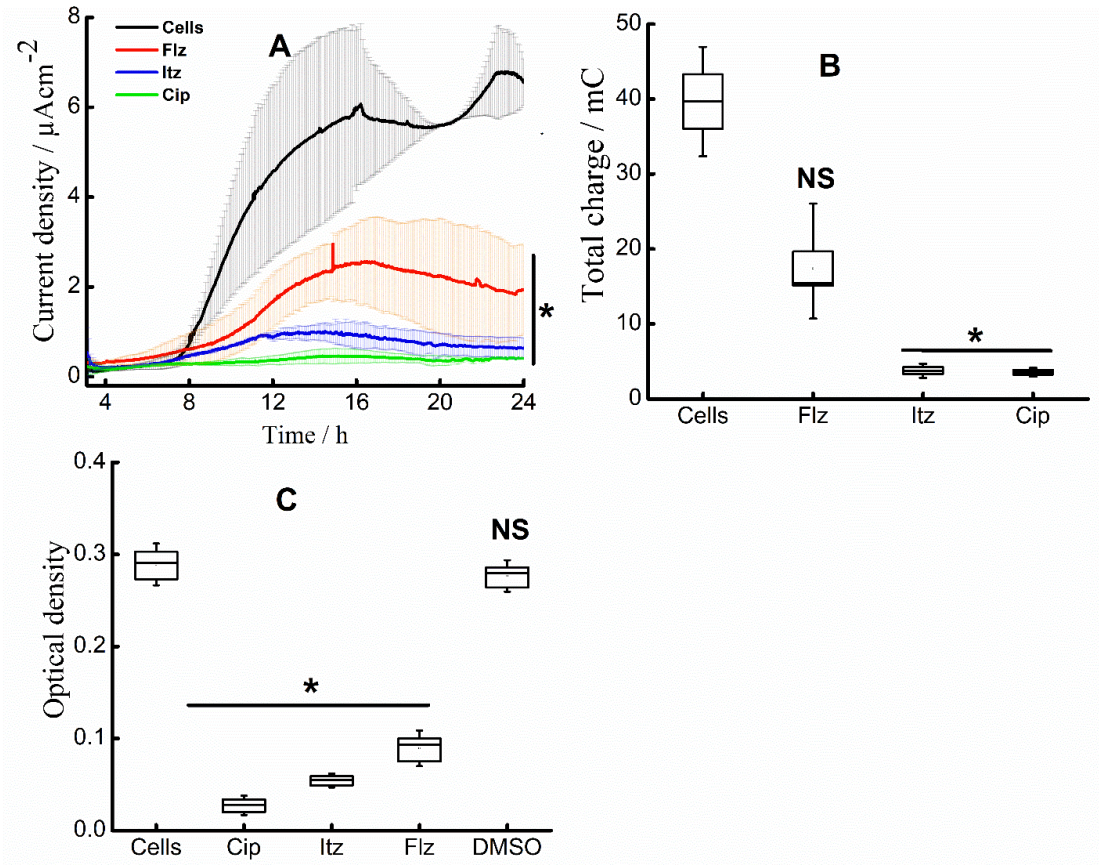

Fig. 5.3. (A) Chronoamperometry of *A. baumannii* biofilms with and without the drugs: cells not exposed to drugs (black trace); cells exposed to Flz (red trace); cells exposed to Itz (blue trace); cells exposed to Cip (green). (B) Total Q obtained after 24 h of incubation at E = 400 mV (C). Crystal violet estimates of biofilms on the WE surface determined after a 24 h potentiostatic experiment. (n=3). Asterisk (*) indicates significant difference between control and treated biofilms ($p < 0.05$) according to Tukey's test. NS means not significant.

Quantitatively, at approximately 16 h, the current response for biofilm not exposed to drugs was 6.00±1.74 µA/cm^2, while biofilms exposed to Itz, Flz and Cip exhibited current responses of 0.92±0.03 µA/cm^2, 2.53±0.87 µA/cm^2, and 0.45±0.15 µA/cm^2, respectively. Similarly, the total charge output (Q, mC) calculated upon completion of electroanalysis (Fig. 5.3B), showed that *A. baumannii* biofilms produced lower Q under drug treatments relative to the untreated biofilms. Therefore, both current density and Q estimates validate the effect of the tested drugs on *A. baumannii* biofilms.

Biofilm measurement via crystal violet staining (Fig. 5.3C) after 24 h of chronoamperometric measurements also indicated a significant difference between treated and untreated biofilms, with Cip, Itz, and Flz producing 90.5±333.3 %, 81.2±33.3 %, and 69.1±13.3 % reduction in biofilm formation, respectively, in comparison with untreated biofilm (Appendix 5.12). These findings (Appendixes 5.10, 5.11 and 5.12) are statistically significant ($p<0.05$), and they support the biochemical findings (section 5.3.1). Independent control experiments with sterile medium only, redox mediator only, and medium and mediator only, all produced near-zero current response (Appendix 5.1), confirming that the electrochemical responses are due to the 2-HNQ redox coupling by biofilms cells on the electrode.

Biofilms of *A. baumannii* have been found in a number of biotic surfaces (wounds and soft tissue infections) and abiotic niches (particularly health-care-related instruments and devices) (Eze et al., 2018). As a result, it is important to evaluate these drugs for their ability to remove already formed *A. baumannii* biofilms via chronoamperometry. Interestingly, unlike our previous work on pre-formed *C. albicans* biofilms using a similar technique with no substantial result (Olaifa et al., 2021), the antifungals examined in this study were able to eliminate pre-formed *A. baumannii* biofilms.

Upon observation of a stable current response, the test agents were introduced gently into the electrochemical cells using a sterile micro-syringe. Cip induced a rapid current reduction at 2×MIC values (Fig. 5.4A). Both Flz (Fig. 5.4B) and Itz (Fig. 5.4C) exhibited a sharp reduction in current responses when added at 5×MIC values. These observations could be attributed to the detachment of the early biofilm from the solid electrode surface as a result of the high drug doses, as 1×MIC does not show any impact on preformed biofilms under the experimental conditions. While this finding is in line with that of Santoro et al. (2016), who had reported that addition of toluene, a wastewater contaminant, caused a continuous decline in current response of *E. coli* cells, it contradicts with the work of Palanisamy et al. (2019) where almost a complete retrieval of current response was obtained upon addition of a chemical pollutant, 1-cyclohexyl-2-pyrrolidone, on preformed *E. coli* biofilm. This may possibly be attributed to the volatility nature of 1-cyclohexyl-2-pyrrolidone, thus, making it to rapidly evaporate from the

experimental set-up, hence, its rapid loss of antibiofilm activity. As presented in Fig. 5.4, a small recovery (< 5%) of the current signal was observed, even after 45 h. This suggests that the biofilm cells on the electrode surface may be dead or that all *A. baumannii* cells in the electrochemical cell are dead. It is however complicated, to validate via electroanalysis which of these phenomena played out, as both generate analogous effects (i.e., a decline or shutdown of the current flow). Despite this limitation, the bioelectrochemical approach for assessment of antibiofilm efficacy can be faster and less cumbersome than traditional culture-based methods.

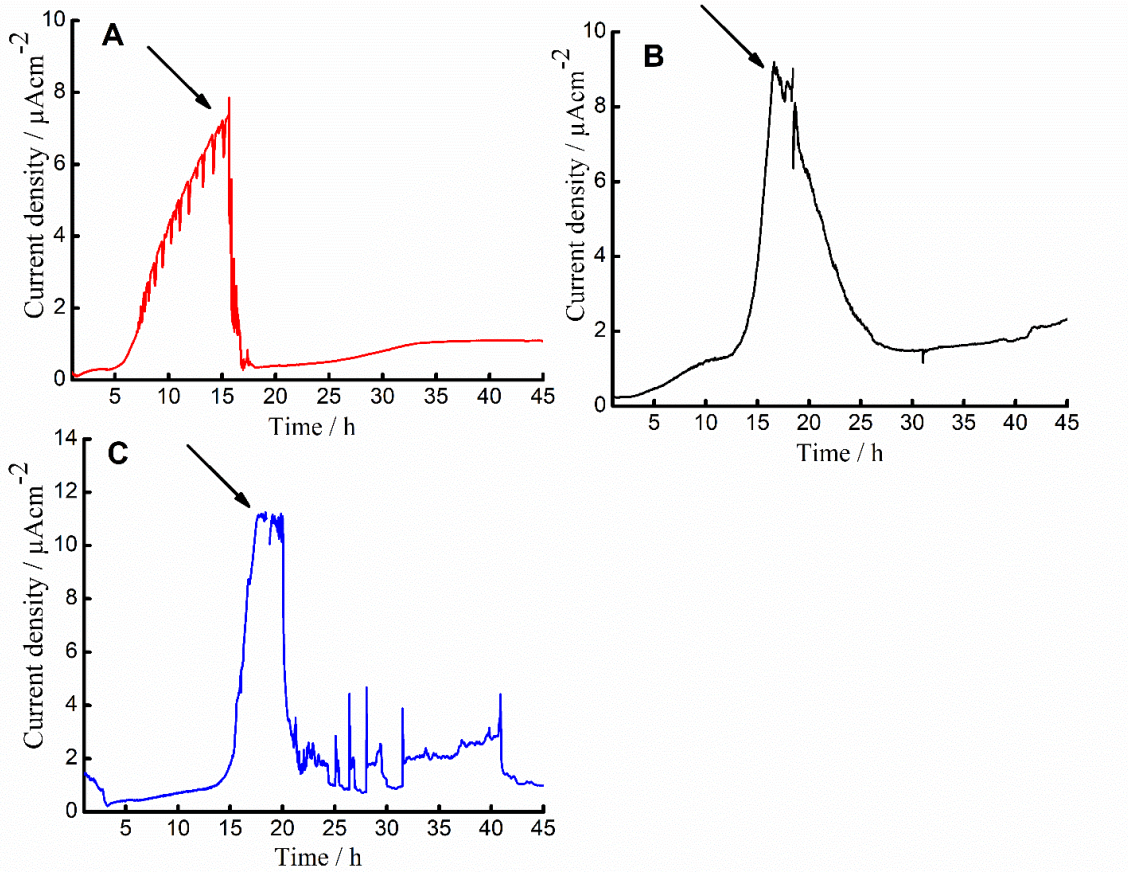

Fig. 5.4. Representative chronoamperometry of *A. baumannii* pre-formed biofilms following addition of the drugs. (A) Cip (2×MIC) (red trace); (B) Flz (5×MIC) (black trace) and (C) Itz (5×MIC) (blue trace).

5.3.3 Microscopy

Microscopy is an important but highly destructive gold standard approach often adopted to determine the efficacy of antimicrobial therapies on biofilms (Gomes & Mergulhão, 2017) and helps qualitatively visualize the degrees of inhibition, killing or removal (Goldbeck et al., 2014). Post-chronoamperometry, microscopic analysis of the SPEs using SEM and CLSM was performed to validate the effects of the tested drugs on *A. baumannii* biofilms.

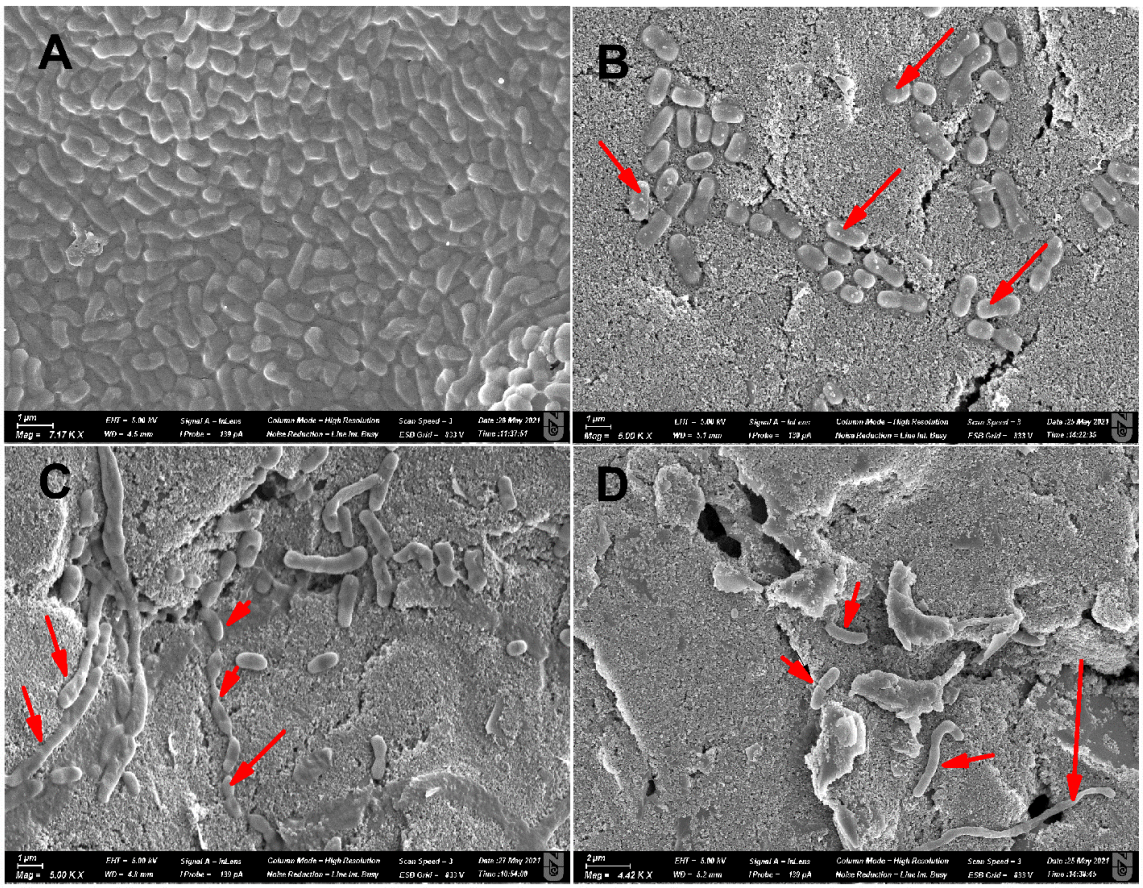

Fig. 5.5. Representative SEM of *A. baumannii* on the WE surface only following completion of electroanalysis. (A) Cells not exposed to any of the drugs (B) Cells exposed to Flz. (C) Cells exposed to Itz. (D) Cells exposed to Cip.

As presented in Fig. 5.5A, SEM images (×5000 magnification) of biofilms without any drugs revealed a completely formed biofilm structure with cells seen surrounded by the matrix. The cells typically appeared homogeneous, with intact membrane integrity and

form (Fig. 5.5A). On the other hand, biofilms exposed to the text drugs at inoculation were unable to form a full biofilm while their cells were mainly monolayered and sparsely distributed. Additionally, morphological damages that include membrane disruptions, unusual cell elongation and other cell shapes and forms (Fig. 5.5B, 5.5C and 5.5D) were observed. Specifically, Fig. 5.5B and 5.5C indicate that Itz and Flz may have disrupted the membrane integrity, leading to cell death and or aberrant surface morphology.

Cell elongation is a well-known physiological reaction to both physical and chemical stressors, including extreme temperature, pH, salinity, and exposure to antimicrobials. It enables cells to increase their exterior surface areas in order to facilitate attachment, cellular contacts, and nutrient uptake during their stress adaptation processes (Uzoechi & Abu-Lail, 2019, 2020), in this case – the treatment of *A. baumannii* with the test drugs (Itz, Flz, and Cip). Furthermore, secretion of membrane-bound molecules that results in an increase in surface roughness has been linked to bacterial membrane integrity and adhesion to surfaces under harsh/stressful/unfavorable conditions (Limoli et al., 2015). Fig. 5.5B, 5.5C, and 5.5D illustrate cell elongation and surface roughness, which could be a feasible survival strategy for *A. baumannii* cells when exposed to drugs under the experimental conditions.

CLSM, in comparison to SEM, is a more advanced imaging technique that has been frequently used to study biofilm morphologies (Palmer & Sternberg, 1999). Cerca and colleagues had previously published a study on CLSM analysis of *S. epidermidis* subjected to rifampicin, vancomycin, and farnesol treatments. They demonstrated that farnesol reduced biofilm biomass, indicating that it could be used as a pharmaceutical adjuvant in clinical practice (Cerca et al., 2012).

The CLSM images in this work corroborates with that of the SEM images, while the biofilm biomass on the electrode of each experimental condition matches to the results obtained using biochemical and bioelectrochemical assays for the same experimental conditions. As qualitatively presented in Fig. 5.6, the order of activity is Cip>Itz>Flz. This is supported by chronoamperometric results (Fig. 5.3A). Fig. 5.6A, however, shows that the biomass was higher in untreated biofilm and lower in the treated biofilms (Fig. 5.6B, 5.6C and 5.6D). In general, the electrochemical data is supported by SEM and CLSM

results, implying that electroanalysis is appropriate for antibiofilm testing of antimicrobials and repurposed compounds.

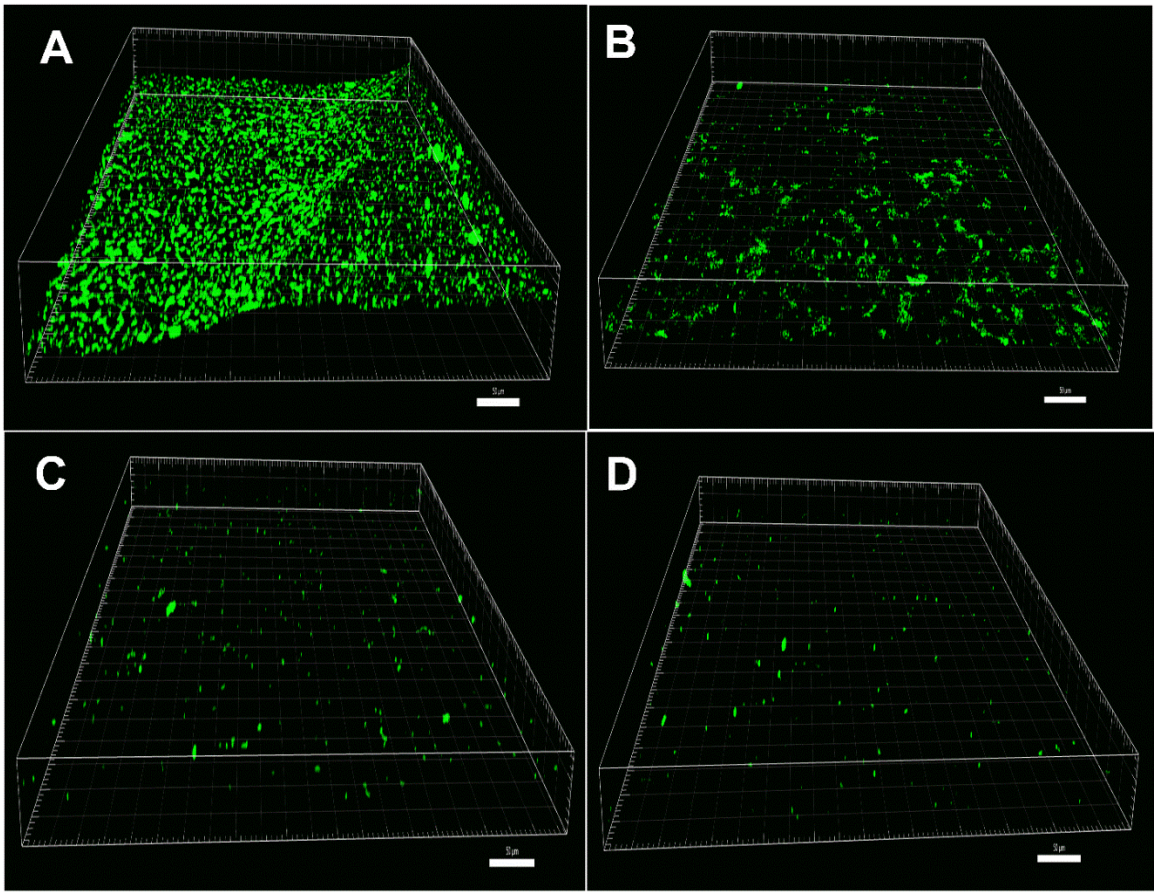

Fig. 5.6. Representative CLSM of *A. baumannii* on the WE surface only following completion of electroanalysis. (A) Cells not exposed to any of the drugs (B) Cells exposed to Flz. (C) Cells exposed to Itz. (D) Cells exposed to Cip. Scale bars indicate 50 µm.

5.4 Possible mechanisms of action of Itz and Flz against *A. baumannii* biofilms

Fungicides' mechanisms of action against fungal biofilms have been extensively researched and documented (Prasad et al., 2016). Despite this, little is known about their activity against bacteria particularly Gram-negative bacterial biofilms. Azole fungicides, such as Itz and Flz, are renowned for their broad-spectrum action and selectivity for interfering with the formation of membrane sterol lipids in fungal cell wall (Campoy & Adrio, 2017). These sterols (e.g., ergosterols, triglycerides, and phospholipids) are critical membrane molecules that maintain or facilitate stability, permeability, and other homeostatic cell

functions. Therefore, any disruption in the formation, structural organization, and/or quantity may eventually affect cell growth and metabolism (Prasad et al., 2016). Bacterial membranes, however, lack sterols, but they do possess hopanoids, which are chemically and functionally analogous to sterols (Lodha et al., 2019).

Hopanoids, like sterols, are known for their physiological functions relating to maintaining the membrane integrity and permeability in bacteria (Mangiarotti et al., 2019; Welander et al., 2009). They have also been identified as key component of bacterial stress responses to pH changes (Kharbush et al., 2018; Schmerk et al., 2011), exposure to chemical detergents and antimicrobial molecules (Willdigg & Helmann, 2021). Additionally, it has been established that hopanoids together with glycolipids found in the outer membrane spaces of bacteria, interact to form a well-organized bilayer structure that is homologous to the sterol-sphingolipids arrangements in fungal membranes (Sáenz et al., 2015).

Consequently, this resemblance in the morphology and physiology of bacterial and fungal membranes could be explored to solving antibiotic resistance problem by designing new drugs or repurposing old drugs with a potential to target the hopanoid biosynthetic pathways (Mingeot-Leclercq & Décout, 2016). As a result, it is hypothesized that the antibiofilm activity against *A. baumannii* biofilms described in this study may be due to interference in the membrane lipids by Itz and Flz treatments. Malott et al. (2014) found similar results when they repurposed fosmidomycin against *Burkholderia multivorans*, commonly associated with lung infections, primarily in persons having cystic fibrosis.

5.5 Summary

Both biochemical and bioelectrochemical results validate that fungicide repurposing for control of bacterial biofilms could be the missing piece in the puzzle of fight against bacterial resistance. While crystal violet assay demonstrated 90.5 %, 81.2 %, and 69.1 % biofilm inhibition, electroanalysis demonstrated 92.5 %, 84.7 %, and 57.8 % reduction in current output of *A. baumannii* biofilm, exposed to Cip, Itz, and Flz, respectively. Though both approaches complement each other, chronoamperometry offers a simple, low-cost, rapid, and real-time platform for antibiofilm assessment.

Furthermore, the activity of Itz and Flz against *A. baumannii* biofilm described in this work could herald a key strategy for enhancing the sensitivity of antibiotic resistant bacteria through a combination therapy of Itz or Flz with other potent antibacterial drugs.

5.6 Outcome

Olaifa, K., Ajunwa, O., & Marsili, E. (2022). Electroanalytic evaluation of antagonistic effect of azole fungicides on Acinetobacter baumannii biofilms. Electrochimica Acta, 405, 139837. https://doi.org/10.1016/j.electacta.2022.139837

Chapter Six: Detection of *C. albicans* cells in urine samples via electroanalysis

6.1 Introduction

As previously established in Chapters 2 and 4, *Candida* species are considered the leading cause of fungal infections (Kainz et al., 2020), ranging from invasive and systemic life-threatening to mild, topical and mucocutaneous diseases. Of all known *Candida* spp., *C. albicans* is the most prevalent and pervasive (Soll & Daniels, 2016), partly because it is a natural commensal and a dominant colonizer of most body parts including the skin, respiratory, reproductive and gastrointestinal tracts (Achkar & Fries, 2010), and partly due to its marked biofilm phenotype (Rodríguez-Cerdeira et al., 2019). *Candida* spp. biofilms exhibit resistance to antifungal treatments, and the resulting infections can be difficult to manage/control, thereby contributing to high morbidity and mortality rate (Cavalheiro & Teixeira, 2018). Nevertheless, early and rapid detection and diagnosis is crucial for effective management of *Candida*-induced infections (Hussain et al., 2020).

Urinary tract infections (UTI) are among the most common infectious diseases worldwide (Behzadi et al., 2019; Flores-Mireles et al., 2015; Murray et al., 2021; Öztürk & Murt, 2020). The term UTI, though very broad, is often used synonymously to describe fungal urinary tract infection potentiated by *Candida* spp, and with a special focus on *C. albicans* as the most implicating agent (Poloni & Rotta, 2020). This is supported by recent evidence suggesting a decline in the occurrence of UTI caused by bacterial species and a rise in the occurrence of UTI caused by fungi, notably the dimorphic yeast *C. albicans*, and especially in critically ill or hospitalized patients (Dias, 2020), a condition generally referred to as genitourinary candidiasis (GC). This may be manifested as candidal balanitis or balanoposthitis in males, vulvovaginal candidiasis in females, and candiduria in both genders. Although these diseases are common in both healthy and immunocompromised individuals, they are of special concern in the latter due to the consequent high morbidity and mortality (Achkar & Fries, 2010; Obisesan et al., 2015).

Candiduria, that is, the presence of *Candida* in urine, may be due to several factors including but not limited to: colonization of the bladder or urinary catheters, UTI, manifestation of candidemia without UTI, candidal prostatitis, and/or contamination of the

urine sample (Odabasi & Mert, 2020). Colonization or contamination is the commonest cause of candiduria in most patients, whether symptomatic or asymptomatic (Kauffman et al., 2011; Odabasi & Mert, 2020). Either ways, the presence of *Candida* in urine often requires diligent clinical evaluation (Kauffman, 2014), as it may be indicative of UTI or other underlying health conditions, such as renal malfunction, diabetes mellitus, and genitourinary structural pathology (Gajdács et al., 2019; Poloni & Rotta, 2020), especially in immunodeficient patients.

Currently, a standard diagnosis for candiduria is not yet available, as criteria, procedures, and methods of detection and analysis vary across laboratories (Alfouzan & Dhar, 2017; Behzadi et al., 2015, 2019; Gharaghani et al., 2018; Obisesan et al., 2015; Odabasi & Mert, 2020; Poloni & Rotta, 2020), which makes therapeutic decisions even more complicated (Dias, 2020; G. M. E. Lima et al., 2017). Initial isolation on routine culture media such as potato dextrose agar (PDA), Sabouraud dextrose agar (SDA) or even CHROMagar™ Candida, followed by microscopic visualization of colonies remains the gold standard (Alfouzan & Dhar, 2017; Gharaghani et al., 2018). This is, however, time and resource consuming, as these laboratory processes may take 48–96 h to give actionable results, causing delay that encourages haphazard and unempirical use of antifungal drugs (Markowitz et al., 2019). Commercial kits (e.g., Dipstick, test strip and other ELISA based techniques), flow cytometry, mass spectrometry, spectroscopic methods (e.g., Infrared, Raman), sequencing and other nucleic acid-based approaches (e.g., PCR, qPCR) are either expensive and thus not readily available, or require some level of expertise to operate and interpret the results (Behzadi et al., 2019; Fazeli et al., 2019; Obisesan et al., 2015).

Momenzadeh and colleagues had recently proposed a computer-aided diagnostic software for detection of vulvovaginal candidiasis (Momenzadeh et al., 2018). Unfortunately, its successful application hinges on the availability of existing microscopic images of yeast cells, which cannot be generated for each patient, particularly in small hospital with limited resources. Therefore, the need for a more direct, simple, fast, sensitive, and cost-effective diagnostic approach cannot be overemphasized. Electrochemical biosensors can be adopted to achieve this purpose (Fritzenwanker et al., 2016; Hussain et al., 2020; Markowitz et al., 2019). We have recently adopted this approach for analysis and

assessment of antifungal drugs against *C. albicans* biofilms (Olaifa et al., 2021) and other clinically important microbial pathogens (Olaifa et al., 2022; N. Savić et al., 2020) using laboratory culture media.

Moreover, there are few studies in the literature on the electrochemical-based detection of *Candida* spp. in clinical samples. Muir and colleagues have proposed electrochemically labelled DNA probes for diagnosis of candidemia, using extracted genomic DNA of *C. albicans* cells isolated from blood samples (Muir et al., 2011). This approach, however, requires some level of expertise and technical knowledge in molecular biology. Also, kits and reagents required for nucleic acid extraction are expensive and not easily available, especially in local and primary health care facilities.

In another recent study by Dutta and coworkers, a glucose meter coupled with a manufactured electrochemical sensor was proposed for the detection of *C. albicans* in urine and serum (Dutta et al., 2021). In their approach, hemicellulase – a hydrolytic extracellular enzyme - was added in the system, while using glucose meter to estimate the amount of glucose released from the enzymatic lysis of the fungal cell wall. The amount of glucose released was proportional to the concentration of *C. albicans*. Similarly, Sá and colleagues employed a lectin-based sensor in a three-electrode system for detection of pathogenic *Candida* spp using a chemically defined growth medium (Sá et al., 2020). However, the need for an analytical grade substance/enzyme and/or additional devices may make these methods relatively expensive.

Consequently, direct, and real-time whole cell detection of *C. albicans* in urine samples using simple and low-cost approach, and with limited or no use of additional materials or reagents is worth investigating. Herein, we demonstrated for the first time the use of cheap and readily available carbon screen-printed electrode for detection of *C. albicans* whole cells in urine samples via electroanalysis. SEM was also done to visualize the attached cells on the electrodes, thus validating the electrochemical measurement.

6.2 Experimental

6.2.1 Materials

Screen-Printed Carbon Electrodes (SPEs) (Reference code: C110) described in previous chapters (sections 3.2, 4.2 and 5.2) were used with no modification. Methacrylate electrochemical cell (ref. CELL) suitable for work-in-solutions SPEs, also obtained from Metrohm DropSens, Spain, were used in electrochemical measurements. Prior to electrochemical measurements, every SPE was sterilized in 70 % (v/v) ethanol, washed in sterile deionized water, and then blotted to dry, while the electrochemical cells were washed, sterilized in 70 % (v/v) ethanol for 30 minutes, followed by exposure to 30 minutes UV-b radiation. During all experiments, the electrochemical cells were maintained at a temperature of 37 °C in steel-beads dry bath.

Urine samples were willfully provided by healthy volunteers (male and female, young and old individuals: age 19-45) following oral description of the project and its objectives, and immediately transported to the laboratory for processing. The samples were homogenously pooled; centrifuged (10,000 rpm for 10 minutes), and then the supernatant was filter-sterilized on 0.22 μm filters (Corning® syringe, USA) to remove living cells and particulate matter. The filtrate obtained was used for electrochemical measurements or stored at 4 °C in the refrigerator when not used.

The standard strain *C. albicans* ATCC 10231 was used. The yeast strain was initially sub-cultured and subsequently maintained in SDA, while RPMI 1640 medium supplemented with 2% glucose was occasionally employed for broth cultivation and inoculum preparation, and urine was employed as sole growth medium for all electrochemical measurements.

6.2.2 Methods

6.2.2.1 Electroanalysis

Detection was done in electrochemical cells containing 8 mL processed urine spiked with freshly prepared inoculum diluted to the corresponding value of colony forming unit (CFU)

of microorganism per mL of urine. After inoculation, cyclic voltammetry (CV) and differential pulsed voltammetry (DPV) and chronoamperometry (CA), were performed in succession using a computer-controlled VSP multichannel potentiostat (BioLogic, France). The parameters for CV included: E_i = −700 mV *vs*. Ag pseudo-reference electrode, E_f = 800 mV *vs*. Ag pseudo-reference electrode, scan rates 1 mV s^{-1} and 10 mV s^{-1} run in succession, current averaged over the last 50% of the step duration and recorded over N = 10 voltage steps. Similarly, the parameters for DPV were E_i = −800 mV *vs*. Ag pseudo-reference electrode, E_f = +800 mV *vs*. Ag pseudo-reference electrode; pulse height 50 mV, pulse width 400 ms, step height 5 mV, step time 500 ms, current average over the last 50 % of the step. CA was performed at 400 mV *vs.* Ag pseudo-reference electrode, and the current output was recorded every 60 s for 24 h, after which CV and DPV were repeated before the experiment was concluded.

6.2.2.2 Crystal violet assessment and microscopic imaging of *C. albicans* cells on the electrodes

Following completion of electrochemical characterization, crystal violet assay for estimation of the attached cells on the working area of the electrodes was done as previously described (Chapter 4, section 4.2). Scanning electron microscopy (SEM) was also done as described previously in Chapter 4 (section 4.2.2.3).

6.3 Results and Discussion

6.3.1 Electroanalysis

Electrochemical signatures of *C. albicans* cells spiked in human urine was characterized by CA, CV and DPV using unmodified graphite screen-printed electrodes. Urine samples from more than 20 healthy individuals were collected and pooled, while a new SPE was used for each independent electrochemical assay to prevent cross-contamination.

The quantitative definition of candiduria is yet to be standardized. Thus, the diagnostic criterion of colony forming unit per milliliter of urine (CFU/mL) varies from one clinical laboratory to another. For example, an estimate of 10^3 to 10^5 CFU/mL (Achkar & Fries, 2010; Behzadi et al., 2015, 2019; Poloni & Rotta, 2020), 10^4 to 10^5 CFU/mL (Gajdács et al., 2019; Odabasi & Mert, 2020) or > 10^4 CFU/mL (Gharaghani et al., 2018) are often

considered candiduria, subject to the gender and age of the patient, and /or the occurrence of a subsisting ailment (e.g., renal infections). Nevertheless, recent studies in collaboration with the National Institute of Health adjudged the adoption of the presence of 10^3 cells of *C. albicans* per mL of a urine sample as the lowest cut-off value for defining candiduria (Alfouzan & Dhar, 2017). While a range of cell concentrations were electrochemically assayed in the present study, assays of 100 CFU/mL provided the most informative diagnostic information. Control experiments with urine only, urine spiked with *Escherichia coli*, *Acinetobacter baumannii*, and a co-culture of *C. albicans* and *E. coli* were also carried out. Our results however indicate that the sensor, having graphite as its working electrode, showed bioaffinity for *Candida* cells probably because of the unique structural and biochemical configurations its cell wall surface, which contains ~ 90% carbon rich compounds including mannose polymers, β-glucans and chitin (Sá et al., 2020).

The CA of filter-sterilized urine spiked with known concentration of viable microorganisms is shown in Fig. 6.1 A. While 10 CFU/mL (black trace) and 1000 CFU/mL (blue trace) *C. albicans*, 100 CFU/mL *E. coli* (olive trace), 100 CFU/mL *A. baumannii* (navy trace), and a co-culture of 100 CFU/mL of *E. coli* and *C. albicans* (violet trace) do not show a defined pattern just as the sterile urine (magenta trace), 100 CFU/mL of *E. coli*, however, showed a poorly reproducible rapid rise in current output within 2 h of inoculation, with a maximum current yield of 18.12±1.15 μA at ~1.6 h, followed with a rapid decline. Additionally, 100 CFU/mL of *C. albicans* (red trace) produced a reproducible current output that could be qualitatively described as a sigmoid curve, a pattern common to most weak electroactive microorganisms when grown under favorable laboratory conditions (Olaifa et al., 2021).

The current trend of 100 CFU/mL of *C. albicans* (red trace) can be categorized into three distinct parts: (i) a slow adaptation period (0–2 h), followed by a gradual increase (2–4 h), probably due to rapid utilization of available nutrient coupled with rapid proliferation of cells; (ii) a very short stationary phase (4–4.5 h) marked with a current peak of 30.12±2.45 μA, probably due to nutrients limitations; (iii) a gradual decline (> 4.5 h), probably due to exhaustion of functional nutrients.

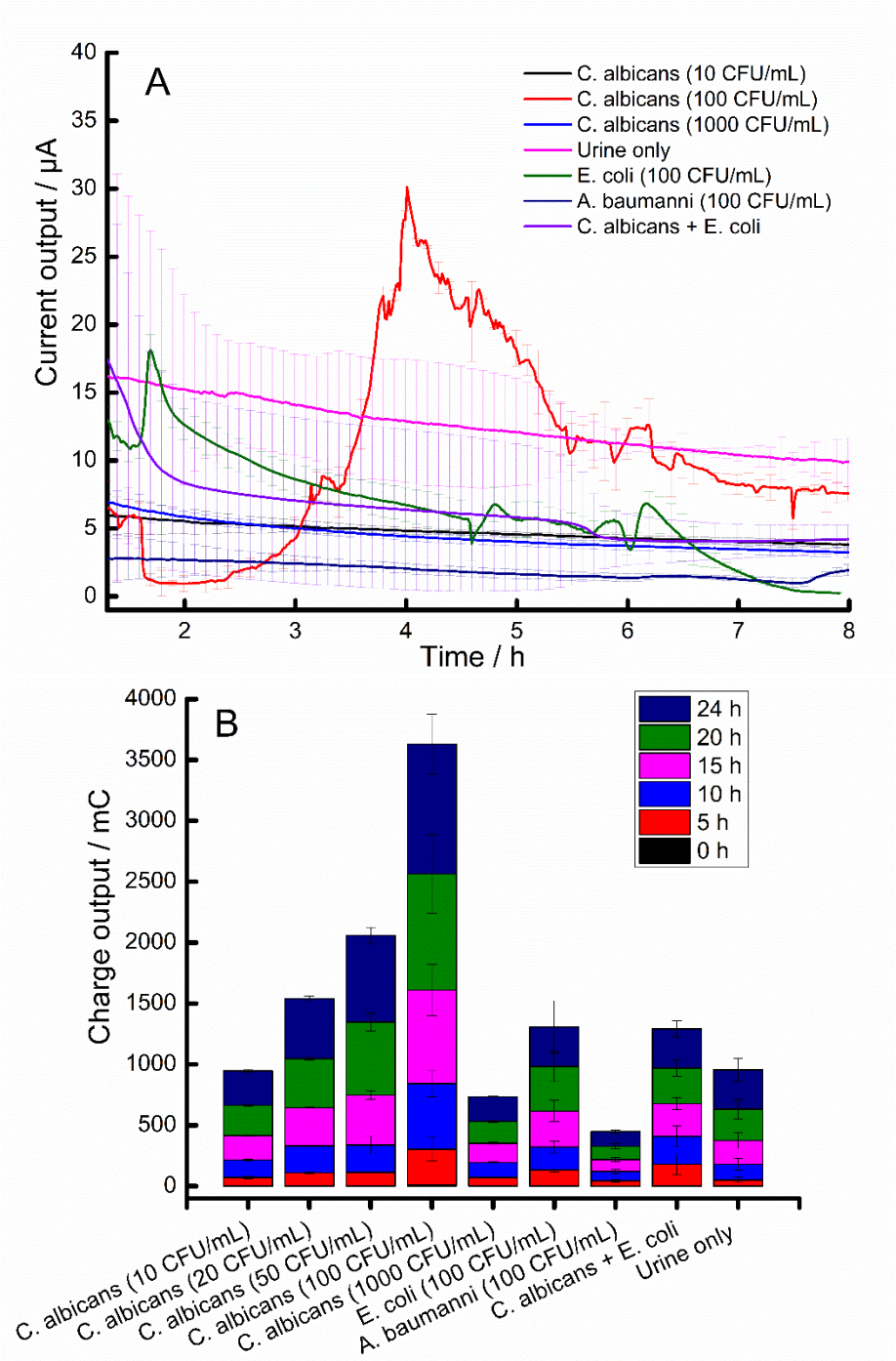

Fig. 6.1. (A) CA of sterile urine (magenta trace) and urine spiked with 10, 100 and 1000 CFU/mL *C. albicans* (black, red, and blue trace, respectively), 100 CFU/mL *E. coli* (olive trace), 100 CFU/mL *A. baumannii* (navy trace), co-culture of *C. albicans* and *E. coli* (violet trace). (B) Cumulative charge outputs at varying times of potentiostatic incubation of spiked and sterile urine samples.

The concentration of planktonic cell at the end of the analysis was much higher than the inoculum, while biofilm estimates on the WE area did not return quantifiable estimates following crystal violet staining and spectrophotometric measurement. It is therefore a possibility that the overall current response is contributed also by the planktonic growth of *Candida* cells under the electrochemical growth conditions adopted. Interestingly, growth of *C. albicans* in conventional 96-well microtiter plates with an initial OD similar to that of electrochemical experiment (~ 10^2 CFU/mL) using both urine and conventional RPMI (with 2% glucose) as growth media (Appendix 6.1), showed urine could support *Candida* growth beyond 48 h, although its growth is about 2× less in comparison to the conventional RPMI medium (Appendix 6.1).

Furthermore, the cumulative charge output obtained via integration of the current output over a specified period, using the EC-Lab software, was also used to describe the electrochemical behavior of *Candida* cells spiked in filter-sterilized urine samples. As presented in Fig. 6.1B, the charge output increases with the number of *C. albicans* cells in the inoculum, in the range 10-100 CFU/mL. However, the charge output decreased again at 1000 CFU/mL. This is suggestive that the sensitivity of the sensor decreased at high cell concentration in the inoculum. Interestingly the current output decreased slowly after 8 h for all the *C. albicans* inocula. Nonetheless, the highest difference in current and charge output was observed at $t < 5$ h, which can be adopted as a suitable time for electrochemical detection of *Candida* under these experimental conditions.

The sensitivity and limit of detection (LOD) of the sensor were estimated as 8.19±1.87 mC/CFU/mL and 39 CFU/mL, respectively, from the plot of maximum charge output (mC) versus different CFU/mL of *Candida* in urine (Appendix 6.2) This plot showed that a linear relationship existed between the two variables in the range of 10–100 CFU/mL, with a coefficient of determination (R^2) of 0.9664. Unfortunately, this range falls short of the most range concentrations (10^3 – 10^5 CFU/mL) typical of candiduria (as previously discussed) that may warrant medical intervention, thus preliminary dilution of the urine samples may be needed. Additionally, the low sensitivity observed in this study may be attributed to the complex nature of urine, as previously observed for most biofluids (sputum, blood, urine) used for electrochemical detection of *Pseudomonas aeruginosa* (Ostrov et al., 2017;

Webster et al., 2014). In a related study on electrochemical detection of *C. albicans* in blood samples (candidemia), a detection limit of 10 CFU/mL blood was obtained (Muir et al., 2011). While this falls within the lower clinical range for candidemia (5–100 CFU/mL blood) (Loeffler et al., 2000), Muir and colleagues opined that a lower LOD outside the range (i.e., < 5 CFU/mL blood) is preferable to minimize the chances of false-negative results (Muir et al., 2011).

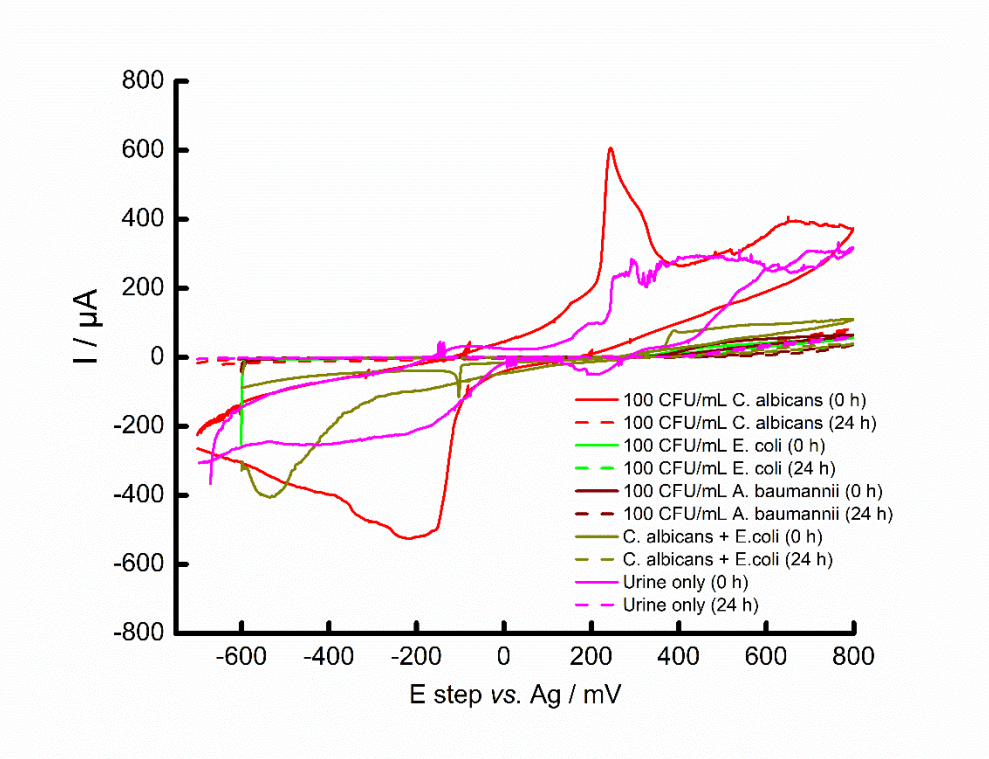

Fig. 6.2. Representative cyclic voltammograms at 1 mV/s scan rate of sterile urine (magenta trace) and urine spiked with 100 CFU/mL *C. albicans* (red trace), 100 CFU/mL *E. coli* (green trace), 100 CFU/mL *A. baumannii* (wine trace), co-culture of *C. albicans* and *E. coli* (dark yellow trace) at 0 h (solid trace) and 24 h.

Cyclic voltammetry (CV) is another important electrochemical technique relevant for characterization of biological phenomena including microbial growth and metabolism (Kang et al., 2012; Marsili, Rollefson, et al., 2008; Teravest & Angenent, 2014). It is, however, necessary to carry out preliminary investigations to determine the optimal potential range that would produce reproducible results and does no damage to the microbial cells. Nonetheless, low scan rates (in the range of 1–5 mV/s) is mostly preferred

for microbial studies and analysis, as it minimizes charging currents, and allows detection of sluggish electron flow phenomena at the electrode interface (Olaifa et al., 2021). In this study, CV was performed at both scan rates of 1 mV/s and 10 mV/s, respectively, under non-turnover (0 h) and turnover (24 h) conditions, as we do not have prior knowledge of the voltammetric behavior of *C. albicans* in human urine samples.

The voltammetric responses observed at both scan rates were similar (Fig. 6.2 and Appendix 6.3), demonstrating that EET rate was fast. This may be attributed to the complex biochemical nature of human urine, which contains relatively high concentration of undefined redox substances, thus, causing high redox reaction rates but also instability of current outputs. While no clear definitive cyclic voltammetric patterns were observed in most of the experimental conditions, a larger non-turnover CVs with defined anodic and cathodic peaks were repeatedly observed for *C. albicans* 100 CFU/mL (Fig. 6.2), suggesting microbial metabolism of a redox molecule in the urine samples. The onset of the anodic peak was observed at a positive potential of approximately 260 mV *vs.* Ag while the reverse cathodic peak occurred at a negative potential of –200 mV *vs.* Ag (Fig. 6.2). Additionally, the absolute values of both anodic and cathodic currents were maximum for *C. albicans* 100 CFU/mL, indicating the sensitivity of the sensor towards this cell count. Furthermore, the non-turnover CVs at 0 h for the co-culture of *C. albicans* and *E. coli* caused a shift in the electrocatalytic peak, with anodic peak drifted towards positive potential at 400 mV *vs.* Ag and cathodic peak drifted to the negative at –540 mV *vs.* Ag., while their respective absolute current values reduced significantly (Fig. 6.2). It is important to emphasize that, while there is defined peaks in sterile urine, the relatively large redox response is suggestive of the presence of minute concentrations of undefined native active redox substances. In general, these results agree with that observed for CA.

Differential pulse voltammetry (DPV) is mostly adopted for bioanalytical studies as a complementary technique to CV, so as to further elucidate the redox mechanisms involved in microbial growth and metabolism (Besant et al., 2015; Buzid et al., 2016; Campuzano et al., 2017; Marsili, Rollefson, et al., 2008; Naradasu, Guionet, Okinaga, et al., 2020; Seviour et al., 2015). Fig. 6.3 shows the representative raw DPV scans obtained at 0 and 24 h of electroanalysis, for urine samples with and without inoculation. The absence of

peaks in sterile urine at both 0 and 24 h (magenta solid and dot traces, respectively) is of significant relevance, suggesting that there may be no reversible electroactive molecules in these samples, or that the constitutive redox molecules in these samples require a biogenic redox coupling for it to be electrochemically manifested. Nonetheless, it is evident that the urine samples were rich in undefined complex substances, leading to generation of noise, as characterized by a relatively high resistivity (with a charging current of ~ 50 µA) and instability and fluctuations in the current outputs (of sterile urine at both 0 and 24 h (magenta solid and dot traces, respectively). Repeated experiments with same and different batches of urine samples produced similar results.

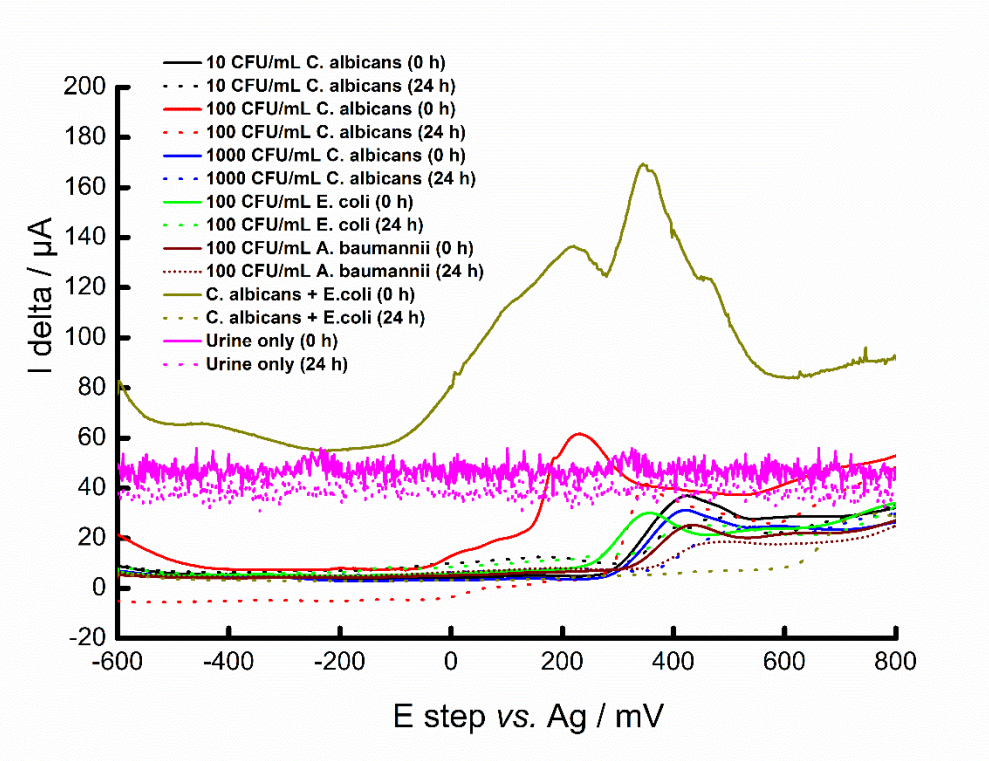

Fig. 6.3. DPV of sterile urine (magenta trace) and urine spiked with 10, 100 and 1000 CFU/mL *C. albicans* (black, red, and blue trace, respectively), 100 CFU/mL *E. coli* (green trace), 100 CFU/mL *A. baumannii* (wine trace), co-culture of *C. albicans* and *E. coli* (dark yellow trace) at 0 h (solid trace) and 24 h.

This observation is, however, in variance with that reported by Webster and colleagues on their work on electrochemical detection of *P. aeruginosa* in biofluids, wherein a fine scan with a negligible peak was observed for sterile urine (Webster et al., 2014). This could be because ultra-processed urine samples purchased from commercial outlets and may have

been long-stored on the shelves, were used in their study, while fresh urine samples subjected only to simple filter-sterilization was used in the current study.

Two observations were common in the DPV scans, namely (a) all characteristic redox peaks of spiked urine samples were observed at positive potential, and (b) all scans of spiked urine show reduced peak intensity after 24 h of electroanalysis, suggesting a decrease in microbial/metabolic activity probably due to exhaustion of nutrients. Following peak analyses (Appendix 6.4), at inoculation, 10 and 1000 CFU/mL *C. albicans* and 100 CFU/mL *A. baumannii* exhibit similar peak patterns with peak intensity of 14.90±0.14 µA, 29.16±1.84 µA, and 27.87±5.26 µA at 411±16 mV, 419±2 mV and 439±5 mV potentials, respectively, while 100 CFU/mL *E. coli* exhibit a similar peak intensity but at 279±10 mV potential. Furthermore, at inoculation (0 h), 100 CFU/mL *C. albicans* exhibits a broader peak intensity of 461.37±36.46 µA at 421±14 mV, while at 24 h, the anodic peak reduced to 24.07±2.59 µA and shifted positively to 494±21 mV. Additionally, the DPV scans at inoculation, of urine spiked with a co-culture of *C. albicans* and *E. coli* exhibit two redox peaks, each similar to the representative peak of the individual strains, though with increased peak intensity (Fig. 6.3). This is suggestive that the two strains exhibit a mutualistic metabolism, and that DPV is sensitive enough to detect each strain, individually or as co-culture.

6.3.2 Microscopic analysis

The application of microscopy as a supporting technique for microbial studies is well documented in the literature (Chandra et al., 2001; Hrubanova et al., 2018; Jarosz et al., 2019; Kleine et al., 2019; Meireles et al., 2015; Méndez-Tovar et al., 2019; Veloz et al., 2019). Thus, following completion of electrochemical characterization, the electrodes were removed and processed as previously described for SEM imaging. Bare electrodes without inoculation were also imaged using the same procedures. Presented in Fig. 6.4 is the representative SEM images of inoculated and bare electrodes. The low frequency and sparse distribution of attached cells on the inoculated electrodes (Fig. 6.4A–B) further alludes to the results of electroanalysis, validating that the electrochemical responses obtained in this study were partly due to the planktonic cells. Fig. 6.4A shows a look-alike

of the *C. albicans* biofilm matrix; Fig. 6.4C confirms the vegetative budding formation, typical of *C. albicans* cells, while Fig. 6.4D is a representative SEM image of a bare SPE, confirming the graphitic surface configuration.

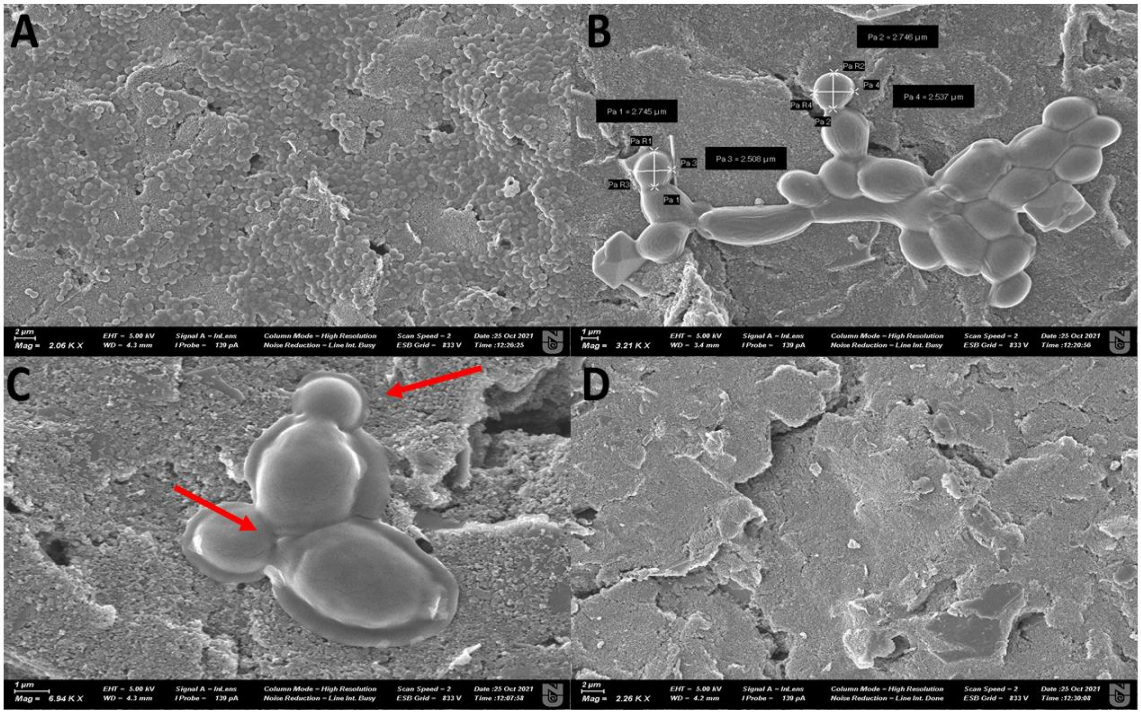

Fig. 6.4. Representative SEM images of early biofilm formation of *C. albicans* on graphite electrode SPE surface after 24 h of potentiostatic growth. (A) Sample showing biofilm matrix; (B, C) Samples showing budding formation in young cells; (D) sample bare electrode from a control sterile urine following completion of electroanalysis.

6.4 Summary

The conventional gold standard approach for *C. albicans* detection and characterization in clinical settings, especially in local and poor communities, remains the culture-dependent techniques which is tedious and require longer duration to obtain actionable results. Consequently, the need for a more simple and rapid diagnostic platform is exigent. In this study, we report for the first time the electrochemical characterization of *C. albicans* cells in human urine using commercially available, low-cost, unmodified SPEs. Chronoamperometry provided the most informative diagnostic information within 2-5 h of inoculation. The assay was shown to be sensitive to detect 39 CFU *C. albicans* cells per mL of human urine but was less sensitive when the cell counts become too low or too high. The high ionic strength and the constitutive chemical components of urine may have

impacted the sensitivity. Nonetheless, this work could provide a basis for further improvement and optimization of low-cost, simple-to-use bioelectrochemical platforms using unmodified SPEs. Additionally, SEM images indicated early biofilm formation on the electrode surface. However, the low biofilm biomass and sparse distribution of cells on electrode surface is indicative that both planktonic and attached cells may have contributed to the electrochemical response.

6.5 Outcome

Olaifa, K., Monari, M., Ajunwa, O., & Marsili, E. Real-time electroanalysis of *Candida albicans* in human urine samples via screen-printed electrochemical assay. **[Manuscript 90% completed].**

Chapter Seven: Limitations, concluding remarks and future prospects

7.1 Comments on our choice of SPEs, its limitations and comparison with the classical 3-electrode system

The choice of screen-printed electrodes (SPEs) or the classical 3-electrode system is often dependent on a number of factors including the experimental purpose vis-à-vis the pros and cons of the method. In cathodic microbial electrochemical systems where electrons are transferred from the electrode to the biofilms for the purpose of bioelectrosynthesis or electrochemical fermentation, the 3-electrode system is encouraged as it allows maximum electron transfer from the electrodes to the biofilms, efficient upscaling, and proper down-stream processing. On the other hand, in anodic microbial electrochemical systems where electrons are transferred from the biofilms to the electrode, a more relevant phenomenon for clinical application in the development of biofilm sensor and antimicrobial testing especially for weak electricigens (the two focal areas in the thesis), SPEs are best suited as it is more sensitive for detection and monitoring of early biofilm formation signatures due to their compact size and structural arrangement. Furthermore, each electrode in the case of the 3-electrode system needs to be acquired/made/fabricated and processed/cleaned separately, thus contributing to high cost and tediousness - luxuries that cannot be afforded in most local and rural healthcare facilities, especially in the developing countries. The possibility of reusing each of these electrodes also pose concerns about contamination and erroneous outcomes. SPEs on the other hand are inexpensive and disposable, with the 3 electrodes integrated into one small compact configuration. It requires only a mild cleaning/processing and allows testing with microvolumes of samples (typical of healthcare settings), a critical advantage completely lacking in the classical 3-electrode system. Use of SPEs requires small volume of sample and antimicrobials, making it feasible for high-throughput screening.

Pseudo-reference, as in the case of SPEs used in the thesis, forms an essential part of the eelectrochemical transducer for the maintenance of the reference potential of the system. The reference electrode provides a stable potential towards which the working electrode of an electrochemical cell can be measured or controlled. This is critical in potentiometric sensor, where any drift in the reference electrode potential may lead to a change in the

electrochemical output. Indeed, the properties of the electrode materials are prone to change in structure and composition over time. This is even more possible when the sensor system is used in longer experimental set-up, thus, possibly influencing the electrochemical output due to oxide layer formation, corrosion, desorption, degradation etc. SPEs are, however, not designed for a long-term experiment. They are best suited for a one-time short duration experiment, so their stability and responsibility are conserved. All experiments reported with SPEs in the thesis were completed in 24 hours (about 90 %), and in few cases 48 hours (< 10 %). Within such durations, SPEs are known to be stable, and yield reproducible results. This is supported by the work of Søpstad et al. (2018) on the long-term stability study of screen-printed pseudo-reference electrodes for electrochemical biosensors. In their experimental design, different pseudo-reference electrodes including the pseudo-Ag electrode used and reported in the thesis, were tested for a long-term duration of 40 days. All electrode surfaces remain unchanged in structure and composition after a measurement period of 40 days, while electrodes with a printed Ag ink (same as what is used and reported in the thesis) exhibited a potential stability beyond 48 hours. In general, and as what is known of SPEs, the study concluded that SPEs are best suited for short-term experiments. This is same as what is recommended in the thesis, that significant biosensing and antimicrobial testing results were obtained within 10 hours of inoculation, as against the minimum of 2-3 days most often recorded with the conventional biochemical approaches.

Furthermore, the roughness and porosity of electrode surface, together with its chemical characteristics, contribute to biofilm formation, and by extension, to its electroactivity. For instance, the larger the surface area, the more biofilm will form, thus resulting in a higher electrochemical output. Therefore, the current density for a typical working electrode in a 3-electrode setup and for a SPE will be different, due to the different surface roughness and chemical composition of the electrodes, even if both of them are made of graphite. However, it can be assumed that the current density will follow a similar pattern with time for the WE of 3-electrode setup and for a SPE, which mainly depends on the concentration and structure of the biofilm formed on the WE in both setups. It should be noted that the current output depends also on the metabolic activity of the biofilms (e.g., the summatory of the viable cells that are in the biofilm). To allow comparison of the results reported in

the thesis with other studies, the current output and the charge output has been reported as current density and charge density with respect to the geometric surface of the WE, i.e., $\mu A\ cm^{-2}$ (Koch & Harnisch, 2016).

7.2 Concluding remarks and future prospects

Based on the results obtained from the studies conducted and presented in this thesis, it is concluded that our hypotheses have been proven correct. That is, electrochemical techniques could be successfully adopted for analysis of clinically relevant microbial species, evaluation of antimicrobial/antibiofilm compounds' efficacy, and detection of selected microbial pathogens in relevant clinical biofluids.

The bioelectrochemical platform discussed in this thesis has been applied only under well-controlled laboratory conditions so far. Its implementation for drug testing, including existing clinically relevant antimicrobial/antibiofilm drugs, new compounds with promising antimicrobial/antibiofilm activity, or repurposed drugs, against clinically relevant microbial species, and detection of relevant microbial cells in actual biofluids (e.g., urine) was done with a number of samples that may be yet inadequate to ascertain a satisfactory validation for real-life clinical practice. Nonetheless, the distinctive features and practical advantages – versatility, portability, low cost, commercial availability of basic components, simplicity of technique, ease of implementation and interpretation of results, potential for miniaturization, and possible integration with microfluidics and other advanced technologies, potential for optimization through modification and/or functionalization of electrode surface, of the bioelectrochemical approach, and most importantly, its real-time feature, make it a methodology of choice for further exploration and research, and adoption in healthcare settings particularly in low-income, poor and local communities with no access to modern diagnostic facilities.

Sequel to the remarkable findings reported in this thesis, further research may be necessary to extend this approach to other infectious agents, including viruses. Additionally, the application of our bioelectrochemical platform for direct detection of microbial pathogens in biological fluids may require additional electrode modification with compatible biorecognition elements so as to improve specificity, and/or with antifouling peptides

especially in situations where extended incubation period may be required. Future research should also be directed to testing of this platform for other microbial species using other variety of biofluids (e.g., blood, serum, saliva, sputum) so as to extend the range of possible applications.

It is remarkable to mention that the early presentation of glucometers (glucose sensors) for clinical use many decades ago was greeted with significant cynicism on whether it would be helpful or cost effective (Cohen & Zimmet, 1980; Mach et al., 2012). Today, the rest is history, as the significance of glucose sensors in the present-day clinical diagnosis cannot be overemphasized. Therefore, to prevent a repeat of history, there is an urgent need to improve the market outlook and adoption of bioelectrochemical sensors in clinical practice. This may be achieved through, first, gradual and successive integration of electrochemical techniques with the existing traditional diagnostic methodologies, and second, funding of collaborative R&D between academics in universities/research centers and clinical practitioners. This would ensure adequate access to sufficient number of clinical samples, thus, foster significant improvement in the design and development of relevant bioelectrochemical devices, leading to a more rapid diagnoses and better patient outcomes.

Prevention, they say, is better than cure. Thus, it has become a priority that ongoing efforts on health education and awareness among the populace on relevance of basic hygiene, pros and cons of microbial pathogenesis, antimicrobial resistance, and the implications of both self-medication and delayed presentation of medical illnesses, should be intensified. Additionally, drug repurposing should be further explored as sustainable strategy in the fight against resistant microbial species, as it holds promising potential in complementing the conventional drug discovery programs. It is also cheap, fast, and poses little or no toxicity concerns.

Moreover, as all the essential known mechanisms of action of most clinically relevant antimicrobials/antibiotics are becoming compromised (as highlighted in Chapter 2), leading to loss of drug efficacy, rapid emergence and spread of antimicrobial resistance factors, it is becoming exigent to investigate other cellular targets for antimicrobial activity. Interestingly, arguments about adoption of microbial energetics, in this case EET as presented in this thesis, as a proxy for cellular growth activities, are now being made. It is

equally logical that a laser attention is beamed to same microbial energetics (EET and its related respiratory machineries) for the design and development of new and novel drugs.

Finally, while the field of bioelectrochemical sensing continues to evolve and advance, it is becoming increasingly necessary to have a centralized library for collection of electrochemical signatures of microorganisms and/or their metabolites, just as we have gene maps and banks for genetic characterizations of microbes. This, I believe, would open new frontiers and opportunities in microbial electrochemistry and its potentials for biosensing applications.

References

Abebe, G. M. (2020). The Role of Bacterial Biofilm in Antibiotic Resistance and Food Contamination. *International Journal of Microbiology*, *2020*. https://doi.org/10.1155/2020/1705814

Achinas, S., Charalampogiannis, N., & Euverink, G. J. W. (2019). A brief recap of microbial adhesion and biofilms. *Applied Sciences (Switzerland)*, *9*(14), 1–15. https://doi.org/10.3390/app9142801

Achkar, J. M., & Fries, B. C. (2010). Candida infections of the genitourinary tract. *Clinical Microbiology Reviews*, *23*(2), 253–273. https://doi.org/10.1128/CMR.00076-09

Aiyer, K., & Doyle, L. (2021). Capturing the signal of weak electricigens : a worthy endeavour. *Trends in Biotechnology*, 1–12. https://doi.org/https://doi.org/10.1016/j.tibtech.2021.10.002

Albanese, D., Sannini, A., Malvano, F., Pilloton, R., & Di Matteo, M. (2014). Optimisation of Glucose Biosensors Based on Sol-Gel Entrapment and Prussian Blue-Modified Screen-Printed Electrodes for Real Food Analysis. *Food Analytical Methods*, *7*(5), 1002–1008. https://doi.org/10.1007/s12161-013-9705-6

Alfouzan, W. A., & Dhar, R. (2017). Candiduria: Evidence-based approach to management, are we there yet? *Journal de Mycologie Medicale*, *27*(3), 293–302. https://doi.org/10.1016/j.mycmed.2017.04.005

Aliane, S., & Meliani, A. (2021). Bacterial biofilms: formation, advantages for community members, clinical implications, and antibiotic resistance. *Environmental and Experimental Biology*, *19*(3), 121–130. https://doi.org/10.22364/eeb.19.12

Almaghrabi, M. K., Joseph, M. R. P., Assiry, M. M., & Hamid, M. E. (2018). Multidrug-Resistant Acinetobacter baumannii: An Emerging Health Threat in Aseer Region, Kingdom of Saudi Arabia. *Canadian Journal of Infectious Diseases and Medical Microbiology*, *2018*. https://doi.org/10.1155/2018/9182747

Alonso-Lomillo, M. A., Domínguez-Renedo, O., & Arcos-Martínez, M. J. (2010). Screen-printed biosensors in microbiology; A review. *Talanta*, *82*(5), 1629–1636. https://doi.org/10.1016/j.talanta.2010.08.033

Amiri, M., Bezaatpour, A., Jafari, H., Boukherroub, R., & Szunerits, S. (2018). Electrochemical methodologies for the detection of pathogens. *ACS Sensors*, *3*(6), 1059–1086. https://doi.org/10.1021/acssensors.8b00239

Andrei, V., Sharpe, E., Vasilescu, A., & Andreescu, S. (2016). A single use electrochemical sensor based on biomimetic nanoceria for the detection of wine antioxidants. *Talanta*, *156–157*, 112–118. https://doi.org/10.1016/j.talanta.2016.04.067

Arthur, P. K., Yeboah, A. B., Issah, I., Balapangu, S., Kwofie, S. K., Asimeng, B. O., Foster, E. J., & Tiburu, E. K. (2019). Electrochemical response of saccharomyces cerevisiae corresponds to cell viability upon exposure to dioclea reflexa seed extracts and antifungal drugs. *Biosensors*, *9*(1), 1–12. https://doi.org/10.3390/bios9010045

Aslam, B., Wang, W., Arshad, M. I., Khurshid, M., Muzammil, S., Rasool, M. H., Nisar, M. A., Alvi, R. F., Aslam, M. A., Qamar, M. U., Salamat, M. K. F., & Baloch, Z. (2018). Antibiotic resistance: a rundown of a global crisis. *Infection and Drug Resistance*, *11*(June), 1645–1658. https://doi.org/10.2147/IDR.S173867

Astorga, S. E., Hu, L. X., Marsili, E., & Huang, Y. (2019). Electrochemical Signature of Escherichia coli on Nickel Micropillar Array Electrode for Early Biofilm Characterization. *ChemElectroChem*, *6*(17), 4674–4680. https://doi.org/10.1002/celc.201901063

Astorga, S. E., Hu, L. X., Marsili, E., & Huang, Y. (2020). Ordered micropillar array gold electrode increases electrochemical signature of early biofilm attachment. *Materials and Design*, *185*. https://doi.org/10.1016/j.matdes.2019.108256

Attoye, B., Pou, C., Blair, E., Rinaldi, C., Thomson, F., Baker, M. J., & Corrigan, D. K. (2020). Developing a Low-Cost, Simple-to-Use Electrochemical Sensor for the Detection of Circulating Tumour DNA in Human Fluids. *Biosensors*, *10*(11). https://doi.org/10.3390/bios10110156

Aulenta, F., Puig, S., & Harnisch, F. (2018). Microbial electrochemical technologies: maturing but not mature. *Microbial Biotechnology*, *11*(1), 18–19. https://doi.org/10.1111/1751-7915.13045

Aydemir, H., Akduman, D., Piskin, N., Comert, F., Horuz, E., Terzi, A., Kokturk, F., Ornek, T., & Celebi, G. (2013). Colistin vs. the combination of colistin and rifampicin for the treatment of carbapenem-resistant Acinetobacter baumannii ventilator-associated pneumonia. *Epidemiology and Infection*, *141*(6), 1214–1222. https://doi.org/10.1017/S095026881200194X

Azeredo, J., Azevedo, N. F., Briandet, R., Cerca, N., Coenye, T., Costa, A. R., Desvaux, M., Di Bonaventura, G., Hébraud, M., Jaglic, Z., Kačániová, M., Knøchel, S., Lourenço, A., Mergulhão, F., Meyer, R. L., Nychas, G., Simões, M., Tresse, O., & Sternberg, C. (2017). Critical review on biofilm methods. *Critical Reviews in Microbiology*, *43*(3), 313–351. https://doi.org/10.1080/1040841X.2016.1208146

Azevedo, N. F., Allkja, J., & Goeres, D. M. (2021). Biofilms vs. cities and humans vs. aliens – a tale of reproducibility in biofilms. *Trends in Microbiology*, *29*(12), 1062–1071. https://doi.org/10.1016/j.tim.2021.05.003

Babapour, E., Haddadi, A., Mirnejad, R., Angaji, S. A., & Amirmozafari, N. (2016). Biofilm formation in clinical isolates of nosocomial Acinetobacter baumannii and its relationship with multidrug resistance. *Asian Pacific Journal of Tropical Biomedicine*, *6*(6), 528–533. https://doi.org/10.1016/j.apjtb.2016.04.006

Babauta, J., Renslow, R., Lewandowski, Z., & Beyenal, H. (2012). Electrochemically active biofilms: Facts and fiction. A review. *Biofouling*, *28*(8), 789–812. https://doi.org/10.1080/08927014.2012.710324

Babauta, J. T., & Beyenal, H. (2014). Mass transfer studies of Geobacter sulfurreducens biofilms on rotating disk electrodes. *Biotechnology and Bioengineering*, *111*(2), 285–294. https://doi.org/10.1002/bit.25105

Balasundaram, P., Veerappapillai, S., Krishnamurthy, S., & Karuppasamy, R. (2018). Drug repurposing: An approach to tackle drug resistance in S. typhimurium. *Journal of Cellular Biochemistry*, *119*(3), 2818–2831. https://doi.org/10.1002/jcb.26457

Beauvais, A., & Latgé, J.-P. (2015). Aspergillus Biofilm In Vitro and In Vivo . *Microbiology Spectrum*, *3*(4). https://doi.org/10.1128/microbiolspec.mb-0017-2015

Becerro, S., Paredes, J., Mujika, M., Pérez Lorenzo, E., & Arana, S. (2016). Electrochemical Real-Time Analysis of Bacterial Biofilm Adhesion and Development by Means of Thin-Film Biosensors. *IEEE Sensors Journal*, *16*(7), 1856–1864. https://doi.org/10.1109/JSEN.2015.2504495

Behzadi, P., Behzadi, E., Agnieszka, E., & Adamska, P. (2019). Urinary tract infections (UTIs) or genital tract infections (GTIs)? It's the diagnostics that count. *GMS Hygiene and Infection Control*, *14*, 1–12.

Behzadi, P., Behzadi, E., & Ranjbar, R. (2015). Urinary tract infections and candida albicans. *Central European Journal of Urology*, *68*(1), 96–101. https://doi.org/10.5173/ceju.2015.01.474

Besant, J. D., Sargent, E. H., & Kelley, S. O. (2015). Rapid electrochemical phenotypic profiling of antibiotic-resistant bacteria. *Lab on a Chip*, *15*(13), 2799–2807. https://doi.org/10.1039/c5lc00375j

Bharatula, L. D., Marsili, E., & Kwan, J. J. (2019). Impedimetric detection of Pseudomonas aeruginosa attachment on flexible ITO-coated polyethylene terephthalate substrates. *Electrochimica Acta*, *332*(135390), 1–10. https://doi.org/10.1016/j.electacta.2019.135390

Bhuvaneswari, A., Navanietha, K. R., & Berchmans, S. (2013). Metamorphosis of pathogen to electrigen at the electrode/electrolyte interface: Direct electron transfer of Staphylococcus aureus leading to superior electrocatalytic activity. *Electrochemistry Communications*, *34*, 25–28. https://doi.org/10.1016/j.elecom.2013.05.013

Bimakr, F., Ginige, M. P., Kaksonen, A. H., Sutton, D. C., Puzon, G. J., & Cheng, K. Y. (2018). Assessing graphite and stainless-steel for electrochemical sensing of biofilm growth in chlorinated drinking water systems. *Sensors and Actuators, B: Chemical*, *277*(August), 526–534. https://doi.org/10.1016/j.snb.2018.09.005

Borole, A. P., Reguera, G., Ringeisen, B., Wang, Z. W., Feng, Y., & Kim, B. H. (2011). Electroactive biofilms: Current status and future research needs. *Energy and Environmental Science*, *4*(12), 4813–4834. https://doi.org/10.1039/c1ee02511b

Bosire, E. M., Blank, L. M., & Rosenbaum, M. A. (2016a). Strain- and substrate-dependent redox mediator and electricity production by pseudomonas aeruginosa. *Applied and Environmental Microbiology*, *82*(16), 5026–5038. https://doi.org/10.1128/AEM.01342-16

Bosire, E. M., Blank, L. M., & Rosenbaum, M. A. (2016b). *Strain- and Substrate-Dependent Redox Mediator and Electricity Production by Pseudomonas aeruginosa*. *82*(16), 5026–5038. https://doi.org/10.1128/AEM.01342-16.Editor

Bosire, E. M., & Rosenbaum, M. A. (2017). Electrochemical potential influences phenazine production, electron transfer and consequently electric current generation by Pseudomonas aeruginosa. *Frontiers in Microbiology*, *8*(MAY), 1–11. https://doi.org/10.3389/fmicb.2017.00892

Bowler, P. G. (2018). Antibiotic resistance and biofilm tolerance: A combined threat in the treatment of chronic infections. *Journal of Wound Care*, *27*(5), 273–277. https://doi.org/10.12968/jowc.2018.27.5.273

Bressel, A., Schultze, J. W., Khan, W., Wolfaardt, G. M., Rohns, H. P., Irmscher, R., & Schöning, M. J. (2003). High resolution gravimetric, optical and electrochemical investigations of microbial biofilm formation in aqueous systems. *Electrochimica Acta*, *48*(20–22), 3363–3372. https://doi.org/10.1016/S0013-4686(03)00406-7

Buzid, A., Muimhneacháin, E., Reen, F. J., Hayes, P. E., Pardo, L. M., Shang, F., O'Gara, F., Sperry, J., Luong, J. H. T., Glennon, J. D., & McGlacken, G. P. (2016). Synthesis and electrochemical detection of a thiazolyl-indole natural product isolated from the nosocomial pathogen Pseudomonas aeruginosa. *Analytical and Bioanalytical Chemistry*, *408*(23), 6361–6367. https://doi.org/10.1007/s00216-016-9749-8

Campoy, S., & Adrio, J. L. (2017). Antifungals. *Biochemical Pharmacology*, *133*, 86–96. https://doi.org/10.1016/j.bcp.2016.11.019

Campuzano, S., Yáñez-Sedeño, P., & Manuel Pingarrón, J. (2017). Molecular biosensors for electrochemical detection of infectious pathogens in liquid biopsies: Current trends and challenges. *Sensors (Switzerland)*, *17*(11). https://doi.org/10.3390/s17112533

Cantón, E., Espinel-Ingroff, A., & Pemán, J. (2009). Trends in antifungal susceptibility testing using CLSI reference and commercial methods. *Expert Review of Anti-Infective Therapy*, *7*(1), 107–119. https://doi.org/10.1586/14787210.7.1.107

Carmona-Martínez, A. A., Harnisch, F., Kuhlicke, U., Neu, T. R., & Schröder, U. (2013). Electron transfer and biofilm formation of Shewanella putrefaciens as function of anode potential. *Bioelectrochemistry*, *93*, 23–29. https://doi.org/10.1016/j.bioelechem.2012.05.002

Castanheira, M., Mendes, R. E., & Jones, R. N. (2014). Update on acinetobacter species: Mechanisms of antimicrobial resistance and contemporary in vitro activity of minocycline and other treatment options. *Clinical Infectious Diseases*, *59*(Suppl 6), S367–S373. https://doi.org/10.1093/cid/ciu706

Cavalheiro, M., & Teixeira, M. C. (2018). Candida Biofilms: Threats, challenges, and promising strategies. *Frontiers in Medicine*, *5*(FEB), 1–15. https://doi.org/10.3389/fmed.2018.00028

CDC. (2019). Antibiotic resistance threats in the United States. In *Centers for Disease Control and Prevention*. https://doi.org/http://dx.doi.org/10.15620/cdc:82532

Cepas, V., López, Y., Gabasa, Y., Martins, C. B., Ferreira, J. D., Correia, M. J., Santos, L. M. A., Oliveira, F., Ramos, V., Reis, M., Castelo-Branco, R., Morais, J., Vasconcelos,

V., Probert, I., Guilloud, E., Mehiri, M., & Soto, S. M. (2019a). Inhibition of bacterial and fungal biofilm formation by 675 extracts from microalgae and cyanobacteria. *Antibiotics*, *8*(2), 1–12. https://doi.org/10.3390/antibiotics8020077

Cepas, V., López, Y., Gabasa, Y., Martins, C. B., Ferreira, J. D., Correia, M. J., Santos, L. M. A., Oliveira, F., Ramos, V., Reis, M., Castelo-Branco, R., Morais, J., Vasconcelos, V., Probert, I., Guilloud, E., Mehiri, M., & Soto, S. M. (2019b). Inhibition of bacterial and fungal biofilm formation by 675 extracts from microalgae and cyanobacteria. *Antibiotics*, *8*(2), 2–3. https://doi.org/10.3390/antibiotics8020077

Cerca, N., Gomes, F., Pereira, S., Teixeira, P., & Oliveira, R. (2012). Confocal laser scanning microscopy analysis of S. epidermidis biofilms exposed to farnesol, vancomycin and rifampicin. *BMC Research Notes*, *5*. https://doi.org/10.1186/1756-0500-5-244

Cesewski, E., & Johnson, B. N. (2020). Electrochemical biosensors for pathogen detection. *Biosensors and Bioelectronics*, *159*, 112214. https://doi.org/10.1016/j.bios.2020.112214

Cha, Y., Erez, T., Reynolds, I. J., Kumar, D., Ross, J., Koytiger, G., Kusko, R., Zeskind, B., Risso, S., Kagan, E., Papapetropoulos, S., Grossman, I., & Laifenfeld, D. (2018). Drug repurposing from the perspective of pharmaceutical companies. *British Journal of Pharmacology*, *175*(2), 168–180. https://doi.org/10.1111/bph.13798

Chalenko, Y., Shumyantseva, V., Ermolaeva, S., & Archakov, A. (2012). Electrochemistry of Escherichia coli JM109: Direct electron transfer and antibiotic resistance. *Biosensors and Bioelectronics*, *32*(1), 219–223. https://doi.org/10.1016/j.bios.2011.12.015

Chandra, J., Kuhn, D. M., Mukherjee, P. K., Hoyer, L. L., Cormick, T. M. C., & Ghannoum, M. A. (2001). Biofilm formation by the fungal pathogen Candida albicans. *Journal of Bacteriology*, *183*(18), 5385–5394. https://doi.org/10.1128/JB.183.18.5385

Chen, L., Cao, C., Wang, S., Varcoe, J. R., Slade, R. C. T., Avignone-Rossa, C., & Zhao, F. (2019). Electron Communication of Bacillus subtilis in Harsh Environments. *IScience*, *12*, 260–269. https://doi.org/10.1016/j.isci.2019.01.020

Cohen, M., & Zimmet, P. (1980). Home blood-glucose monitoring: a new approach to the management of diabetes mellitus. *The Lancet*, 187–188. https://doi.org/10.1016/S0140-6736(80)90068-9

Congdon, R. B., Feldberg, A. S., Ben-yakar, N., Mcgee, D., Ober, C., Sammakia, B., & Sadik, O. A. (2013). Early detection of Candida albicans biofilms at porous electrodes. *ANALYTICAL BIOCHEMISTRY*, *433*(2), 192–201. https://doi.org/10.1016/j.ab.2012.10.016

Czerwińska-Główka, D., & Krukiewicz, K. (2020). A journey in the complex interactions between electrochemistry and bacteriology: From electroactivity to electromodulation of bacterial biofilms. *Bioelectrochemistry*, *131*. https://doi.org/10.1016/j.bioelechem.2019.107401

D'Onofrio, V., Conzemius, R., Varda-Brkić, D., Bogdan, M., Grisold, A., Gyssens, I. C., Bedenić, B., & Barišić, I. (2020). Epidemiology of colistin-resistant, carbapenemase-producing Enterobacteriaceae and Acinetobacter baumannii in Croatia. *Infection, Genetics and Evolution*, *81*(December 2019), 104263. https://doi.org/10.1016/j.meegid.2020.104263

Dadar, M., Tiwari, R., Karthik, K., Chakraborty, S., Shahali, Y., & Dhama, K. (2018). Candida albicans - Biology, molecular characterization, pathogenicity, and advances in diagnosis and control – An update. *Microbial Pathogenesis*, *117*(April), 128–138. https://doi.org/10.1016/j.micpath.2018.02.028

Dahdouh, E., Gómez-Gil, R., Pacho, S., Mingorance, J., Daoud, Z., & Suárez, M. (2017). Clonality, virulence determinants, and profiles of resistance of clinical Acinetobacter baumannii isolates obtained from a Spanish hospital. *PLoS ONE*, *12*(4), 1–18. https://doi.org/10.1371/journal.pone.0176824

Davenport, M., Mach, K. E., Shortliffe, L. M. D., Banaei, N., Wang, T. H., & Liao, J. C. (2017). New and developing diagnostic technologies for urinary tract infections. *Nature Reviews Urology*, *14*(5), 298–310. https://doi.org/10.1038/nrurol.2017.20

Davies, J. (1996). Origins and evolution of antibiotic resistance. *Microbiología (Madrid, Spain)*, *12*(1), 9–16. https://doi.org/10.1128/mmbr.00016-10

de Barros, P. P., Rossoni, R. D., de Souza, C. M., Scorzoni, L., Fenley, J. D. C., & Junqueira, J. C. (2020). Candida Biofilms: An Update on Developmental Mechanisms and Therapeutic Challenges. *Mycopathologia*, *0123456789*. https://doi.org/10.1007/s11046-020-00445-w

de Kraker, M. E. A., Stewardson, A. J., & Harbarth, S. (2016). Will 10 Million People Die a Year due to Antimicrobial Resistance by 2050? *PLoS Medicine*, *13*(11), 1–6. https://doi.org/10.1371/journal.pmed.1002184

Della Pelle, F., Angelini, C., Sergi, M., Del Carlo, M., Pepe, A., & Compagnone, D. (2018). Nano carbon black-based screen printed sensor for carbofuran, isoprocarb, carbaryl and fenobucarb detection: application to grain samples. *Talanta*, *186*(March), 389–396. https://doi.org/10.1016/j.talanta.2018.04.082

Di Domenico, E. G., Cavallo, I., Guembe, M., Prignano, G., Gallo, M. T., Bordignon, V., D'Agosto, G., Sperduti, I., Toma, L., & Ensoli, F. (2018). The clinical Biofilm Ring Test: A promising tool for the clinical assessment of biofilm-producing Candida species. *FEMS Yeast Research*, *18*(3), 1–8. https://doi.org/10.1093/femsyr/foy025

Dias, V. (2020). Candida species in the urinary tract: Is it a fungal infection or not? *Future Microbiology*, *15*(2), 81–83. https://doi.org/10.2217/fmb-2019-0262

Dieltjens, L., Appermans, K., Lissens, M., Lories, B., Kim, W., Van der Eycken, E. V., Foster, K. R., & Steenackers, H. P. (2020). Inhibiting bacterial cooperation is an evolutionarily robust anti-biofilm strategy. *Nature Communications*, *11*(1), 1–11. https://doi.org/10.1038/s41467-019-13660-x

Dincer, C., Bruch, R., Costa-Rama, E., Fernández-Abedul, M. T., Merkoçi, A., Manz, A.,

Urban, G. A., & Güder, F. (2019). Disposable Sensors in Diagnostics, Food, and Environmental Monitoring. *Advanced Materials*, *31*(30). https://doi.org/10.1002/adma.201806739

Doelling, R. (1998). Hans Wenking, born August 18th, 1923 A problem-solver for electrochemists. *Materials and Corrosion*, *49*(8), 535–538. https://doi.org/10.1002/(sici)1521-4176(199808)49:8<535::aid-maco535>3.0.co;2-m

Doelling, R. (2000). Potentiostats: An introduction to the principle of potentiostatic control, including basic potentiostatic circuits, electrochemical applications, and some notes on electrode and cell design. *Bank Elektronik Intelligent Controls*, *March*. http://www.bank-ic.de/encms/downloads/potstae2.pdf

Domínguez, A., Mejías, M. E., & Smani, Y. (2016). Drugs Repurposing for Multi-Drug Resistant Bacterial Infections. In *Intech* (Issue tourism). https://doi.org/DOI: http://dx.doi.org/10.5772/intechopen.93635 against

Domínguez, A. V., Algaba, R. A., Canturri, A. M., Villodres, Á. R., & Smani, Y. (2020). Antibacterial activity of colloidal silver against gram-negative and gram-positive bacteria. *Antibiotics*, *9*(1), 1–10. https://doi.org/10.3390/antibiotics9010036

Doyle, L. E., & Marsili, E. (2018a). Weak electricigens: A new avenue for bioelectrochemical research. *Bioresource Technology*, *258*(February), 354–364. https://doi.org/10.1016/j.biortech.2018.02.073

Doyle, L. E., & Marsili, E. (2018b). Weak electricigens: A new avenue for bioelectrochemical research. *Bioresource Technology*, *258*(December 2017), 354–364. https://doi.org/10.1016/j.biortech.2018.02.073

Doyle, L. E., Yung, P. Y., Mitra, S. D., Wuertz, S., Williams, R. B. H., Lauro, F. M., & Marsili, E. (2017). Electrochemical and genomic analysis of novel electroactive isolates obtained via potentiostatic enrichment from tropical sediment. *Journal of Power Sources*, *356*, 539–548. https://doi.org/10.1016/j.jpowsour.2017.03.147

Dutta, P., Lu, Y. J., Hsieh, H. Y., Lee, T. Y., Lee, Y. T., Cheng, C. M., & Fan, Y. J. (2021). Detection of candida albicans using a manufactured electrochemical sensor. *Micromachines*, *12*(2). https://doi.org/10.3390/mi12020166

El-Nahas, H. A., Salem, D. A., El-Henawy, A. A., El-Nimr, H. I., Abdel-Ghaffar, H. A., & El-Meadawy, A. M. (2013). Giardia diagnostic methods in human fecal samples: a comparative study. *Cytometry. Part B, Clinical Cytometry*, *84*(1), 44–49. https://doi.org/10.1002/cyto.b.21048

Elabed, A., Ezziat, L., Ibnsouda, S., Elabed, S., & Erable, B. (2021). Bioelectrochemical Characterization of Heavy Metals Resistant yeast: Hansenula fabianii Isolated from Tannery Wastewater. *International Journal of Electrochemical Science*, *16*, 140128. https://doi.org/10.20964/2021.01.31

Elbardisy, H. M., García-Miranda Ferrari, A., Foster, C. W., Sutcliffe, O. B., Brownson, D. A. C., Belal, T. S., Talaat, W., Daabees, H. G., & Banks, C. E. (2019). Forensic

Electrochemistry: The Electroanalytical Sensing of Mephedrone Metabolites. *ACS Omega*, *4*(1), 1947–1954. https://doi.org/10.1021/acsomega.8b02586

Enke, C. G. (2015). The Analog Revolution and Its On-Going Role in Modern Analytical Measurements. *Analytical Chemistry*, *87*(24), 11935–11947. https://doi.org/10.1021/acs.analchem.5b02405

Ernst, E. (2007). Antifungal Agents: Methods and Protocols. *Methods in Molecular Medicine*, *118*, 1–10. http://cx2ef4jw8j.search.serialssolutions.com/?url_ver=Z39.88-2004&rfr_id=info:sid/udel.worldcat.org:worldcat&rft_val_fmt=info:ofi/fmt:kev:mtx:book&rft.genre=unknown&req_dat=%3Csessionid%3E&rfe_dat=%3Caccessionnumber%3E65284672%3C/accessionnumber%3E&rft_i

Ertl, P., Robello, E., Battaglini, F., & Mikkelsen, S. R. (2000). Rapid antibiotic susceptibility testing via electrochemical measurement of ferricyanide reduction by Escherichia coli and Clostridium sporogenes. *Analytical Chemistry*, *72*(20), 4957–4964. https://doi.org/10.1021/ac0003596

Eze, E. C., Chenia, H. Y., & El Zowalaty, M. E. (2018). Acinetobacter baumannii biofilms: Effects of physicochemical factors, virulence, antibiotic resistance determinants, gene regulation, and future antimicrobial treatments. *Infection and Drug Resistance*, *11*, 2277–2299. https://doi.org/10.2147/IDR.S169894

Farha, M. A., & Brown, E. D. (2019). Drug repurposing for antimicrobial discovery. *Nature Microbiology*, *4*(4), 565–577. https://doi.org/10.1038/s41564-019-0357-1

Farrer, N. J., & Sadler, P. J. (2011). Medicinal Inorganic Chemistry: State of the Art, New Trends, and a Vision of the Future. In E. Alessio (Ed.), *Bioinorganic Medicinal Chemistry* (pp. 1–37). Wiley-VCH Verlag & Co. KGaA, Boschstr. 12, 69469 Weinheim, Germany All.

Fazeli, A., Kordbacheh, P., Nazari, A., Daie Ghazvini, R., Mirhendi, H., Safara, M., Bakhshi, H., & Yaghoubi, R. (2019). Candiduria in hospitalized patients and identification of isolated candida species by morphological and molecular methods in Ilam, Iran. *Iranian Journal of Public Health*, *48*(1), 156–161. https://doi.org/10.18502/ijph.v48i1.804

Flemming, H. C., Wingender, J., Szewzyk, U., Steinberg, P., Rice, S. A., & Kjelleberg, S. (2016). Biofilms: An emergent form of bacterial life. *Nature Reviews Microbiology*, *14*(9), 563–575. https://doi.org/10.1038/nrmicro.2016.94

Flores-Mireles, A. L., Walker, N., J., Caparon, M., & Hultgren, S. J. (2015). Urinary tract infections: epidemiology, mechanisms of infection and treatment options. *Nature Reviews Microbiology*, *13*(5), 269–284. https://doi.org/10.1038/nrmicro3432

Franco-Duarte, R., Černáková, L., Kadam, S., Kaushik, K. S., Salehi, B., Bevilacqua, A., Corbo, M. R., Antolak, H., Dybka-Stępień, K., Leszczewicz, M., Tintino, S. R., de Souza, V. C. A., Sharifi-Rad, J., Coutinho, H. D. M., Martins, N., & Rodrigues, C. F. (2019). Advances in chemical and biological methods to identify microorganisms—from past to present. *Microorganisms*, *7*(5). https://doi.org/10.3390/microorganisms7050130

Frassinetti, S., Falleni, A., & Del Carratore, R. (2020). Effect of itraconazole on Staphylococcus aureus biofilm and extracellular vesicles formation. *Microbial Pathogenesis, 147*, 104267. https://doi.org/10.1016/j.micpath.2020.104267

Freguia, S., Masuda, M., Tsujimura, S., & Kano, K. (2009). Lactococcus lactis catalyses electricity generation at microbial fuel cell anodes via excretion of a soluble quinone. *Bioelectrochemistry*, *76*(1–2), 14–18. https://doi.org/10.1016/j.bioelechem.2009.04.001

Fritzenwanker, M., Imirzalioglu, C., Chakraborty, T., & Wagenlehner, F. M. (2016). Modern diagnostic methods for urinary tract infections. *Expert Review of Anti-Infective Therapy*, *14*(11), 1047–1063. https://doi.org/10.1080/14787210.2016.1236685

Furst, A. L., & Francis, M. B. (2019). Impedance-Based Detection of Bacteria [Review-article]. *Chemical Reviews*, *119*(1), 700–726. https://doi.org/10.1021/acs.chemrev.8b00381

Gajdács, M., Dóczi, I., Ábrók, M., Lázár, A., & Burián, K. (2019). Epidemiology of candiduria and Candida urinary tract infections in inpatients and outpatients: Results from a 10-year retrospective survey. *Central European Journal of Urology*, *72*(2), 209–214. https://doi.org/10.5173/ceju.2019.1909

Garciá-Miranda Ferrari, A., Carrington, P., Rowley-Neale, S. J., & Banks, C. E. (2020). Recent advances in portable heavy metal electrochemical sensing platforms. *Environmental Science: Water Research and Technology*, *6*(10), 2676–2690. https://doi.org/10.1039/d0ew00407c

García-Miranda Ferrari, A., Rowley-Neale, S. J., & Banks, C. E. (2021). Screen-printed electrodes: Transitioning the laboratory in-to-the field. *Talanta Open*, *3*(January). https://doi.org/10.1016/j.talo.2021.100032

Gharaghani, M., Taghipour, S., Halvaeezadeh, M., & Mahmoudabadi, A. Z. (2018). Candiduria; a review article with specific data from Iran. *Turkish Journal of Urology*, *44*(6), 445–452. https://doi.org/10.5152/tud.2018.54069

Ghosh, A., Jayaraman, N., & Chatterji, D. (2020). Small-Molecule Inhibition of Bacterial Biofilm. *ACS Omega*, *5*(7), 3108–3115. https://doi.org/10.1021/acsomega.9b03695

Glišić, B. A., Senerovic, L., Comba, P., Wadepohl, H., Veselinovic, A., Milivojevic, D. R., Djuran, M. I., & Nikodinovic-Runic, J. (2016). Silver(I) complexes with phthalazine and quinazoline as effective agents against pathogenic Pseudomonas aeruginosa strains. *Journal of Inorganic Biochemistry*, *155*(I), 115–128. https://doi.org/10.1016/j.jinorgbio.2015.11.026

Goeres, D. M., Walker, D. K., Buckingham-Meyer, K., Lorenz, L., Summers, J., Fritz, B., Goveia, D., Dickerman, G., Schultz, J., & Parker, A. E. (2019). Development, standardization, and validation of a biofilm efficacy test: The single tube method. *Journal of Microbiological Methods*, *165*, 105694. https://doi.org/10.1016/j.mimet.2019.105694

Goldbeck, J. C., Victoria, F. N., Motta, A., Savegnago, L., Jacob, R. G., Perin, G., Lenardão, E. J., & Padilha da Silva, W. (2014). Bioactivity and morphological changes of bacterial cells after exposure to 3-(p-chlorophenyl)thio citronellal. *LWT - Food Science and Technology*, *59*(2P1), 813–819. https://doi.org/10.1016/j.lwt.2014.05.036

Golichenari, B., Nosrati, R., Farokhi-Fard, A., Faal Maleki, M., Gheibi Hayat, S. M., Ghazvini, K., Vaziri, F., & Behravan, J. (2019). Electrochemical-based biosensors for detection of Mycobacterium tuberculosis and tuberculosis biomarkers. *Critical Reviews in Biotechnology*, *39*(8), 1056–1077. https://doi.org/10.1080/07388551.2019.1668348

Gomes, L. C., & Mergulhão, F. J. (2017). SEM analysis of surface impact on biofilm antibiotic treatment. *Scanning*, *2017*(c). https://doi.org/10.1155/2017/2960194

Gómez-Gaviria, M., & Mora-Montes, H. M. (2020). Current aspects in the biology, pathogeny, and treatment of candida krusei, a neglected fungal pathogen. *Infection and Drug Resistance*, *13*, 1673–1689. https://doi.org/10.2147/IDR.S247944

Gonzalez-Villoria, A. M., & Valverde-Garduno, V. (2016). Antibiotic-Resistant Acinetobacter baumannii Increasing Success Remains a Challenge as a Nosocomial Pathogen . *Journal of Pathogens*, *2016*, 1–10. https://doi.org/10.1155/2016/7318075

Guette-Marquet, S., Basseguy, R., Roques, C., & Bergel, A. (2021). The electrochemical potential is a key parameter for cell adhesion and proliferation on carbon surface. *Bioelectrochemistry*, *144*, 108045. https://doi.org/10.1016/j.bioelechem.2021.108045

Gulati, M. and, & Nobile, C. (2016). Candida albicans biofilms. *Chinese Pharmaceutical Journal*, *18*(5), 310–321. https://doi.org/10.1016/j.micinf.2016.01.002.Candida

Gulati, M., Ennis, C. L., Rodriguez, D. L., & Nobile, C. J. (2017). Visualization of biofilm formation in Candida albicans using an automated microfluidic device. *Journal of Visualized Experiments*, *2017*(130), 1–8. https://doi.org/10.3791/56743

Gulati, M., Lohse, M. B., Ennis, C. L., Gonzalez, R. E., Perry, A. M., Bapat, P., Arevalo, A. V., Rodriguez, D. L., & Nobile, C. J. (2018). In Vitro Culturing and Screening of Candida albicans Biofilms. *Current Protocols in Microbiology*, *50*(1), 1–45. https://doi.org/10.1002/cpmc.60

Gunsalus, K. T. W., Tornberg-Belanger, S. N., Matthan, N. R., Lichtenstein, A. H., & Kumamoto, C. A. (2016). Manipulation of Host Diet To Reduce Gastrointestinal Colonization by the Opportunistic Pathogen Candida albicans. *MSphere*, *1*(1), 1–16. https://doi.org/10.1128/msphere.00020-15

Haque, A., Ilmi, R., Al-Busaidi, I. J., & Khan, M. S. (2017). Coordination chemistry and application of mono- and oligopyridine-based macrocycles. *Coordination Chemistry Reviews*, *350*, 320–339. https://doi.org/10.1016/j.ccr.2017.07.008

Harba, N. M., Rady, A. A., & Khalefa, K. A. (2012). Evaluation of Flow Cytometry as a Diagnostic Method for Detection of Giardia lamblia in Comparison to IFAT and Other Conventional Staining Techniques in Fecal Samples. *Parasitologists United Journal*

(PUJ), *5*(2), 165–174.

Hards, K., & Cook, G. M. (2018). Targeting bacterial energetics to produce new antimicrobials. *Drug Resistance Updates*, *36*(October 2017), 1–12. https://doi.org/10.1016/j.drup.2017.11.001

Hassan, R. Y. A., & Bilitewski, U. (2013). Direct electrochemical determination of Candida albicans activity. *Biosensors and Bioelectronics*, *49*, 192–198. https://doi.org/10.1016/j.bios.2013.05.015

Hawser, S. (1996). Adhesion of different Candida spp. to plastic: XTT formazan determinations. *Journal of Medical and Veterinary Mycology*, *34*(6), 407–410. https://doi.org/10.1080/02681219680000721

Hawser, S. P., & Douglas, L. J. (1995). Resistance of Candida albicans biofilms to antifungal agents in vitro. *Antimicrobial Agents and Chemotherapy*, *39*(9), 2128–2131. https://doi.org/10.1128/AAC.39.9.2128

Hederstedt, L., Gorton, L., & Pankratovab, G. (2020). Two Routes for Extracellular Electron Transfer in Enterococcus faecalis. *Journal of Bacteriology*, *202*(7), 1–18. https://doi.org/10.1128/JB.00725-19

Hernández-Fernández, F. J., Pérez De Los Ríos, A., Salar-García, M. J., Ortiz-Martínez, V. M., Lozano-Blanco, L. J., Godínez, C., Tomás-Alonso, F., & Quesada-Medina, J. (2015). Recent progress and perspectives in microbial fuel cells for bioenergy generation and wastewater treatment. *Fuel Processing Technology*, *138*, 284–297. https://doi.org/10.1016/j.fuproc.2015.05.022

Holm, A., Cordoba, G., Møller Sørensen, T., Rem Jessen, L., Frimodt-Møller, N., Siersma, V., & Bjerrum, L. (2017). Effect of point-of-care susceptibility testing in general practice on appropriate prescription of antibiotics for patients with uncomplicated urinary tract infection: A diagnostic randomised controlled trial. *BMJ Open*, *7*(10). https://doi.org/10.1136/bmjopen-2017-018028

Hrubanova, K., Krzyzanek, V., Nebesarova, J., Ruzicka, F., Pilat, Z., & Samek, O. (2018). Monitoring Candida parapsilosis and Staphylococcus epidermidis Biofilms by a Combination of Scanning Electron Microscopy and Raman Spectroscopy. *Sensors (Basel, Switzerland)*, *18*(12), 1–19. https://doi.org/10.3390/s18124089

Huang, X., Xu, D., Chen, J., Liu, J., Li, Y., Song, J., Ma, X., & Guo, J. (2018). Smartphone-based analytical biosensors. *Analyst*, *143*(22), 5339–5351. https://doi.org/10.1039/c8an01269e

Huang, Y., Chakraborty, S., & Liang, H. (2020). Methods to probe the formation of biofilms: Applications in foods and related surfaces. *Analytical Methods*, *12*(4), 416–432. https://doi.org/10.1039/c9ay02214g

Hubenova, Y., Bakalska, R., Hubenova, E., & Mitov, M. (2016). Mechanisms of electron transfer between a styrylquinolinium dye and yeast in biofuel cell. *Bioelectrochemistry*, *112*, 158–165. https://doi.org/10.1016/j.bioelechem.2016.02.005

Hudzicki, J. (2012). Kirby-Bauer Disk Diffusion Susceptibility Test Protocol Author Information. *American Society For Microbiology*, *December 2009*, 1–13. https://www.asm.org/Protocols/Kirby-Bauer-Disk-Diffusion-Susceptibility-Test-Pro

Hussain, K. K., Malavia, D., Johnson, E. M., Littlechild, J., Winlove, C. P., Vollmer, F., & Gow, N. A. R. (2020). Biosensors and diagnostics for fungal detection. *Journal of Fungi*, *6*(4), 1–26. https://doi.org/10.3390/jof6040349

Ibáñez-Redín, G., Furuta, R. H. M., Wilson, D., Shimizu, F. M., Materon, E. M., Arantes, L. M. R. B., Melendez, M. E., Carvalho, A. L., Reis, R. M., Chaur, M. N., Gonçalves, D., & Oliveira, O. N. (2019). Screen-printed interdigitated electrodes modified with nanostructured carbon nano-onion films for detecting the cancer biomarker CA19-9. *Materials Science and Engineering C*, *99*(September 2018), 1502–1508. https://doi.org/10.1016/j.msec.2019.02.065

Ibberson, C. B., & Whiteley, M. (2020). The social life of microbes in chronic infection. *Current Opinion in Microbiology*, *53*, 44–50. https://doi.org/10.1016/j.mib.2020.02.003

Imperi, F., Massai, F., Pillai, C. R., Longo, F., Zennaro, E., Rampioni, G., Visc, P., & Leoni, L. (2013). New life for an old Drug: The anthelmintic drug niclosamide inhibits pseudomonas aeruginosa quorum sensing. *Antimicrobial Agents and Chemotherapy*, *57*(2), 996–1005. https://doi.org/10.1128/AAC.01952-12

Islam, R., Luu, H. T. Le, & Kuss, S. (2020). Review—Electrochemical Approaches and Advances towards the Detection of Drug Resistance. *Journal of The Electrochemical Society*, *167*(4), 045501. https://doi.org/10.1149/1945-7111/ab6ff3

Jarosz, M., Grudzień, J., Kamiński, K., Gawlak, K., Wolski, K., Nowakowska, M., & Sulka, G. D. (2019). Novel bioelectrodes based on polysaccharide modified gold surfaces and electrochemically active Lactobacillus rhamnosus GG biofilms. *Electrochimica Acta*, *296*, 999–1008. https://doi.org/10.1016/j.electacta.2018.11.154

Johnson, E. M. (2008). Issues in antifungal susceptibility testing. *Journal of Antimicrobial Chemotherapy*, *61*(SUPPL. 1), 13–18. https://doi.org/10.1093/jac/dkm427

Jubeh, B., Breijyeh, Z., & Karaman, R. (2020). Resistance of gram-positive bacteria to current antibacterial agents and overcoming approaches. *Molecules*, *25*(12). https://doi.org/10.3390/molecules25122888

Kainz, K., Bauer, M. A., Madeo, F., & Carmona-Gutierrez, D. (2020). Fungal infections in humans: the silent crisis. *Microbial Cell*, *7*(6), 143–145. https://doi.org/10.15698/mic2020.06.718

Kalinowska-Lis, U., Felczak, A., Checińska, L., Zawadzka, K., Patyna, E., Lisowska, K., & Ochocki, J. (2015). Synthesis, characterization and antimicrobial activity of water-soluble silver(I) complexes of metronidazole drug and selected counter-ions. *Dalton Transactions*, *44*(17), 8178–8189. https://doi.org/10.1039/c5dt00403a

Kamurai, B., Mombeshora, M., & Mukanganyama, S. (2020). Repurposing of Drugs for Antibacterial Activities on Selected ESKAPE Bacteria Staphylococcus aureus and

Pseudomonas aeruginosa. *International Journal of Microbiology*, *2020*. https://doi.org/10.1155/2020/8885338

Kang, J., Kim, T., Tak, Y., Lee, J. H., & Yoon, J. (2012). Cyclic voltammetry for monitoring bacterial attachment and biofilm formation. *Journal of Industrial and Engineering Chemistry*, *18*(2), 800–807. https://doi.org/10.1016/j.jiec.2011.10.002

Kannan, P., Jogdeo, P., Mohidin, A. F., Yung, P. Y., Santoro, C., Seviour, T., Hinks, J., Lauro, F. M., & Marsili, E. (2019). A novel microbial - Bioelectrochemical sensor for the detection of n-cyclohexyl-2-pyrrolidone in wastewater. *Electrochimica Acta*, *317*, 604–611. https://doi.org/10.1016/j.electacta.2019.06.018

Karbelkar, A. A., & Furst, A. L. (2020). Electrochemical Diagnostics for Bacterial Infectious Diseases. *ACS Infectious Diseases*, *6*(7), 1567–1571. https://doi.org/10.1021/acsinfecdis.0c00342

Kauffman, C. A. (2014). Diagnosis and management of fungal urinary tract infection. *Infectious Disease Clinics of North America*, *28*(1), 61–74. https://doi.org/10.1016/j.idc.2013.09.004

Kauffman, C. A., Fisher, J. F., Sobel, J. D., & Newman, C. A. (2011). Candida urinary tract infections - Diagnosis. *Clinical Infectious Diseases*, *52*(SUPPL. 6). https://doi.org/10.1093/cid/cir111

Kaul, G., Shukla, M., Dasgupta, A., & Chopra, S. (2019). Update on drug-repurposing: Is it useful for tackling antimicrobial resistance? *Future Microbiology*, *14*(10), 829–831. https://doi.org/10.2217/fmb-2019-0122

Kędziora, A., Speruda, M., Krzyżewska, E., Rybka, J., Łukowiak, A., & Bugla-Płoskońska, G. (2018). Similarities and differences between silver ions and silver in nanoforms as antibacterial agents. *International Journal of Molecular Sciences*, *19*(2). https://doi.org/10.3390/ijms19020444

Keogh, D., Lam, L. N., Doyle, L. E., Matysik, A., Pavagadhi, S., Umashankar, S., Low, P. M., Dale, J. L., Song, Y., Ng, S. P., Boothroyd, C. B., Dunny, G. M., Swarup, S., Williams, R. B. H., Marsili, E., & Kline, K. A. (2018). Extracellular electron transfer powers Enterococcus faecalis biofilm metabolism. *MBio*, *9*(2), 1–16. https://doi.org/10.1128/mBio.00626-17

Kharbush, J. J., Thompson, L. R., Haroon, M. F., Knight, R., & Aluwihare, L. I. (2018). Hopanoid-producing bacteria in the Red Sea include the major marine nitrite oxidizers. *FEMS Microbiology Ecology*, *94*(6), 1–9. https://doi.org/10.1093/femsec/fiy063

Khater, D. Z., El-Khatib, K. M., Hazaa, M. M., & Hassan, R. Y. A. (2015). Development of Bioelectrochemical System for Monitoring the Biodegradation Performance of Activated Sludge. *Applied Biochemistry and Biotechnology*, *175*(7), 3519–3530. https://doi.org/10.1007/s12010-015-1522-5

Kim, J. H., Cheng, L. W., Chan, K. L., Tam, C. C., Mahoney, N., Friedman, M., Shilman, M. M., & Land, K. M. (2020). Antifungal drug repurposing. *Antibiotics*, *9*(11), 1–29.

https://doi.org/10.3390/antibiotics9110812

Klasen, H. J. (2000). A historical review of the use of silver in the treatment of burns. II. Renewed interest for silver. *Burns*, *26*(2), 131–138. https://doi.org/10.1016/S0305-4179(99)00116-3

Kleine, D., Chodorski, J., Mitra, S., Schlegel, C., Huttenlochner, K., Müller-Renno, C., Mukherjee, J., Ziegler, C., & Ulber, R. (2019). Monitoring of biofilms grown on differentially structured metallic surfaces using confocal laser scanning microscopy. *Engineering in Life Sciences*, *19*(7), 513–521. https://doi.org/10.1002/elsc.201800176

Koch, C., & Harnisch, F. (2016). What is the essence of microbial electroactivity? *Frontiers in Microbiology*, *7*(NOV), 1–5. https://doi.org/10.3389/fmicb.2016.01890

Koch, C., Korth, B., & Harnisch, F. (2018). Microbial ecology-based engineering of Microbial Electrochemical Technologies. *Microbial Biotechnology*, *11*(1), 22–38. https://doi.org/10.1111/1751-7915.12802

Kong, C., Chee, C. F., Richter, K., Thomas, N., Abd. Rahman, N., & Nathan, S. (2018). Suppression of Staphylococcus aureus biofilm formation and virulence by a benzimidazole derivative, UM-C162. *Scientific Reports*, *8*(1), 1–16. https://doi.org/10.1038/s41598-018-21141-2

Konreddy, A. K., Rani, G. U., Lee, K., & Choi, Y. (2018). Recent Drug-Repurposing-Driven Advances in the Discovery of Novel Antibiotics. *Current Medicinal Chemistry*, *26*(28), 5363–5388. https://doi.org/10.2174/0929867325666180706101404

Krstić, M. P., Petković, B. B., Milčić, M., Mišić, D., & Santibanez, J. F. (2019). Synthesis, characterization and biological study of new dinuclear zinc(Ii) and nickel(Ii) octaaza macrocyclic complexes. *Macedonian Journal of Chemistry and Chemical Engineering*, *38*(1), 1–11. https://doi.org/10.20450/mjcce.2019.1599

Kuhn, D. M., Balkis, M., Chandra, J., Mukherjee, P. K., & Ghannoum, M. A. (2003). Uses and limitations of the XTT assay in studies of Candida growth and metabolism. *Journal of Clinical Microbiology*, *41*(1), 506–508. https://doi.org/10.1128/JCM.41.1.506-508.2003

Kumar, M., Sarma, D. K., Shubham, S., Kumawat, M., Verma, V., Nina, P. B., JP, D., Kumar, S., Singh, B., & Tiwari, R. R. (2021). Futuristic Non-antibiotic Therapies to Combat Antibiotic Resistance: A Review. *Frontiers in Microbiology*, *12*(January), 1–15. https://doi.org/10.3389/fmicb.2021.609459

Kuper, K. M., Pharm, D., Coyle, E. a, Wanger, A., & Ph, D. (2012). Antifungal Susceptibility Testing: A Primer for Clinicians. *Pharmacotherapy*, *32*(12), 1112–1122.

Kurihara, M. N. L., Sales, R. O. de, Silva, K. E. da, Maciel, W. G., & Simionatto, S. (2020). Multidrug-resistant Acinetobacter baumannii outbreaks: a global problem in healthcare settings. *Revista Da Sociedade Brasileira de Medicina Tropical*,

53(September), e20200248. https://doi.org/10.1590/0037-8682-0248-2020

Kuss, S., Amin, H. M. A., & Compton, R. G. (2018). Electrochemical Detection of Pathogenic Bacteria—Recent Strategies, Advances and Challenges. *Chemistry - An Asian Journal*, *13*(19), 2758–2769. https://doi.org/10.1002/asia.201800798

Kyriakidis, I., Vasileiou, E., Pana, Z. D., & Tragiannidis, A. (2021). Acinetobacter baumannii antibiotic resistance mechanisms. *Pathogens*, *10*(3), 1–31. https://doi.org/10.3390/pathogens10030373

LaFleur, M. D., Kumamoto, C. A., & Lewis, K. (2006). Candida albicans biofilms produce antifungal-tolerant persister cells. *Antimicrobial Agents and Chemotherapy*, *50*(11), 3839–3846. https://doi.org/10.1128/AAC.00684-06

Lass-Flör, C., Mayr, A., Perkhofer, S., Hinterberger, G., Hausdorfer, J., Speth, C., & Fille, M. (2008). Activities of antifungal agents against yeasts and filamentous fungi: Assessment according to the methodology of the European Committee on Antimicrobial Susceptibility Testing. *Antimicrobial Agents and Chemotherapy*, *52*(10), 3637–3641. https://doi.org/10.1128/AAC.00662-08

Lass-Flörl, C., Mayr, A., Aigner, M., Lackner, M., & Orth-Höller, D. (2018). A nationwide passive surveillance on fungal infections shows a low burden of azole resistance in molds and yeasts in Tyrol, Austria. *Infection*, *46*(5), 701–704. https://doi.org/10.1007/s15010-018-1170-0

Lass-Flörl, C., Perkhofer, S., & Mayr, A. (2010). In vitro susceptibility testing in fungi: A global perspective on a variety of methods. *Mycoses*, *53*(1), 1–11. https://doi.org/10.1111/j.1439-0507.2009.01813.x

Leão, C., Borges, A., & Simões, M. (2020). Nsaids as a drug repurposing strategy for biofilm control. *Antibiotics*, *9*(9), 1–19. https://doi.org/10.3390/antibiotics9090591

Lee, C. R., Lee, J. H., Park, M., Park, K. S., Bae, I. K., Kim, Y. B., Cha, C. J., Jeong, B. C., & Lee, S. H. (2017). Biology of Acinetobacter baumannii: Pathogenesis, antibiotic resistance mechanisms, and prospective treatment options. *Frontiers in Cellular and Infection Microbiology*, *7*(MAR). https://doi.org/10.3389/fcimb.2017.00055

Lee, J., Park, C., Kim, Y., & Park, S. (2017). Signal enhancement in ATP bioluminescence to detect bacterial pathogens via heat treatment. *Biochip Journal*, *11*(4), 287–293. https://doi.org/10.1007/s13206-017-1404-8

Lenhard, J. R., Smith, N. M., Bulman, Z. P., & Tao, X. (2017). *High-Dose Ampicillin-Sulbactam Combinations Combat Polymyxin- Resistant Acinetobacter baumannii in a Hollow-Fiber Infection Model*. *61*(3), 1–6.

Li, X. H., & Lee, J. H. (2017). Antibiofilm agents: A new perspective for antimicrobial strategy. *Journal of Microbiology*, *55*(10), 753–766. https://doi.org/10.1007/s12275-017-7274-x

Li, X., Liu, L., Liu, T., Yuan, T., Zhang, W., Li, F., Zhou, S., & Li, Y. (2013). Electron transfer capacity dependence of quinone-mediated Fe(III) reduction and current generation by Klebsiella pneumoniae L17. *Chemosphere*, *92*(2), 218–224.

https://doi.org/10.1016/j.chemosphere.2013.01.098

Liang, P., Duan, R., Jiang, Y., Zhang, X., Qiu, Y., & Huang, X. (2018). One-year operation of 1000-L modularized microbial fuel cell for municipal wastewater treatment. *Water Research*, *141*, 1–8. https://doi.org/10.1016/j.watres.2018.04.066

Light, S. H., Su, L., Rivera-Lugo, R., Cornejo, J. A., Louie, A., Iavarone, A. T., Ajo-Franklin, C. M., & Portnoy, D. A. (2018). A flavin-based extracellular electron transfer mechanism in diverse Gram-positive bacteria. *Nature*, *562*(7725), 140–157. https://doi.org/10.1038/s41586-018-0498-z

Lima, C. D., Couto, R. A. S., Arantes, L. C., Marinho, P. A., Pimentel, D. M., Quinaz, M. B., da Silva, R. A. B., Richter, E. M., Barbosa, S. L., & dos Santos, W. T. P. (2020). Electrochemical detection of the synthetic cathinone 3,4-methylenedioxypyrovalerone using carbon screen-printed electrodes: A fast, simple and sensitive screening method for forensic samples. *Electrochimica Acta*, *354*, 136728. https://doi.org/10.1016/j.electacta.2020.136728

Lima, G. M. E., Nunes, M. de O., Chang, M. R., Tsujisaki, R. A. de S., Nunes, J. de O., Taira, C. L., Thomaz, D. Y., Del Negro, G. M. B., Mendes, R. P., & Paniago, A. M. M. (2017). Identification and antifungal susceptibility of Candida species isolated from the urine of patients in a university hospital in Brazil. *Revista Do Instituto de Medicina Tropical de Sao Paulo*, *59*(April). https://doi.org/10.1590/S1678-9946201759075

Limoli, D. H., Jones, C. J., & Wozniak, D. J. (2015). Bacterial Extracellular Polysaccharides in Biofilm Formation and Function. *Microbiology Spectrum*, *3*(3), 1–19. https://doi.org/10.1128/microbiolspec.mb-0011-2014

Liu, D. F., & Li, W. W. (2020). Potential-dependent extracellular electron transfer pathways of exoelectrogens. *Current Opinion in Chemical Biology*, *59*, 140–146. https://doi.org/10.1016/j.cbpa.2020.06.005

Liu, L., Xu, Y., Cui, F., Xia, Y., Chen, L., Mou, X., & Lv, J. (2018). Monitoring of bacteria biofilms forming process by in-situ impedimetric biosensor chip. *Biosensors and Bioelectronics*, *112*(March), 86–92. https://doi.org/10.1016/j.bios.2018.04.019

Liu, X., Wu, X., Tang, J., Zhang, L., & Jia, X. (2020). Trends and development in the antibiotic-resistance of acinetobacter baumannii: A scientometric research study (1991–2019). *Infection and Drug Resistance*, *13*, 3195–3208. https://doi.org/10.2147/idr.s264391

Lockhart, S. R., & Guarner, J. (2019). Emerging and reemerging fungal infections. *Seminars in Diagnostic Pathology*, *36*(3), 177–181. https://doi.org/10.1053/j.semdp.2019.04.010

Lodha, T. D., Indu, B., Ch., S., & Ch.V., R. (2019). Transcriptome analysis of hopanoid deficient mutant of Rhodopseuodomonas palustris TIE-1. *Microbiological Research*, *218*(July 2018), 108–117. https://doi.org/10.1016/j.micres.2018.10.009

Loeffler, J., Henke, N., Hebart, H., Schmidt, D., Hagmeyer, L., Schumacher, U., & Einsele,

H. (2000). *Quantification of Fungal DNA by Using Fluorescence Resonance Energy Transfer and the Light Cycler System*. *38*(2), 586–590.

Logan, B. E., Rossi, R., Ragab, A., & Saikaly, P. E. (2019). Electroactive microorganisms in bioel ectrochemical systems. *Nature Reviews Microbiology*, *17*(5), 307–319. https://doi.org/10.1038/s41579-019-0173-x

Lohsea, M. B., Gulatic, M., Fishburnc, Ashley Valle Arevaloc, A., & Alexander, Johnson Clarissa, N. (2017). Assessment and Optimizations of Candida albicans In Vitro Biofilm Assays. *Antimicrobial Agents and Chemotherapy*, *61*(5), 1–13. https://doi.org/https://doi .org/10.1128/AAC.02749-16

Lv, X., Ge, W., Li, Q., Wu, Y., Jiang, H., & Wang, X. (2014). Rapid and ultrasensitive electrochemical detection of multidrug-resistant bacteria based on nanostructured gold coated ITO electrode. *ACS Applied Materials and Interfaces*, *6*(14), 11025–11031. https://doi.org/10.1021/am5016099

Mach, E. K., Wong, K. P., & Liao, C. J. (2012). Biosensor diagnosis of urinary tract infections: a path to better treatment? *Trends in Pharmacological Sciences*, *32*(6), 1–12. https://doi.org/10.1016/j.tips.2011.03.001.Biosensor

Madadi-Goli, N., Moniri, R., Bagheri-Josheghani, S., & Dasteh-Goli, N. (2017). Sensitivity of levofloxacin in combination with ampicillin-sulbactam and tigecycline against multidrug-resistant Acinetobacter baumannii. *Iranian Journal of Microbiology*, *9*(1), 19–25.

Maillard, J. Y., & Hartemann, P. (2013). Silver as an antimicrobial: facts and gaps in knowledge. *Critical Reviews in Microbiology*, *39*(4), 373–383. https://doi.org/10.3109/1040841X.2012.713323

Malott, R. J., Wu, C. H., Lee, T. D., Hird, T. J., Dalleska, N. F., Zlosnik, J. E. A., Newman, D. K., & Speert, D. P. (2014). Fosmidomycin decreases membrane hopanoids and potentiates the effects of colistin on burkholderia multivorans clinical isolates. *Antimicrobial Agents and Chemotherapy*, *58*(9), 5211–5219. https://doi.org/10.1128/AAC.02705-14

Mangiarotti, A., Genovese, D. M., Naumann, C. A., Monti, M. R., & Wilke, N. (2019). Hopanoids, like sterols, modulate dynamics, compaction, phase segregation and permeability of membranes. *Biochimica et Biophysica Acta - Biomembranes*, *1861*(12), 183060. https://doi.org/10.1016/j.bbamem.2019.183060

Mansour, A. M., & Radacki, K. (2019). Structural Studies, Antimicrobial Activity and Protein Interaction of Photostable Terpyridine Silver(I) Complexes. *European Journal of Inorganic Chemistry*, *2019*(37), 4020–4030. https://doi.org/10.1002/ejic.201900701

Markowitz, M. A., Monti, G. K., Kim, J. H., & Haake, D. A. (2019). Rapid diagnostic testing in the management of urinary tract infection: Potentials and limitations. *Diagnostic Microbiology and Infectious Disease*, *94*(4), 371–377. https://doi.org/10.1016/j.diagmicrobio.2019.02.019

Marsili, E., Baron, D. B., Shikhare, I. D., Coursolle, D., Gralnick, J. A., & Bond, D. R. (2008). Shewanella secretes flavins that mediate extracellular electron transfer. *Proceedings of the National Academy of Sciences of the United States of America*, *105*(10), 3968–3973. https://doi.org/10.1073/pnas.0710525105

Marsili, E., Rollefson, J. B., Baron, D. B., Hozalski, R. M., & Bond, D. R. (2008). Microbial biofilm voltammetry: Direct electrochemical characterization of catalytic electrode-attached biofilms. *Applied and Environmental Microbiology*, *74*(23), 7329–7337. https://doi.org/10.1128/AEM.00177-08

Marsili, E., Sun, J., & Bond, D. R. (2010). Voltammetry and growth physiology of Geobacter sulfurreducens biofilms as a function of growth stage and imposed electrode potential. *Electroanalysis*, *22*(7–8), 865–874. https://doi.org/10.1002/elan.200800007

Martinez, C. M., & Alvarez, L. H. (2018a). Application of redox mediators in bioelectrochemical systems. *Biotechnology Advances*, *36*(5), 1412–1423. https://doi.org/10.1016/j.biotechadv.2018.05.005

Martinez, C. M., & Alvarez, L. H. (2018b). Application of redox mediators in bioelectrochemical systems. *Biotechnology Advances*, *36*(5), 1412–1423. https://doi.org/10.1016/j.biotechadv.2018.05.005

Masi, E., Ciszak, M., Santopolo, L., Frascella, A., Giovannetti, L., Marchi, E., Viti, C., & Mancuso, S. (2015). Electrical spiking in bacterial biofilms. *Journal of the Royal Society Interface*, *12*(102). https://doi.org/10.1098/rsif.2014.1036

Mathur, H., Field, D., Rea, M. C., Cotter, P. D., Hill, C., & Ross, R. P. (2018). Fighting biofilms with lantibiotics and other groups of bacteriocins. *Npj Biofilms and Microbiomes*, *4*(1), 1–13. https://doi.org/10.1038/s41522-018-0053-6

Mayer, F. L., Wilson, D., & Hube, B. (2013). Candida albicans pathogenicity mechanisms. *Virulence*, *4*(2), 119–128. https://doi.org/10.4161/viru.22913

McEachern, F., Harvey, E., & Merle, G. (2020). Emerging Technologies for the Electrochemical Detection of Bacteria. *Biotechnology Journal*, 2000140. https://doi.org/10.1002/biot.202000140

Medici, S., Peana, M., Nurchi, V. M., & Zoroddu, M. A. (2019). Medical Uses of Silver: History, Myths, and Scientific Evidence [Review-article]. *Journal of Medicinal Chemistry*, *62*(13), 5923–5943. https://doi.org/10.1021/acs.jmedchem.8b01439

Meireles, A., L. Gonçalves, A., B. Gomes, I., Chaves Simões, L., & Simões, M. (2015). Methods to study microbial adhesion on abiotic surfaces. *AIMS Bioengineering*, *2*(4), 297–309. https://doi.org/10.3934/bioeng.2015.4.297

Melo, A. S., Bizerra, F. C., Freymüller, E., Arthington-Skaggs, B. A., & Colombo, A. L. (2011). Biofilm production and evaluation of antifungal susceptibility amongst clinical Candida spp. isolates, including strains of the Candida parapsilosis complex. *Medical Mycology*, *49*(3), 253–262. https://doi.org/10.3109/13693786.2010.530032

Méndez-Tovar, M., García-Meza, J. V., & González, I. (2019). Electrochemical

monitoring of Acidithiobacillus thiooxidans biofilm formation on graphite surface with elemental sulfur. *Bioelectrochemistry*, *128*, 30–38. https://doi.org/10.1016/j.bioelechem.2019.03.004

Meshulam, T., Levitz, S. M., Christin, L., & Diamond, R. D. (1995). A Simplified New Assay for Assessment of Fungal Cell Damage with the Tetrazolium Dye, (2,3)-bis-(2-Methoxy-4-Nitro-5-Sulphenyl)-(2H)-Tetrazolium-5- Carboxanilide (XTT). *The Journal of Infectious Diseases*, *172*, 1153–1156.

Metters, J. P., Kadara, R. O., & Banks, C. E. (2011). New directions in screen printed electroanalytical sensors: An overview of recent developments. *Analyst*, *136*(6), 1067–1076. https://doi.org/10.1039/c0an00894j

Mewis, R. E., & Archibald, S. J. (2019). Side-bridged cyclam transition metal complexes bearing a phenolic ether or a phenolate pendent arm. *Polyhedron*, *171*, 578–589. https://doi.org/10.1016/j.poly.2019.08.003

Mingeot-Leclercq, M. P., & Décout, J. L. (2016). Bacterial lipid membranes as promising targets to fight antimicrobial resistance, molecular foundations and illustration through the renewal of aminoglycoside antibiotics and emergence of amphiphilic aminoglycosides. *MedChemComm*, *7*(4), 586–611. https://doi.org/10.1039/c5md00503e

Miran, W., Naradasu, D., & Okamoto, A. (2021). Pathogens electrogenicity as a tool for in-situ metabolic activity monitoring and drug assessment in biofilms. *IScience*, *24*(2), 102068. https://doi.org/10.1016/j.isci.2021.102068

Miró-Canturri, A., Ayerbe-Algaba, R., & Smani, Y. (2019). Drug repurposing for the treatment of bacterial and fungal infections. *Frontiers in Microbiology*, *10*(JAN). https://doi.org/10.3389/fmicb.2019.00041

Momenzadeh, M., Vard, A., Talebi, A., Mehri Dehnavi, A., & Rabbani, H. (2018). Computer-aided diagnosis software for vulvovaginal candidiasis detection from Pap smear images. *Microscopy Research and Technique*, *81*(1), 13–21. https://doi.org/10.1002/jemt.22951

Monem, S., Furmanek-Blaszk, B., Łupkowska, A., Kuczyńska-Wiśnik, D., Stojowska-Swędrzyńska, K., & Laskowska, E. (2020). Mechanisms protecting acinetobacter baumannii against multiple stresses triggered by the host immune response, antibiotics, and outside host environment. *International Journal of Molecular Sciences*, *21*(15), 1–30. https://doi.org/10.3390/ijms21155498

Moraes, D. C., & Ferreira-Pereira, A. (2019). Insights on the anticandidal activity of non-antifungal drugs. *Journal de Mycologie Medicale*, *29*(3), 253–259. https://doi.org/10.1016/j.mycmed.2019.07.004

Moreira, F. T. C., Ferreira, M. J. M. S., Puga, J. R. T., & Sales, M. G. F. (2016). Screen-printed electrode produced by printed-circuit board technology. Application to cancer biomarker detection by means of plastic antibody as sensing material. *Sensors and Actuators, B: Chemical*, *223*, 927–935. https://doi.org/10.1016/j.snb.2015.09.157

Moriarty, T. F., Grainger, D. W., & Richards, R. G. (2014). Challenges in linking preclinical anti-microbial research strategies with clinical outcomes for device-associated infections. *European Cells and Materials*, *28*, 112–128. https://doi.org/10.22203/eCM.v028a09

Moubareck, C. A., & Halat, D. H. (2020). Insights into Acinetobacter baumannii: A review of microbiological, virulence, and resistance traits in a threatening nosocomial pathogen. *Antibiotics*, *9*(3). https://doi.org/10.3390/antibiotics9030119

Mourenza, Á., Gil, J. A., Mateos, L. M., & Letek, M. (2020). Novel treatments against mycobacterium tuberculosis based on drug repurposing. *Antibiotics*, *9*(9), 1–12. https://doi.org/10.3390/antibiotics9090550

Muir, A., Forrest, G., Clarkson, J., & Wheals, A. (2011). Detection of Candida albicans DNA from blood samples using a novel electrochemical assay. *Journal of Medical Microbiology*, *60*(4), 467–471. https://doi.org/10.1099/jmm.0.026229-0

Mukherjee, P. K., & Chandra, J. (2004). Candida biofilm resistance. *Drug Resistance Updates*, *7*(4–5), 301–309. https://doi.org/10.1016/j.drup.2004.09.002

Munteanu, F. D., Titoiu, A. M., Marty, J. L., & Vasilescu, A. (2018). Detection of antibiotics and evaluation of antibacterial activity with screen-printed electrodes. *Sensors (Switzerland)*, *18*(3). https://doi.org/10.3390/s18030901

Murray, B. O., Flores, C., Williams, C., Flusberg, D. A., Marr, E. E., Kwiatkowska, K. M., Charest, J. L., Isenberg, B. C., & Rohn, J. L. (2021). Recurrent Urinary Tract Infection: A Mystery in Search of Better Model Systems. *Frontiers in Cellular and Infection Microbiology*, *11*(May), 1–29. https://doi.org/10.3389/fcimb.2021.691210

Naradasu, D., Guionet, A., Miran, W., & Okamoto, A. (2020). Microbial current production from Streptococcus mutans correlates with biofilm metabolic activity. *Biosensors and Bioelectronics*, *162*(April), 112236. https://doi.org/10.1016/j.bios.2020.112236

Naradasu, D., Guionet, A., Okinaga, T., Nishihara, T., & Okamoto, A. (2020). Electrochemical Characterization of Current-Producing Human Oral Pathogens by Whole-Cell Electrochemistry. *ChemElectroChem*, *7*(9), 2012–2019. https://doi.org/10.1002/celc.202000117

Naradasu, D., Miran, W., & Okamoto, A. (2020). Metabolic current production by an oral biofilm pathogen corynebacterium matruchotii. *Molecules*, *25*(14). https://doi.org/10.3390/molecules25143141

Naradasu, D., Miran, W., Sakamoto, M., & Okamoto, A. (2019). Isolation and characterization of human gut bacteria capable of extracellular electron transport by electrochemical techniques. *Frontiers in Microbiology*, *10*(JAN). https://doi.org/10.3389/fmicb.2018.03267

Narayanan, J., Sosa-torres, M. E., & Toscano, A. (2002). 1,4,8,11-tetrakis(2 pyridylmethyl)-1,4,8,11- tetraazacyclotetradecane. *Journal OfChemical Crystallography*, *31*(3), 129–133.

Nealson, K. H. (2017). Bioelectricity (electromicrobiology) and sustainability. *Microbial Biotechnology*, *10*(5), 1114–1119. https://doi.org/10.1111/1751-7915.12834

Nett, J., Lincoln, L., Marchillo, K., Massey, R., Holoyda, K., Hoff, B., VanHandel, M., & Andes, D. (2007). Putative role of β-1,3 glucans in Candida albicans biofilm resistance. *Antimicrobial Agents and Chemotherapy*, *51*(2), 510–520. https://doi.org/10.1128/AAC.01056-06

Nobile, C. J., & Johnson, A. D. (2015). Candida albicans Biofilms and Human Disease. *Annual Review of Microbiology*, *69*(1), 71–92. https://doi.org/10.1146/annurev-micro-091014-104330

Nocera, F. P., Attili, A. R., & De Martino, L. (2021). Acinetobacter baumannii: Its clinical significance in human and veterinary medicine. *Pathogens*, *10*(2), 1–13. https://doi.org/10.3390/pathogens10020127

Obisesan, O. J., Olowe, O. A., & Taiwo, S. S. (2015). Phenotypic Detection of Genitourinary Candidiasis among Sexually Transmitted Disease Clinic Attendees in Ladoke Akintola University Teaching Hospital, Osogbo, Nigeria. *Journal of Environmental and Public Health*, *2015*. https://doi.org/10.1155/2015/401340

Odabasi, Z., & Mert, A. (2020). Candida urinary tract infections in adults. *World Journal of Urology*, *38*(11), 2699–2707. https://doi.org/10.1007/s00345-019-02991-5

Olaifa, K., Ajunwa, O., & Marsili, E. (2022). Electroanalytic evaluation of antagonistic effect of azole fungicides on Acinetobacter baumannii biofilms. *Electrochimica Acta*, *405*, 139837. https://doi.org/10.1016/j.electacta.2022.139837

Olaifa, K., Nikodinovic-Runic, J., Glišić, B., Boschetto, F., Marin, E., Segreto, F., & Marsili, E. (2021). Electroanalysis of Candida albicans biofilms: a suitable real-time tool for antifungal testing. *Electrochimica Acta*, *389*, 138757. https://doi.org/10.1016/j.electacta.2021.138757

Oliot, M., Chong, P., Erable, B., & Bergel, A. (2017). Influence of the electrode size on microbial anode performance. *Chemical Engineering Journal*, *327*(June), 218–227. https://doi.org/10.1016/j.cej.2017.06.044

Oliveira, I. M., Borges, A., & Simões, M. (2020). The potential of drug repurposing to face bacterial and fungal biofilm infections. In *Recent Trends in Biofilm Science and Technology* (pp. 307–328). Elsevier Inc. https://doi.org/10.1016/b978-0-12-819497-3.00014-3

Opulente, D. A., Langdon, Q. K., Buh, K. V., Haase, M. A. B., Sylvester, K., Moriarty, R. V., Jarzyna, M., Considine, S. L., Schneider, R. M., & Hittinger, C. T. (2019). Pathogenic budding yeasts isolated outside of clinical settings. *FEMS Yeast Research*, *19*(3), 1–6. https://doi.org/10.1093/femsyr/foz032

Ostrov, N., Jimenez, M., Billerbeck, S., Brisbois, J., Matragrano, J., Ager, A., & Cornish, V. W. (2017). A modular yeast biosensor for low-cost point-of-care pathogen detection. *Science Advances*, *3*(6). https://doi.org/10.1126/sciadv.1603221

Ott, C. E., Cunha-Silva, H., Kuberski, S. L., Cox, J. A., Arcos-Martínez, M. J., & Arroyo-

Mora, L. E. (2020). Electrochemical detection of fentanyl with screen-printed carbon electrodes using square-wave adsorptive stripping voltammetry for forensic applications. *Journal of Electroanalytical Chemistry*, *873*. https://doi.org/10.1016/j.jelechem.2020.114425

Öztürk, R., & Murt, A. (2020). Epidemiology of urological infections: a global burden. *World Journal of Urology*, *38*(11), 2669–2679. https://doi.org/10.1007/s00345-019-03071-4

Pacios, O., Blasco, L., Bleriot, I., Fernandez-Garcia, L., Bardanca, Mónica González Ambroa, A., López, M., Bou, G., & Tomas, M. (2020). Strategies to Combat Multidrug-Resistant and Persistent Infectious Diseases. *Antibiotics*, *9*(65), 1–20.

Palmer, R. J., & Sternberg, C. (1999). Modern microscopy in biofilm research: Confocal microscopy and other approaches. *Current Opinion in Biotechnology*, *10*(3), 263–268. https://doi.org/10.1016/S0958-1669(99)80046-9

Pankratova, G., Leech, D., Gorton, L., & Hederstedt, L. (2018). Extracellular Electron Transfer by the Gram-Positive Bacterium Enterococcus faecalis. *Biochemistry*, *57*(30), 4597–4603. https://doi.org/10.1021/acs.biochem.8b00600

Paquete, C. M. (2020). Electroactivity across the cell wall of Gram-positive bacteria. *Computational and Structural Biotechnology Journal*, *18*, 3796–3802. https://doi.org/10.1016/j.csbj.2020.11.021

Parvathaneni, V., Kulkarni, N. S., Muth, A., & Gupta, V. (2019). Drug repurposing: a promising tool to accelerate the drug discovery process. *Drug Discovery Today*, *24*(10), 2076–2085. https://doi.org/10.1016/j.drudis.2019.06.014

Peck, K. R., Kim, M. J., Choi, J. Y., Kim, H. S., Kang, C. I., Cho, Y. K., Park, D. W., Lee, H. J., Lee, M. S., & Ko, K. S. (2012). In vitro time-kill studies of antimicrobial agents against blood isolates of imipenem-resistant acinetobacter baumannii, including colistin- or tigecycline-resistant isolates. *Journal of Medical Microbiology*, *61*(3), 353–360. https://doi.org/10.1099/jmm.0.036939-0

Perez, F., Hujer, A. M., Hujer, K. M., Decker, B. K., Rather, P. N., & Bonomo, R. A. (2007). Global challenge of multidrug-resistant Acinetobacter baumanni. *Antimicrobial Agents and Chemotherapy*, *51*(10), 3471–3484. https://doi.org/10.1128/AAC.01464-06

Perlin, D. S., Rautemaa-Richardson, R., & Alastruey-Izquierdo, A. (2017). The global problem of antifungal resistance: prevalence, mechanisms, and management. *The Lancet Infectious Diseases*, *17*(12), e383–e392. https://doi.org/10.1016/S1473-3099(17)30316-X

Petković, B. B., Milčić, M., Stanković, D., Stambolić, I., Manojlović, D., Jovanović, V. M., & Sovilj, S. P. (2013). Complexation ability of octaazamacrocyclic ligand toward Co2+, Ni2+, Cu2+ and Zn2+ metal cations: Experimental and theoretical study. *Electrochimica Acta*, *89*, 680–687. https://doi.org/10.1016/j.electacta.2012.11.100

Peyclit, L., Baron, S. A., & Rolain, J. M. (2019). Drug repurposing to fight colistin and

carbapenem-resistant bacteria. *Frontiers in Cellular and Infection Microbiology*, *9*(JUN), 1–11. https://doi.org/10.3389/fcimb.2019.00193

Pierce, C. G., Uppuluri, P., Tristan, A. R., Wormley, F. L., Mowat, E., Ramage, G., & Lopez-Ribot, J. L. (2008). A simple and reproducible 96-well plate-based method for the formation of fungal biofilms and its application to antifungal susceptibility testing. *Nature Protocols*, *3*(9), 1494–1500. https://doi.org/10.1038/nprot.2008.141

Pierini, G. D., Maccio, S. A., Robledo, S. N., Ferrari, A. G. M., Banks, C. E., Fernández, H., & Zon, M. A. (2020). Screen-printed electrochemical-based sensor for taxifolin determination in edible peanut oils. *Microchemical Journal*, *159*(August), 105442. https://doi.org/10.1016/j.microc.2020.105442

Polke, M., Hube, B., & Jacobsen, I. D. (2015). Candida survival strategies. In *Advances in Applied Microbiology* (Vol. 91). Elsevier Ltd. https://doi.org/10.1016/bs.aambs.2014.12.002

Poloni, J. A. T., & Rotta, L. N. (2020). Urine sediment findings and the immune response to pathologies in fungal urinary tract infections caused by candida spp. *Journal of Fungi*, *6*(4), 1–12. https://doi.org/10.3390/jof6040245

Posseckardt, J., Schirmer, C., Kick, A., Rebatschek, K., Lamz, T., & Mertig, M. (2018). Monitoring of Saccharomyces cerevisiae viability by non-Faradaic impedance spectroscopy using interdigitated screen-printed platinum electrodes. *Sensors and Actuators, B: Chemical*, *255*, 3417–3424. https://doi.org/10.1016/j.snb.2017.09.171

Potocki, L., Depciuch, J., Kuna, E., Worek, M., Lewinska, A., & Wnuk, M. (2019). FTIR and raman spectroscopy-based biochemical profiling reflects genomic diversity of clinical candida isolates that may be useful for diagnosis and targeted therapy of candidiasis. *International Journal of Molecular Sciences*, *20*(4). https://doi.org/10.3390/ijms20040988

Potter, M. C., & B, P. R. S. L. (1911). Electrical effects accompanying the decomposition of organic compounds. *Proceedings of the Royal Society of London. Series B, Containing Papers of a Biological Character*, *84*(571), 260–276. https://doi.org/10.1098/rspb.1911.0073

Prasad, R., Shah, A. H., & Rawal, M. K. (2016). Antifungals: Mechanism of action and drug resistance. *Advances in Experimental Medicine and Biology*, *892*, 327–349. https://doi.org/10.1007/978-3-319-25304-6_14

Prévoteau, A., & Rabaey, K. (2017). Electroactive Biofilms for Sensing: Reflections and Perspectives. *ACS Sensors*, *2*(8), 1072–1085. https://doi.org/10.1021/acssensors.7b00418

Prindle, A., Liu, J., Asally, M., Ly, S., Garcia-Ojalvo, J., & Süel, G. M. (2015). Ion channels enable electrical communication in bacterial communities. *Nature*, *527*(7576), 59–63. https://doi.org/10.1038/nature15709

Pulido, M. R., García-Quintanilla, M., Martín-Peña, R., Cisneros, J. M., & McConnell, M. J. (2013). Progress on the development of rapid methods for antimicrobial

susceptibility testing. *Journal of Antimicrobial Chemotherapy*, *68*(12), 2710–2717. https://doi.org/10.1093/jac/dkt253

Pushpakom, S., Iorio, F., Eyers, P. A., Escott, K. J., Hopper, S., Wells, A., Doig, A., Guilliams, T., Latimer, J., McNamee, C., Norris, A., Sanseau, P., Cavalla, D., & Pirmohamed, M. (2018). Drug repurposing: Progress, challenges and recommendations. *Nature Reviews Drug Discovery*, *18*(1), 41–58. https://doi.org/10.1038/nrd.2018.168

Qi, L., Li, H., Zhang, C., Liang, B., Li, J., Wang, L., Du, X., Liu, X., Qiu, S., & Song, H. (2016). Relationship between antibiotic resistance, biofilm formation, and biofilm-specific resistance in Acinetobacter baumannii. *Frontiers in Microbiology*, *7*(APR), 1–10. https://doi.org/10.3389/fmicb.2016.00483

Qiao, Y. J., Qiao, Y., Zou, L., Wu, X. S., & Liu, J. H. (2017). Biofilm promoted current generation of Pseudomonas aeruginosa microbial fuel cell via improving the interfacial redox reaction of phenazines. *Bioelectrochemistry*, *117*, 34–39. https://doi.org/10.1016/j.bioelechem.2017.04.003

Qiao, Y., Li, C. M., Bao, S. J., Lu, Z., & Hong, Y. (2008). Direct electrochemistry and electrocatalytic mechanism of evolved Escherichia coli cells in microbial fuel cells. *Chemical Communications*, *11*, 1290–1292. https://doi.org/10.1039/b719955d

Rajapaksha, P., Elbourne, A., Gangadoo, S., Brown, R., Cozzolino, D., & Chapman, J. (2019). A review of methods for the detection of pathogenic microorganisms. *Analyst*, *144*(2), 396–411. https://doi.org/10.1039/c8an01488d

Ramage, G. (2016). Comparing apples and oranges: Considerations for quantifying candidal biofilms with XTT [2,3-bis(2-methoxy-4-nitro-5-sulfo-phenyl)-2H-tetrazolium-5-carboxanilide] and the need for standardized testing. *Journal of Medical Microbiology*, *65*(4), 259–260. https://doi.org/10.1099/jmm.0.000237

Ramage, G., & Williams, C. (2013). The clinical importance of fungal biofilms. In *Advances in Applied Microbiology* (1st ed., Vol. 84). Elsevier Inc. https://doi.org/10.1016/B978-0-12-407673-0.00002-3

Ramanavicius, A., Morkvenaite-Vilkonciene, I., Kisieliute, A., Petroniene, J., & Ramanaviciene, A. (2017). Scanning electrochemical microscopy based evaluation of influence of pH on bioelectrochemical activity of yeast cells − Saccharomyces cerevisiae. *Colloids and Surfaces B: Biointerfaces*, *149*, 1–6. https://doi.org/10.1016/j.colsurfb.2016.09.039

Rangel-Vega, A., Bernstein, L. R., Mandujano-Tinoco, E. A., García-Contreras, S. J., & García-Contreras, R. (2015). Drug repurposing as an alternative for the treatment of recalcitrant bacterial infections. *Frontiers in Microbiology*, *6*(APR), 1–8. https://doi.org/10.3389/fmicb.2015.00282

Rao, M., Rashid, F. A., Shukor, S., Hashim, R., & Ahmad, N. (2020). Detection of Antimicrobial Resistance Genes Associated with Carbapenem Resistance from the Whole-Genome Sequence of Acinetobacter baumannii Isolates from Malaysia. *Canadian Journal of Infectious Diseases and Medical Microbiology*, *2020*.

https://doi.org/10.1155/2020/5021064

Rao R, P., Sharma, S., Mehrotra, T., Das, R., Kumar, R., Singh, R., Roy, I., & Basu, T. (2020). Rapid Electrochemical Monitoring of Bacterial Respiration for Gram-Positive and Gram-Negative Microbes: Potential Application in Antimicrobial Susceptibility Testing. *Analytical Chemistry*, *92*(6), 4266–4274. https://doi.org/10.1021/acs.analchem.9b04810

Reguera, G. (2018). Harnessing the power of microbial nanowires. *Microbial Biotechnology*, *11*(6), 979–994. https://doi.org/10.1111/1751-7915.13280

Richards, C., O'Connor, N., Jose, D., Barrett, A., & Regan, F. (2020). Selection and optimization of protein and carbohydrate assays for the characterization of marine biofouling. *Analytical Methods*, *12*(17), 2228–2236. https://doi.org/10.1039/d0ay00272k

Richter, K., Van Den Driessche, F., & Coenye, T. (2017). Innovative approaches to treat Staphylococcus aureus biofilm-related infections. *Essays in Biochemistry*, *61*(1), 61–70. https://doi.org/10.1042/EBC20160056

Rodríguez-Cerdeira, C., Gregorio, M. C., Molares-Vila, A., López-Barcenas, A., Fabbrocini, G., Bardhi, B., Sinani, A., Sánchez-Blanco, E., Arenas-Guzmán, R., & Hernandez-Castro, R. (2019). Biofilms and vulvovaginal candidiasis. *Colloids and Surfaces B: Biointerfaces*, *174*(November 2018), 110–125. https://doi.org/10.1016/j.colsurfb.2018.11.011

Rodríguez-Cerdeira, C., Martínez-Herrera, E., Carnero-Gregorio, M., López-Barcenas, A., Fabbrocini, G., Fida, M., El-Samahy, M., & González-Cespón, J. L. (2020). Pathogenesis and Clinical Relevance of Candida Biofilms in Vulvovaginal Candidiasis. *Frontiers in Microbiology*, *11*(November). https://doi.org/10.3389/fmicb.2020.544480

Ruiz-Herrera, B. L., Flores-Álamo, M., Toscano, R. A., Escudero, R., & Sosa-Torres, M. E. (2016). Adsorption of water induces a reversible structural phase transition and colour change in new nickel(II) macrocyclic complexes forming flexible supramolecular networks. *New Journal of Chemistry*, *40*(9), 7465–7475. https://doi.org/10.1039/c6nj01621a

Sá, S. R., Silva Junior, A. G., Lima-Neto, R. G., Andrade, C. A. S., & Oliveira, M. D. L. (2020). Lectin-based impedimetric biosensor for differentiation of pathogenic candida species. *Talanta*, *220*(March), 121375. https://doi.org/10.1016/j.talanta.2020.121375

Sáenz, J. P., Grosser, D., Bradley, A. S., Lagny, T. J., Lavrynenko, O., Broda, M., & Simons, K. (2015). Hopanoids as functional analogues of cholesterol in bacterial membranes. *Proceedings of the National Academy of Sciences of the United States of America*, *112*(38), 11971–11976. https://doi.org/10.1073/pnas.1515607112

Sainis, I., Banti, C. N., Owczarzak, A. M., Kyros, L., Kourkoumelis, N., Kubicki, M., & Hadjikakou, S. K. (2016). New antibacterial, non-genotoxic materials, derived from the functionalization of the anti-thyroid drug methimazole with silver ions. *Journal of Inorganic Biochemistry*, *160*, 114–124.

https://doi.org/10.1016/j.jinorgbio.2015.12.013

Saito, J., Murugan, M., Deng, X., Guionet, A., Miran, W., & Okamoto, A. (2019). Electrochemical techniques and applications to characterize single- and multicellular electric microbial functions. *Bioelectrochemical Interface Engineering*, 37–53. https://doi.org/10.1002/9781119611103.ch3

Sánchez, C., Dessì, P., Duffy, M., & Lens, P. N. L. (2020). Microbial electrochemical technologies: Electronic circuitry and characterization tools. *Biosensors and Bioelectronics*, *150*(September 2019). https://doi.org/10.1016/j.bios.2019.111884

Sanguinetti, M., & Posteraro, B. (2017). New approaches for antifungal susceptibility testing. *Clinical Microbiology and Infection*, *23*(12), 931–934. https://doi.org/10.1016/j.cmi.2017.03.025

Sanguinetti, Maurizio, & Posteraro, B. (2018). Susceptibility testing of fungi to antifungal drugs. *Journal of Fungi*, *4*(3), 1–16. https://doi.org/10.3390/jof4030110

Sanguinetti, Maurizio, Posteraro, B., & Lass-Flörl, C. (2015). Antifungal drug resistance among Candida species: Mechanisms and clinical impact. *Mycoses*, *58*(S2), 2–13. https://doi.org/10.1111/myc.12330

Santoro, C., Mohidin, A. F., Grasso, L. Lo, Seviour, T., Palanisamy, K., Hinks, J., Lauro, F. M., & Marsili, E. (2016). Sub-toxic concentrations of volatile organic compounds inhibit extracellular respiration of Escherichia coli cells grown in anodic bioelectrochemical systems. *Bioelectrochemistry*, *112*, 173–177. https://doi.org/10.1016/j.bioelechem.2016.02.003

Sarshar, M., Behzadi, P., Scribano, D., Palamara, A. T., & Ambrosi, C. (2021). Acinetobacter baumannii: An ancient commensal with weapons of a pathogen. *Pathogens*, *10*(4). https://doi.org/10.3390/pathogens10040387

Savić, N. D., Glišić, B. D., Wadepohl, H., Pavic, A., Senerovic, L., Nikodinovic-Runic, J., & Djuran, M. I. (2016). Silver(i) complexes with quinazoline and phthalazine: Synthesis, structural characterization and evaluation of biological activities. *MedChemComm*, *7*(2), 282–291. https://doi.org/10.1039/c5md00494b

Savić, N. D., Milivojevic, D. R., Glišić, B. D., Ilic-Tomic, T., Veselinovic, J., Pavic, A., Vasiljevic, B., Nikodinovic-Runic, J., & Djuran, M. I. (2016). A comparative antimicrobial and toxicological study of gold(III) and silver(i) complexes with aromatic nitrogen-containing heterocycles: Synergistic activity and improved selectivity index of Au(III)/Ag(i) complexes mixture. *RSC Advances*, *6*(16), 13193–13206. https://doi.org/10.1039/c5ra26002g

Savić, N., Petković, B., Vojnovic, S., Mojicevic, M., Wadepohl, H., Olaifa, K., Marsili, E., Nikodinovic-Runic, J., Djuran, M., & Glisic, B. (2020). Dinuclear silver(I) complexes with pyridine-based macrocyclic type of ligand as antimicrobial agents against clinically relevant species: the influence of counter anion on the structure diversification of the complexes. *Dalton Transactions*, *49*, 10880–10894. https://doi.org/10.1039/D0DT01272F

Schmerk, C. L., Bernards, M. A., & Valvano, M. A. (2011). Hopanoid production is required for low-pH tolerance, antimicrobial resistance, and motility in Burkholderia cenocepacia. *Journal of Bacteriology*, *193*(23), 6712–6723. https://doi.org/10.1128/JB.05979-11

Schofield, Z., Meloni, G. N., Tran, P., Zerfass, C., Sena, G., Hayashi, Y., Grant, M., Contera, S. A., Minteer, S. D., Kim, M., Prindle, A., Rocha, P., Djamgoz, M. B. A., Pilizota, T., Unwin, P. R., Asally, M., & Soyer, O. S. (2020). Bioelectrical understanding and engineering of cell biology. *Journal of the Royal Society Interface*, *17*(166). https://doi.org/10.1098/rsif.2020.0013

Schröder, U., Harnisch, F., & Angenent, L. T. (2015). Microbial electrochemistry and technology: Terminology and classification. *Energy and Environmental Science*, *8*(2), 513–519. https://doi.org/10.1039/c4ee03359k

Schwab, L., Rago, L., Koch, C., & Harnisch, F. (2019). Identification of Clostridium cochlearium as an electroactive microorganism from the mouse gut microbiome. *Bioelectrochemistry*, *130*, 107334. https://doi.org/10.1016/j.bioelechem.2019.107334

Seneviratne, C. J., Jin, L., & Samaranayake, L. P. (2008). Biofilm lifestyle of Candida: A mini review. *Oral Diseases*, *14*(7), 582–590. https://doi.org/10.1111/j.1601-0825.2007.01424.x

Seviour, T., Doyle, L. E., Lauw, S. J. L., Hinks, J., Rice, S. A., Nesatyy, V. J., Webster, R. D., Kjelleberg, S., & Marsili, E. (2015). Voltammetric profiling of redox-active metabolites expressed by Pseudomonas aeruginosa for diagnostic purposes. *Chemical Communications*, *51*(18), 3789–3792. https://doi.org/10.1039/c4cc08590f

Shafiei, M., Peyton, L., Hashemzadeh, M., & Foroumadi, A. (2020). History of the development of antifungal azoles: A review on structures, SAR, and mechanism of action. *Bioorganic Chemistry*, *104*(August), 104240. https://doi.org/10.1016/j.bioorg.2020.104240

Shenkutie, A. M., Yao, M. Z., Siu, G. K. H., Wong, B. K. C., & Leung, P. H. M. (2020). Biofilm-induced antibiotic resistance in clinical acinetobacter baumannii isolates. *Antibiotics*, *9*(11), 1–15. https://doi.org/10.3390/antibiotics9110817

Sheybani, R., & Shukla, A. (2017). Highly sensitive label-free dual sensor array for rapid detection of wound bacteria. *Biosensors and Bioelectronics*, *92*(July), 425–433. https://doi.org/10.1016/j.bios.2016.10.084

Siala, W., Kucharíková, S., Braem, A., Vleugels, J., Tulkens, P. M., Mingeot-Leclercq, M. P., Van Dijck, P., & Van Bambeke, F. (2016). The antifungal caspofungin increases fluoroquinolone activity against Staphylococcus aureus biofilms by inhibiting N-acetylglucosamine transferase. *Nature Communications*, *7*. https://doi.org/10.1038/ncomms13286

Simoska, O., Sans, M., Eberlin, L. S., Shear, J. B., & Stevenson, K. J. (2019). Electrochemical monitoring of the impact of polymicrobial infections on Pseudomonas aeruginosa and growth dependent medium. *Biosensors and Bioelectronics*, *142*(June), 111538. https://doi.org/10.1016/j.bios.2019.111538

Simoska, O., Sans, M., Fitzpatrick, M. D., Crittenden, C. M., Eberlin, L. S., Shear, J. B., & Stevenson, K. J. (2019). Real-Time Electrochemical Detection of Pseudomonas aeruginosa Phenazine Metabolites Using Transparent Carbon Ultramicroelectrode Arrays. *ACS Sensors*, *4*(1), 170–179. https://doi.org/10.1021/acssensors.8b01152

Simoska, O., & Stevenson, K. J. (2019). Electrochemical sensors for rapid diagnosis of pathogens in real time. *Analyst*, *144*(22), 6461–6478. https://doi.org/10.1039/c9an01747j

Smith, J. P., Metters, J. P., Kampouris, D. K., Lledo-Fernandez, C., Sutcliffe, O. B., & Banks, C. E. (2013). Forensic electrochemistry: The electroanalytical sensing of Rohypnol® (flunitrazepam) using screen-printed graphite electrodes without recourse for electrode or sample pre-treatment. *Analyst*, *138*(20), 6185–6191. https://doi.org/10.1039/c3an01352a

Soley, A., Lecina, M., Gámez, X., Cairó, J. J., Riu, P., Rosell, X., Bragós, R., & Gòdia, F. (2005). On-line monitoring of yeast cell growth by impedance spectroscopy. *Journal of Biotechnology*, *118*(4), 398–405. https://doi.org/10.1016/j.jbiotec.2005.05.022

Soll, D. R., & Daniels, K. J. (2016). Plasticity of Candida albicans Biofilms. *Microbiology and Molecular Biology Reviews*, *80*(3), 565–595. https://doi.org/10.1128/mmbr.00068-15

Søpstad, S., Johannessen, E. A., Seland, F., & Imenes, K. (2018). Long-term stability of screen-printed pseudo-reference electrodes for electrochemical biosensors. *Electrochimica Acta*, *287*, 29–36. https://doi.org/10.1016/j.electacta.2018.08.045

Soulis, D., Trigazi, M., Tsekenis, G., Chrysoula, C., Klinakis, A., & Zergioti, I. (2020). Facile and Low-Cost SPE Modification Towards Ultra-Sensitive Organophosphorus and Carbamate Pesticide Detection in Olive Oil. *Molecules*, *25*(4988), 1–19. https://doi.org/doi:10.3390/molecules25214988

Srikanth, S., Marsili, E., Flickinger, M. C., & Bond, D. R. (2008). Electrochemical characterization of Geobacter sulfurreducens cells immobilized on graphite paper electrodes. *Biotechnology and Bioengineering*, *99*(5), 1065–1073. https://doi.org/10.1002/bit.21671

Stokes, J. M., Macnair, C. R., Ilyas, B., French, S., Côté, J. P., Bouwman, C., Farha, M. A., Sieron, A. O., Whitfield, C., Coombes, B. K., & Brown, E. D. (2017). Pentamidine sensitizes Gram-negative pathogens to antibiotics and overcomes acquired colistin resistance. *Nature Microbiology*, *2*(March). https://doi.org/10.1038/nmicrobiol.2017.28

Su, Y., Liu, C., Fang, H., & Zhang, D. (2020). Bacillus subtilis: A universal cell factory for industry, agriculture, biomaterials and medicine. *Microbial Cell Factories*, *19*(1), 1–12. https://doi.org/10.1186/s12934-020-01436-8

Sun, H., Angelidaki, I., Wu, S., Dong, R., & Zhang, Y. (2019). The potential of bioelectrochemical sensor for monitoring of acetate during anaerobic digestion: Focusing on novel reactor design. *Frontiers in Microbiology*, *10*(JAN), 1–10. https://doi.org/10.3389/fmicb.2018.03357

Sun, J., Warden, A. R., Huang, J., Wang, W., & Ding, X. (2019). Colorimetric and Electrochemical Detection of Escherichia coli and Antibiotic Resistance Based on a p-Benzoquinone-Mediated Bioassay. *Analytical Chemistry*, *91*(12), 7524–7530. https://doi.org/10.1021/acs.analchem.8b04997

Sypabekova, M., Dukenbayev, K., Tsepke, A., Akisheva, A., Oralbayev, N., & Kanayeva, D. (2019). An aptasensor for the detection of Mycobacterium tuberculosis secreted immunogenic protein MPT64 in clinical samples towards tuberculosis detection. *Scientific Reports*, *9*(1), 1–11. https://doi.org/10.1038/s41598-019-52685-6

Tacconelli, E., & Pezzani, M. D. (2019). Public health burden of antimicrobial resistance in Europe. *The Lancet Infectious Diseases*, *19*(1), 4–6. https://doi.org/10.1016/S1473-3099(18)30648-0

Tadesse, B., Shimelis, T., & Worku, M. (2019). Bacterial profile and antibacterial susceptibility of otitis media among pediatric patients in Hawassa, Southern Ethiopia: Cross-sectional study. *BMC Pediatrics*, *19*(1), 1–8. https://doi.org/10.1186/s12887-019-1781-3

Tanasković, S. B., Vučković, G., Antonijević-Nikolić, M., Stanojković, T., & Gojgić-Cvijović, G. (2012). Binuclear biologically active Co(II) complexes with octazamacrocycle and aliphatic dicarboxylates. *Journal of Molecular Structure*, *1029*, 1–7. https://doi.org/10.1016/j.molstruc.2012.06.055

Tao, Y., Wang, Y., Huang, S., Zhu, P., Huang, W. E., Ling, J., & Xu, J. (2017). Metabolic-Activity-Based Assessment of Antimicrobial Effects by D2O-Labeled Single-Cell Raman Microspectroscopy. *Analytical Chemistry*, *89*(7), 4108–4115. https://doi.org/10.1021/acs.analchem.6b05051

Teravest, M. A., & Angenent, L. T. (2014). Oxidizing Electrode Potentials Decrease Current Production and Coulombic Efficiency through Cytochromec Inactivation in Shewanella oneidensis MR-1. *ChemElectroChem*, *1*(11), 2000–2006. https://doi.org/10.1002/celc.201402128

Tharali, A. D., Sain, N., & Osborne, W. J. (2016). Microbial fuel cells in bioelectricity production. *Frontiers in Life Science*, *9*(4), 252–266. https://doi.org/10.1080/21553769.2016.1230787

Tian, T., Fan, X., Feng, M., Su, L., Zhang, W., Chi, H., & Fu, D. (2019). Flavin-mediated extracellular electron transfer in Gram-positive bacteria: Bacillus cereus DIF1 and Rhodococcus ruber DIF2. *RSC Advances*, *9*(70), 40903–40909. https://doi.org/10.1039/c9ra08045g

Tokonami, S., & Iida, T. (2017). Review: Novel sensing strategies for bacterial detection based on active and passive methods driven by external field. *Analytica Chimica Acta*, *988*, 1–16. https://doi.org/10.1016/j.aca.2017.07.034

Torre, R., Costa-Rama, E., Nouws, H. P. A., & Delerue-Matos, C. (2020). Screen-printed electrode-based sensors for food spoilage control: Bacteria and biogenic amines detection. *Biosensors*, *10*(10). https://doi.org/10.3390/BIOS10100139

Tsay, S., Williams, S. ;, Mu, Y., Epson, E., & Helen Johnston; Monica M. Farley, Lee H. Harrison, Brittany Vonbank, Sarah Shrum, Ghinwa Dumyati, Alexia Zhang, William SchaffnerNational Burden of Candidemia, United States, 2017. (2018). National Burden of Candidemia, United States, 2017. *Fungal Disease: Management and Outcomes*, *5*(Suppl 1), S142–S143. https://doi.org/10.1093/ofid/ofy210.374

Tsay, S., Williams, S., Mu, Y., Epson, E., Johnston, H., Farley, M. M., Lee, ;, Harrison, H., Vonbank, B., Shrum, S., Dumyati, G., Zhang, A., & Schaffner, ; William. (2017). National Burden of Candidemia, United States, 2017. *Poster Abstracts • OFID*, *362*(5), S142–S143. https://academic.oup.com/ofid/article-abstract/5/suppl_1/S142/5207783

Tsubouchi, T., Suzuki, M., Niki, M., Oinuma, K.-I., Niki, M., Kakeya, H., & Kaneko, Y. (2020). Complete Genome Sequence of Acinetobacter baumannii ATCC 19606 T , a Model Strain of Pathogenic Bacteria Causing Nosocomial Infection . *Microbiology Resource Announcements*, *9*(20), 8–9. https://doi.org/10.1128/mra.00289-20

Tsui, C., Kong, E. F., & Jabra-Rizk, M. A. (2016). Pathogenesis of Candida albicans biofilm. *Pathogens and Disease*, *74*(4), ftw018. https://doi.org/10.1093/femspd/ftw018

Tuddenham, S. & Sears, C. L. (2015). Candida Biofilms: Development, Architecture, and Resistance. *Microbiology Spectrum*, *176*(3(4)), 139–148. https://doi.org/10.1016/j.physbeh.2017.03.040

Turick, C. E., Shimpalee, S., Satjaritanun, P., Weidner, J., & Greenway, S. (2019). Convenient non-invasive electrochemical techniques to monitor microbial processes: current state and perspectives. *Applied Microbiology and Biotechnology*, *103*(20), 8327–8338. https://doi.org/10.1007/s00253-019-10091-y

Uchil, R. R., Kohli, G. S., Katekhaye, V. M., & Swami, O. C. (2014). Strategies to combat antimicrobial resistance. *Journal of Clinical and Diagnostic Research*, *8*(7), 8–11. https://doi.org/10.7860/JCDR/2014/8925.4529

Uria, N., Fiset, E., Pellitero, M. A., Muñoz, F. X., Rabaey, K., & Campo, F. J. de. (2020). Immobilisation of electrochemically active bacteria on screen-printed electrodes for rapid in situ toxicity biosensing. *Environmental Science and Ecotechnology*, *3*, 100053. https://doi.org/10.1016/j.ese.2020.100053

Uzoechi, S. C., & Abu-Lail, N. I. (2019). The effects of β-lactam antibiotics on surface modifications of multidrug-resistant Escherichia coli: A multiscale approach. *Microscopy and Microanalysis*, *25*(1), 135–150. https://doi.org/10.1017/S1431927618015696

Uzoechi, S. C., & Abu-Lail, N. I. (2020). Variations in the morphology, mechanics and adhesion of persister and resister E. Coli cells in reponses to ampicillin: AFM study. *Antibiotics*, *9*(5). https://doi.org/10.3390/antibiotics9050235

Van Dijck, P., Sjollema, J., Cammue, B. P. A., Lagrou, K., Berman, J., d'Enfert, C., Andes, D. R., Arendrup, M. C., Brakhage, A. A., Calderone, R., Cantón, E., Coenye, T., Cos, P., Cowen, L. E., Edgerton, M., Espinel-Ingroff, A., Filler, S. G., Ghannoum, M.,

Gow, N. A. R., … Thevissen, K. (2018). Methodologies for in vitro and in vivo evaluation of efficacy of antifungal and antibiofilm agents and surface coatings against fungal biofilms. *Microbial Cell*, *5*(7), 300–326. https://doi.org/10.15698/mic2018.07.638

VanArsdale, E., Pitzer, J., Payne, G. F., & Bentley, W. E. (2020). Redox Electrochemistry to Interrogate and Control Biomolecular Communication. *IScience*, *23*(9), 101545. https://doi.org/10.1016/j.isci.2020.101545

Vasilescu, A., Fanjul-Bolado, P., Titoiu, A. M., Porumb, R., & Epure, P. (2019). Progress in electrochemical (bio)sensors for monitoring wine production. *Chemosensors*, *7*(4). https://doi.org/10.3390/chemosensors7040066

Vázquez-López, R., Solano-Gálvez, S. G., Vignon-Whaley, J. J. J., Vaamonde, J. A. A., Alonzo, L. A. P., Reséndiz, A. R., Álvarez, M. M., López, E. N. V., Franyuti-Kelly, G., Álvarez-Hernández, D. A., Guzmán, V. M., Bañuelos, J. E. J., Felix, J. M., Barrios, J. A. G., & Fortes, T. B. (2020). Acinetobacter baumannii resistance: A real challenge for clinicians. *Antibiotics*, *9*(4), 1–22. https://doi.org/10.3390/antibiotics9040205

Veloz, J. J., Alvear, M., & Salazar, L. A. (2019). Evaluation of Alternative Methods to Assess the Biological Properties of Propolis on Metabolic Activity and Biofilm Formation in Streptococcus mutans. *Evidence-Based Complementary and Alternative Medicine*, *2019*. https://doi.org/10.1155/2019/1524195

Verma, J., Kumar, D., Singh, N., Katti, S. S., & Shah, Y. T. (2021). Electricigens and microbial fuel cells for bioremediation and bioenergy production: a review. In *Environmental Chemistry Letters* (Vol. 19, Issue 3). Springer International Publishing. https://doi.org/10.1007/s10311-021-01199-7

Vrancianu, C. O., Gheorghe, I., Czobor, I. B., & Chifiriuc, M. C. (2020). Antibiotic resistance profiles, molecular mechanisms and innovative treatment strategies of acinetobacter baumannii. *Microorganisms*, *8*(6), 1–40. https://doi.org/10.3390/microorganisms8060935

Wang, C. H., Hsieh, Y. H., Powers, Z. M., & Kao, C. Y. (2020). Defeating antibiotic-resistant bacteria: Exploring alternative therapies for a post-antibiotic era. *International Journal of Molecular Sciences*, *21*(3), 1–18. https://doi.org/10.3390/ijms21031061

Wang, V. B., Chua, S. L., Cao, B., Seviour, T., Nesatyy, V. J., Marsili, E., Kjelleberg, S., Givskov, M., Tolker-Nielsen, T., Song, H., Loo, J. S. C., & Yang, L. (2013). Engineering PQS Biosynthesis Pathway for Enhancement of Bioelectricity Production in Pseudomonas aeruginosa Microbial Fuel Cells. *PLoS ONE*, *8*(5), 1–7. https://doi.org/10.1371/journal.pone.0063129

Wang, W., Du, Y., Yang, S., Du, X., Li, M., Lin, B., Zhou, J., Lin, L., Song, Y., Li, J., Zuo, X., & Yang, C. (2019). Bacterial Extracellular Electron Transfer Occurs in Mammalian Gut. *Analytical Chemistry*, *91*(19), 12138–12141. https://doi.org/10.1021/acs.analchem.9b03176

Wang, Y., Xu, J., Kong, L., Liu, T., Yi, L., Wang, H., Huang, W. E., & Zheng, C. (2020). Raman–deuterium isotope probing to study metabolic activities of single bacterial cells in human intestinal microbiota. *Microbial Biotechnology*, *13*(2), 572–583. https://doi.org/10.1111/1751-7915.13519

Ward, A. C., Hannah, A. J., Kendrick, S. L., Tucker, N. P., MacGregor, G., & Connolly, P. (2018). Identification and characterisation of Staphylococcus aureus on low cost screen printed carbon electrodes using impedance spectroscopy. *Biosensors and Bioelectronics*, *110*, 65–70. https://doi.org/10.1016/j.bios.2018.03.048

Ward, Andrew C., Connolly, P., & Tucker, N. P. (2014). Pseudomonas aeruginosacan be detected in a polymicrobial competition model using impedance spectroscopy with a novel biosensor. *PLoS ONE*, *9*(3). https://doi.org/10.1371/journal.pone.0091732

Webster, T. A., Sismaet, H. J., Conte, J. L., Chan, I. ping J., & Goluch, E. D. (2014). Electrochemical detection of Pseudomonas aeruginosa in human fluid samples via pyocyanin. *Biosensors and Bioelectronics*, *60*, 265–270. https://doi.org/10.1016/j.bios.2014.04.028

Wei, J., Liang, P., Cao, X., & Huang, X. (2010). A new insight into potential regulation on growth and power generation of geobacter sulfurreducens in microbial fuel cells based on energy viewpoint. *Environmental Science and Technology*, *44*(8), 3187–3191. https://doi.org/10.1021/es903758m

Welander, P. V., Hunter, R. C., Zhang, L., Sessions, A. L., Summons, R. E., & Newman, D. K. (2009). Hopanoids play a role in membrane integrity and pH homeostasis in Rhodopseudomonas palustris TIE-1. *Journal of Bacteriology*, *191*(19), 6145–6156. https://doi.org/10.1128/JB.00460-09

Whited, J., & Levin, M. (2019). Bioelectrical controls of morphogenesis: from ancient mechanisms of cell coordination to biomedical opportunities. *Physiology & Behavior*, *57*, 61–69. https://doi.org/10.1016/j.gde.2019.06.014.

Whiteway, C., Breine, A., Philippe, C., & Van der Henst, C. (2022). Acinetobacter baumannii. *Trends in Microbiology*, *30*(2), 199–200. https://doi.org/10.1016/j.tim.2021.11.008

Willdigg, J. R., & Helmann, J. D. (2021). *Mini Review : Bacterial Membrane Composition and Its Modulation in Response to Stress*. *8*(May), 1–11. https://doi.org/10.3389/fmolb.2021.634438

Wilson, D. (2019). Candida albicans. *Trends in Microbiology*, *27*(2), 188–189. https://doi.org/10.1016/j.tim.2018.10.010

Winkelströter, L. K., Teixeira, F. B. dos R., Silva, E. P., Alves, V. F., & De Martinis, E. C. P. (2014). Unraveling Microbial Biofilms of Importance for Food Microbiology. *Microbial Ecology*, *68*(1), 35–46. https://doi.org/10.1007/s00248-013-0347-4

Wong, D., Nielsen, T. B., Bonomo, R. A., Pantapalangkoor, P., Luna, B., & Spellberg, B. (2017). Clinical and pathophysiological overview of Acinetobacter infections: A century of challenges. *Clinical Microbiology Reviews*, *30*(1), 409–447.

https://doi.org/10.1128/CMR.00058-16

World Health Organization. (2017). *WHO Publishes List of Bacteria for Which New Antibiotics Are Urgently Needed*. https://doi.org/https://www.who.int/news/item/27-02-2017-who-publishes-list-of-bacteria-for-which-new-antibiotics-are-urgently-needed

Xiao, Y., Zhang, E., Zhang, J., Dai, Y., Yang, Z., Christensen, H. E. M., Ulstrup, J., & Zhao, F. (2017). Extracellular polymeric substances are transient media for microbial extracellular electron transfer. *Science Advances*, *3*(7), 1–8. https://doi.org/10.1126/sciadv.1700623

Yamanaka, K., Vestergaard, M. C., & Tamiya, E. (2016). Printable electrochemical biosensors: A focus on screen-printed electrodes and their application. *Sensors (Switzerland)*, *16*(10), 1–16. https://doi.org/10.3390/s16101761

Yáñez-Sedeño, P., Campuzano, S., & Pingarrón, J. M. (2019). Pushing the limits of electrochemistry toward challenging applications in clinical diagnosis, prognosis, and therapeutic action. *Chemical Communications*, *55*(18), 2563–2592. https://doi.org/10.1039/c8cc08815b

Yáñez-Sedeño, Paloma, Campuzano, S., & Pingarrón, J. M. (2018). Integrated affinity biosensing platforms on screen-printed electrodes electrografted with diazonium salts. *Sensors (Switzerland)*, *18*(2). https://doi.org/10.3390/s18020675

Yang, C. H., Su, P. W., Moi, S. H., & Chuang, L. Y. (2019). Biofilm formation in Acinetobacter baumannii: Genotype-phenotype correlation. *Molecules*, *24*(10), 1–12. https://doi.org/10.3390/molecules24101849

Yong, X. Y., Feng, J., Chen, Y. L., Shi, D. Y., Xu, Y. S., Zhou, J., Wang, S. Y., Xu, L., Yong, Y. C., Sun, Y. M., Shi, C. L., OuYang, P. K., & Zheng, T. (2014). Enhancement of bioelectricity generation by cofactor manipulation in microbial fuel cell. *Biosensors and Bioelectronics*, *56*, 19–25. https://doi.org/10.1016/j.bios.2013.12.058

You, J., Chen, H., Xu, L., Zhao, J., Ye, J., Zhang, S., Chen, J., & Cheng, Z. (2021). Anodic-potential-tuned bioanode for efficient gaseous toluene removal in an MFC. *Electrochimica Acta*, *375*, 137992. https://doi.org/10.1016/j.electacta.2021.137992

You, L. X., Liu, L. D., Xiao, Y., Dai, Y. F., Chen, B. L., Jiang, Y. X., & Zhao, F. (2018). Flavins mediate extracellular electron transfer in Gram-positive Bacillus megaterium strain LLD-1. *Bioelectrochemistry*, *119*, 196–202. https://doi.org/10.1016/j.bioelechem.2017.10.005

Yudin, A. K. (2015). Macrocycles: Lessons from the distant past, recent developments, and future directions. *Chemical Science*, *6*(1), 30–49. https://doi.org/10.1039/c4sc03089c

Zarnowski, R., Westler, W. M., Lacmbouh, G. A., Marita, J. M., Bothe, J. R., Bernhardt, J., Sahraoui, A. L. H., Fontainei, J., Sanchez, H., Hatfeld, R. D., Ntambi, J. M., Nett, J. E., Mitchell, A. P., & Andes, D. R. (2014). Novel entries in a fungal biofilm matrix encyclopedia. *MBio*, *5*(4), 1–13. https://doi.org/10.1128/mBio.01333-14

Zeng, X., She, P., Zhou, L., Li, S., Hussain, Z., Chen, L., & Wu, Y. (2020). Drug repurposing: Antimicrobial and antibiofilm effects of penfluridol against Enterococcus faecalis. *MicrobiologyOpen*, *December*, 1–8. https://doi.org/10.1002/mbo3.1148

Zhang, F., Pant, D., & Logan, B. E. (2011). Long-term performance of activated carbon air cathodes with different diffusion layer porosities in microbial fuel cells. *Biosensors and Bioelectronics*, *30*(1), 49–55. https://doi.org/10.1016/j.bios.2011.08.025

Zhang, S., Miran, W., Naradasu, D., Guo, S., & Okamoto, A. (2020). A human pathogen Capnocytophaga ochracea exhibits current producing capability. *Electrochemistry*, *88*(3), 224–229. https://doi.org/10.5796/electrochemistry.20-00021

Zhu, K., Chen, S., Sysoeva, T. A., & You, L. (2019). Universal antibiotic tolerance arising from antibiotic-triggered accumulation of pyocyanin in Pseudomonas aeruginosa. *PLoS Biology*, *17*(12), 1–9. https://doi.org/10.1371/journal.pbio.3000573

Appendixes

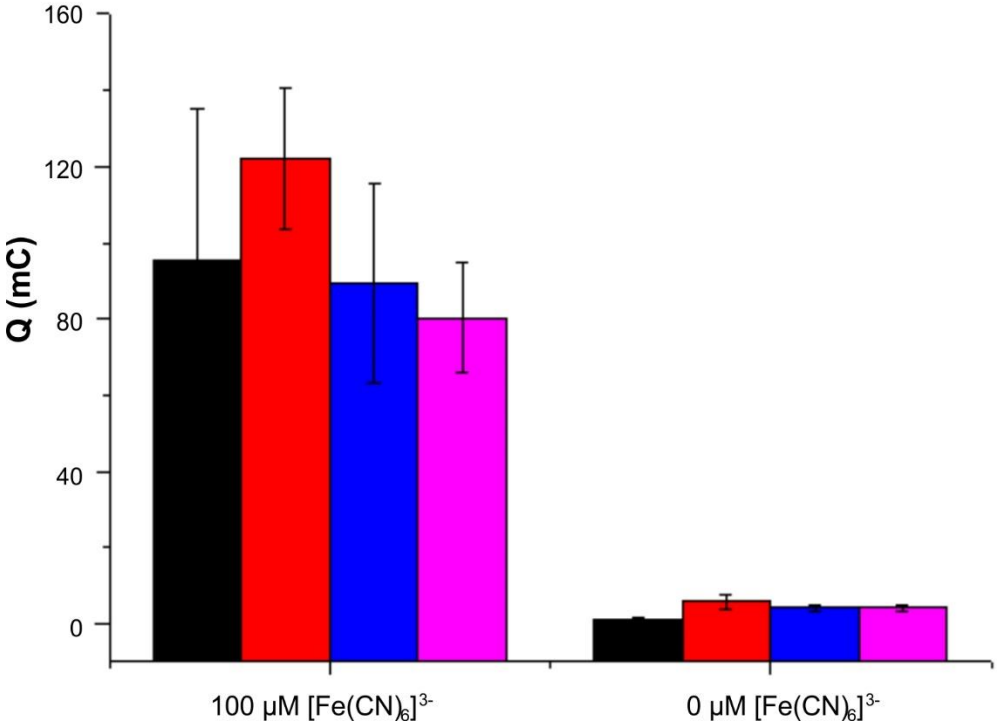

Appendix 3.1. Total Q (mC) of biofilms grown with and without $[Fe(CN)_6]^{3-}$ as redox mediator for *C. albicans* isolate 24 (black) , *A. baumannii* (ATCC 19606) (violet), *C. parapsilosis* (ATCC 22019) (red) and *C. albicans* (ATCC 10231) (blue).

Appendix 4.1(A)**:** Analysis of variance for planktonic and biofilm cells estimates at varying time intervals of growth at E = 0.4 *vs*. Ag pseudo-reference electrode.

Null hypothesis: no difference in planktonic and biofilm cell counts.
Alternate hypothesis: there is difference in planktonic and biofilm cell counts.

SUMMARY

Groups	*Count*	*Sum*	*Average*	*Variance*
Planktonic cells	5	3.758083	0.751617	0.29806
Biofilms cells	5	2.089167	0.417833	0.126838

Source of variation	**Sum of squares**	**Deg. of freedom**	**Mean square**	**Mean square ratio (F)**	**P-value**	**F crit**
Between groups	0.278528284	1	0.278528284	1.311034168	0.285304834	5.317655072
Within groups	1.699594356	8	0.212449294			
Total	1.97812264	9				

As F < F crit, we accept the null hypothesis; there is no significant difference between planktonic and biofilm cell counts at varying time intervals of growth at E = 0.4 *vs*. Ag pseudo-reference electrode.

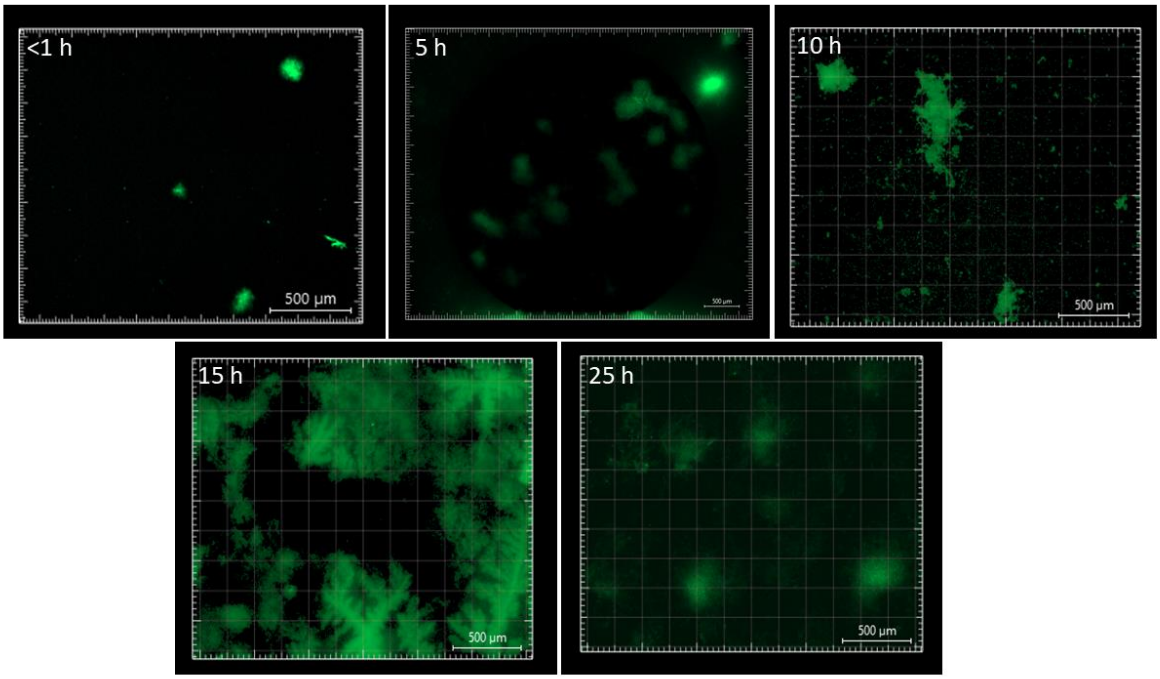

Appendix 4.1(B)**:** Representative fluorescent microscopic images of C. albicans biofilms at varying times interval.

Appendix 4.2: ANOVA for optical density of planktonic cells in different experimental conditions after 24 h growth at $E = 0.4$ *vs*. Ag pseudo-reference electrode.

Null hypothesis: no difference in the optical density of planktonic cells among the experimental conditions.
Alternate hypothesis: there is difference in the optical density of planktonic cells among the experimental conditions.

SUMMARY

Groups	*Count*	*Sum*	*Average*	*Variance*
Cells+mediator only	3	4.055	1.351666667	0.058565
Cells+mediator+complex 3	3	1.023	0.341	0.0031
Cells+mediator+Flz	3	2.137	0.712333333	0.024904
Cells+mediator+AmB	3	1.857	0.619	0.010036

ANOVA

Source of variation	**Sum of squares**	**Deg. of freedom**	**Mean square**	**Mean square ratio (F)**	**P-value**	**F crit**
Between groups	1.643158667	3	0.547719556	22.67857	0.000289	4.066181
Within groups	0.193211333	8	0.024151417			
Total	1.83637	11				

As F > F crit, we accept the alternate hypothesis; there is a significant difference in the optical density of planktonic cells among the experimental conditions.

Appendix 4.3: ANOVA for biofilm cells concentration measured with crystal violet assay for different experimental conditions after 24 h growth at E = 0.4 *vs*. Ag pseudo-reference electrode.

Null hypothesis: no difference in the optical density of biofilm cells among the experimental conditions.
Alternate hypothesis: there is difference in the optical density of biofilm cells among the experimental conditions.

Summary

Groups	*Count*	*Sum*	*Average*	*Variance*
Cells+mediator only	3	2.243	0.747666667	0.008217
Cells+mediator+complex 3	3	0.032	0.010666667	1.43E-05
Cells+mediator+Flz	3	0.345	0.115	0.001171
Cells+mediator+AmB	3	0.516	0.172	0.002107

ANOVA

Source of variation	**Sum of squares**	**Degrees of freedom**	**Mean square**	**Mean square ratio (F)**	**P-value**	**F crit**
Between groups	0.986243333	3	0.328747778	114.251	6.6E-07	4.066181
Within groups	0.023019333	8	0.002877417			
Total	1.009262667	11				

As F > F crit, we accept the alternate hypothesis; there is a significant difference in the optical density of biofilm cells among the experimental conditions.

Appendix 4.4: ANOVA for total charge output for different experimental conditions after 24 h growth at E = 0.4 *vs*. Ag pseudo-reference electrode

Null hypothesis: no difference in the total charge output among the experimental conditions; **Alternate hypothesis:** there is difference in the total charge output among the experimental conditions.

SUMMARY

Groups	*Count*	*Sum*	*Average*	*Variance*
Cells+mediator only	2	1983.26895	991.634475	35235.24644
Cells+complex 3	3	295.05123	98.35041	435.6692775
Cells+Flz	2	1127.59401	563.797005	2.77779521
Cells+AmB	2	312.456	156.228	1165.575762
Mediator+Medium only	2	0.317595474	0.158797737	0.050544361
Cells+medium only	2	6.10467	3.052335	0.271768781
Mediator+complex 3	2	110.445	55.2225	4.23754272
Cells+mediator+DMSO	2	1832.423	916.2115	14499.85292

ANOVA

Source of variation	**Sum of squares**	**Degrees of freedom**	**Mean square**	**Mean square ratio (F)**	**P-value**	**F crit**
Between groups	2475698.061	7	353671.1515	61.47316028	7.00268E-07	3.292745839
Within groups	51779.35133	9	5753.261259			
Total	2527477.412	16				

As F > F crit, we accept the alternate hypothesis; there is a significant difference in the total charge output among the experimental conditions.

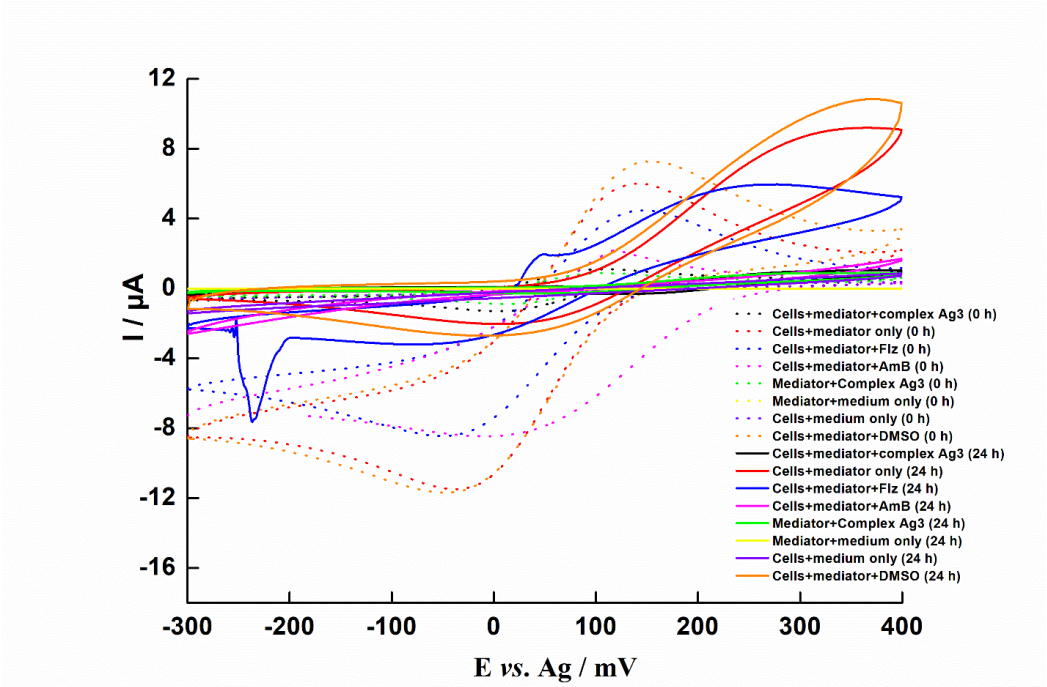

Appendix 4.5: Cyclic voltammogram of *C. albicans* ATTC 10231 at 0 h (dot traces) and 24 h (solid traces) at 10 mV s^{-1}. Cells with 0.1 mM $K_3[Fe(CN)_6]$ as a redox mediator (red trace); cells with 0.1 mM $K_3[Fe(CN)_6]$ and MIC of complex 3 dissolved in DMSO (black trace); cells with 0.1 mM $K_3[Fe(CN)_6]$ and MIC of Flz dissolved in DMSO (blue trace); cells with 0.1 mM $K_3[Fe(CN)_6]$ and MIC of AmB dissolved in DMSO (magenta trace); cells with 0.1 mM $K_3[Fe(CN)_6]$ and 0.1% (v/v) DMSO (orange trace); cells and RPMI medium only (with no mediator) (violet trace); 0.1 mM $K_3[Fe(CN)_6]$ and complex 3 only (green trace); RPMI medium and 0.1 mM $K_3[Fe(CN)_6]$ (yellow trace). Results are the average of two independent biological replicates except for cells with 0.1 mM $K_3[Fe(CN)_6]$ as a redox mediator (red trace), and cells with 0.1 mM $K_3[Fe(CN)_6]$ and MIC of complex 3 dissolved in DMSO (black trace) with three independent biological replicates.

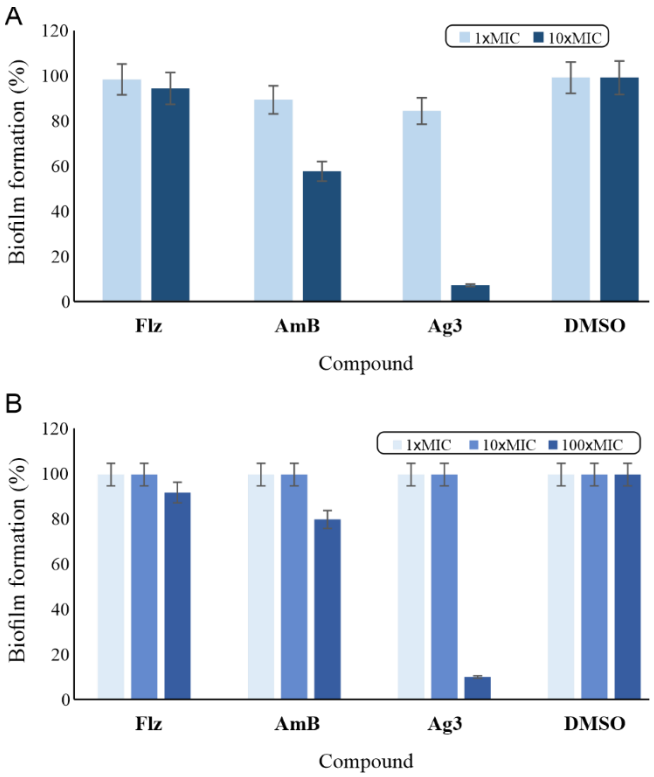

Appendix 4.6: Effect of antifungal compounds Flz, AmB, and complex 3 at 1-100 × MIC on pre-formed *C. albicans* biofilm, as determined by XTT reduction assay. (A) Biofilm pre-formed for 8 h; (B) Biofilm pre-formed for 48 h.

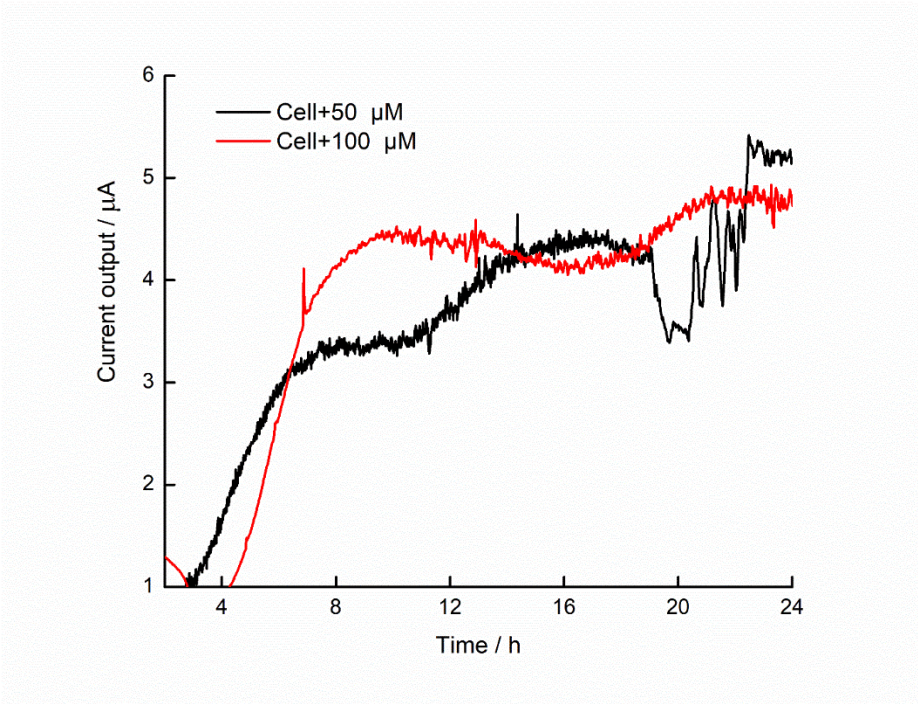

Appendix 5.1. Chronoamperometry of cells with 0.1 mM 2-HNQ (red trace); 0.05 mM 2-HNQ (black trace).

Appendix 5.2. One-way ANOVA followed by Tukey's test on the comparative susceptibility (MICs, μM) of *A. baumannii* against tested drugs.

Overall ANOVA

	DF	Sum of Squares	Mean Square	F Value	Prob>F
Model	2	5581.08667	2790.54333	244.45094	1.78195E-6
Error	6	68.49333	11.41556		
Total	8	5649.58			

Null Hypothesis: The means of all levels are equal.
Alternative Hypothesis: The means of one or more levels are different.
At the 0.05 level, the population means are significantly different.

Results of mean comparisons - Tukey's post hoc test.

	MeanDiff	SEM	q Value	Prob	Alpha	Sig	LCL	UCL
Itz *vs* Cip	48.26667	2.75869	24.7434	5.50416E-6	0.05	1	39.80205	56.73129
Flz *vs* Cip	56.43333	2.75869	28.92996	2.15903E-6	0.05	1	47.96871	64.89795
Flz *vs* Itz	8.16667	2.75869	4.18656	0.05714	0.05	0	-0.29795	16.63129

Sig equals 1 indicates that the difference of the means is significant at the 0.05 level.
Sig equals 0 indicates that the difference of the means is not significant at the 0.05 level.

Appendix 5.3(A). One-way ANOVA followed by Tukey's test on the effect of different concentrations of Amp on growth (OD_{600}) of *A. baumannii.*

Overall ANOVA

	DF	Sum of Squares	Mean Square	F Value	Prob>F
Model	5	2.12778	0.42556	2.1574	0.05785
Error	432	85.21381	0.19725		
Total	437	87.3416			

Null Hypothesis: The means of all levels are equal.
Alternative Hypothesis: The means of one or more levels are different.
At the 0.05 level, the population means are not significantly different.

Results of mean comparisons - Tukey's post hoc test.

	MeanDiff	SEM	q Value	Prob	Alpha	Sig	LCL	UCL
5 µM *vs* 0 µM	-0.13595	0.07351	2.61533	0.43519	0.05	0	-0.34639	0.07449
10 µM *vs* 0 µM	-0.18176	0.07351	3.49657	0.13464	0.05	0	-0.3922	0.02868
10 µM *vs* 5 µM	-0.04581	0.07351	0.88123	0.9893	0.05	0	-0.25625	0.16463
20 µM *vs* 0 µM	-0.19734	0.07351	3.79628	0.08045	0.05	0	-0.40778	0.0131
20 µM *vs* 5 µM	-0.06139	0.07351	1.18095	0.96086	0.05	0	-0.27183	0.14905
20 µM *vs* 10 µM	-0.01558	0.07351	0.29972	0.99994	0.05	0	-0.22602	0.19486
50 µM *vs* 0 µM	-0.19408	0.07351	3.73365	0.09001	0.05	0	-0.40452	0.01636
50 µM *vs* 5 µM	-0.05813	0.07351	1.11832	0.96902	0.05	0	-0.26857	0.15231
50 µM *vs* 10 µM	-0.01232	0.07351	0.23709	0.99998	0.05	0	-0.22276	0.19811
50 µM *vs* 20 µM	0.00326	0.07351	0.06263	1	0.05	0	-0.20718	0.21369
DMSO *vs* 0 µM	-0.09812	0.07351	1.8876	0.76552	0.05	0	-0.30856	0.11232
DMSO *vs* 5 µM	0.03783	0.07351	0.72773	0.9956	0.05	0	-0.17261	0.24827
DMSO *vs* 10 µM	0.08364	0.07351	1.60897	0.86541	0.05	0	-0.1268	0.29407
DMSO *vs* 20 µM	0.09922	0.07351	1.90868	0.75694	0.05	0	-0.11122	0.30965
DMSO *vs* 50 µM	0.09596	0.07351	1.84605	0.78206	0.05	0	-0.11448	0.3064

Sig equals 1 indicates that the difference of the means is significant at the 0.05 level.
Sig equals 0 indicates that the difference of the means is not significant at the 0.05 level.

Appendix 5.3(B). One-way ANOVA followed by Tukey's test on the effect of different concentrations of Flz on growth (OD_{600}) of *A. baumannii*.

Overall ANOVA

	DF	Sum of Squares	Mean Square	F Value	Prob>F
Model	6	44.07018	7.34503	83.0609	0
Error	503	44.48001	0.08843		
Total	509	88.55019			

Null Hypothesis: The means of all levels are equal.
Alternative Hypothesis: The means of one or more levels are different.
At the 0.05 level, the population means are significantly different.

Results of mean comparisons - Tukey's post hoc test.

	MeanDiff	SEM	q Value	Prob	Alpha	Sig	LCL	UCL
1 µM *vs* 0 µM	-0.33984	0.04939	9.7305	2.3479E-8	0.05	1	-0.48606	-0.19362
5 µM *vs* 0 µM	-0.66131	0.04922	19.00052	0	0.05	1	-0.80702	-0.51559
5 µM *vs* 1 µM	-0.32147	0.04939	9.20439	1.58593E-8	0.05	1	-0.46768	-0.17525
10 µM *vs* 0 µM	-0.69407	0.04922	19.94178	0	0.05	1	-0.83978	-0.54835
10 µM *vs* 1 µM	-0.35423	0.04939	10.1424	2.21447E-8	0.05	1	-0.50044	-0.20801
10 µM *vs* 5 µM	-0.03276	0.04922	0.94126	0.99435	0.05	0	-0.17847	0.11295
20 µM *vs* 0 µM	-0.73653	0.04922	21.1619	0	0.05	1	-0.88224	-0.59082
20 µM *vs* 1 µM	-0.39669	0.04939	11.3583	1.92182E-8	0.05	1	-0.54291	-0.25047
20 µM *vs* 5 µM	-0.07523	0.04922	2.16138	0.72764	0.05	0	-0.22094	0.07049
20 µM *vs* 10 µM	-0.04247	0.04922	1.22012	0.97778	0.05	0	-0.18818	0.10325
50 µM *vs* 0 µM	-0.73464	0.04922	21.10758	0	0.05	1	-0.88035	-0.58893
50 µM *vs* 1 µM	-0.3948	0.04939	11.30417	1.9342E-8	0.05	1	-0.54102	-0.24858
50 µM *vs* 5 µM	-0.07334	0.04922	2.10706	0.75086	0.05	0	-0.21905	0.07238
50 µM *vs* 10 µM	-0.04058	0.04922	1.1658	0.9824	0.05	0	-0.18629	0.10514
50 µM *vs* 20 µM	0.00189	0.04922	0.05431	1	0.05	0	-0.14382	0.1476
DMSO *vs* 0 µM	-0.09812	0.04922	2.81919	0.42007	0.05	0	-0.24383	0.04759
DMSO *vs* 1 µM	0.24172	0.04939	6.92104	2.74571E-5	0.05	1	0.0955	0.38794
DMSO *vs* 5 µM	0.56318	0.04922	16.18132	0	0.05	1	0.41747	0.7089
DMSO *vs* 10 µM	0.59595	0.04922	17.12258	0	0.05	1	0.45023	0.74166
DMSO *vs* 20 µM	0.63841	0.04922	18.3427	0	0.05	1	0.4927	0.78412
DMSO *vs* 50 µM	0.63652	0.04922	18.28839	0	0.05	1	0.49081	0.78223

Sig equals 1 indicates that the difference of the means is significant at the 0.05 level.
Sig equals 0 indicates that the difference of the means is not significant at the 0.05 level.

Appendix 5.3(C). One-way ANOVA followed by Tukey's test on the effect of different concentrations of Itz on growth (OD_{600}) of *A. baumannii.*

Overall ANOVA

	DF	Sum of Squares	Mean Square	F Value	Prob>F
Model	6	21.29897	3.54983	43.3342	0
Error	504	41.2864	0.08192		
Total	510	62.58537			

Null Hypothesis: The means of all levels are equal.
Alternative Hypothesis: The means of one or more levels are different.
At the 0.05 level, the population means are significantly different.

Results of mean comparisons - Tukey's post hoc test.

	MeanDiff	SEM	q Value	Prob	Alpha	Sig	LCL	UCL
1 µM *vs* 0 µM	-0.34574	0.04737	10.32115	2.14858E-8	0.05	1	-0.48599	-0.2055
5 µM *vs* 0 µM	-0.35231	0.04737	10.51724	2.10033E-8	0.05	1	-0.49256	-0.21207
5 µM *vs* 1 µM	-0.00657	0.04737	0.19608	1	0.05	0	-0.14681	0.13367
10 µM *vs* 0 µM	-0.35112	0.04737	10.48166	2.10896E-8	0.05	1	-0.49136	-0.21088
10 µM *vs* 1 µM	-0.00538	0.04737	0.16051	1	0.05	0	-0.14562	0.13487
10 µM *vs* 5 µM	0.00119	0.04737	0.03558	1	0.05	0	-0.13905	0.14143
20 µM *vs* 0 µM	-0.53672	0.04737	16.02227	0	0.05	1	-0.67697	-0.39648
20 µM *vs* 1 µM	-0.19098	0.04737	5.70112	0.00125	0.05	1	-0.33122	-0.05074
20 µM *vs* 5 µM	-0.18441	0.04737	5.50503	0.00215	0.05	1	-0.32465	-0.04417
20 µM *vs* 10 µM	-0.1856	0.04737	5.54061	0.00195	0.05	1	-0.32585	-0.04536
50 µM *vs* 0 µM	-0.62185	0.04737	18.56337	0	0.05	1	-0.76209	-0.4816
50 µM *vs* 1 µM	-0.2761	0.04737	8.24221	2.24318E-7	0.05	1	-0.41635	-0.13586
50 µM *vs* 5 µM	-0.26953	0.04737	8.04613	4.67431E-7	0.05	1	-0.40978	-0.12929
50 µM *vs* 10 µM	-0.27073	0.04737	8.08171	4.08911E-7	0.05	1	-0.41097	-0.13048
50 µM *vs* 20 µM	-0.08512	0.04737	2.5411	0.55081	0.05	0	-0.22537	0.05512
DMSO *vs* 0 µM	-0.09812	0.04737	2.92911	0.37152	0.05	0	-0.23836	0.04212
DMSO *vs* 1 µM	0.24762	0.04737	7.39205	5.2623E-6	0.05	1	0.10738	0.38787
DMSO *vs* 5 µM	0.25419	0.04737	7.58813	2.57953E-6	0.05	1	0.11395	0.39443
DMSO *vs* 10 µM	0.253	0.04737	7.55255	2.93876E-6	0.05	1	0.11276	0.39324
DMSO *vs* 20 µM	0.4386	0.04737	13.09316	0	0.05	1	0.29836	0.57885
DMSO *vs* 50 µM	0.52373	0.04737	15.63426	0	0.05	1	0.38348	0.66397

Sig equals 1 indicates that the difference of the means is significant at the 0.05 level.
Sig equals 0 indicates that the difference of the means is not significant at the 0.05 level.

Appendix 5.3(D). One-way ANOVA followed by Tukey's test on the effect of different concentrations of Cip on growth (OD_{600}) of *A. baumannii.*

Overall ANOVA

	DF	Sum of Squares	Mean Square	F Value	Prob>F
Model	6	53.68216	8.94703	121.13737	0
Error	504	37.22469	0.07386		
Total	510	90.90685			

Null Hypothesis: The means of all levels are equal.
Alternative Hypothesis: The means of one or more levels are different.
At the 0.05 level, the population means are significantly different.

Results of mean comparisons - Tukey's post hoc test.

	MeanDiff	SEM	q Value	Prob	Alpha	Sig	LCL	UCL
1 µM *vs* 0 µM	-0.36295	0.04498	11.41072	1.8925E-8	0.05	1	-0.49612	-0.22979
5 µM *vs* 0 µM	-0.68486	0.04498	21.53096	0	0.05	1	-0.81803	-0.55169
5 µM *vs* 1 µM	-0.32191	0.04498	10.12024	2.20083E-8	0.05	1	-0.45507	-0.18874
10 µM *vs* 0 µM	-0.78624	0.04498	24.7183	0	0.05	1	-0.91941	-0.65308
10 µM *vs* 1 µM	-0.42329	0.04498	13.30758	0	0.05	1	-0.55646	-0.29012
10 µM *vs* 5 µM	-0.10138	0.04498	3.18734	0.26894	0.05	0	-0.23455	0.03178
20 µM *vs* 0 µM	-0.80849	0.04498	25.4177	0	0.05	1	-0.94166	-0.67532
20 µM *vs* 1 µM	-0.44554	0.04498	14.00698	0	0.05	1	-0.5787	-0.31237
20 µM *vs* 5 µM	-0.12363	0.04498	3.88674	0.08873	0.05	0	-0.2568	0.00954
20 µM *vs* 10 µM	-0.02225	0.04498	0.6994	0.99892	0.05	0	-0.15541	0.11092
50 µM *vs* 0 µM	-0.80681	0.04498	25.36473	0	0.05	1	-0.93997	-0.67364
50 µM *vs* 1 µM	-0.44385	0.04498	13.95401	0	0.05	1	-0.57702	-0.31069
50 µM *vs* 5 µM	-0.12195	0.04498	3.83377	0.09762	0.05	0	-0.25511	0.01122
50 µM *vs* 10 µM	-0.02056	0.04498	0.64643	0.99931	0.05	0	-0.15373	0.1126
50 µM *vs* 20 µM	0.00168	0.04498	0.05297	1	0.05	0	-0.13148	0.13485
DMSO *vs* 0 µM	-0.09812	0.04498	3.08477	0.30754	0.05	0	-0.23129	0.03505
DMSO *vs* 1 µM	0.26483	0.04498	8.32595	1.6471E-7	0.05	1	0.13167	0.398
DMSO *vs* 5 µM	0.58674	0.04498	18.44619	0	0.05	1	0.45357	0.71991
DMSO *vs* 10 µM	0.68812	0.04498	21.63353	0	0.05	1	0.55496	0.82129
DMSO *vs* 20 µM	0.71037	0.04498	22.33293	0	0.05	1	0.5772	0.84354
DMSO *vs* 50 µM	0.70868	0.04498	22.27996	0	0.05	1	0.57552	0.84185

Sig equals 1 indicates that the difference of the means is significant at the 0.05 level.
Sig equals 0 indicates that the difference of the means is not significant at the 0.05 level.

Appendix 5.4. One-way ANOVA followed by Tukey's test on the effect of tested compounds (Cip, Flz and Itz) on biofilm formation by *A. baumannii* at two different concentrations (1×MIC and 10×MIC) upon addition at the start of incubation.

Overall ANOVA

	DF	Sum of Squares	Mean Square	F Value	Prob>F
Model	7	0.85316	0.12188	47.3734	1.61167E-9
Error	16	0.04116	0.00257		
Total	23	0.89432			

Null Hypothesis: The means of all levels are equal.
Alternative Hypothesis: The means of one or more levels are different.
At the 0.05 level, the population means are significantly different.

Results of mean comparisons - Tukey's post hoc test.

	MeanDiff	SEM	q Value	Prob	Alpha	Sig	LCL	UCL
Cip 10×MIC *vs* Cip 1×MIC	-0.103	0.04141	3.51722	0.2675	0.05	0	-0.24638	0.04038
Flz 1×MIC *vs* Cip 1×MIC	0.04667	0.04141	1.59356	0.94109	0.05	0	-0.09672	0.19005
Flz 1×MIC *vs* Cip 10×MIC	0.14967	0.04141	5.11078	0.03756	0.05	1	0.00628	0.29305
Flz 10×MIC *vs* Cip 1×MIC	-0.089	0.04141	3.03915	0.42726	0.05	0	-0.23238	0.05438
Flz 10×MIC *vs* Cip 10×MIC	0.014	0.04141	0.47807	0.99996	0.05	0	-0.12938	0.15738
Flz 10×MIC *vs* Flz 1×MIC	-0.13567	0.04141	4.63271	0.07061	0.05	0	-0.27905	0.00772
Itz 1×MIC *vs* Cip 1×MIC	0.09133	0.04141	3.11883	0.39749	0.05	0	-0.05205	0.23472
Itz 1×MIC *vs* Cip 10×MIC	0.19433	0.04141	6.63604	0.00464	0.05	1	0.05095	0.33772
Itz 1×MIC *vs* Flz 1×MIC	0.04467	0.04141	1.52527	0.95255	0.05	0	-0.09872	0.18805
Itz 1×MIC *vs* Flz 10×MIC	0.18033	0.04141	6.15797	0.00897	0.05	1	0.03695	0.32372
Itz 10×MIC *vs* Cip 1×MIC	-0.085	0.04141	2.90256	0.48068	0.05	0	-0.22838	0.05838
Itz 10×MIC *vs* Cip 10×MIC	0.018	0.04141	0.61466	0.9998	0.05	0	-0.12538	0.16138
Itz 10×MIC *vs* Flz 1×MIC	-0.13167	0.04141	4.49612	0.08416	0.05	0	-0.27505	0.01172
Itz 10×MIC *vs* Flz 10×MIC	0.004	0.04141	0.13659	1	0.05	0	-0.13938	0.14738
Itz 10×MIC *vs* Itz 1×MIC	-0.17633	0.04141	6.02138	0.01083	0.05	1	-0.31972	-0.03295
DMSO 1×MIC *vs* Cip 1×MIC	0.38533	0.04141	13.15826	1.60366E-6	0.05	1	0.24195	0.52872
DMSO 1×MIC *vs* Cip 10×MIC	0.48833	0.04141	16.67547	1.36818E-7	0.05	1	0.34495	0.63172
DMSO 1×MIC *vs* Flz 1×MIC	0.33867	0.04141	11.5647	9.23931E-6	0.05	1	0.19528	0.48205
DMSO 1×MIC *vs* Flz 10×MIC	0.47433	0.04141	16.19741	1.53507E-7	0.05	1	0.33095	0.61772
DMSO 1×MIC *vs* Itz 1×MIC	0.294	0.04141	10.03943	5.4853E-5	0.05	1	0.15062	0.43738
DMSO 1×MIC *vs* Itz 10×MIC	0.47033	0.04141	16.06082	1.60721E-7	0.05	1	0.32695	0.61372
DMSO 10×MIC *vs* Cip 1×MIC	0.387	0.04141	13.21517	1.50792E-6	0.05	1	0.24362	0.53038
DMSO 10×MIC *vs* Cip 10×MIC	0.49	0.04141	16.73239	1.34523E-7	0.05	1	0.34662	0.63338
DMSO 10×MIC *vs* Flz 1×MIC	0.34033	0.04141	11.62161	8.66564E-6	0.05	1	0.19695	0.48372
DMSO 10×MIC *vs* Flz 10×MIC	0.476	0.04141	16.25432	1.509E-7	0.05	1	0.33262	0.61938
DMSO 10×MIC *vs* Itz 1×MIC	0.29567	0.04141	10.09635	5.12057E-5	0.05	1	0.15228	0.43905
DMSO 10×MIC *vs* Itz 10×MIC	0.472	0.04141	16.11773	1.46035E-7	0.05	1	0.32862	0.61538
DMSO 10×MIC *vs* DMSO 1×MIC	0.00167	0.04141	0.05691	1	0.05	0	-0.14172	0.14505

Sig equals 1 indicates that the difference of the means is significant at the 0.05 level.
Sig equals 0 indicates that the difference of the means is not significant at the 0.05 level.

Appendix 5.5. One-way ANOVA followed by Tukey's test on the effect of tested compounds (Cip, Flz and Itz) on preformed biofilm of *A. baumannii* at two different concentrations (1×MIC and 10×MIC) (B), as determined by crystal violet staining assay.

Overall ANOVA

DF	Sum of Squares	Mean Square	F Value	Prob>F	
Model	7	1.34614	0.19231	74.08119	5.3468E-11
Error	16	0.04153	0.0026		
Total	23	1.38767			

Null Hypothesis: The means of all levels are equal.
Alternative Hypothesis: The means of one or more levels are different.
At the 0.05 level, the population means are significantly different.

Results of mean comparisons - Tukey's post hoc test.

	MeanDiff	SEM	q Value	Prob	Alpha	Sig	LCL	UCL
Cip 10×MIC *vs* Cip 1×MIC	-0.22867	0.0416	7.77359	9.88851E-4	0.05	1	-0.37269	-0.08464
Flz 1×MIC *vs* Cip 1×MIC	-0.01333	0.0416	0.45327	0.99997	0.05	0	-0.15736	0.13069
Flz 1×MIC *vs* Cip 10×MIC	0.21533	0.0416	7.32032	0.00182	0.05	1	0.07131	0.35936
Flz 10×MIC *vs* Cip 1×MIC	-0.07967	0.0416	2.70829	0.56044	0.05	0	-0.22369	0.06436
Flz 10×MIC *vs* Cip 10×MIC	0.149	0.0416	5.0653	0.03992	0.05	1	0.00497	0.29303
Flz 10×MIC *vs* Flz 1×MIC	-0.06633	0.0416	2.25502	0.74711	0.05	0	-0.21036	0.07769
Itz 1×MIC *vs* Cip 1×MIC	-0.03833	0.0416	1.30315	0.97923	0.05	0	-0.18236	0.10569
Itz 1×MIC *vs* Cip 10×MIC	0.19033	0.0416	6.47044	0.00583	0.05	1	0.04631	0.33436
Itz 1×MIC *vs* Flz 1×MIC	-0.025	0.0416	0.84988	0.99835	0.05	0	-0.16903	0.11903
Itz 1×MIC *vs* Flz 10×MIC	0.04133	0.0416	1.40514	0.96887	0.05	0	-0.10269	0.18536
Itz 10×MIC *vs* Cip 1×MIC	-0.12067	0.0416	4.1021	0.13738	0.05	0	-0.26469	0.02336
Itz 10×MIC *vs* Cip 10×MIC	0.108	0.0416	3.67149	0.22633	0.05	0	-0.03603	0.25203
Itz 10×MIC *vs* Flz 1×MIC	-0.10733	0.0416	3.64883	0.23205	0.05	0	-0.25136	0.03669
Itz 10×MIC *vs* Flz 10×MIC	-0.041	0.0416	1.39381	0.97018	0.05	0	-0.18503	0.10303
Itz 10×MIC *vs* Itz 1×MIC	-0.08233	0.0416	2.79895	0.5228	0.05	0	-0.22636	0.06169
DMSO 1×MIC *vs* Cip 1×MIC	0.457	0.0416	15.53585	1.08379E-7	0.05	1	0.31297	0.60103
DMSO 1×MIC *vs* Cip 10×MIC	0.68567	0.0416	23.30944	5.12984E-7	0.05	1	0.54164	0.82969
DMSO 1×MIC *vs* Flz 1×MIC	0.47033	0.0416	15.98912	1.65105E-7	0.05	1	0.32631	0.61436
DMSO 1×MIC *vs* Flz 10×MIC	0.53667	0.0416	18.24414	1.08037E-7	0.05	1	0.39264	0.68069
DMSO 1×MIC *vs* Itz 1×MIC	0.49533	0.0416	16.839	1.30625E-7	0.05	1	0.35131	0.63936
DMSO 1×MIC *vs* Itz 10×MIC	0.57767	0.0416	19.63795	1.4488E-7	0.05	1	0.43364	0.72169
DMSO 10×MIC *vs* Cip 1×MIC	0.431	0.0416	14.65197	3.14805E-7	0.05	1	0.28697	0.57503
DMSO 10×MIC *vs* Cip 10×MIC	0.65967	0.0416	22.42556	1.64952E-7	0.05	1	0.51564	0.80369
DMSO 10×MIC *vs* Flz 1×MIC	0.44433	0.0416	15.10524	1.85656E-7	0.05	1	0.30031	0.58836
DMSO 10×MIC *vs* Flz 10×MIC	0.51067	0.0416	17.36026	1.17645E-7	0.05	1	0.36664	0.65469
DMSO 10×MIC *vs* Itz 1×MIC	0.46933	0.0416	15.95512	1.67341E-7	0.05	1	0.32531	0.61336
DMSO 10×MIC *vs* Itz 10×MIC	0.55167	0.0416	18.75407	1.44505E-7	0.05	1	0.40764	0.69569
DMSO 10×MIC *vs* DMSO 1×MIC	-0.026	0.0416	0.88388	0.99789	0.05	0	-0.17003	0.11803

Sig equals 1 indicates that the difference of the means is significant at the 0.05 level.
Sig equals 0 indicates that the difference of the means is not significant at the 0.05 level.

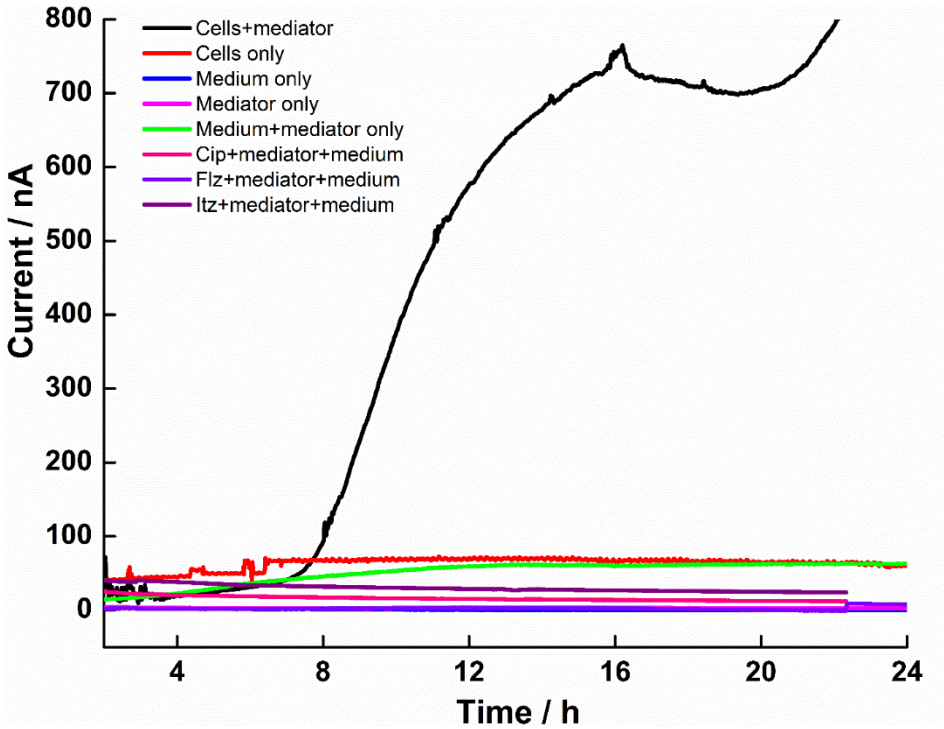

Appendix 5.6. Chronoamperometry of cells with 0.1 mM 2-HNQ (black trace); cells only (no mediator) (red trace); medium only (no mediator) (blue trace); mediator only (magenta trace); medium with 0.1 mM 2-HNQ (green trace); 1×MIC Cip with with 0.1 mM 2-HNQ (pink trace); 1×MIC Flz with with 0.1 mM 2-HNQ (violet trace); 1×MIC Itz with with 0.1 mM 2-HNQ (purple trace). The curves are the average of at least two independent biological replicates.

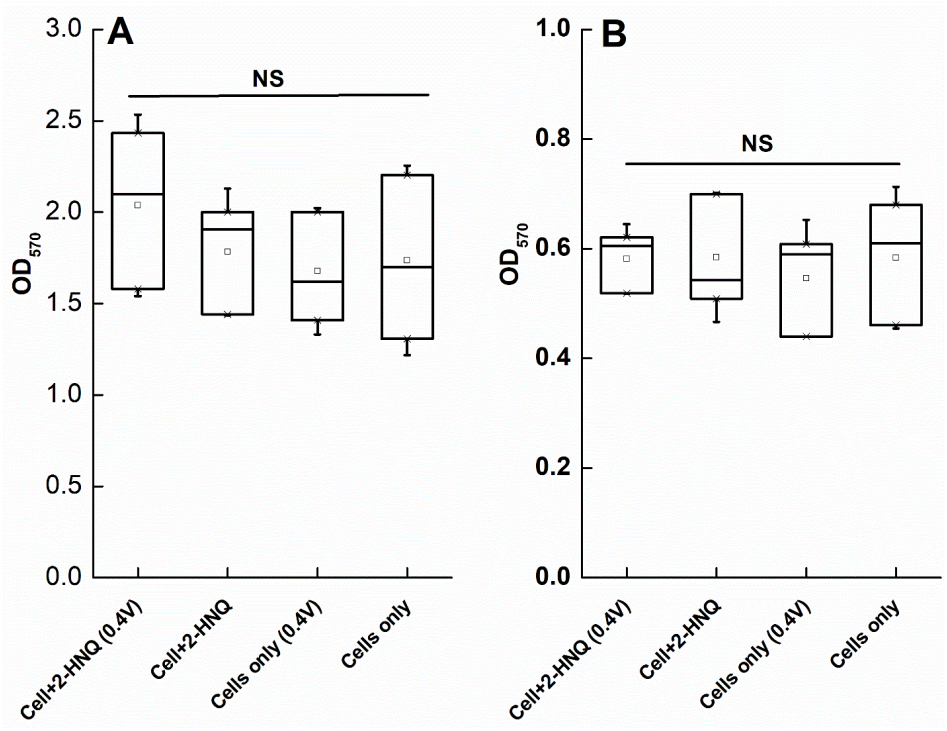

Appendix 5.7. (A) OD of planktonic cells with and without mediator after 24 h growth under conventional (no potential) and at E = 400 mV. (B) Biofilm cells concentration measured with crystal violet assay for cells with and without mediator after 24 h growth under conventional (no potential) and at E = 400 mV. The difference between each pair of conditions is statistically insignificant ($p < 0.05$). NS means not significant.

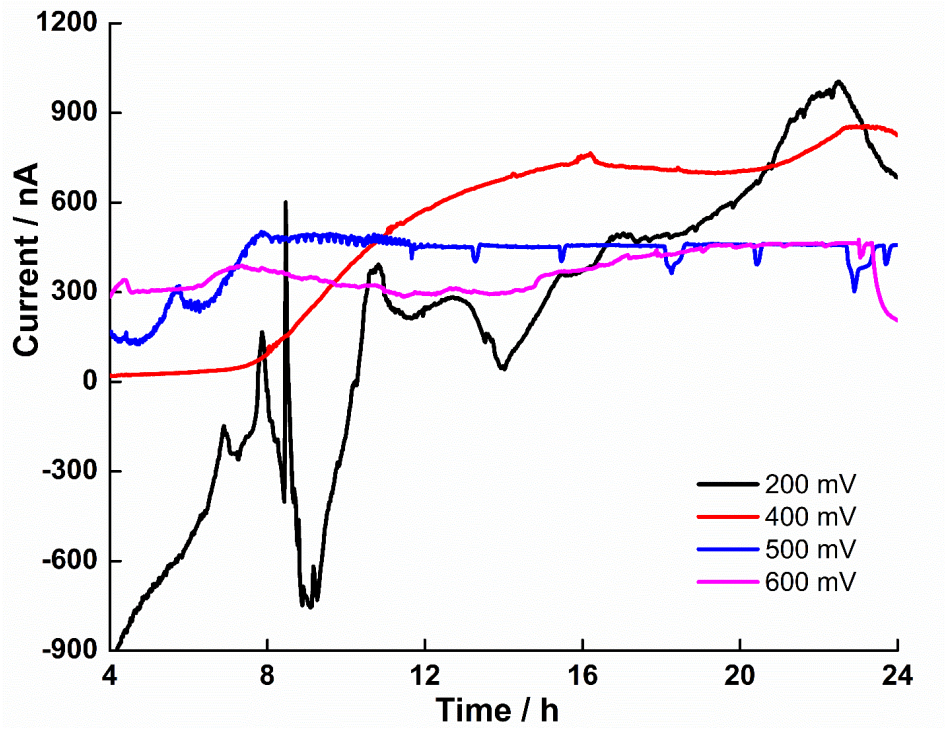

Appendix 5.8**.** Current output of *A. baumannii* biofilm over 24 h poised at different potential (mV). The curves are the average of at least two independent biological replicates.

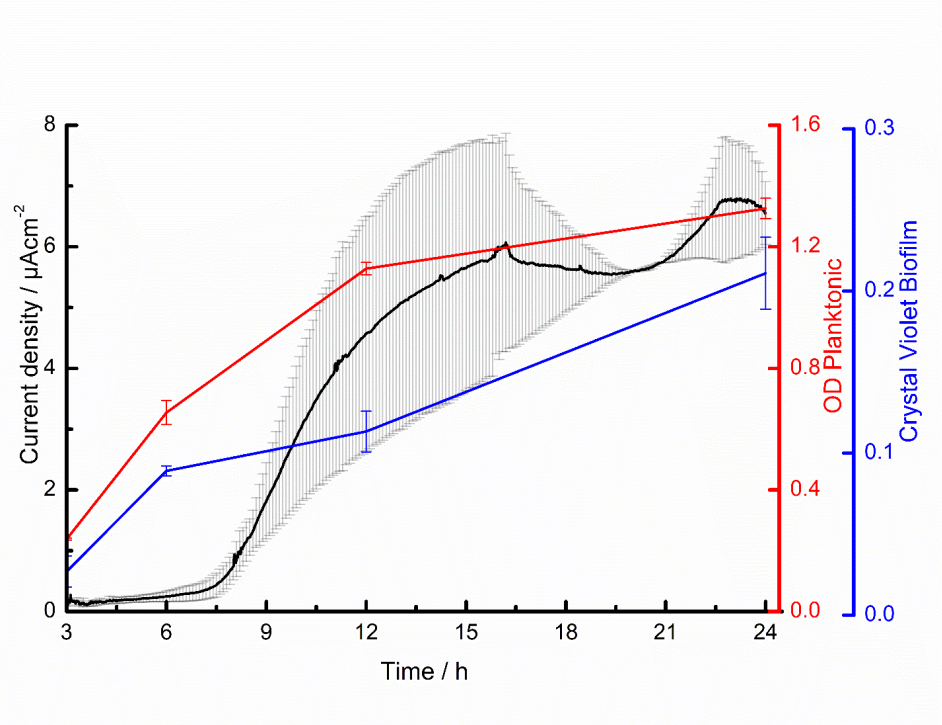

Appendix **5.9.** biofilm and planktonic cells estimate at varying time intervals under potentiostatic growth at E = 0.4 *vs*. Ag pseudo-reference electrode (n=3). No statistical significance between the estimates ($p < 0.05$) (Appendix 5.10).

Appendix 5.10. One-way ANOVA followed by Tukey's test on the chronoamperometric measurements on the effect of Flz, Itz and Cip at their MIC values on the current output of *A. baumannii* biofilms.

Overall ANOVA

	DF	Sum of Squares	Mean Square	F Value	Prob>F
Model	3	1.44301E8	4.81004E7	948.24823	0
Error	5543	2.81172E8	50725.54469		
Total	5546	4.25473E8			

Null Hypothesis: The means of all levels are equal.
Alternative Hypothesis: The means of one or more levels are different.
At the 0.05 level, the population means are significantly different.

Results of mean comparisons - Tukey's post hoc test.

	MeanDiff	SEM	q Value	Prob	Alpha	Sig	LCL	UCL
Flz *vs* Cells	-269.77805	8.55244	44.60992	2.22045E-16	0.05	1	-291.74957	-247.80653
Itz *vs* Cells	-328.89043	8.55244	54.38462	2.22045E-16	0.05	1	-350.86196	-306.91891
Itz *vs* Flz	-59.11238	8.55244	9.7747	2.87191E-11	0.05	1	-81.08391	-37.14086
Cip *vs* Cells	-437.82848	8.55398	72.38533	2.22045E-16	0.05	1	-459.80396	-415.85299
Cip *vs* Flz	-168.05043	8.55398	27.78345	2.22045E-16	0.05	1	-190.02591	-146.07494
Cip *vs* Itz	-108.93804	8.55398	18.01051	2.22045E-16	0.05	1	-130.91353	-86.96256

Sig equals 1 indicates that the difference of the means is significant at the 0.05 level.
Sig equals 0 indicates that the difference of the means is not significant at the 0.05 level.

Appendix 5.11. One-way ANOVA followed by Tukey's test on the columbic charge output obtained after 24 h of incubation of treated and untreated *A. baumannii* biofilm at E = 400 mV.

Overall ANOVA

	DF	Sum of Squares	Mean Square	F Value	Prob>F
Model	3	1.73587E9	5.78624E8	12.4449	0.00934
Error	5	2.32474E8	4.64949E7		
Total	8	1.96835E9			

Null Hypothesis: The means of all levels are equal.
Alternative Hypothesis: The means of one or more levels are different.
At the 0.05 level, the population means are significantly different.

Results of mean comparisons - Tukey's post hoc test.

	MeanDiff	SEM	q Value	Prob	Alpha	Sig	LCL	UCL
Flz *vs* Cells	-22261.58333	6224.60806	5.05777	0.05598	0.05	0	-45229.88104	706.71438
Itz *vs* Cells	-35912.065	6818.71649	7.44822	0.0122	0.05	1	-61072.57453	-10751.55547
Itz *vs* Flz	-13650.48167	6224.60806	3.10135	0.24389	0.05	0	-36618.77938	9317.81604
Cip *vs* Cells	-36123.37	6818.71649	7.49205	0.0119	0.05	1	-61283.87953	-10962.86047
Cip *vs* Flz	-13861.78667	6224.60806	3.14936	0.23504	0.05	0	-36830.08438	9106.51104
Cip *vs* Itz	-211.305	6818.71649	0.04383	0.99999	0.05	0	-25371.81453	24949.20453

Sig equals 1 indicates that the difference of the means is significant at the 0.05 level.
Sig equals 0 indicates that the difference of the means is not significant at the 0.05 level.

Appendix 5.12. One-way ANOVA followed by Tukey's test on the crystal violet estimates of treated and untreated *A. baumannii* biofilm on the working electrode area only; after potentiostatic experiment.

Overall ANOVA

	DF	Sum of Squares	Mean Square	F Value	Prob>F
Model	4	0.18963	0.04741	396.16017	5.78844E-11
Error	10	0.0012	1.19667E-4		
Total	14	0.19083			

Null Hypothesis: The means of all levels are equal.
Alternative Hypothesis: The means of one or more levels are different.
At the 0.05 level, the population means are significantly different.

Mean comparisons - Tukey's post hoc test.

	MeanDiff	SEM	q Value	Prob	Alpha	Sig	LCL	UCL
Cip *vs* Cells	-0.26167	0.00893	41.43072	0	0.05	1	-0.29106	-0.23227
Itz *vs* Cells	-0.23467	0.00893	37.1557	0	0.05	1	-0.26406	-0.20527
Itz *vs* Cip	0.027	0.00893	4.27502	0.07571	0.05	0	-0.0024	0.0564
Flz *vs* Cells	-0.19967	0.00893	31.61401	0	0.05	1	-0.22906	-0.17027
Flz *vs* Cip	0.062	0.00893	9.8167	2.98173E-4	0.05	1	0.0326	0.0914
Flz *vs* Itz	0.035	0.00893	5.54169	0.01893	0.05	1	0.0056	0.0644
DMSO *vs* Cells	-0.01233	0.00893	1.95279	0.65197	0.05	0	-0.04173	0.01706
DMSO *vs* Cip	0.24933	0.00893	39.47793	0	0.05	1	0.21994	0.27873
DMSO *vs* Itz	0.22233	0.00893	35.20291	0	0.05	1	0.19294	0.25173
DMSO *vs* Flz	0.18733	0.00893	29.66123	0	0.05	1	0.15794	0.21673

Sig equals 1 indicates that the difference of the means is significant at the 0.05 level.
Sig equals 0 indicates that the difference of the means is not significant at the 0.05 level.

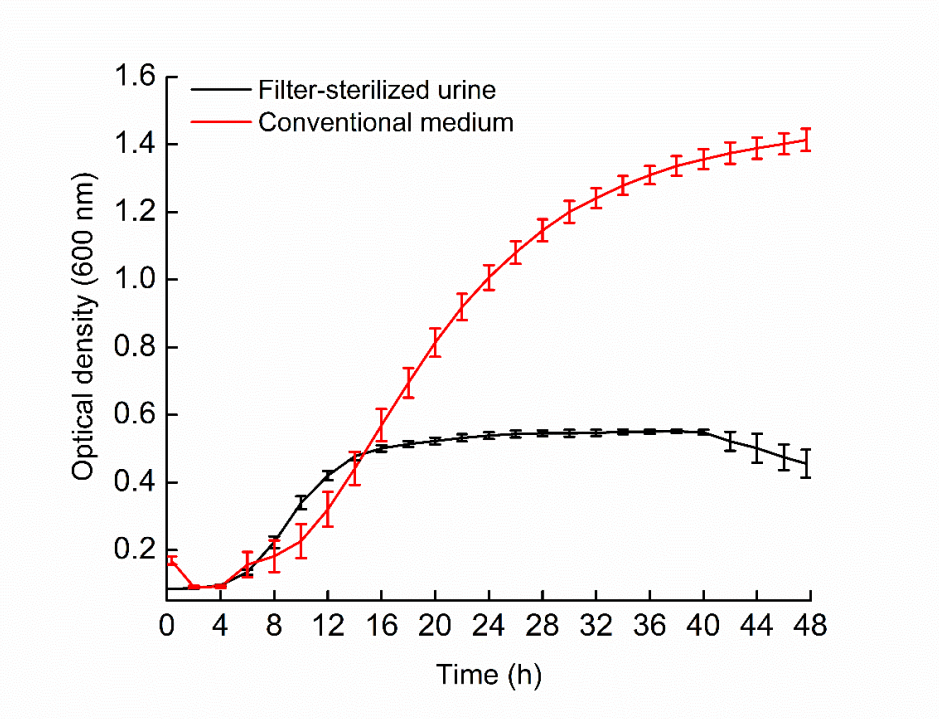

Appendix 6.1. Comparative growth curves of *C. albicans* in filter-sterilized urine and conventional RPMI (supplemented with 2% glucose) medium. (n=4)

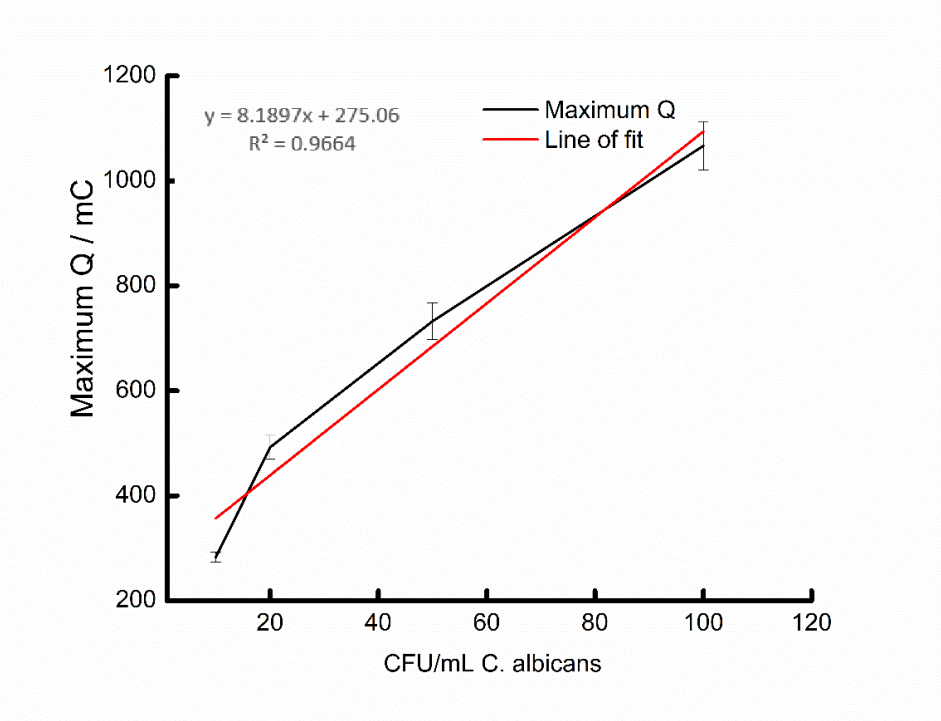

Appendix 6.2. Plot of maximum charge output (mC) obtained at different CFU/mL of *C. albicans*.

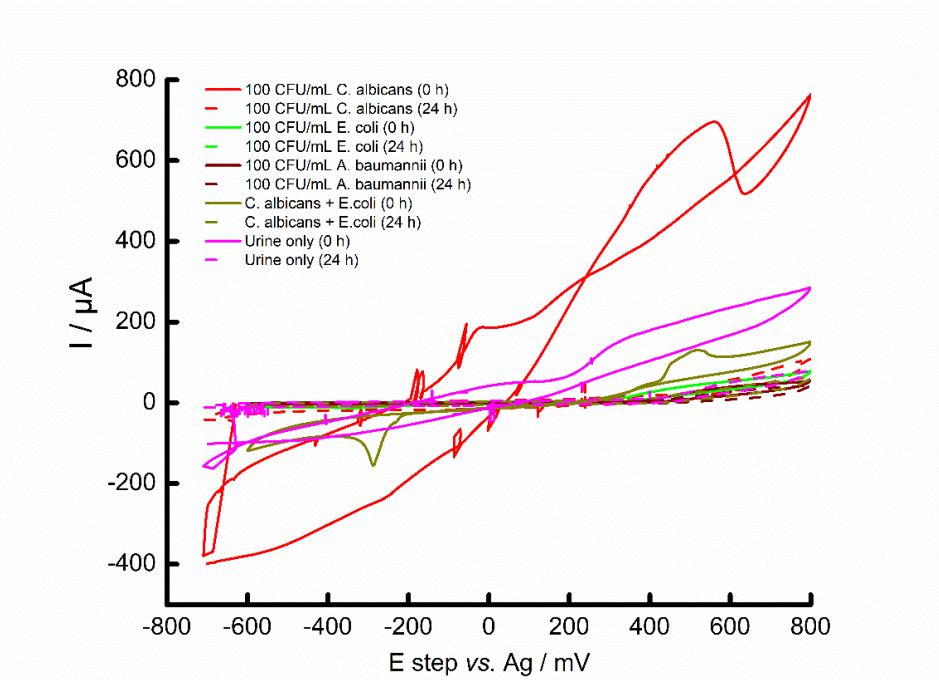

Appendix 6.3. Representative cyclic voltammograms at 10 mV/s scan rate of sterile urine (magenta trace) and urine spiked with 100 CFU/mL *C. albicans* (red trace), 100 CFU/mL *E. coli* (green trace), 100 CFU/mL *A. baumannii* (wine trace), co-culture of *C. albicans* and *E. coli* (dark yellow trace) at 0 h (solid trace) and 24 h.

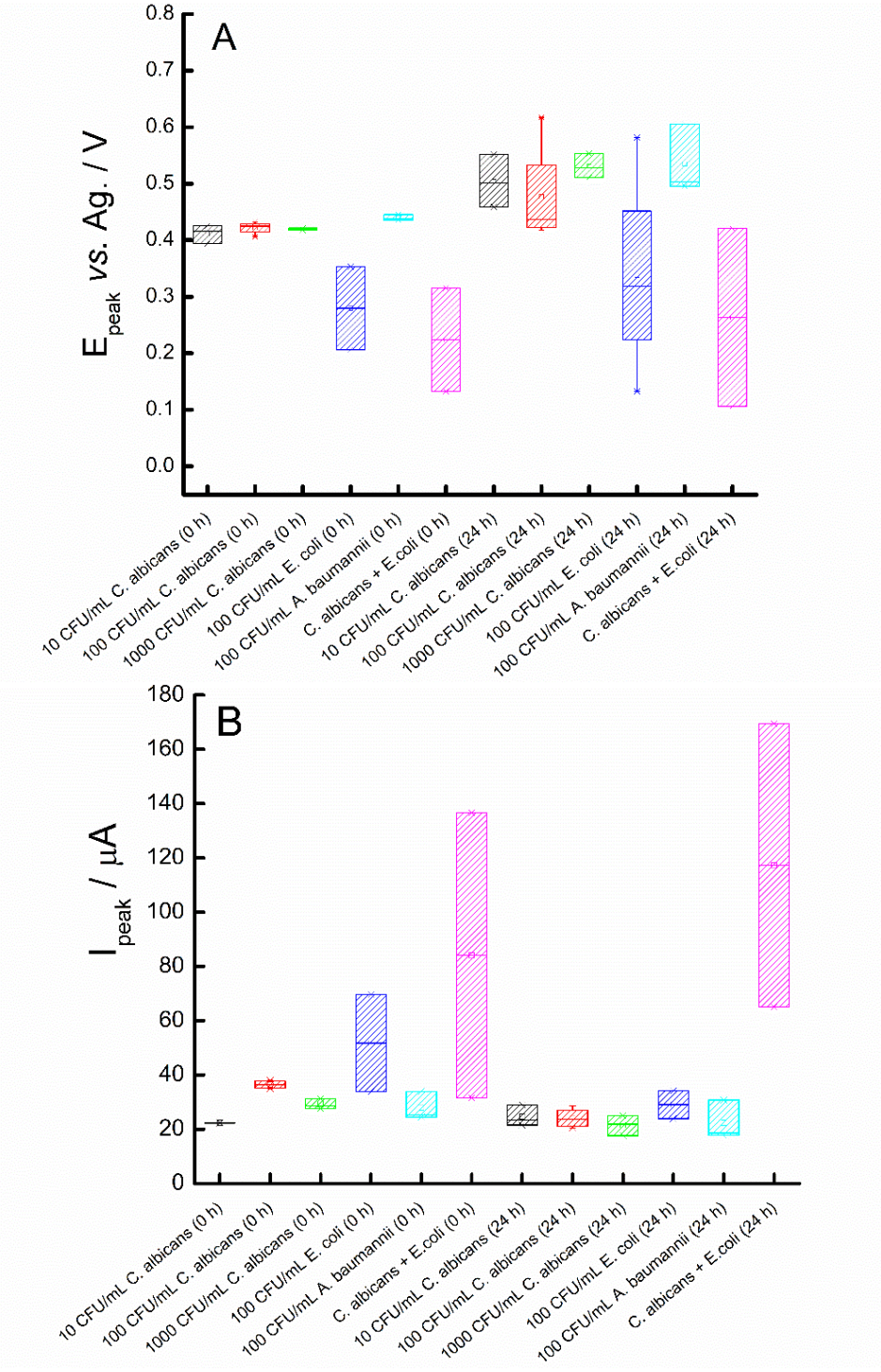

Appendix 6.**4.** (A) Peak position and (B) peak intensity of DPV spiked urine samples at *E* = 0.4 *vs.* Ag. Control experiments with sterile urine show no peaks and are therefore excluded.